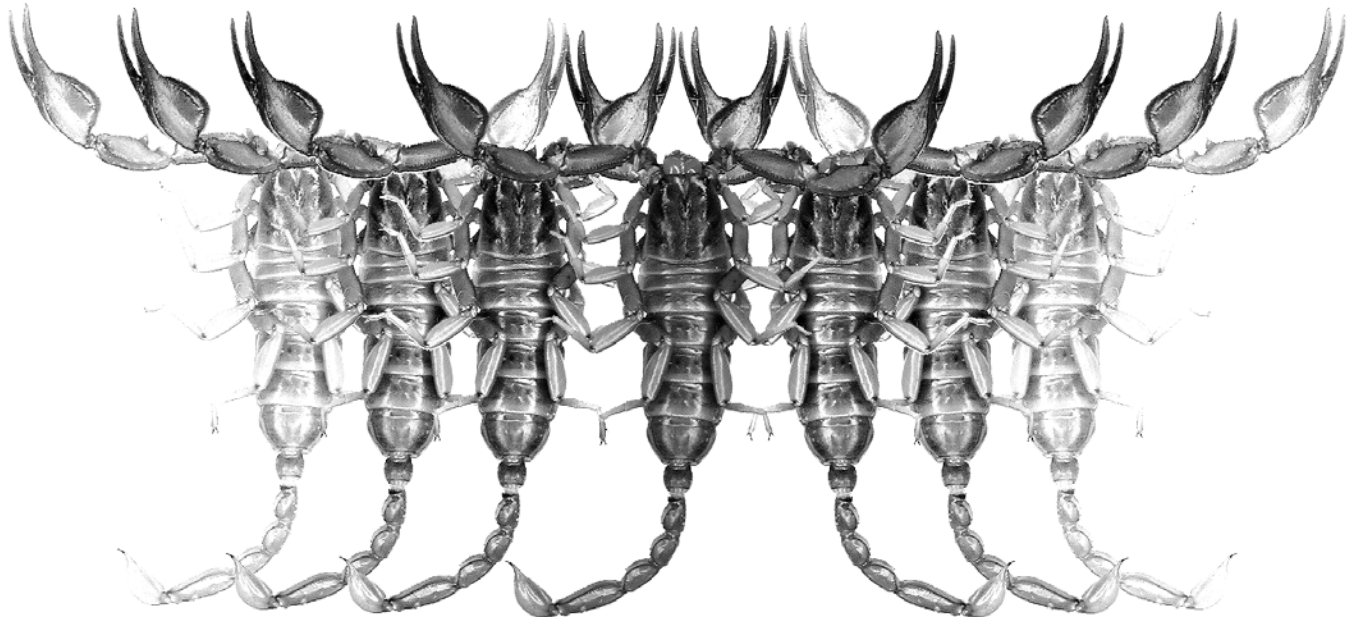


Euscorpius

Occasional Publications in Scorpiology



**Etudes on Iurids, III. Revision of the Genus
Iurus Thorell, 1876 (Scorpiones: Iuridae), with a
Description of Two New Species from Turkey**

František Kovařík, Victor Fet, Michael E. Soleglad & Ersen Aydın Yağmur

April 2010 – No. 95

Euscorpius

Occasional Publications in Scorpiology

EDITOR: Victor Fet, Marshall University, ‘fet@marshall.edu’

ASSOCIATE EDITOR: Michael E. Soleglad, ‘soleglad@la.znet.com’

Euscorpius is the first research publication completely devoted to scorpions (Arachnida: Scorpiones). *Euscorpius* takes advantage of the rapidly evolving medium of quick online publication, at the same time maintaining high research standards for the burgeoning field of scorpion science (scorpiology). *Euscorpius* is an expedient and viable medium for the publication of serious papers in scorpiology, including (but not limited to): systematics, evolution, ecology, biogeography, and general biology of scorpions. Review papers, descriptions of new taxa, faunistic surveys, lists of museum collections, and book reviews are welcome.

Derivatio Nominis

The name *Euscorpius* Thorell, 1876 refers to the most common genus of scorpions in the Mediterranean region and southern Europe (family Euscorpiidae).

Euscorpius is located on Website ‘<http://www.science.marshall.edu/fet/euscorpius/>’ at Marshall University, Huntington, WV 25755-2510, USA.

The International Code of Zoological Nomenclature (ICZN, 4th Edition, 1999) does not accept online texts as published work (Article 9.8); however, it accepts CD-ROM publications (Article 8). *Euscorpius* is produced in two *identical* versions: online (ISSN 1536-9307) and CD-ROM (ISSN 1536-9293). Only copies distributed on a CD-ROM from *Euscorpius* are considered published work in compliance with the ICZN, i.e. for the purposes of new names and new nomenclatural acts. All *Euscorpius* publications are distributed on a CD-ROM medium to the following museums/libraries:

- **ZR**, Zoological Record, York, UK
- **LC**, Library of Congress, Washington, DC, USA
- **USNM**, United States National Museum of Natural History (Smithsonian Institution), Washington, DC, USA
- **AMNH**, American Museum of Natural History, New York, USA
- **CAS**, California Academy of Sciences, San Francisco, USA
- **FMNH**, Field Museum of Natural History, Chicago, USA
- **MCZ**, Museum of Comparative Zoology, Cambridge, Massachusetts, USA
- **MNHN**, Museum National d'Histoire Naturelle, Paris, France
- **NMW**, Naturhistorisches Museum Wien, Vienna, Austria
- **BMNH**, British Museum of Natural History, London, England, UK
- **MZUC**, Museo Zoologico “La Specola” dell’Universita de Firenze, Florence, Italy
- **ZISP**, Zoological Institute, Russian Academy of Sciences, St. Petersburg, Russia
- **WAM**, Western Australian Museum, Perth, Australia
- **NTNU**, Norwegian University of Science and Technology, Trondheim, Norway
- **OUMNH**, Oxford University Museum of Natural History, Oxford, UK
- **NEV**, Library Netherlands Entomological Society, Amsterdam, Netherlands

Etudes on iurids, III. Revision of the genus *Iurus* Thorell, 1876 (Scorpiones: Iuridae), with a description of two new species from Turkey

František Kovařík¹, Victor Fet², Michael E. Soleglad³ & Ersen Aydin Yağmur⁴

¹ P.O. Box 27, CZ-145 01 Praha 45, Czech Republic; email: kovarik.scorpio@gmail.com; website: www.kovarex.com/scorpio

² Department of Biological Sciences, Marshall University, Huntington, West Virginia 25755-2510, USA; email: fet@marshall.edu

³ P.O. Box 250, Borrego Springs, California 92004, USA; email: soleglad@znet.com

⁴ Science Faculty, Biology Department, Zoology Section, Ege University, TR-35100, İzmir, Turkey; email: ersen.yagmur@gmail.com

Summary

This revision is based on a comprehensive analysis of largely new, very extensive material encompassing 341 specimens (58 from Greece and 283 from Turkey). The type species *Iurus dufourei* (Brullé, 1832) is restricted to Greece. *Iurus asiaticus* Birula, 1903 is confirmed as a distinct species, limited to eastern Anatolia. Most widespread in southern Turkey is another species, *Iurus kraepelini* von Ubisch, 1922, which is here restored from synonymy. We also describe two new species from Turkey: *Iurus kadleci*, sp. nov. from Antalya and Mersin Provinces (sympatric with *I. kraepelini*), and *Iurus kinzelbachi*, sp. nov. from İzmir and Aydin Provinces; therefore, fauna of Turkey includes four species of *Iurus*. Neotypes of *I. dufourei* and *I. kraepelini*, and lectotype and paralectotypes of *I. asiaticus* are designated. Status of *Iurus* populations from the eastern Aegean islands of Greece (Fourni, Karpathos, Kasos, Rhodes, Samos, Saria) remains to be determined. A map of the distribution of *Iurus* is presented, based on 198 localities (79 in Greece and 119 in Turkey).

Introduction

This large work represents a revision of the genus *Iurus* Thorell, 1876 (Iuridae). Our analysis of the extensive material (341 specimens, 58 from Greece and 283 from Turkey) revealed an unexpected and complex structure of the genus *Iurus*, which currently includes at least five species.

We restrict the nominotypical *Iurus dufourei* (Brullé, 1832) to the “Western clade” of Parmakelis et al. (2006), i.e. mainland Greece (Peloponnese) and Crete, as well as small islands of Kythira and Gavdos. A neotype for *I. dufourei* from the Peloponnese is designated since the syntypes of Brullé are lost.

Within Anatolia, we discover four species, of which two are new. We justify the species status of *Iurus asiaticus* Birula, 1903 (originally described as a subspecies of *I. dufourei* from Gülek Pass, Adana Province), and designate a lectotype and paralectotype for its existing syntype series. We demonstrate, however, that this species is limited to the eastern Anatolian mountains, mainly in the eastern Mersin, Adana, Kahramanmaraş, and Adiyaman Provinces.

Most of the southern Anatolian populations belong to the forgotten species *Iurus kraepelini* von Ubisch,

1922, described from Finike (Antalya Province), which is here restored from synonymy. We designate a neotype for it since the holotype is lost. This species is widespread in Muğla, Antalya, and western Mersin Provinces. The ranges of *I. asiaticus* and *I. kraepelini* appear to be closely allopatric, separated in Mersin by the Bolkar range of the eastern Taurus Mountains, one of the most important biogeographic boundaries in Anatolia (Çiplak, 2003).

We also describe two new, peripheral and distinct species of *Iurus* from Turkey. One of these, *Iurus kinzelbachi* sp. nov., occupies a limited range in western Anatolia, first discovered and studied there by Koç & Yağmur (2007, as *I. d. asiaticus*). We know that the range of this species has been reduced recently since we also studied old material from the now extinct population from the suburbs of İzmir. Some features of *I. kinzelbachi* sp. nov. point at its relatedness to the Greek *Iurus dufourei* rather than to three other Anatolian species.

Another new species, *Iurus kadleci* sp. nov., is described from Antalya and Mersin Provinces. This species is sympatric with *I. kraepelini* (in Akseki, Antalya, both were collected in the same habitat) but clearly different morphologically.

Finally, the status of the populations from six eastern Aegean islands (Fourni, Karpathos, Kasos, Rhodos, Saria, and Samos) remains to be determined; limited material does not allow us to associate them with *I. dufourei* or with any of the Anatolian species.

In this paper, following the historical **introduction**, we present the detailed section on **systematics**, which includes the genus-level discussion highlighted with many SEM micrographs, where *Iurus* is compared to its sister genus *Calchas*; distribution maps and an illustrated key; and detailed descriptions of five *Iurus* species, including two new species; **breeding**, which includes data highlighting the rearing of *Iurus kraepelini*, accompanied by photographs of all ontogenetic stages from the first instar to adult; **embryo morphology**, where, for the first time, a detailed description is given of the *I. dufourei* late embryo, accompanied by photographs and SEM micrographs; **ecology and biogeography** that provides a brief discussion of the distribution of *Iurus* and preferred habitats; and, finally, three **appendices** that provide complete locality data (including latitude/longitude), summary of neobothriotaxy in *Iurus*, and complete morphometric comparisons of all five *Iurus* species (separately for males and females).

History of study

The genus *Iurus* (Iuridae) was described by Thorell (1876) and has a relatively brief but confusing taxonomic history. Its type species was described by Brullé (1832: 58–59, pl. 28, fig. 1) as *Buthus dufourei*, from the ancient Messene, in Peloponnese (then called Morea), in newly independent Greece. Messene (now Messini, Messinia Prefecture) is located on the slopes of Mt. Ithomi (798 m a.s.l.), 30 km NW of Kalamata. A brief description of Brullé (1832) includes number of pectinal teeth as 10 for female and 11 for male. These historical syntypes of Brullé are lost. Later in this paper, we designate a neotype from Peloponnese, a female chosen from the available material from the closest locality to Messini, between Artemisia and Kalamata.

C. L. Koch (1837: 46–49, pl. 122, fig. 279) described the same species from Peloponnese (no exact locality) as *Buthus granulatus*. The two species were synonymized by Karsch (1879: 102), shortly after Thorell (1876) established genus *Iurus*, naming *Buthus granulatus* Koch as its type species.

The first records of *Iurus* for Crete (as “*Scorpius gibbus*”) were published by Lucas (1853) and Raulin (1869); and for Rhodes, by Thorell (1877). Werner (1938) had already listed *Iurus* from Peloponnese, Kythira, Crete, Karpathos, Rhodes, and Samos.

The first record of *I. dufourei* for Anatolia (Birula, 1898: 135) was of three specimens, a large (maybe adult) female and two juveniles, collected by Martin Holtz in 1897 at Gülek, a famous pass in the

Taurus Mts., called “Cilician Gates” by the ancients. The Gülek female was later discussed in comparison with Crete specimens by Birula (1903: 297–298), and was given the name as a new subspecies, *Iurus dufourei* *asiaticus*, with a rather brief description. The type series, which includes the large female, designated below as lectotype of *I. asiaticus*, and two juvenile paralectotypes, still exists in Zoological Institute, St. Petersburg, Russia, where Birula’s scorpion collection is kept.

A new species *Iurus kraepelini* was described from “Fineka” (now Finike) in southern Anatolia by Magda von Ubisch (1922). Its holotype, with pectinal teeth count of 13–11, formerly in Stuttgart, was lost in World War II (W. Schawaller, pers. comm., 2008). Based on its rather general description, Vachon (1947b: 26) synonymized *I. kraepelini* with *I. dufourei* *asiaticus*; however, Vachon never analyzed Birula’s types of *I. d. asiaticus*.

Roewer (1943), in a bizarre confusion, described a new genus *Chaerilomma* (with one species, *Chaerilomma dekanum*, allegedly from India; type was in SMFD but not found by Kovářík, 2002), which much later was discovered to be a synonym of *Iurus* (Vachon, 1966a; Francke, 1981). The label was obviously wrong, and we do not know the true provenance of Roewer’s specimen, other than its morphology matched the Crete population (Francke, 1981). Interestingly, the same paper (Roewer, 1943: 235) lists a specimen of *Iurus* from Anatolia (Ovacik), collected and correctly identified by Roewer himself (!), also deposited in SMFD.

Vachon (1947a, 1947b, 1948, 1951) mentioned *Iurus* in his works on scorpions of Turkey, as new records became available, still extremely scarce (only two specimens collected by C. Kosswig in 1946 and 1949 in Silifke and Korykos, near Silifke). Map of Vachon (1951: 343) shows only two localities for *Iurus* in Anatolia (Silifke and Gülek). A special biogeographic paper on *Iurus* was also published by Vachon (1953) who outlined its range as Peloponnese, Kythira, Crete, Karpathos, Rhodes, Samos, and southern Anatolia; the map of Vachon (1953: 98) shows four localities, adding Finike (after von Ubisch, 1922) and Tarsus (a new locality). The Ovacik locality near Fethiye, which was reported by both Werner (1902, 1936a) and Roewer (1943), was never mentioned by Vachon. No new Anatolian records were published for the following 20 years; in fact, *Iurus* was so poorly known that it was altogether omitted from a brief review of Turkish scorpions by Tolunay (1959), who otherwise correctly reproduced Vachon’s data.

Marking the history of study of this genus is a constant dearth of specimens. *Iurus* seems to be a rare scorpion in nature, and few museums had a chance to amass a large series of material. As a result, the true diversity of the genus *Iurus* has never been assessed

properly. Even when Vachon (1953) specifically wrote on this “*grand scorpion noir*” and recognized its biogeographic importance and taxonomic uniqueness, he never studied more than a couple of specimens. When he published an insightful and detailed revision of Roewer’s *Chaerilomma*, Vachon (1966a) only compared Roewer’s male of an alleged Indian species to a *single* male from Tarsus (MNHN RS 3007), both marvellously pictured by Maurice Gailliard. Even images of *Iurus* appearing in the great monograph of Vachon (1974) were based on the same Tarsus specimen (which we had a chance to examine in the present study).

After many decades of a relative neglect, the first modern and comprehensive review of *Iurus* was published by Kinzelbach (1975) who studied all circum-Aegean scorpion fauna and listed a number of new localities based on several European museum collections as well as personal field studies. Kinzelbach (1975) treated *Iurus* as monotypic, with only one species, *Iurus dufoureius*.

The map of Kinzelbach (1975, fig. 9) included *Iurus dufoureius* range in Greece as the Peloponnese, Crete, Karpathos, Rhodes, and Samos. The islands of Kythira, Kos, and Leros were listed as “known only from the locals but not confirmed by specimens.” A record from Kythira, however, had already been published by Werner (1937), and is now confirmed (Stathi & Mylonas, 2001). Records from Kos (Kinzelbach, 1975) and Samos (Vachon, 1953; Francke, 1981) were considered as dubious by Stathi & Mylonas (2001). However, Kritscher (1993) collected a specimen from Samos, as did Vignoli in 2003 (Francke & Prendini, 2008; FKCP). In addition, Fet (2000) reported a specimen from Kasos Island, collected by P. Beron and V. Beshkov in Stylokamara Cave. For Anatolia, the insert on the map of Kinzelbach (1975) covered the entire southern peninsula to the Gulf of Iskenderun in the east. Only three exact Anatolian localities were plotted, all coastal; however, in his map legend, Kinzelbach (1975: 25) listed twelve localities as new for Anatolia, based on the examination of several European museum collections: Pazarkoy (SE Egridir), Silifke, Cennet (NE Silifke), Çiglikara, Narli Kioi (“Marli Kioi”) near İzmir, Bodrum, Aspendos (E Antalya), Gazane, Dodurga (“Dorduga”), Mersin, Antalya, and Şile. Similar extrapolated maps were later published by Kinzelbach (1985) and Vachon & Kinzelbach (1987).

Detailed field studies of Crucitti (1995a, 1995b, 1998, 1999b) in the Peloponnese for the first time provided substantial data on distribution and ecology of *Iurus dufoureius*. For Anatolia, Crucitti (1999: 87–88) described the range of *Iurus* as “the whole Mediterranean region of Turkey, including the Chain of Taurus between the districts of Mugla and Tarsus.” For the southwestern Peloponnese, the map of Crucitti (1998, fig. 1) shows 18 localities. These and other

distributional records for Greece, along with some new data, were recently summarized by Facheris (2007a, 2007b), whose map shows over 30 localities for Peloponnese and 13 localities for Crete, as well as localities on Kythira and Gavdos islands.

More records from Anatolia were published by Crucitti & Malori (1998) and Francke & Prendini (2008). The map of Crucitti (1999, fig. 2) does not plot precise localities but shows a “presumptive” range from İzmir to Adana, but not as far east as maps of Kinzelbach (1975, 1985). The map given by Crucitti & Cicuzza (2001) had 13 localities plotted for Anatolia. Most recently, Yağmur, Koç & Akkaya (2009) listed 29 new localities for Anatolia based on extensive new collections by Turkish zoologists, and extended the known range of *Iurus* considerably to the east.

Recently, Parmakelis et al. (2006) published a phylogeographic study of *Iurus* based on mtDNA (16S rDNA) marker, recovering two clades for seven localities across the range of the genus: three for the western clade (Peloponnese, Kythira, Crete) and four for the eastern clade (Rhodes, Karpathos, Megisti, Anatolia). They indicated that the level of mtDNA sequence divergence (above 5 %) between all pairwise comparisons could justify elevation of the two described subspecies (*I. d. dufoureius* and *I. d. asiaticus*) to species rank (see below on the history of this issue). Parmakelis et al. (2006), however, refrained from making taxonomic decisions until a detailed morphological study. We offer such a study here, focusing primarily on largely unexplored Anatolian populations of *Iurus*.

Probably the fact that *Iurus* was classified for over 100 years in Vaejovidae did not facilitate its revision: no modern European researcher studied vaejovids at generic level, while North American taxonomists were unfamiliar with *Iurus*. Note that Stahnke (1974: 215), in the first comprehensive revision of high-level taxa of Vaejovidae, studied only a single female of *Iurus*. Both Vachon (1966a, 1974) and Stahnke (1974) noted a separate position of this genus, and of then monotypic Iurinae (equivalent to current Iuridae). Francke & Soleglad (1981) outlined Iuridae as a family (equivalent to the current superfamily Iuroidea), which in fact is not closely related to Vaejovidae (Stockwell, 1989; Soleglad & Fet, 2003b; Fet & Soleglad, 2008). Still, a few attempts to address taxonomy of *Iurus* (Francke, 1981; Kritscher, 1993) were not conclusive due to the limited material available. In addition, no connection between *Iurus* and its sister genus *Calchas* Birula, 1899, then classified in Chactidae, was made until Vachon (1971) who was the first modern researcher to see a specimen of *Calchas*. Francke & Soleglad (1981) first brought the two genera together under Iuridae (again, examining only a single female *Calchas*). See Fet, Soleglad & Kovařík (2009) for detailed information on *Calchas*, a very important taxon for understanding *Iurus*.

Our attention to *Iurus* was warranted by several factors. First, it was the importance of Iuroidea and Iuridae for the high-level scorpion systematics and phylogeny, namely a separate, basal position of this group (Stockwell, 1989; Soleglad & Fet, 2003b; Fet et al., 2004; Fet & Soleglad, 2008). Second, the unusual trichobothrial pattern of Iuridae, noticed by Vachon (1974) and Stahnke (1974), when studied in more detail, yielded previously unknown extensive and variable neobothriotaxy (Soleglad, Kovařík & Fet, 2009), including that in the unique population near İzmir (described here as *I. kinzelbachi*, sp. nov.). Third, our recent revision of the sister genus *Calchas* (Fet, Soleglad & Kovařík, 2009) revealed its “hidden diversity” in Anatolia, which prompted us to pay more attention to *Iurus* that is even more widespread in this area. Fourth, a tentative identification of a distinctive, new species from Anatolia (described here as *I. kadleci*, sp. nov.), required a careful reanalysis of the Anatolian populations. Finally, the availability of numerous new material, which has been recently collected by Turkish zoologists, allowed us to assess many populations across the entire range of *Iurus*.

Subspecies controversy

Iurus dufoureius dufoureius (Brullé, 1832) and *I. d. asiaticus* Birula, 1903 have been traditionally treated as subspecies by the authors who maintained the monotypy of the genus (e.g. Vachon, 1947b; Kinzelbach, 1975, 1982). These subspecies, however, were never revised until Francke (1981) first suggested that *I. d. asiaticus* should be given species status.

Francke (1981) studied the type of *Chaerilomma dekanum* Roewer from SMFD (no correct locality known, assumed to be from Greece), and compared it to “additional specimens from Crete, Rhodes and Turkey.” In his paper, however, Francke (1981) listed the data only for one male from Crete and four specimens from Turkey: two from “Namrum” (=Namrun, now Çamliyayla; but see below for corrected labels), and two from Antalya; no data were listed for Rhodes. Francke (1981: 221) mentioned that Birula’s subspecies was described as having 12 pectinal teeth versus 9 in the “nominate subspecies from Crete.” This is not exact: Birula (1903: 297) clearly stated that Crete specimens have 9 pectinal teeth but otherwise do not differ from typical “Greek” (i.e. Peloponnese) specimens, which have 10 or 11. Birula’s ZISP collection, in fact, has an unpublished specimen from Taygetos Mts. (Peloponnese) as well as Gülek and Crete specimens. Birula (1903) did not address Crete as part of Greece because Crete since 1898 was an autonomous state still under Ottoman rule, and joined Greece only in 1913. Francke

(1981) concluded that his Anatolian specimens were a separate species, *I. asiaticus*. He suggested that populations from Rhodes and Karpathos Islands also belong to *I. asiaticus*.

Francke (1981: 222) also suggested that, since Thorell (1877: 193–195) placed under *Iurus granulatus* a female from Greece as well as a male from Rhodes, this makes *Buthus granulatus* C. L. Koch, 1837 an available senior synonym of *Iurus asiaticus* Birula, 1903. This is, however, incorrect, since Koch’s original name was clearly given to a Peloponnese population. Therefore *Buthus granulatus* C. L. Koch, 1837 is a junior synonym of *Iurus dufoureius* (Brullé, 1832), as synonymized by Karsch (1879); the Rhodes specimens of Thorell are not name-bearing.

The opinions on species or subspecies status of *I. asiaticus*, as well as on its volume, have varied after its elevation to species level by Francke (1981). Kritscher (1993) analyzed a larger series of specimens, mostly from Karpathos, and treated *I. d. asiaticus* as a subspecies found in Karpathos, Rhodes, Samos, and Turkey.

Sissom & Fet (2000) listed *I. d. asiaticus* as a subspecies and explained: “Francke (1981) considered *Iurus dufoureius asiaticus* Birula, 1903 from Turkey and the Aegean a separate species. Kritscher (1993) analyzed a larger series of specimens and concluded that this form has only a status of subspecies.” The subspecies rank was followed by Fet (2000), Fet & Braunwalder (2000), Parmakelis et al. (2006), Facheris (2007a, 2007b), Kaltsas, Stathi & Fet, (2008), and Yağmur, Koç & Akkaya (2009).

At the same time, other authors (Crucitti & Malori, 1998; Kovařík, 1999, 2002; Crucitti & Cicuzza, 2001; Stathi & Mylonas, 2001) continued recognizing *I. asiaticus* as a separate species. Stathi & Mylonas (2001: 293) noted also that they “found specimens from Rodos and Karpathos that are clearly *I. dufoureius*, similar to individuals from Crete,” thus disagreeing with both Francke (1981) and Kritscher (1993) on the geographic scope of *I. dufoureius* (or *I. d. dufoureius*). On the contrary, the mitochondrial DNA-based phylogeny by Parmakelis et al. (2006) did not group Rhodes and Karpathos populations with the nominotypical *I. dufoureius* from the Peloponnese; instead, these populations formed a clade with populations from Anatolia and Megisti (*I. kraepelini*, see below).

In the present paper, we do not employ the subspecies category as we demonstrate that species-level differences exist between several of *Iurus* populations in Greece and Turkey, amounting to at least five species. The Rhodes and Karpathos populations, as well as those from other Eastern Aegean islands, designated here as *Iurus* sp., are a subject of a separate study (Soleglad et al., in progress).

Material and Methods

Abbreviations

The four-letter institutional abbreviations listed below and used throughout are mostly after Arnett et al. (1993), or introduced here to accommodate other collections: BMNH, Natural History Museum, London, UK; FKCP, personal collection of František Kovařík, Prague, Czech Republic; MBCH, personal collection of Matt E. Braunwalder, Zürich, Switzerland; MCNH, Natural History Museum of Crete, Iraklio, Crete, Greece; MESB, personal collection of Michael E. Soleglad, Borrego Springs, California, USA; MNHN, Muséum national d'Histoire naturelle, Paris, France; MTAS, Museum of the Turkish Society of Arachnology, Ankara, Turkey; MZUF, Sezione di Zoologia "La Specola", Museo di Storia Naturale dell'Università di Firenze, Florence, Italy; NHMW, Naturhistorisches Museum Wien, Vienna, Austria; NMPC, National Museum, Prague, Czech Republic; RKRO, personal collection of Ragnar Kinzelbach, Rostock, Germany; SMFD, Senckenberg Museum, Frankfurt, Germany; SMNS, Staatliches Museum für Naturkunde, Stuttgart, Germany; SOFM, National Museum of Natural History, Sofia, Bulgaria; VFWV, personal collection of Victor Fet, Huntington, West Virginia, USA; ZISP, Zoological Institute, Russian Academy of Sciences, St. Petersburg, Russia; ZMHB, Museum für Naturkunde der Humboldt-Universität zu Berlin, Berlin, Germany.

Terminology and conventions

The systematics adhered to in this paper follows the classification as established in Fet & Soleglad (2005) and as modified in Fet & Soleglad (2008). Terminology describing pedipalp chelal finger dentition follows that described and illustrated in Soleglad & Sissom (2001), that of the sternum follows that in Soleglad & Fet (2003a), and the metasomal and pedipalp carination, and leg tarsus armature follows that described in Soleglad & Fet (2003b). Trichobothrial nomenclature and hypothesized homologies are those described and illustrated in Vachon (1974). Techniques using maximized morphometric ratios follow those described in Fet & Soleglad (2002: 5) and further established in Soleglad & Fet (2008: 57–69).

SEM microscopy

To investigate *Iurus* morphology, various structures were dehydrated in an ethanol series (50, 75, 95, and two changes of 100%) before being dried and coated with gold/palladium (ca. 10 nm thickness) in a Hummer sputter coater. Digital SEM images were acquired with a

JEOL JSM-5310LV at Marshall University, West Virginia. Acceleration voltage (10–20 kV), spot size, and working distance were adjusted as necessary to optimize resolution, adjust depth of field, and to minimize charging. The SEM fixation protocol for the embryos was as follows. The embryos were transferred from 70% ethyl alcohol into Phosphate-Buffered Saline (PBS) with two changes (in ca. 15 ml vial) about 30 min each; fixed in fresh 5% glutaraldehyde with 4% formaldehyde in 0.1M cacodylate buffer in refrigerator for 48 hrs; rinsed ten times with distilled water; fixed in 2% OsO₄ for 2–3 hours; rinsed three times in distilled water, and placed into 50% ethanol.

Material Examined

We examined the total of 341 specimens of *Iurus* (58 from Greece and 283 from Turkey). For the list of material with labels, see below under species names.

In addition to the five species described and defined in detail below, we also examined the following 7 specimens from Greece (eastern Aegean islands), currently under further study, and identified here as *Iurus* sp.:

Greece: *Karpathos*: eastern part of the island, Apella Beach, ♂ sbad., born in captivity from a ♀ collected 6 July 2005, leg. M. Colombo (MESB; Figs. 48, 95). *Kasos*: Stylokamara Cave, 6 May 1984, 1 ♂, leg. P. Beron (SOFM 96). *Rhodes*: 1 ♂, Kritia ("Kastelo"), May 1887, leg. E. von Oertzen (ZMHB 8069) (Figs. 49, 94, 102); Mt. Filerimos (Eremofilo), 1 ♀, 1 juv (MZUF 1069); Archangelos, 2 May 1987, 1 ♀, leg. P. Beron (SOFM 158). *Samos*: Aghios Nikolaos, 3 km W of Karlovasi, 27 June 2003, 1 ♀, leg. V. Vignoli (FKCP) (Fig. 96, 104). Fig. 103 shows a live juvenile specimen from Rhodes.

Our map (Fig. 74) is based on 198 localities from literature as well as unpublished museum and private collections, including 35 localities from Peloponnese and 119 from Anatolia. For a full list of localities, sources, and geographic coordinates, see Appendix A. We exclude Kos and Leros islands from the distribution of *Iurus* until confirmed. We also did not plot obviously introduced specimens from Egypt (Thorell, 1877; Kraepelin, 1899; Birula, 1903), Beirut ("Syria", Kinzelbach, 1975), and records from Gökce-Kısık near Eskişehir (Werner, 1902) and Şile near Istanbul (Kinzelbach, 1975), far from the main range and probably also introductions or incorrect labels. We also did not include the single existing record from Cyprus, published only recently (Kamenz & Prendini, 2008: 43) but based on an old series of specimens, identified as *I. d. dufourei*, with an unclear label ("Cyprus: Rolle", ZMHB 7497). We suspect that this locality was confused with Crete, since there have been no other records of *Iurus* from Cyprus. Franz Hermann Rolle

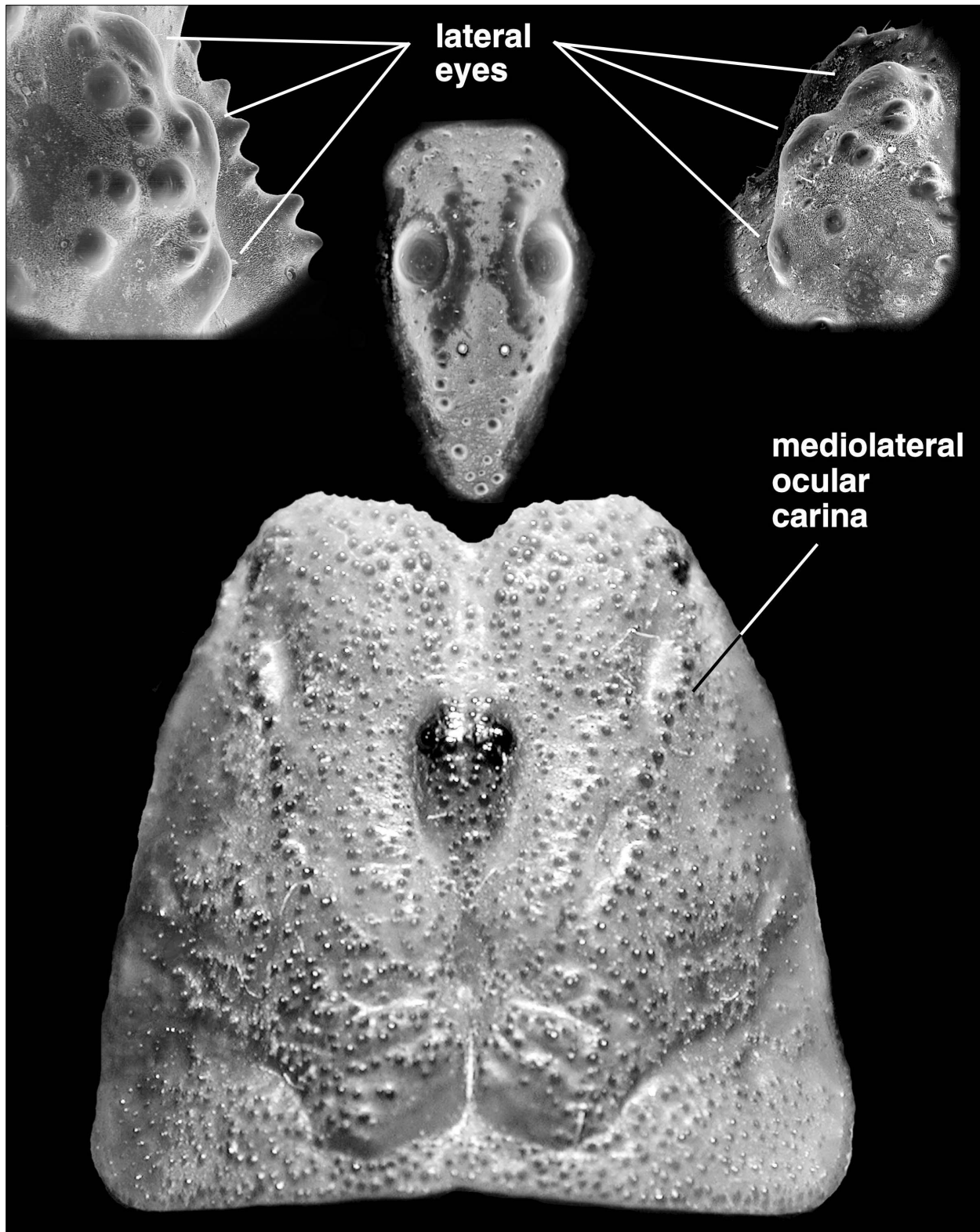


Figure 1: Carapace and close-up of median and lateral eyes. Carapace of *Iurus kinzelbachi*, sp. nov., adult male, İzmir, İzmir, Turkey. Median and left lateral eyes (right, 50x) of *I. dufourieius*, subadult female, Krini, Gythio, Laconia, Greece. Right lateral eyes (left, 75x) of *I. asiaticus*, 4 km E Kaşlıca Village, Adiyaman, Turkey. Three lateral eyes and a well developed mediolateral ocular carina are indicated.

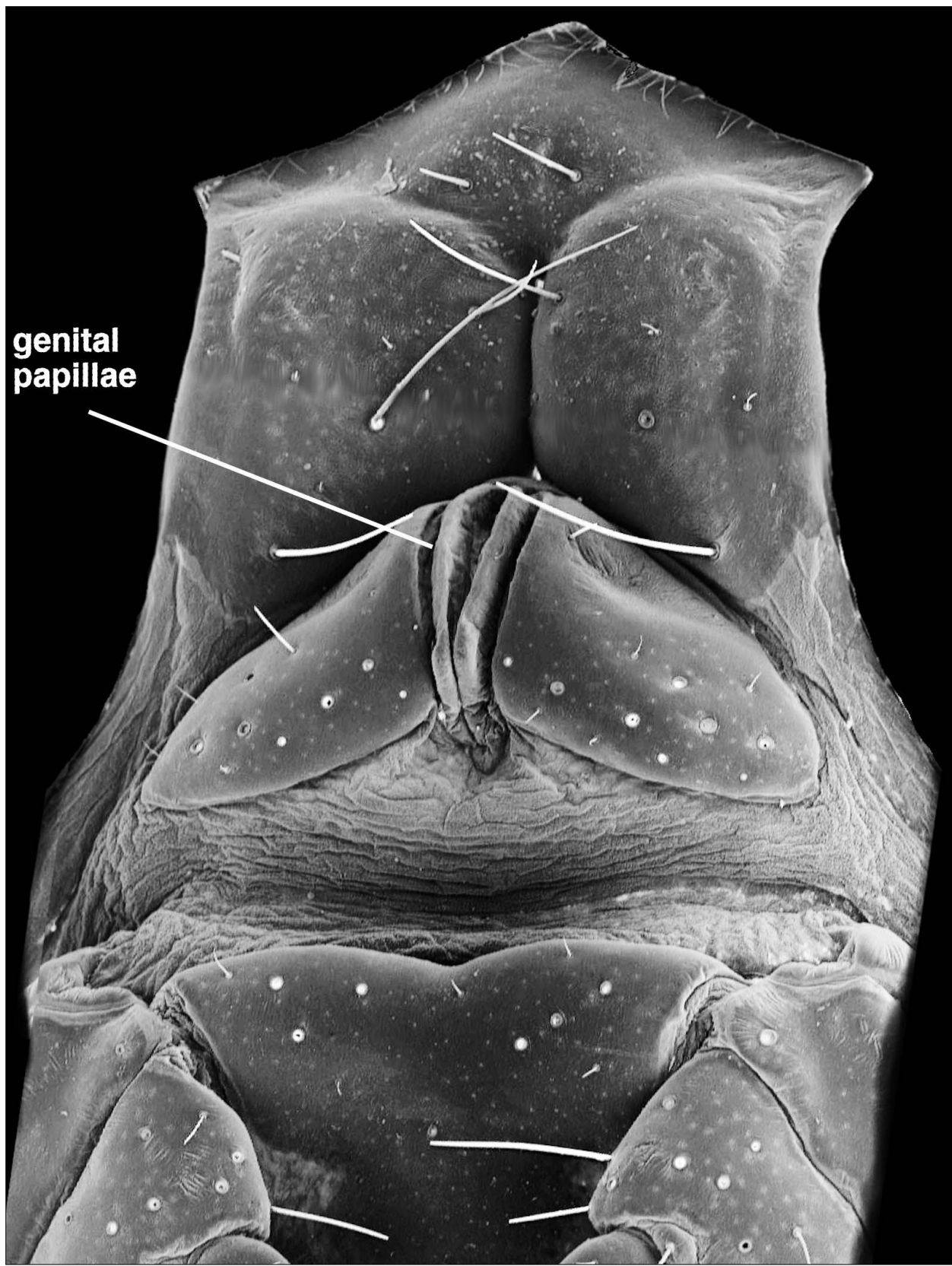


Figure 2: Sternopectinal area (35x) of *Iurus kraepelini*, juvenile male, Akseki, Antalya, Turkey. The conspicuous genital papillae visible between the genital operculum sclerites are indicated.

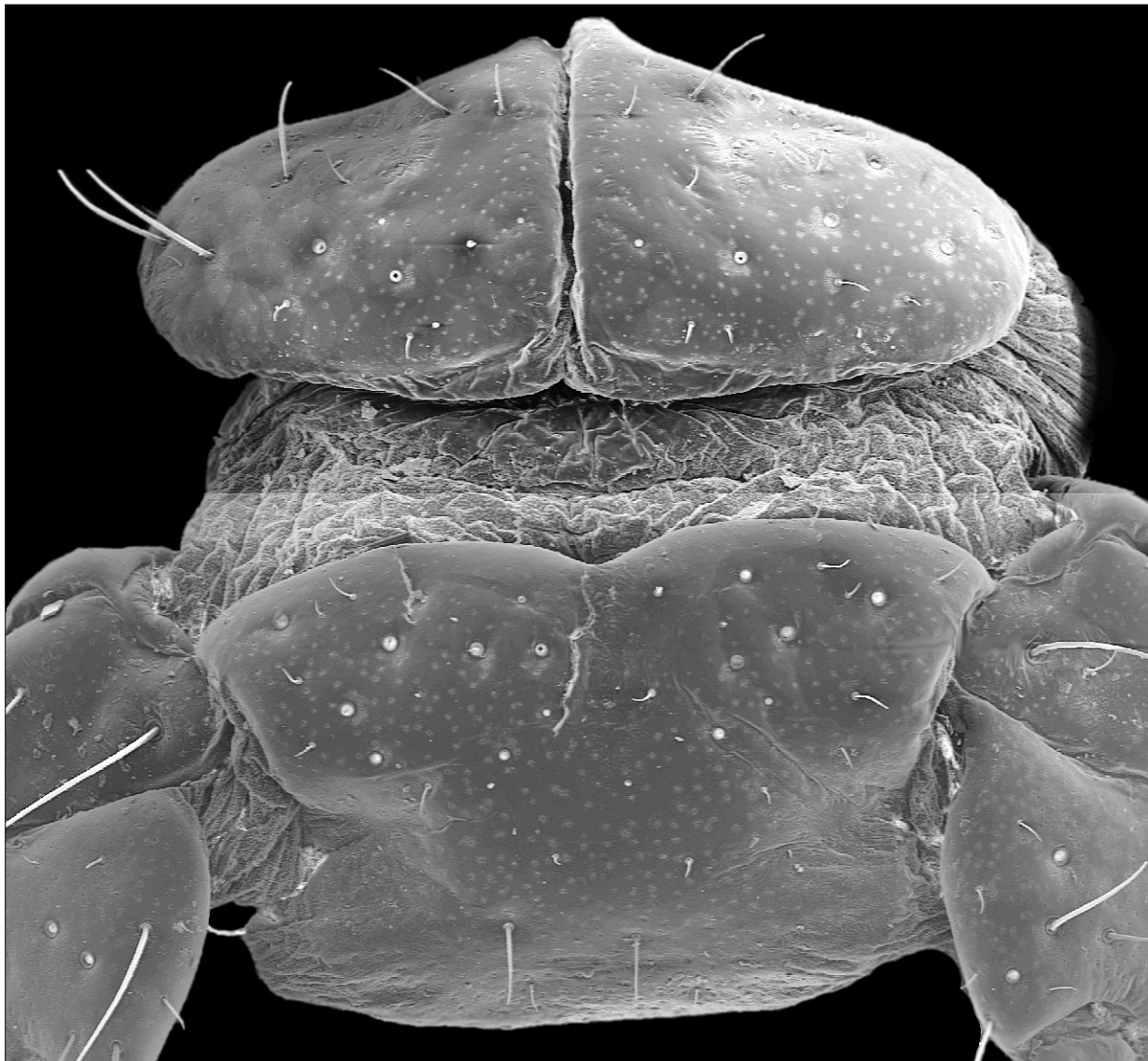


Figure 3: Genital operculum and pectinal basal piece (35x) of *Iurus asiaticus*, adult female, 4 km east of Kaşlıca Village, Adiyaman, Turkey. Note the wide genital operculum with sclerites fused medially.

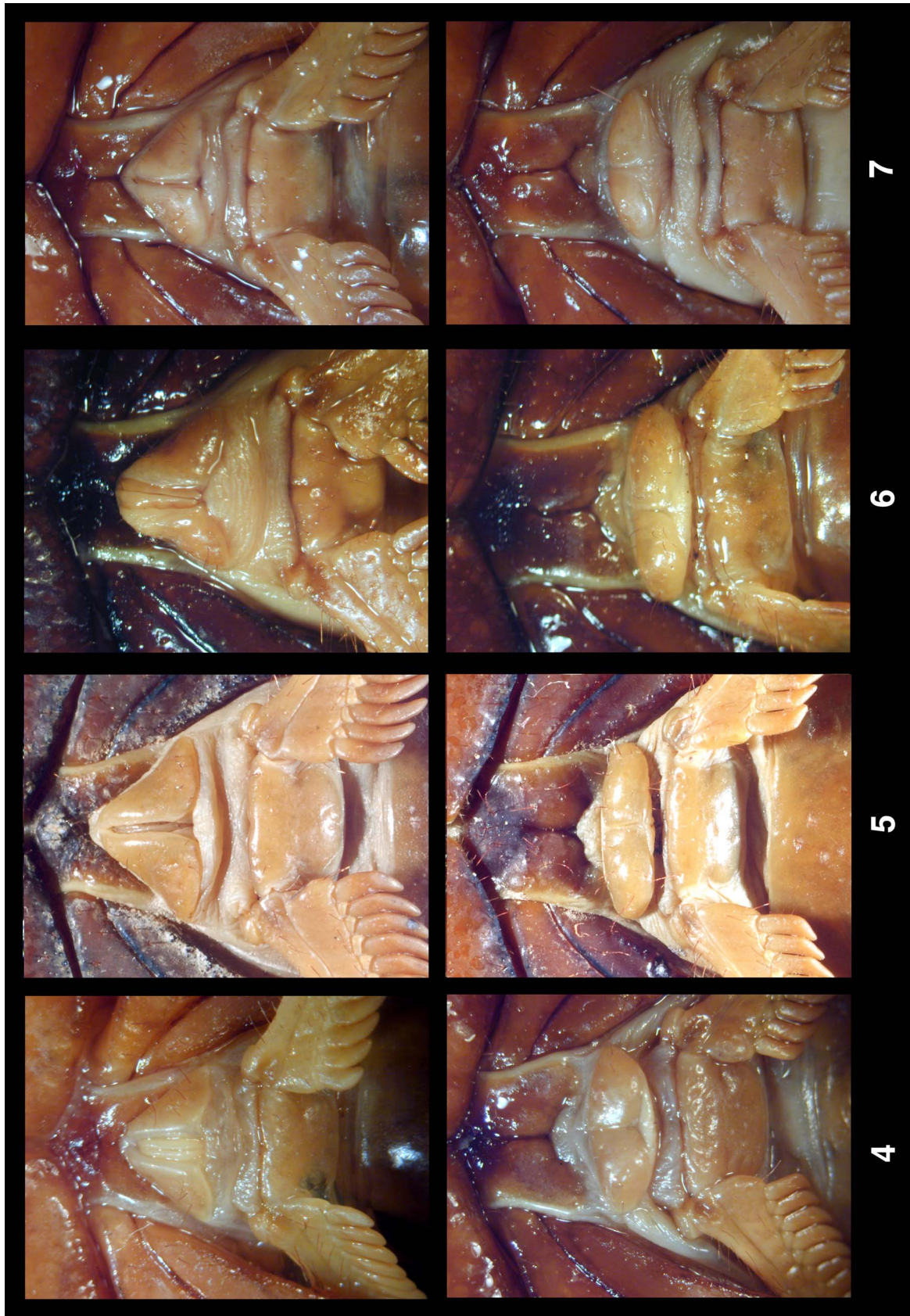
(1864–1929), a German zoologist, was also a dealer who supplied scorpions to the museums; his other specimens of *Iurus* without any exact label exist in ZMHB (see Material Examined) and BMNH (“Mersina”, 95-11.9.14; J. Beccaloni, pers. comm.).

Systematics

The systematics of superfamily Iuroidea has been discussed in detail in four recent papers: (1) Soleglad & Fet (2003b), a high-level cladistic analysis of extant scorpions, where Iuroidea was originally declared; (2) Fet et al. (2004), an analysis of the leg tarsal spination of

Iuroidea, where a key to all six genera was provided and genus *Hoffmannihadrurus* was described; (3) Fet & Soleglad (2008), a cladistic analysis of Iuroidea with an emphasis on subfamily Hadrurinae, where *Hoffmannihadrurus* was reestablished; and (4) Fet, Soleglad & Kovařík (2009), a systematic revision of the genus *Calchas*, where two new species were described.

Order **SCORPIONES** C. L. Koch, 1850
 Suborder Neoscorpiones Thorell et Lindström, 1885
 Infraorder Orthosterni Pocock, 1911
 Parvorder Iurida Soleglad et Fet, 2003
 Superfamily Iuroidea Thorell, 1876
 Family Iuridae Thorell, 1876



Figures 4–7: Sternum, genital operculum, and pectinal basal piece of *Iurus* male (top) and female (bottom). **4.** *I. dufoureius*, Kurtaina, Greece (male); Nedontas River, between Artemisia and Kalamata, Greece (female neotype). **5.** *I. kinzelbachi*, sp. nov., Dilek Peninsula, Aydin, Turkey. **6.** *I. kraepelini*, Akseki, Antalya, Turkey. **7.** *I. kalleci*, sp. nov., Akseki, Antalya, Turkey.

Genus *Iurus* Thorell, 1876

Iurus Thorell, 1876: 11; type species by original designation *Iurus granulatus* (C. L. Koch, 1837) [= *Iurus dufoureius* (Brullé, 1832)].

Synonyms:

Chaerilomma Roewer, 1943: 237–238; type species *Chaerilomma dekanum* Roewer, 1943 [= *Iurus dufoureius* (Brullé, 1832)] (synonymized by Vachon, 1966a: 453–461).

References (selected):

Iurus: Thorell, 1877: 193; Pavesi, 1878: 360; Simon, 1879: 115; Kraepelin, 1894: 183; Kraepelin, 1899: 178; Werner, 1902: 605; Borelli, 1913: 2; Caporiacco, 1928: 240; Werner, 1936b: 17; Menozzi, 1941: 234; Gruber, 1963: 308; Gruber, 1966: 424; Vachon, 1966a: 453; Vachon, 1966b: 215; Stahnke, 1974: 114; Vachon, 1974, fig. 141, etc.; Kinzelbach, 1975: 21; Francke, 1981: 221; Kinzelbach, 1982: 58; Kinzelbach, 1985: Map IV; Vachon & Kinzelbach, 1987: 102; Kovařík, 1992: 185; Kritscher, 1993: 381; Crucitti, 1995a: 1; Crucitti, 1995b: 91; Crucitti, 1998: 31; Crucitti & Malori, 1998: 133; Kovařík, 1998: 136; Crucitti, 1999a: 87; Crucitti, 1999b: 251; Kovařík, 1999: 40; Fet, 2000: 49; Fet & Braunwalder, 2000: 18; Sissom & Fet, 2000: 419; Crucitti & Cicuzza, 2001: 227; Karataş, 2001: 14; Stathi & Mylonas, 2001: 290; Kovařík, 2002: 16; Fet et al., 2004: 18; Kovařík & Whitman, 2005: 113; Parmakelis et al., 2006: 253; Facheris, 2007a: 1; Facheris, 2007b: 1; Koç & Yağmur, 2007: 57; Fet & Soleglad, 2008: 256; Francke & Prendini, 2008: 218; Kaltsas, Stathi & Fet, 2008: 228; Soleglad, Kovařík & Fet, 2009: 2; Yağmur, Koç & Akkaya, 2009: 154.

Jurus (incorrect subsequent spelling): Karsch, 1879: 101; Karsch, 1881: 90; Simon, 1884: 351; Kraepelin, 1894: 183; Birula, 1898: 135; Birula, 1903: 297; Penther, 1906: 62; von Ubisch, 1922: 503; Werner, 1934a: 162; Werner, 1934b: 282; Werner, 1937: 136; Werner, 1938: 172; Vachon, 1947a: 162; Vachon, 1947b: 2; Vachon, 1948: 62; Vachon, 1951: 343; Vachon, 1953: 96.

Distribution. GREECE: mainland: Peloponnese; islands: Crete, Fourni, Gavdos, Karpathos, Kasos, Kithyra, Megisti, Rhodes, Samos, Saria. TURKEY (Anatolia): Adana, Adiyaman, Antalya, Aydın, Isparta, İzmir, Kahramanmaraş, Karaman, Konya, Mersin, Muğla, and Niğde Provinces.

Diagnosis

General appearance. Large-sized scorpion (85–100 mm); generally dark grey to black in color; chelae

elongate, robust and carinated, exaggerated lobe found on movable finger in males; metasoma with well-developed carinae, dorsal carinae highly serrated; telson elongate, vesicle-aculeus juncture subtly defined, vesicle ventral surface covered with setae. Pectinal tooth counts 10–16 in males, 7–14 in females. Carapace granular, with deep narrow indentation; median eyes and tubercle small, located on anterior three-eighths; three lateral eyes; mediolateral ocular carinae strongly developed.

Important taxonomic characters. Tibial spurs absent on legs III–IV; leg tarsus ventral surface with single row of densely populated spinule clusters, terminating in an enlarged pair of distal clusters. Femoral trichobothrium *d* located on external surface; *e* located slightly distal of *d*; chelal trichobothrium *db* positioned at fixed finger midpoint; *Db* located ventrally of external (*E*) carina, in line with *Eb* series; patellar trichobothrium *i* located on internal surface, adjacent to *DI* carina. Prepectinal plate absent in female. Stigma medium to long, slit-like in shape. Large conspicuous ventral accessory (*va*) denticle of cheliceral movable finger located at finger midpoint; vestigial serrula present on juveniles and subadults, essentially absent in adults. Hemispermatophore lamina elongate with non-spatulate, pointed terminus; lamellar internal base lacking triangular protuberance; capsular area with strongly developed acuminate process with truncated tip. Chelal finger median denticle (*MD*) groups number 14–16; inner denticles (*ID*) 11–16. Patellar dorsal (DPS) and ventral (VPS) spurs strongly developed and conspicuously doubled.

Detailed Analysis of Morphology at Genus Level

Here, we describe basic morphology specific to genus *Iurus*. The species assignments are as accepted further in this paper. Since the second iurid genus, *Calchas*, has been revised recently (Fet, Soleglad & Kovařík, 2009), we can now contrast *Iurus* with *Calchas* in great detail for all morphology described below, which follows each structure analysis subsection.

Carapace

The carapace of *Iurus* is characterized by its conspicuous anterior emargination and exaggerated mediolateral ocular carinae (Fig. 1). In general, the entire surface of the carapace is covered with various sized granules, the larger found on the anterior half. There are exceptions, however, within the five species; the interocular area is partially smooth in *I. asiaticus* and *I. kraepelini*.

Three lateral eyes are present in all species, the most posterior eye smaller than the others. Close-up views of

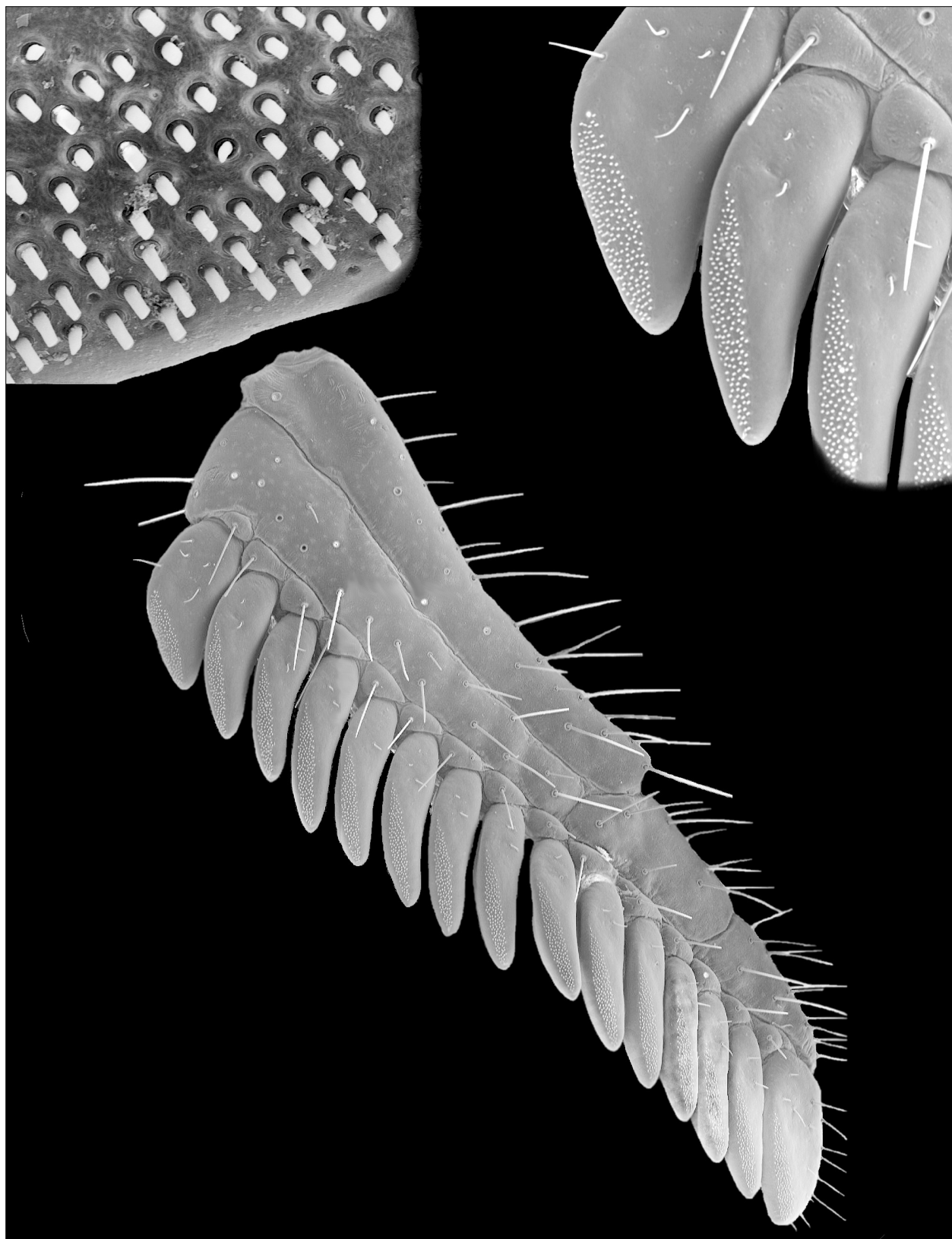


Figure 8: Pecten (35x), close-up of basal teeth (100x), and close-up of peg sensilla of basal tooth (500x) of *Iurus kraepelini*, juvenile male, Akseki, Antalya, Turkey.

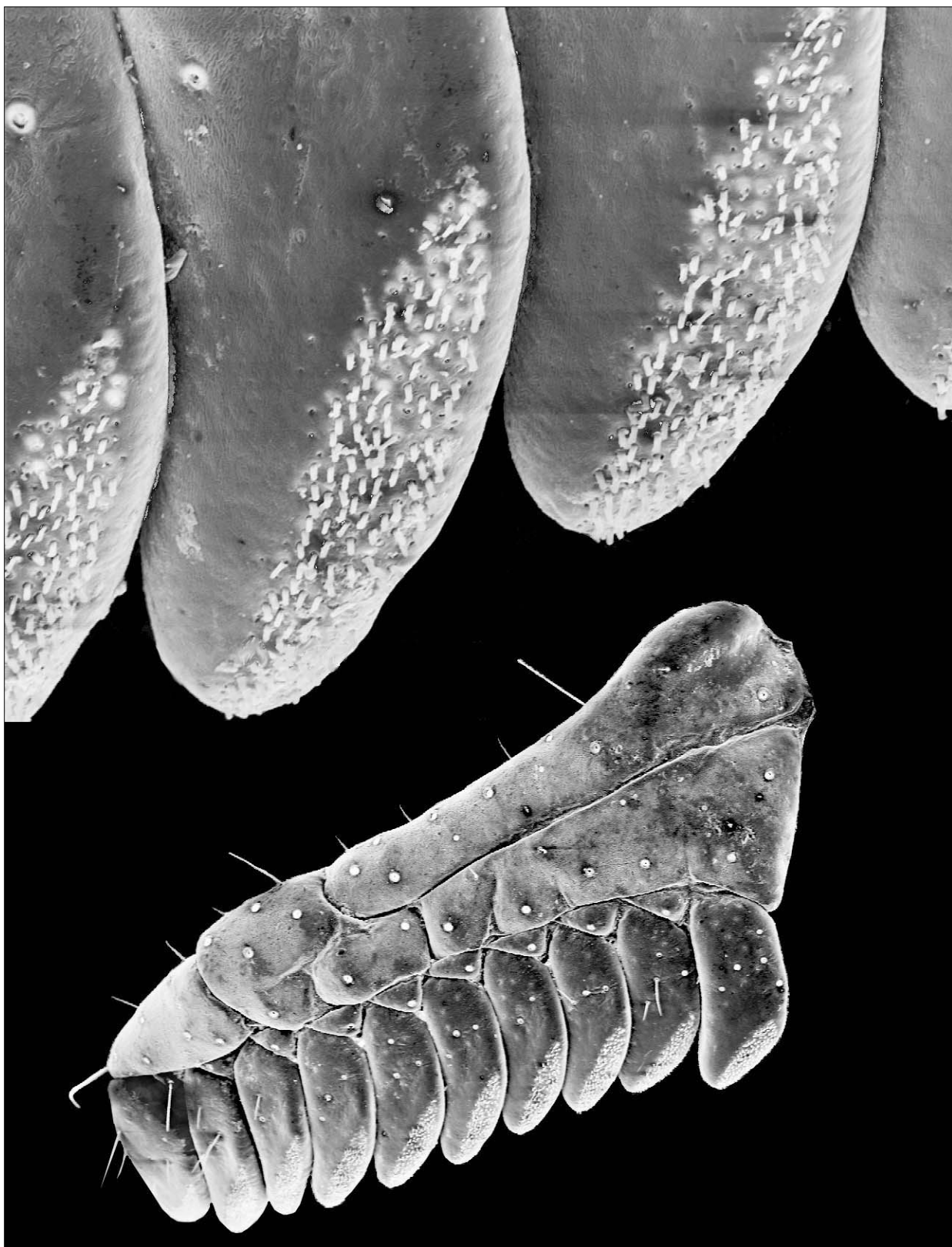


Figure 9: Pecten (35x) and close-up (75x) of peg sensilla of *Iurus dufoureius*, subadult female, Krini, Gythio, Laconia, Greece.

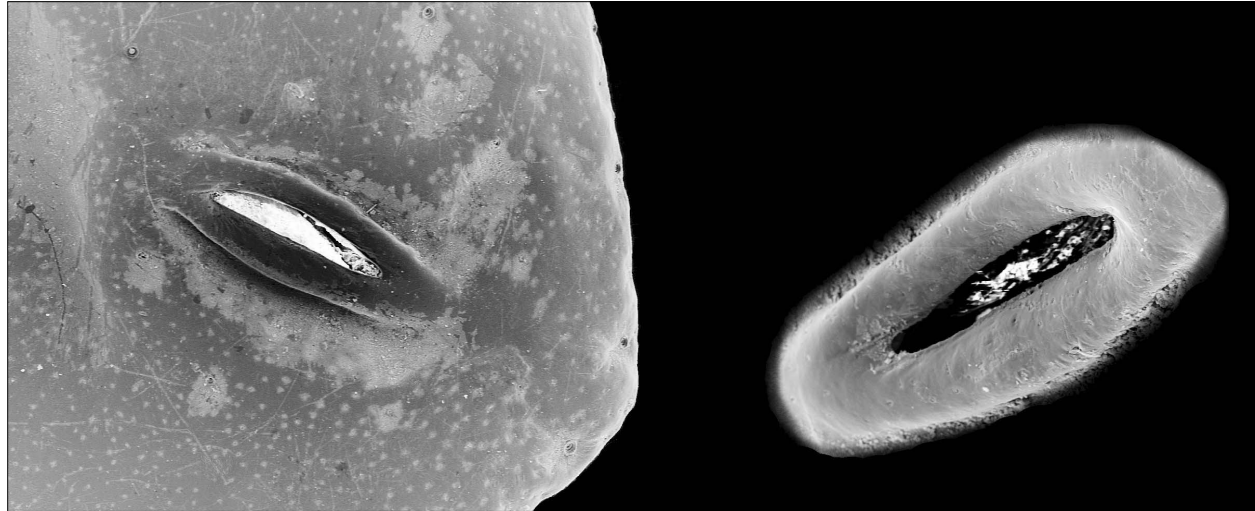


Figure 10: Stigma, *Iurus dufoureius*, subadult female, Krini, Gythio, Laconia, Greece. **Left.** Left stigma III. **Right.** Close-up of right stigma IV.

the eyes for *I. dufoureius* and *I. asiaticus* are shown in Fig. 1. The median tubercle and eyes are relatively small, with the ratio of median tubercle width / carapace width (at that point) ranging 0.134–0.164 (0.147) [5]. The median eyes are situated anteriorly with the median tubercle position / carapace length ranging 0.346–0.402 (0.375) [5].

The anterior emargination and mediolateral ocular carinae of the carapace were first defined as diagnostic of Iuridae by Fet et al. (2004: 23, figs. 53, 54) and presented as characters in their cladistic analysis of Iuroidea (Fet & Soleglad, 2008: character 23 (state=1), character 24 (state=1)) where both were synapomorphies for Iuridae.

Comparison to *Calchas*. As stated above, both *Iurus* and *Calchas* exhibit anterior emarginations and developed mediolateral ocular carinae. Both of these characters, however, are much more exaggerated in *Iurus*, whereas in *Calchas* they are less developed. Both genera have relatively small median eyes and tubercle, their width ratios essentially the same. The median eyes are situated more anteriorly in *Calchas*, with a length ratio of 0.241–0.310 (0.289) [7] (Fet, Soleglad & Kovařík, 2009: 9), exhibiting a mean value difference (MVD) of 30 %. *Iurus* has three lateral eyes per side whereas *Calchas* has only two (interestingly, at one time, this difference was used to place these two genera into separate families!).

Mesosoma

The *Iurus sternum* (Fig. 2) conforms to the type 2 sternum as defined by Soleglad & Fet (2003a). This structure is typically longer than wide (*I. dufoureius* is an exception) with a well-defined posterior emargination

forming two convexed lateral lobes. The apex is not particularly deep or offset from the lobes. The sternum tapers anteriorly. Of particular interest, a membranous plug is present between posterior region of the lateral lobes in female *Iurus*, typically vestigial or absent in the male (Figs. 3–7). The entire sternocoxal area of *I. kraepelini* is illustrated in Soleglad & Fet (2003a: fig. 8; referred to as *I. dufoureius*).

The **genital operculum** exhibits considerable sexual dimorphism in *Iurus*. In the female, the individual sclerites are much wider than long and are fused medially most of their length (all five species are illustrated in Figs. 3–7, and all five species, male and female, are illustrated under the individual species descriptions). In the male, each sclerite is subtriangular in shape, roughly as long or longer than wide, and the sclerites are separated most of their length. In addition, in the male, well-developed **genital papillae** (Fig. 2) are visible between the two plates, but not extending posteriad of the operculum. Fet & Soleglad (2008: character 10 (state=0)) hypothesized this genital papillae configuration (as found in *Iurus*) as symplesiomorphic for family Iuridae; i.e. the same configuration as in the outgroup *Chaerilus* (parvorder Chaerilida).

The **pectines** in *Iurus* are fully developed, exhibiting all major substructures common to most scorpions (Figs. 8, 9). Three anterior lamellae are present, the most basal one significantly longer than the middle and distal lamellae. Middle lamellae, if present, are marginally formed. Well-developed fulcra are present between the inner bases of pectinal teeth. The pectinal teeth are well-developed in *Iurus*, exhibiting well-defined sensorial areas on their inner distal edges. The sensorial areas are densely populated with peg sensilla, which are shaped as uniform, elongated cylin-

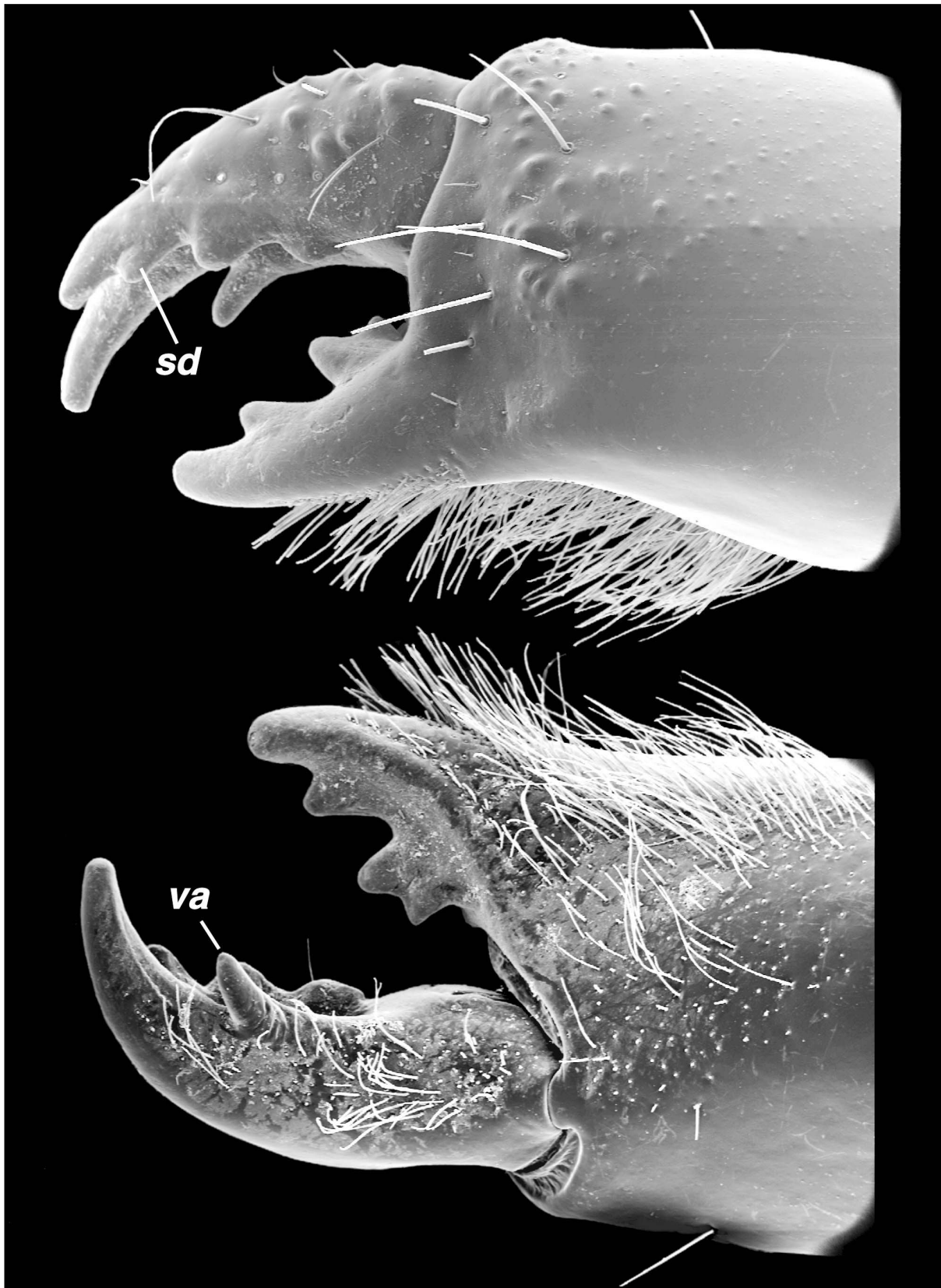


Figure 11: Chelicera (35x), *Iurus dufoureius*, subadult female, Krini, Gythio, Laconia, Greece. Dorsal view (top, left chelicera reversed), ventral view (bottom, right chelicera). Diagnostic large midfinger placed ventral accessory (va) denticle and large single subdistal (sd) denticle indicated.

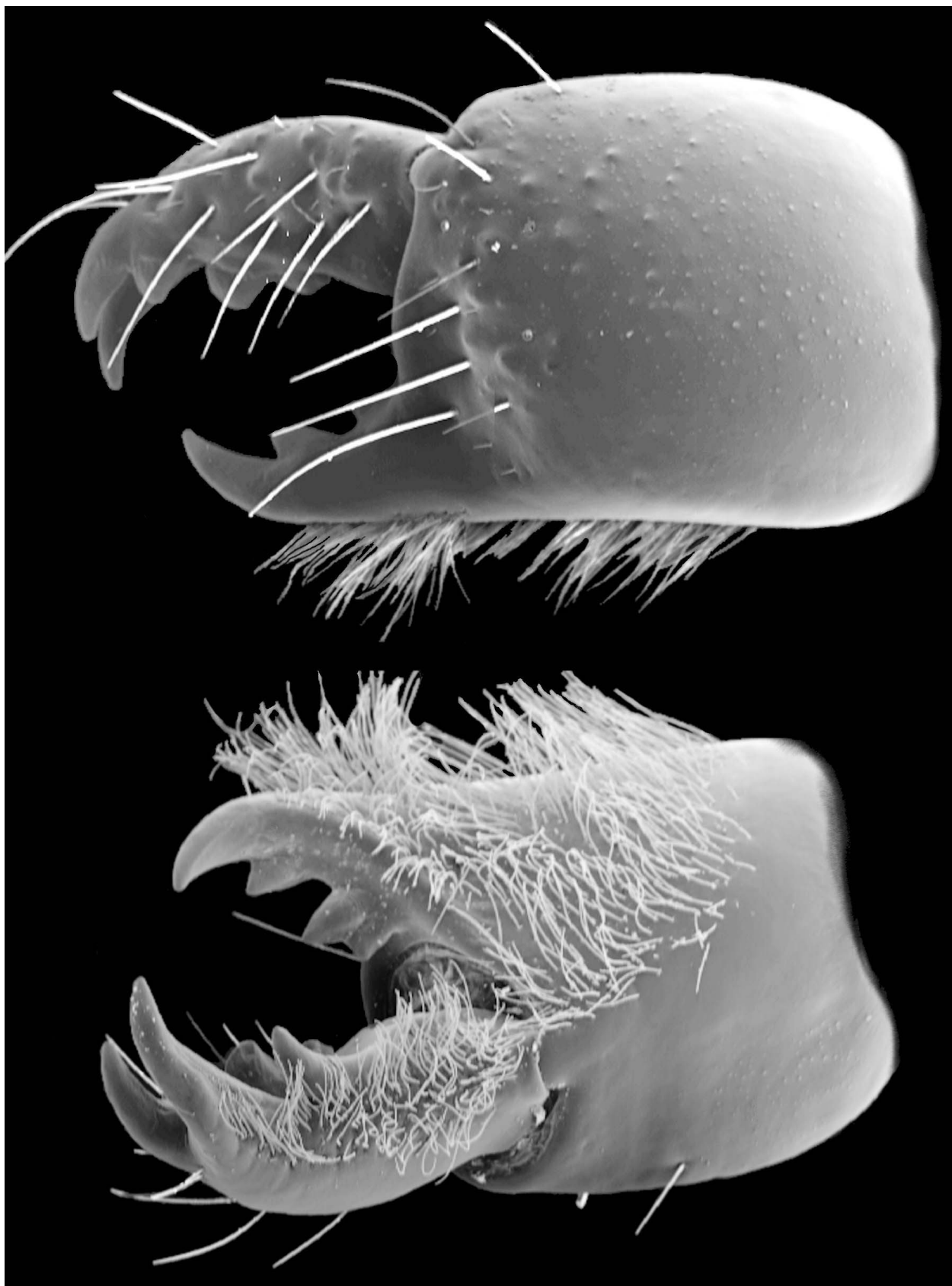


Figure 12: Chelicera (35x), *Iurus kraepelini*, juvenile male, Akseki, Antalya, Turkey. Dorsal view (top, left chelicera reversed), ventral view (bottom, right chelicera).

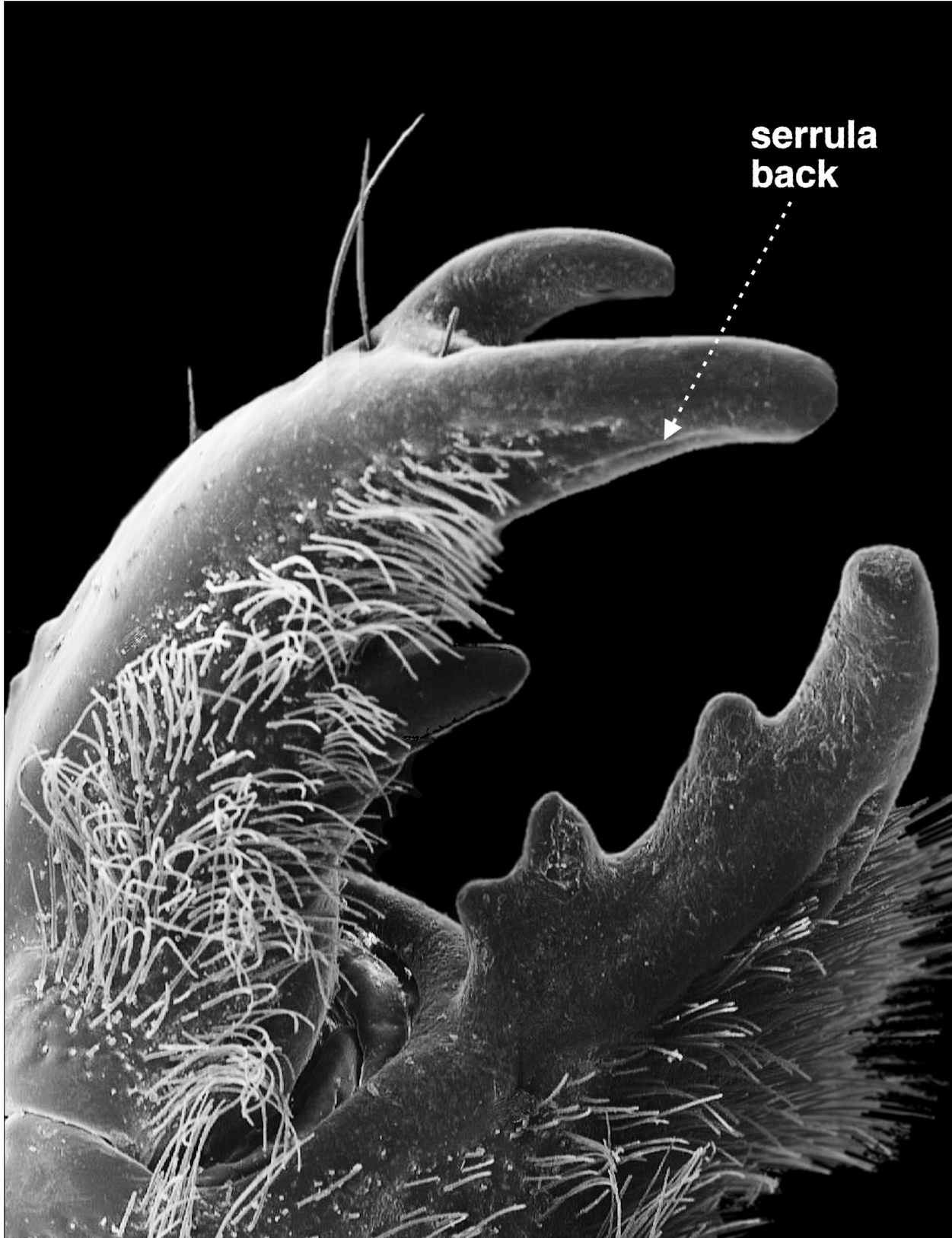


Figure 13: Right chelicera (35x), ventral view, of *Iurus kinzelbachi*, adult male, Dilek Peninsula, Aydin, Turkey. Note that serrula is not present, only the *back* (indicated).

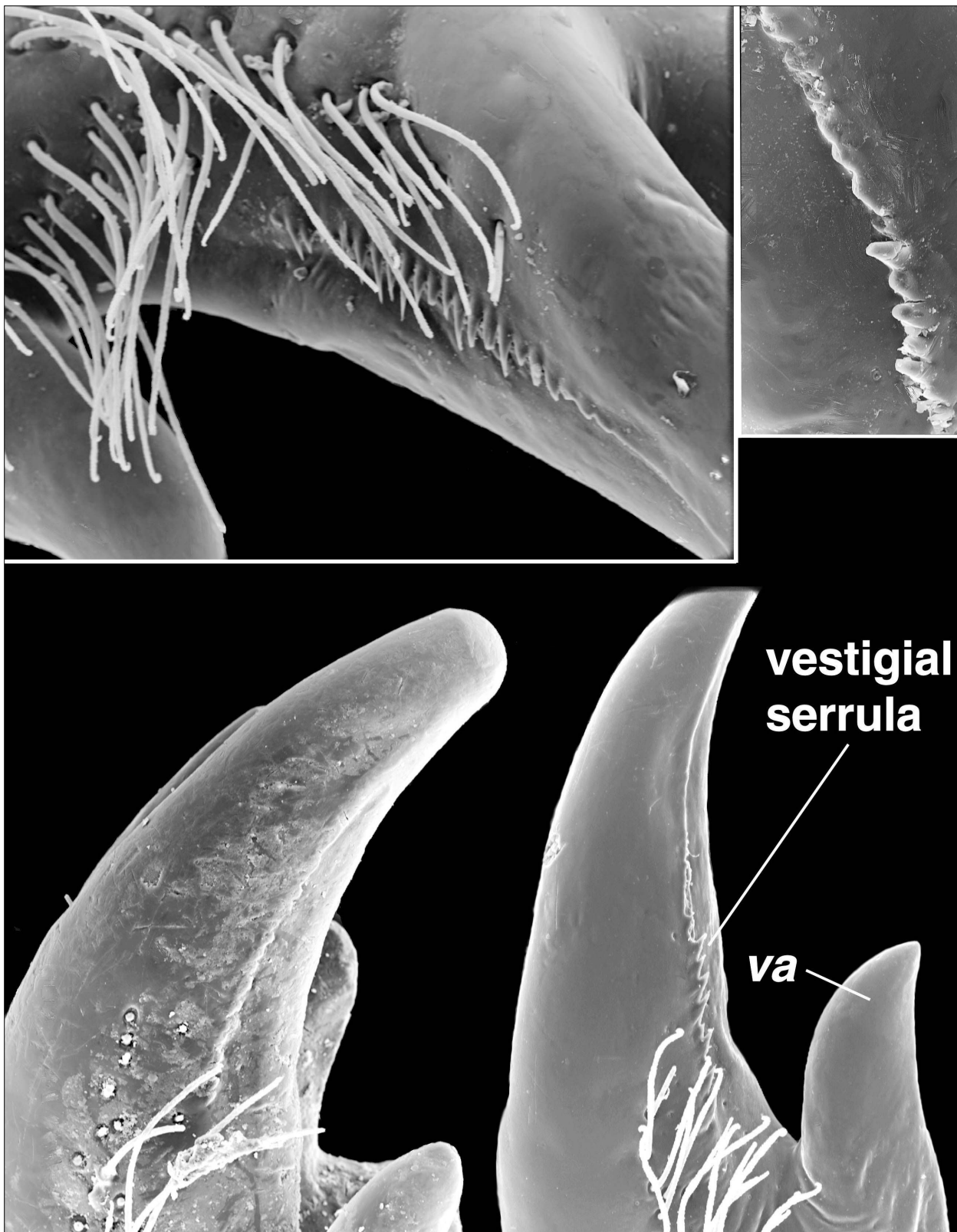


Figure 14: Cheliceral movable finger, ventral view, showing vestigial development of serrula in *Iurus*. **Top Left.** *I. kraepelini*, juvenile male (150x), Akseki, Antalya, Turkey. **Top Right.** *I. asiaticus*, adult female (200x), 4 km east of Kaşlıca Village, Adiyaman, Turkey. **Bottom Left.** *I. dufoureius*, subadult female (150x), Krini, Gythio, Laconia, Greece, showing worn vestigial serrula. **Bottom Right.** *I. dufoureius*, subadult female (150x), Mystras, Laconia, Greece, with vestigial serrula and conspicuous large ventral accessory denticle (va) indicated.

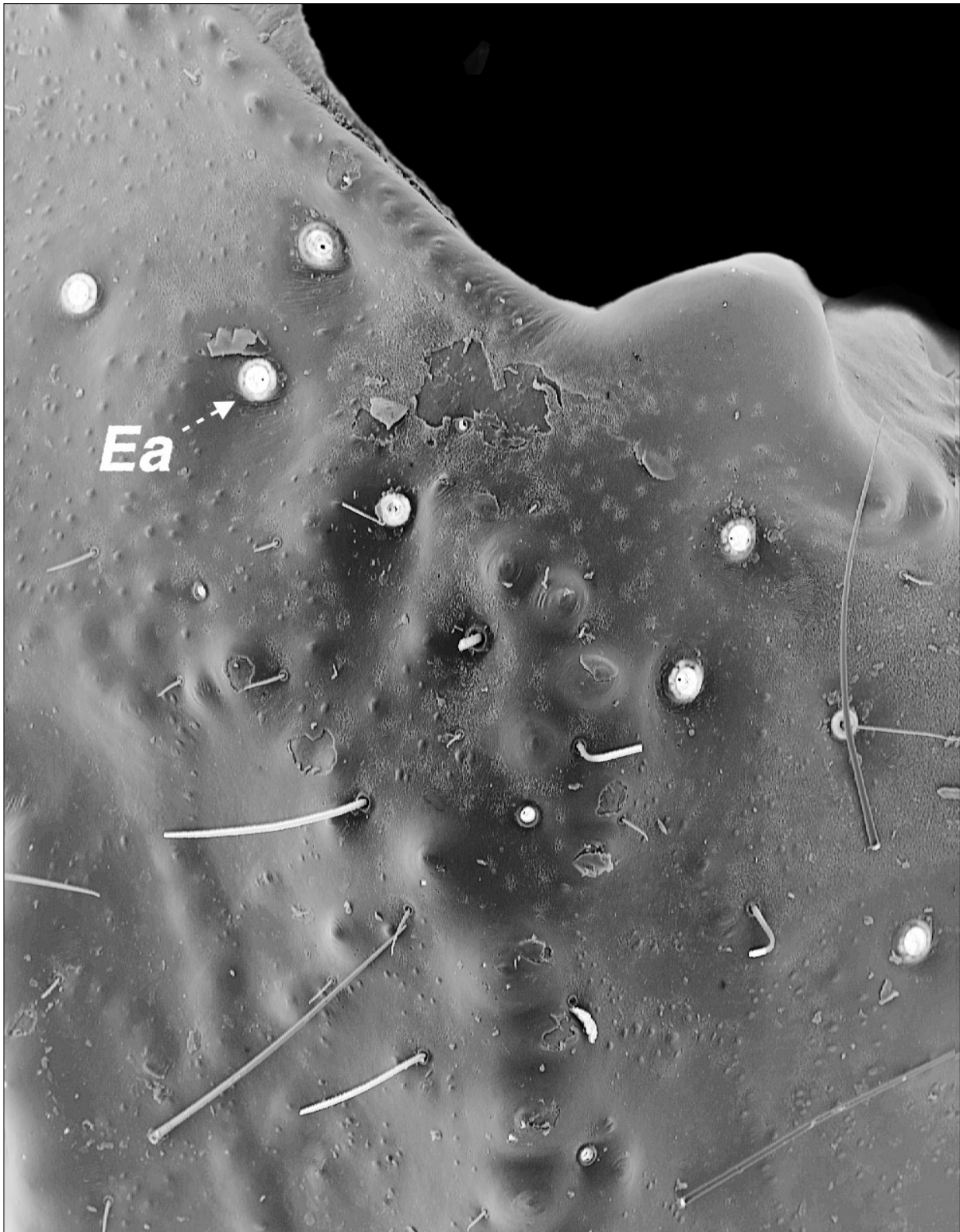


Figure 15: Distal external view of right chelal palm (35x) of *Iurus kraepelini*, juvenile male, Akseki, Antalya, Turkey, showing neobothriotaxy. Trichobothrial series Et_1 – Et_5 , Est , and Dt are shown as well as the solitary accessory trichobothrium, Ea , which is indicated. Note that trichobothria Et_3 and Est are petite, the latter unique to family Iuridae.

ders (see close-up in Figs. 8, 9). The pectinal **basal piece** is well-developed in *Iurus*, longer than the genital operculum in the female. Its anterior edge exhibits a somewhat narrow and shallow emargination.

The lung **stigmata** (spiracles) in *Iurus* are somewhat large, slit-like in shape (Fig. 10). They are angled roughly 45° toward anterointernal direction. The fine structure of the posterior spiracle margin (Kamenz, Dunlop & Scholtz, 2005) can be seen in Fig. 10. The stigmata of all five species are illustrated in the individual species descriptions.

Comparison to *Calchas*. *Iurus* differs from *Calchas* in the following. The sternum membranous plug exhibited in *Iurus* females is considerably reduced in *Calchas*; the sternum is wider than long in *Calchas*, whereas in *Iurus* it is noticeably longer than wide in both genders (*I. dufoureius* an exception). The unique prepectinal plate conspicuous in *Calchas* females is absent in *Iurus*. The anterior emargination on pectinal basal piece in *Calchas* is generally well-developed and somewhat wide, whereas in *Iurus* it is subtle and narrow. The stigmata in *Iurus* are large, elongated and slit-like in shape, whereas in *Calchas* they are small and sub-oval.

Chelicerae

In Figures 11–12, the dorsal and ventral aspects of the *Iurus* chelicera are illustrated for *I. dufoureius* and *I. kraepelini*. This chelicera conforms to the definitive form as described for superfamily Iuroidea: ventral edge equipped with a large denticle (*va*), hypothesized as synapomorphic by Soleglad & Fet (2003b; character 42, state=2) and Fet & Soleglad (2008; character 9, state=1). The dorsal edge has a single large subdistal (*sd*) denticle, classified as symplesiomorphic (Soleglad & Fet, 2001; Fet & Soleglad, 2008). In addition, a characteristic of the chelicerae specific to *Iurus* within the Iuridae is the midfinger position of the large ventral denticle on the ventral edge (in *Calchas*, it is located basally). Weak to vestigial **serrula** is present on the ventral edge of the movable finger (Figs. 13–14), composed of at most 12–14 irregularly developed tines in juveniles and small subadults. In adults, serrula presence is dependent on the wear of the chelicerae. For example, in the adult *I. kinzelbachi*, sp. nov. shown in Fig. 13 only the serrula back is visible, whereas in the adult *I. asiaticus* (Fig. 14), some well defined tines are still present. Serrula in *Iurus* was first mentioned by Francke & Soleglad (1981: fig. 19). See Graham & Fet (2006: 7) for the review of serrula observations; note that fig. 2 in Graham & Fet (2006) was quoted erroneously as a serrula of a juvenile *Iurus dufoureius* from Crete; it in fact belongs to *Calchas gruberi* from Megisti.

The cheliceral fixed finger is typical of Recent scorpions, with four denticles, median (*m*) and basal (*b*)

denticles conjoined on common trunk. Ventral accessory (*va*) denticles are not present.

The ventral surface of the cheliceral palm is covered with a heavy growth of setae (Figs. 11–13) extending along the ventral edge of the movable finger and the inner surface of the fixed finger where it is the heaviest.

Comparison to *Calchas*. The chelicera of *Iurus* differs from that of *Calchas* as follows. The *va* denticle of the movable finger ventral edge is much larger in *Iurus* and is located midfinger whereas in *Calchas* it is located basally on the finger. The ventral distal denticle (*dd*) in *Iurus* does not extend beyond its dorsal counterpart as much as in *Calchas*, where the dorsal *dd* is much shorter than the ventral *dd*. The serrula in *Calchas* is well-developed, in adults as well as in juveniles, whereas in *Iurus* it is only vestigial in juveniles and small subadults, and essentially absent in adults.

Pedipalps

The **trichobothrial pattern** of *Iurus* was illustrated and discussed in detail by Soleglad, Kovařík & Fet (2009: fig. 2) where it was contrasted with its sister genus *Calchas*. Therefore, we will not discuss it here in any detail except to note that the full trichobothrial patterns of the five species of *Iurus* are illustrated in this paper under their individual discussions below (Figs. 86, 119, 120, 158, 191, and 211). We will point out, however, that although a very unusual pattern in itself, representative of the family Iuridae, the pattern seen in *Iurus* does exhibit significant differences in individual trichobothrial positions from that found in *Calchas*, involving the femur, patella, and chela. At the species level, however, we did not uncover any significant positional differences in trichobothria deemed diagnostic between the five species of *Iurus*. Neobothriotaxy was detected in genus *Iurus*, spanning four of the five species recognized in this paper. These occurrences of neobothriotaxy, organized into 13 unique types across four species, were considerably rare in two of the species, *I. dufoureius* and *I. asiaticus*, common but occurring erratically in *I. kraepelini*, and diagnostic for *I. kinzelbachi*, sp. nov. In our Fig. 15, we illustrate a single accessory trichobothrium (*Ea*) in the *Et* series in *I. kraepelini*. Neobothriotaxy is discussed in detail in Appendix B.

The **dorsal patellar and ventral patellar spurs (DPS/VPS)** were illustrated by Soleglad & Fet (2003b: fig. 96) for *Calchas*, with a detailed analysis of these structures. In our Figs. 16–17 we show significantly developed DPS/VPS for *I. dufoureius* and *I. kraepelini*, illustrating two large spurs both dorsally and ventrally. In the femoral view of these spurs, shown in Fig. 17, their size and development are emphasized. We refer to these as “doubled” DPS/VPS. Accompanying the two spur sets is a large seta, represented in our figures only

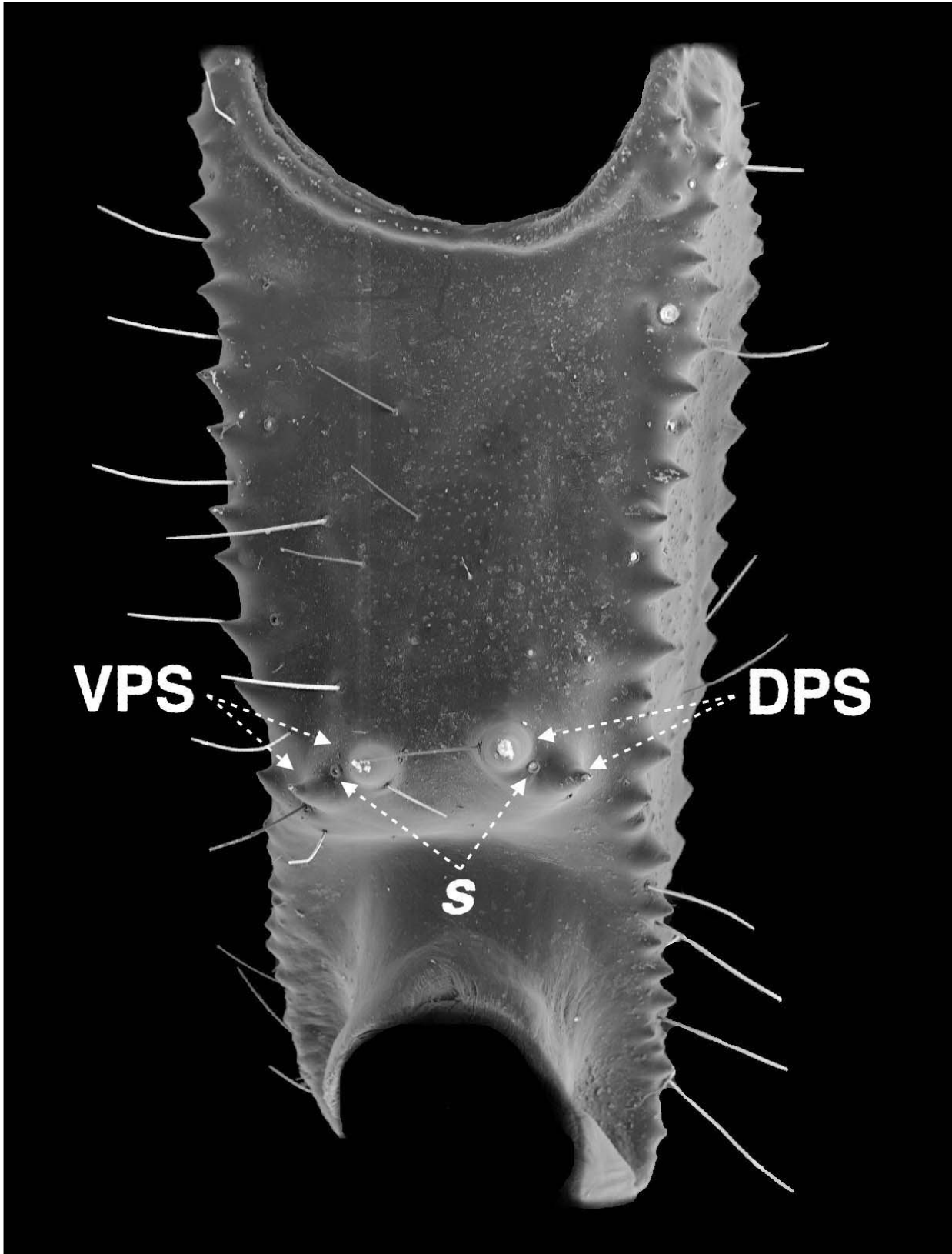


Figure 16: Pedipalp patella, internal view (15x), *Iurus kraepelini*, juvenile male, Akseki, Antalya, Turkey. Note well developed doubled Dorsal (DPS) and Ventral (VPS) Patellar Spurs. *s* = seta areolae.

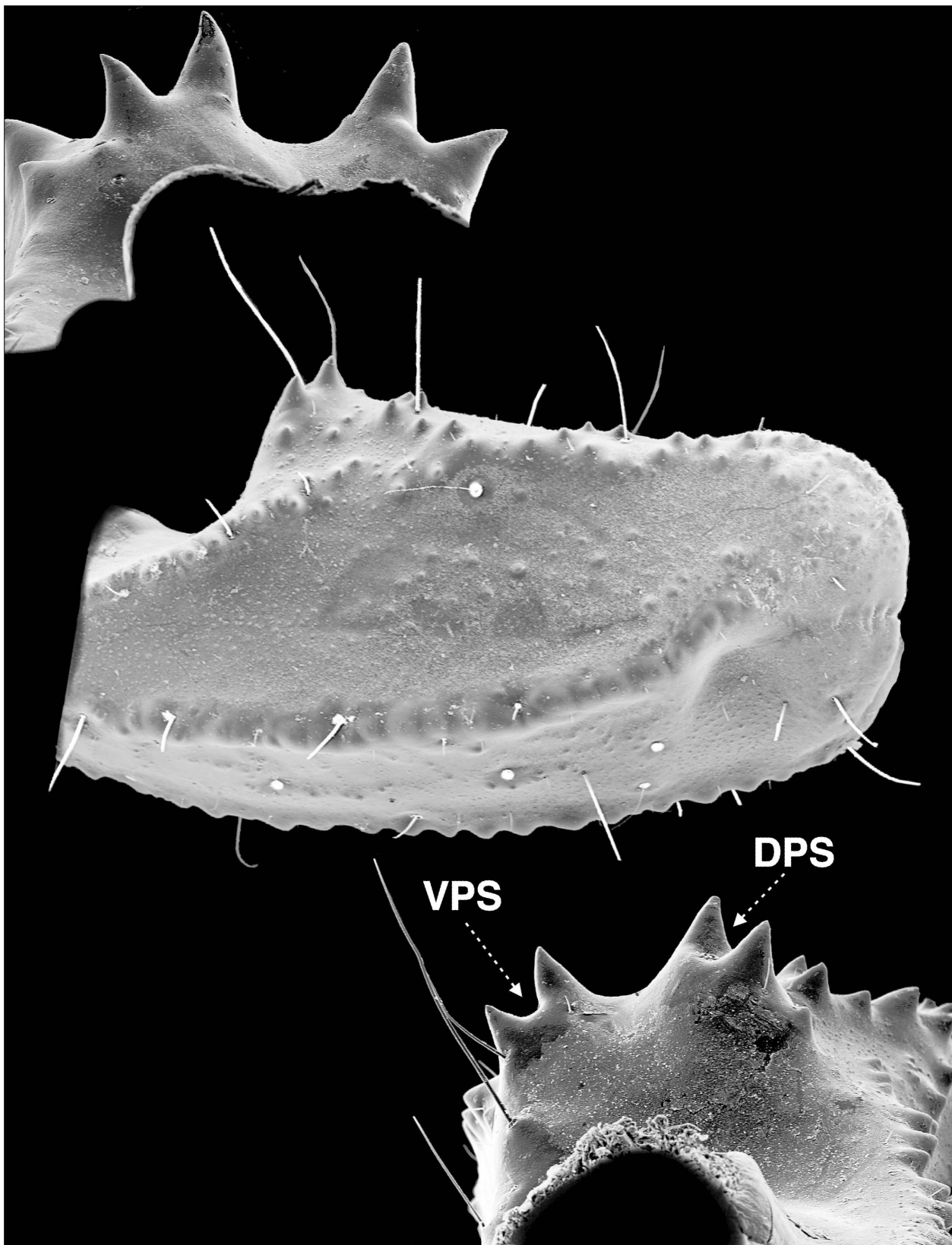


Figure 17: Doubled Dorsal (DPS) and Ventral (VPS) Patellar Spurs. **Top.** Femoral (50x) views, *Iurus kraepelini*, juvenile male, Akseki, Antalya, Turkey. **Middle & Bottom.** Dorsal (15x) and femoral (50x) views *I. dufourieus*, subadult female, Krini, Gythio, Laconia, Greece.

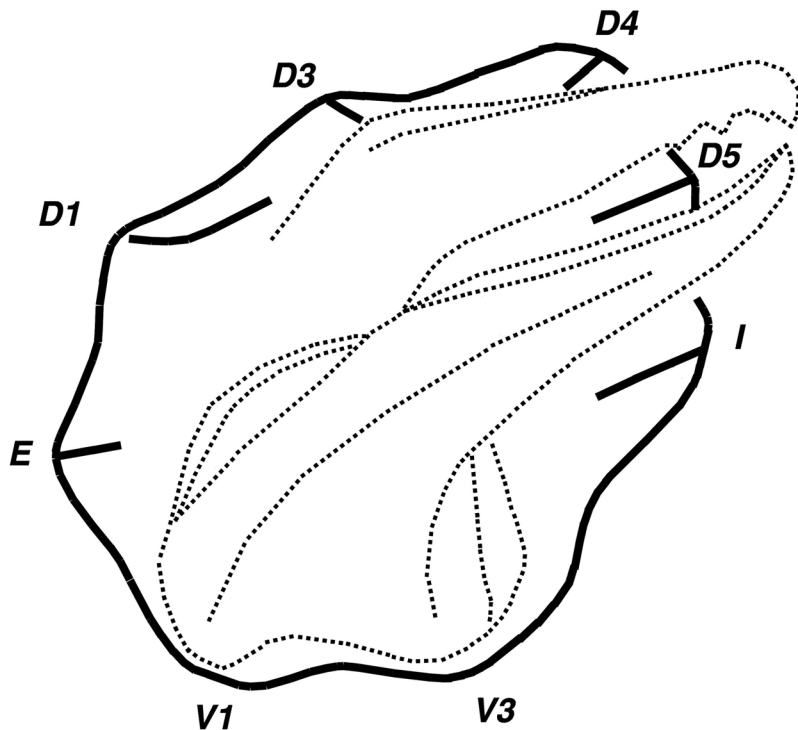


Figure 18: Diagrammatic view of pedipalp chela from the finger's perspective showing the eight primary carinae in genus *Iurus*. This carinal arrangement complies to the “8-carinae” configuration, note the absence of the *V2* (ventromedian) and *D2* (subdigital) carinae. Dotted portions indicate fixed and movable fingers and socket areas. *D1* = digital carina, *D3* = dorsosecondary carina; *D4* = dorsomarginal carina, *D5* = dorsointernal carina, *V1* = ventroexternal carina, *V3* = ventrointernal carina, *E* = external carina, *I* = internal carina.

as enlarged areola (Fig. 16). There is no evidence of the DPSc or VPSc carinae in *Iurus*.

The **chelal carinae** configuration in *Iurus* complies with the “eight-carinae” configuration as identified in Soleglad & Sissom (2001: 41–44; figs. 43–72). As illustrated in our Figure 18, which shows a diagrammatic view of the chela from the fingers, this configuration excludes the ventromedian (*V2*) and subdigital (*D2*) carinae. Soleglad & Sissom (2001: character 20, state=0) characterized genus *Iurus* as conforming to this carinal configuration. Fet & Soleglad (2008: character 6, state=0) showed that this configuration, as reflected in family Iuridae, is symplesiomorphic, being present in other presumably more primitive parvorders, whereas in family Caraboctonidae the “ten-carinae” configuration is present, a demonstrated synapomorphy (state=1).

The **chelal finger dentition** is very distinctive in *Iurus* and is used, in part, to separate its species. The fixed and movable finger dentition is shown in Figs. 19–20 for *I. kraepelini* and *I. dufoureius*. Common to all *Iurus* species, and considered a symplesiomorphy for superfamily Iuroidea, are the oblique highly imbricated median denticle (*MD*) groups, occurring in the three other parvorders, Pseudochactida, Buthida, and Chaerilida. Interestingly, the *MD* denticle groups in sister family Caraboctonidae, though oblique, are not imbricating, which is considered a synapomorphy by Fet & Soleglad (2008: character 5, state=1). The distribution of inner (*ID*) and outer (*OD*) denticles is presented on Fig. 19. As common to most scorpions, two *ID*s are grouped

at the movable finger distal tip close to the distal denticle (*DD*), the remaining *IDs* are positioned at the beginning of *MD* groups distally and moving slightly more proximally in basal groups. The last two to four *MD* groups in either finger are not accompanied by an *ID* (species dependent). All *MD* denticle groups terminate with a slightly enlarged *OD* denticle, except for the basal *MD* group which terminates with increasingly smaller *MD* denticles. The most distal *MD* denticle group is much shorter on the movable finger, exhibiting roughly half the number of denticles than found on the fixed finger. This overall *MD*, *ID* and *OD* distribution is found in all five *Iurus* species, only the number of *ID* and *MD* denticle groups is species-specific, as described in detail below under species descriptions.

Fet et al. (2006) first reported the occurrence of a very unique array of minute sensilla located on the extreme distal external tip of the chelal fixed finger, termed the **constellation array**. Based on current surveys, this array is assumed to be present in one form or another in all Recent scorpions, Fet et al. (2006) having examined all four parvorders and six superfamilies. We have investigated the constellation array in all five *Iurus* species (Figs. 21–25). Interestingly, we find that each species has a different number of sensilla, ranging from two to nine, implying that this array is species-specific. In *I. asiaticus*, we detected variability, with the number of sensilla from two to four (based on two specimens).

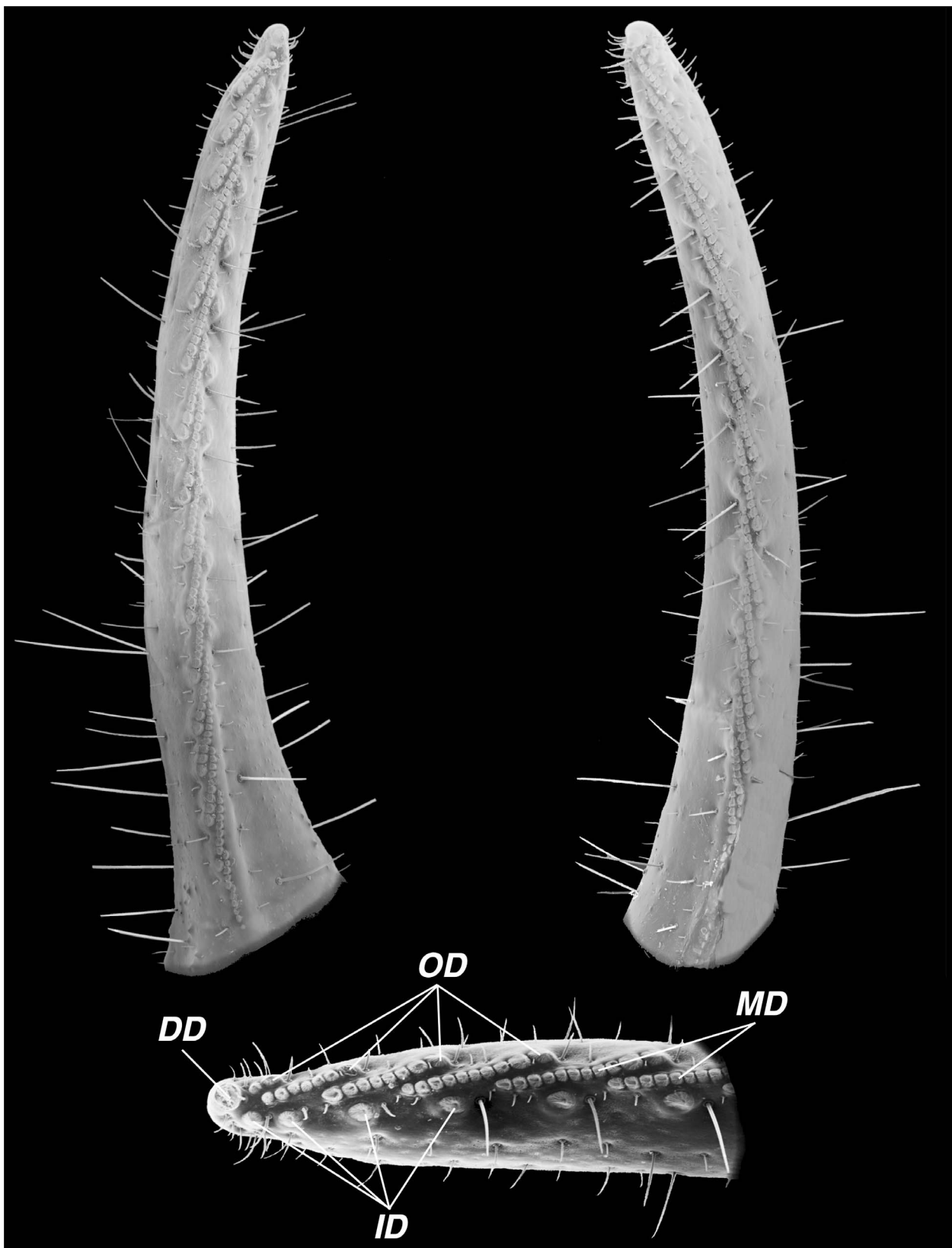


Figure 19: Right chelal finger dentition (fixed left, movable right, 35x), *Iurus kraepelini*, juvenile male, Akseki, Antalya, Turkey. Note that the median denticle (MD) groups are oblique and *highly imbricated*. Bottom figure shows close-up of a movable finger distal aspect with distal denticle (DD), median denticles (MD), outer denticles (OD), and inner denticles (ID) identified (350x).



Figure 20: Right chelal finger dentition (fixed left, movable right), *Iurus dufoureius*, subadult female, Krini, Gythio, Laconia, Greece. Note movable finger is equipped with 16 inner denticles (*ID*), the largest number encountered in *Iurus* (35x).

Comparison to *Calchas*. The trichobothrial pattern in *Iurus* differs from *Calchas* as follows. Femoral trichobothrium *d* is located on the external surface (not dorsal); *e* located slightly distally of *d* (not significantly distally); chelal trichobothrium *db* is positioned at fixed finger midpoint (not basally); *Db* is located ventrally of external (*E*) carina, in line with *Eb* series (not dorsally of *E* and distally of *Eb* series); patellar trichobothrium *i* is located on the internal surface, adjacent to *DI* carina (not on dorsal surface). The doubled DPS/VPS are signif-

icantly developed in *Iurus*, whereas in *Calchas* they are weakly developed. Both genera comply with the “eight-carinae” configuration, but the palm is more vaulted in *Iurus*, and the vertical distance between carinae *D4* and *V3* is greater than the distance between carinae *E* and *I*. In *Calchas*, where palm is not vaulted and somewhat flat, the distance between *D4* and *V3* is less than that between *E* and *I*. In *Iurus*, the chelal finger *MD* rows are highly imbricated and number 14 to 16 on the movable finger, whereas in *Calchas* the *MD* rows are slightly

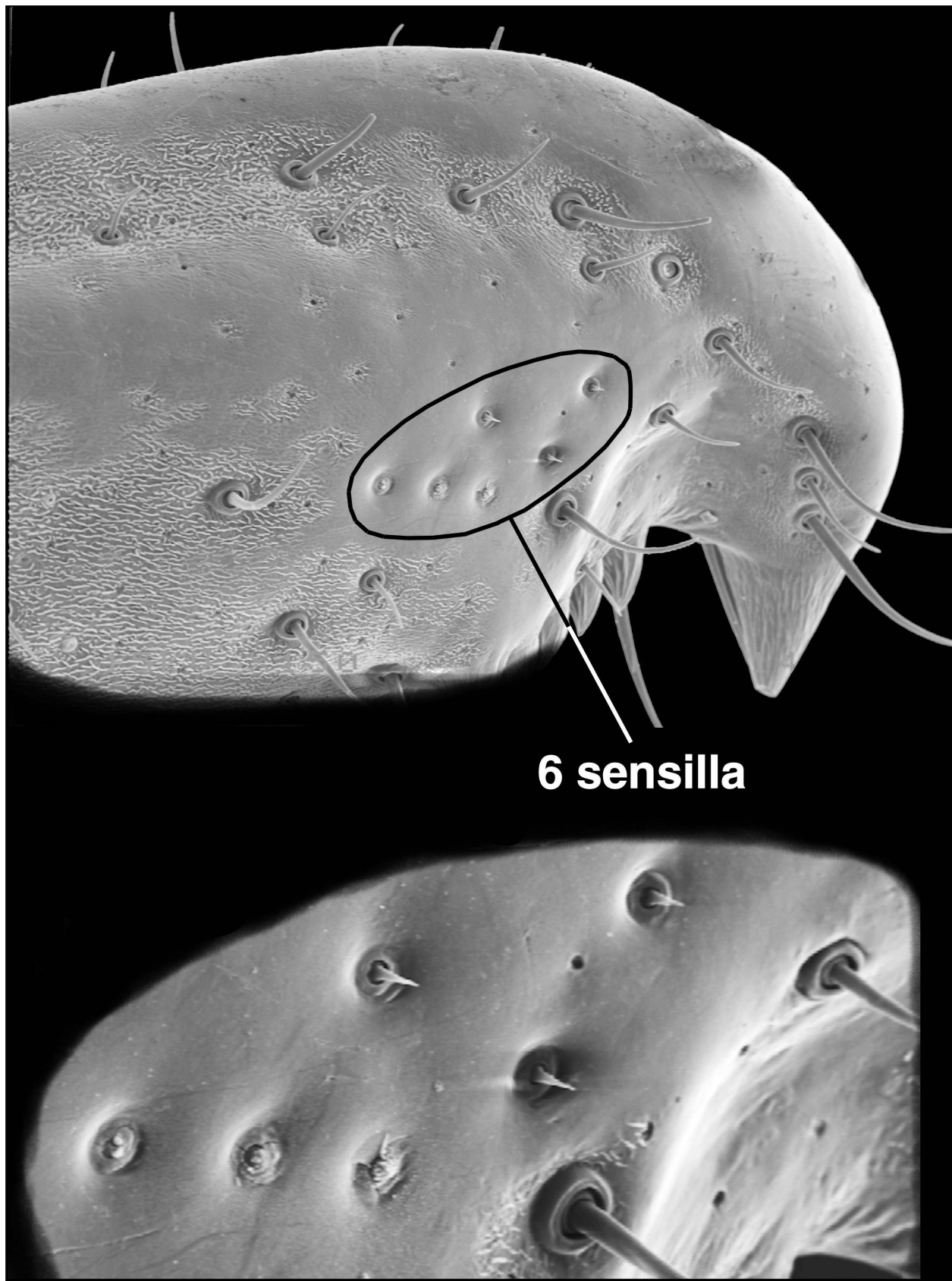


Figure 21: Constellation array in *Iurus dusourei* showing six sensilla, subadult female, Mystras, Laconia, Greece. **Top.** Distal tip of pedipalp fixed finger showing orientation of sensilla (200x). **Bottom.** Close-up of sensilla.

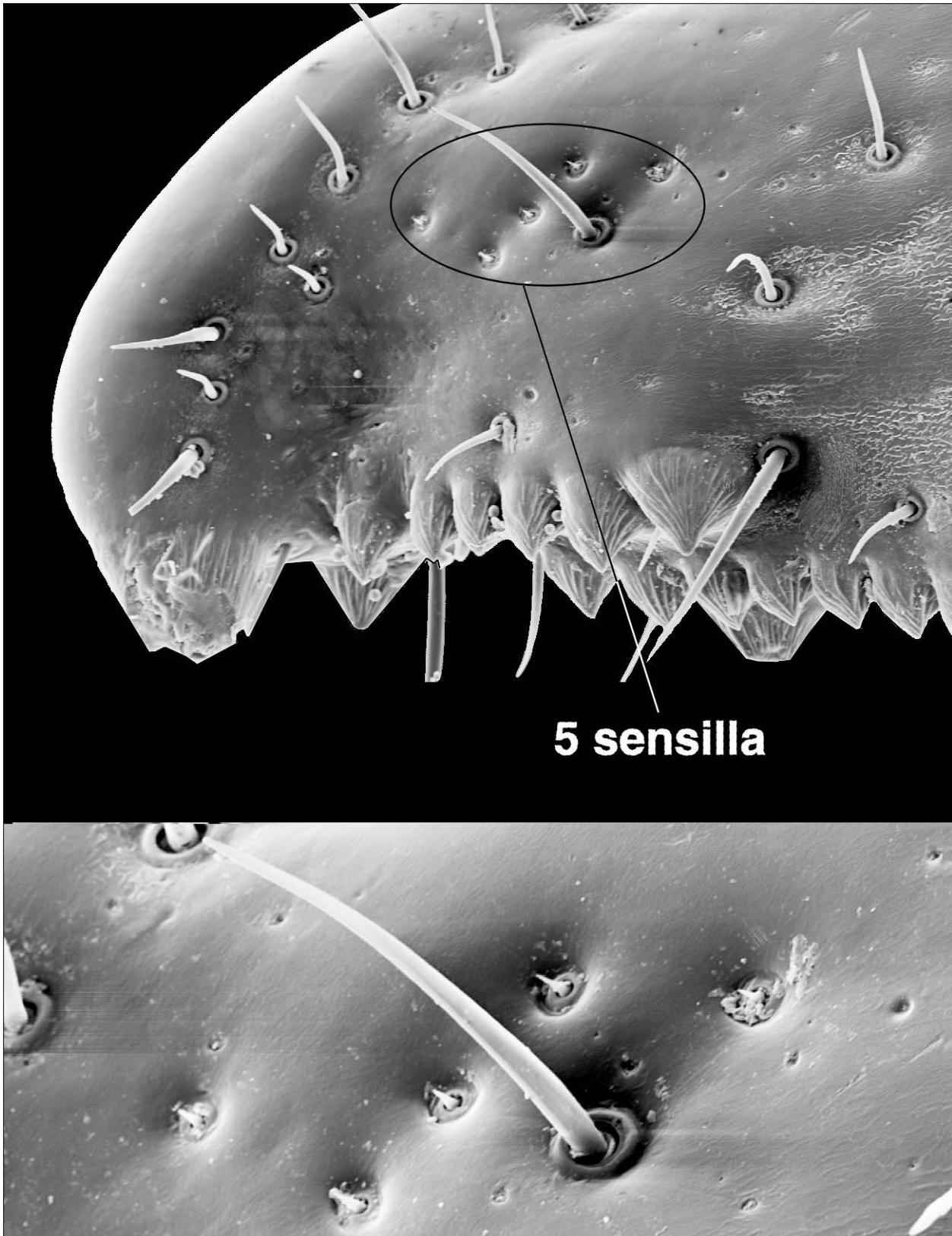


Figure 22: Constellation array in *Iurus kraepelini*, showing five sensilla, male, Akseki, Antalya, Turkey. **Top.** Distal tip of pedipalp fixed finger showing orientation of sensilla (150x). **Bottom.** Close-up of sensilla (350x).

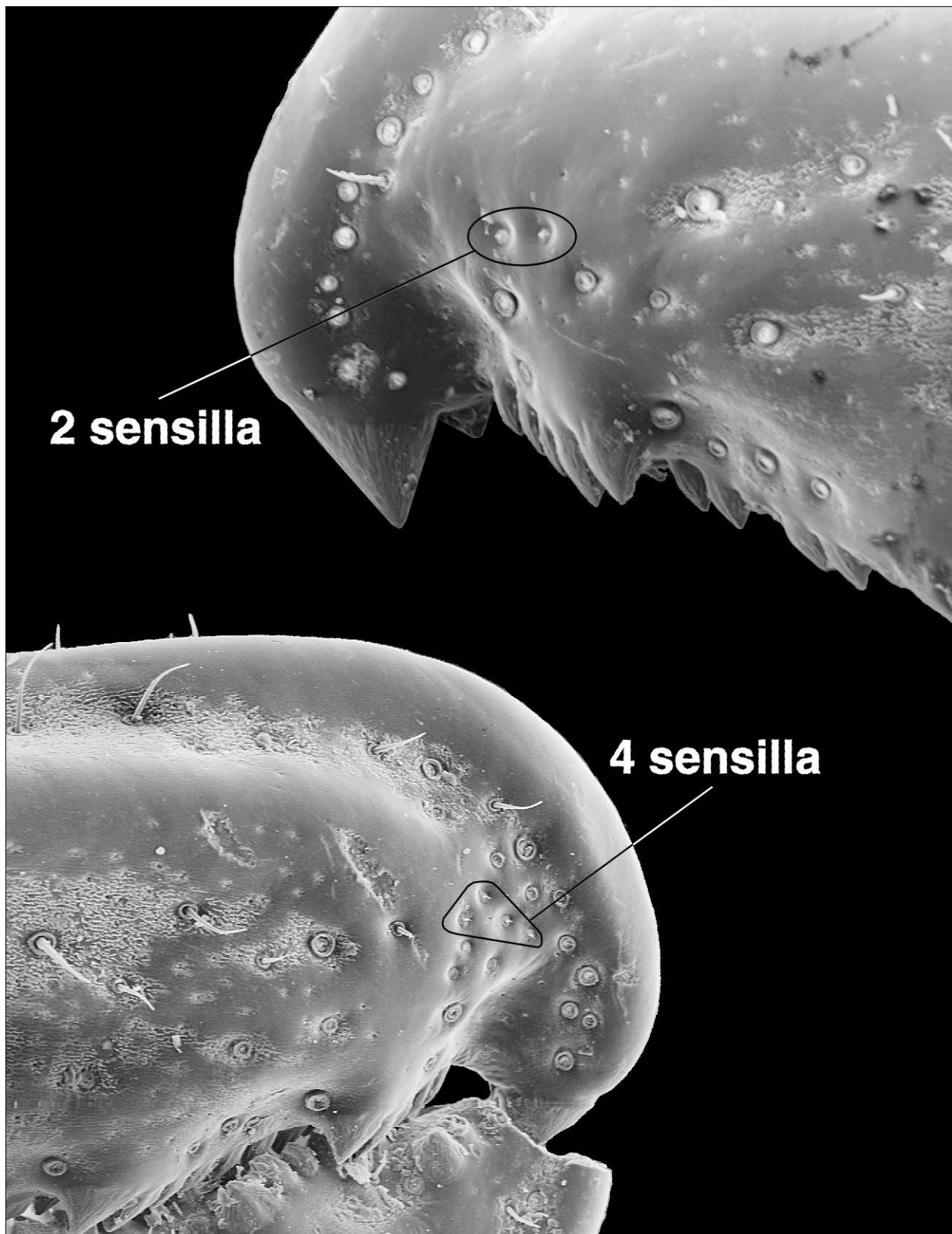


Figure 23: Constellation array in *Iurus asiaticus*, showing two to four sensilla, female, Kaşlica, Adiyaman, Turkey. **Top.** Distal tip of left pedipalp fixed finger showing two sensilla (50x). **Bottom.** Right fixed finger showing four sensilla (75x).

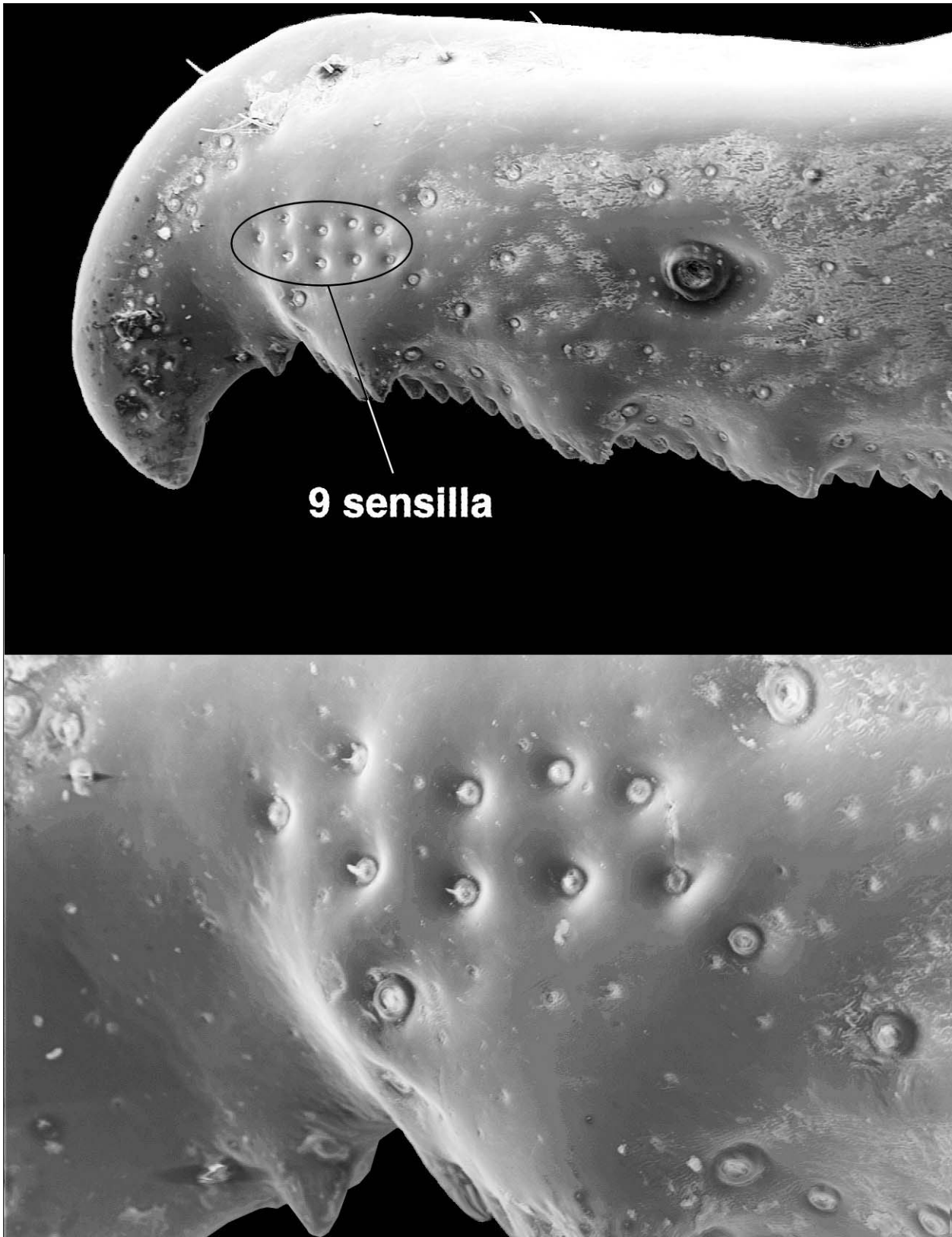


Figure 24: Constellation array in *Iurus kadleci*, sp. nov., showing nine sensilla, male, Akseki, Antalya, Turkey. **Top.** Distal tip of pedipalp fixed finger showing orientation of sensilla (50x). **Bottom.** Close-up of sensilla (150x).

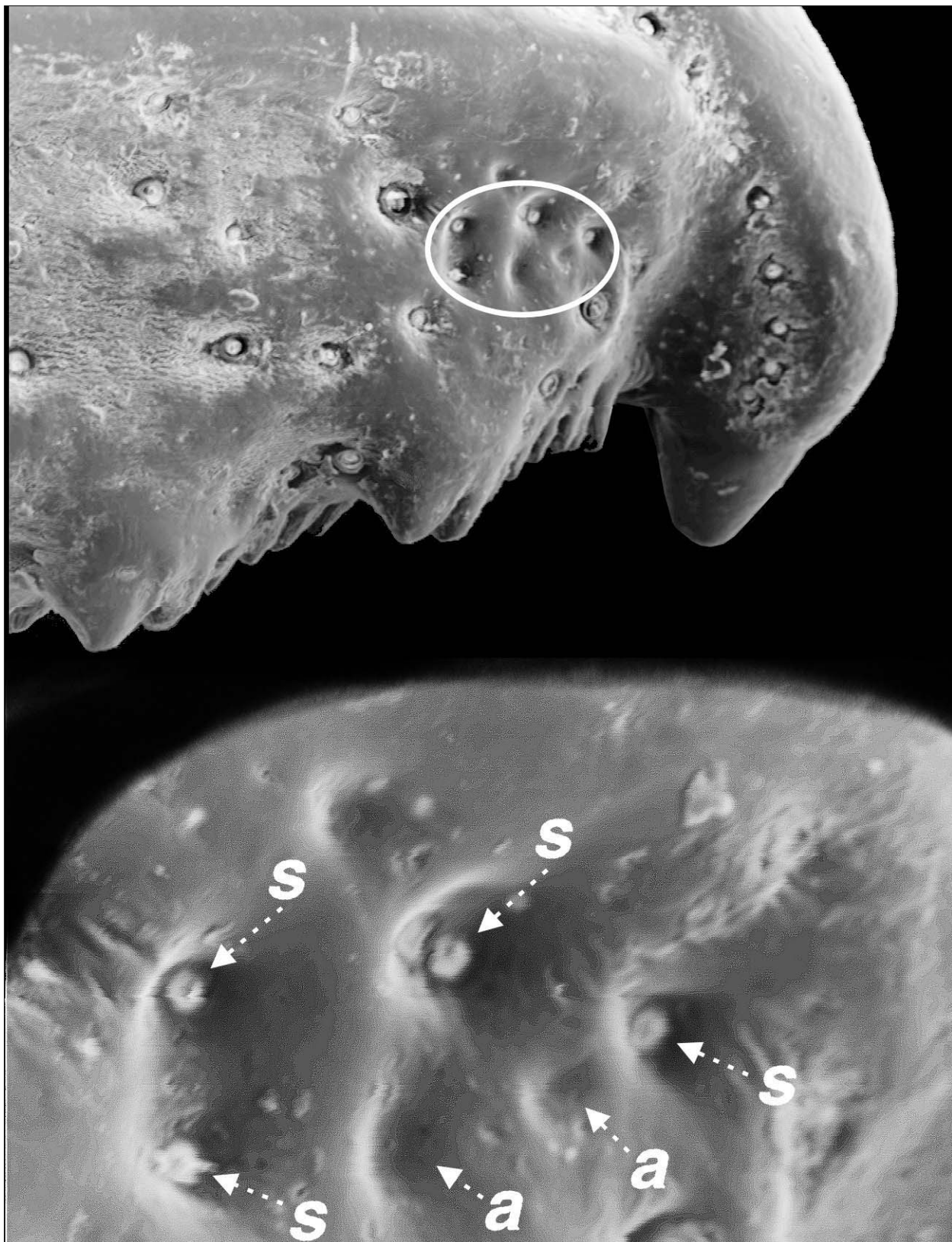


Figure 25: Constellation array in *Iurus kinzelbachi*, sp. nov., showing six sensilla, subadult female, Dilek Peninsula, Aydin, Turkey. **Top.** Distal tip of pedipalp fixed finger showing orientation of sensilla (100x). **Bottom.** Close-up of sensilla (350x). Note two sensilla lack a seta and the areolae are partially formed. *s* = sensilla, *a* = areolae.

imbricated and number 7 to 8. In both genera, the number of constellation array sensilla are species-specific (of eight total species of Iuridae this character is unknown only for *C. nordmanni*).

Legs

Iurus has a pair of **pedal** (tarsal) **spurs** located on the ventral surface at the juncture of the basitarsus and tarsus (Figs. 26, 28). These spurs are typical for Recent scorpions; they are smooth, neither exhibiting spinelets as in *Hadrurus* and *Hoffmannihadrurus* (family Caraboctonidae), nor showing morphometric differences between the spurs as seen in some environmentally adapted scorpions such as psammophiles. The **tibial spur** found in *Calchas* is not present in *Iurus*.

Fet et al. (2004) presented a detailed analysis of the iuroid leg tarsus. In this important study, it was shown that all six iuroid genera had some form of **spinule clusters** on the ventral surface of the **leg tarsus**. The variety and overall manifestation of this spination, however, is considerable across the six genera. In *Iurus*, the individual spinules are exceptionally small and form actual clusters ("tufts") of dense spinules in a medial line along the tarsus, terminating in a pair of enlarged clusters (Figs. 27, 29–31). These clusters are significantly developed in adults, with individual spinule counts exceeding 200 (Fet et al., 2004: tab. I), whereas in juveniles individual spinule clusters may exhibit as few as 3 or 4 spinules (Fig. 31). The leg **basitarsus** also has spinule clusters in two elongated rows on the ventral surface (Fig. 28).

Soleglad & Fet (2003b: character 57, state=3) and Fet & Soleglad (2008: character 4, state=1) demonstrated that the ventral aspect of the tarsus with heavy spination is a synapomorphy for superfamily Iuroidea.

Comparison to *Calchas*. *Iurus* lacks the tibial spur found on legs III–IV in *Calchas*. The spination of the leg tarsus is considerably different between *Iurus* and *Calchas*. In *Iurus*, highly populated spinule clusters are found on ventral surface of the tarsus and the basitarsus, whereas in *Calchas* irregular spinule groups exist on the base of the tarsus, only occurring along the entire length of the tarsus in juveniles and small subadults. In addition, two large rows of setae with large sockets are found on the ventral aspect of the tarsus in *Calchas*; these rows are absent in *Iurus*.

Metasoma and telson

The **metasomal** structure of *Iurus* is typical for many scorpions of the parvorder Iurida (Fig. 32). Segments I–IV become narrower and longer beginning from the basal segment, with segment IV usually the narrowest and longest of the four segments. Segment V is considerably longer than segment IV, 1.60 to 1.80

times longer. Segments I–IV exhibit dorsal, dorsolateral, lateral, ventrolateral, and ventromedian carinal pairs, the lateral being complete on segment I, and decreasing in size to obsolete on segments II–IV. These carinae are well-developed and usually granulated or crenulated; in particular, the dorsal carinae are highly serrated. The dorsal and dorsolateral carinae do not terminate in an enlarged denticle. The dorsolateral carinae of segment IV are not flared distally, but terminate at the condyle. Segment V has dorsolateral, lateral, ventrolateral, and ventromedian carinae, the latter singular. The lateral carinae are present on the anterior two-thirds of the segment. As with the other carinae, segment V carinae are granulated to serrated. The single ventromedian carina is usually straight, but can terminate in an irregular bifurcation.

The **telson** in *Iurus* is somewhat elongate with a long vesicle, roughly twice as long as the aculeus (Figs. 35–40). The vesicle ventrally is covered with dense setation. The vesicle/aculeus juncture is not abrupt, but instead gradually narrowing to the aculeus base. The **subaculear setal pair** (SSP) is located on the base of the aculeus, their areolae forming a slight raised area. This area is more noticeable on juvenile and subadult specimens (Figs. 33–34).

Comparison to *Calchas*. The metasoma in *Iurus* is much thinner than in *Calchas*. All segments are longer than wide except for segment I in *Iurus* (*I. kadleci*, sp. nov., is a noted exception where all segments are longer than wide), whereas in *Calchas* segments I–II are wider than long, and in two species, segment III is also wider than long. In *Iurus*, segment V is 3.00–4.25 times longer than wide in males and 2.95–3.85 in females, whereas in *Calchas* it is 2.10–2.55 times longer in males and 2.03–2.41 in females. The telson vesicle is thinner in *Iurus*, the telson length 3.60–4.10 times longer than deep; ventrally it is densely covered with setae. In *Calchas*, the vesicle is heavier, telson length 2.65–3.05 times longer than deep; ventral setation is not as dense, being irregularly scattered on ventral surface. In all *Iurus* species and two *Calchas* species (*C. gruberi* the only exception), the SSP is located on the aculeus base.

Hemispermatophore

The terminology used in this discussion is derived, in part, from Lamoral (1979: 520–527), Stockwell (1989: figs. 186, 189–203), Hjelle (1990: 59–62), and Soleglad & Fet (2008: 29–40). In some cases, new terminology was instituted for the simplistic but unusual hemispermatophore found in family Iuridae. The four views of this structure are addressed here as dorsal, internal, ventral, and external.

Morphology. The hemispermatophores dissected in this study were, in almost all cases, enclosed in a membranous sac (Fig. 41). The paraxial organ seminal

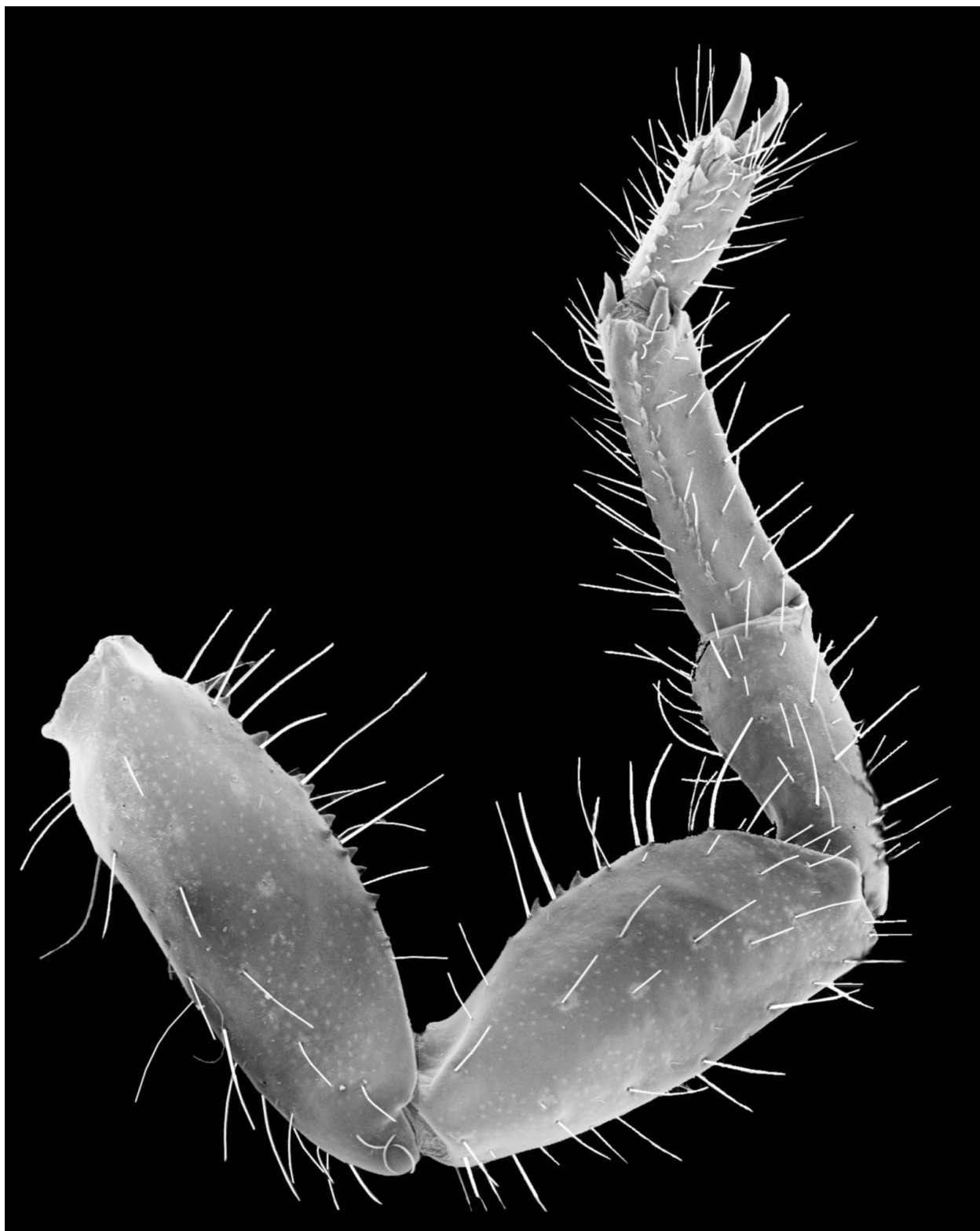


Figure 26: Left leg I, ventral view, *Iurus kraepelini*, juvenile male, Akseki, Antalya, Turkey.

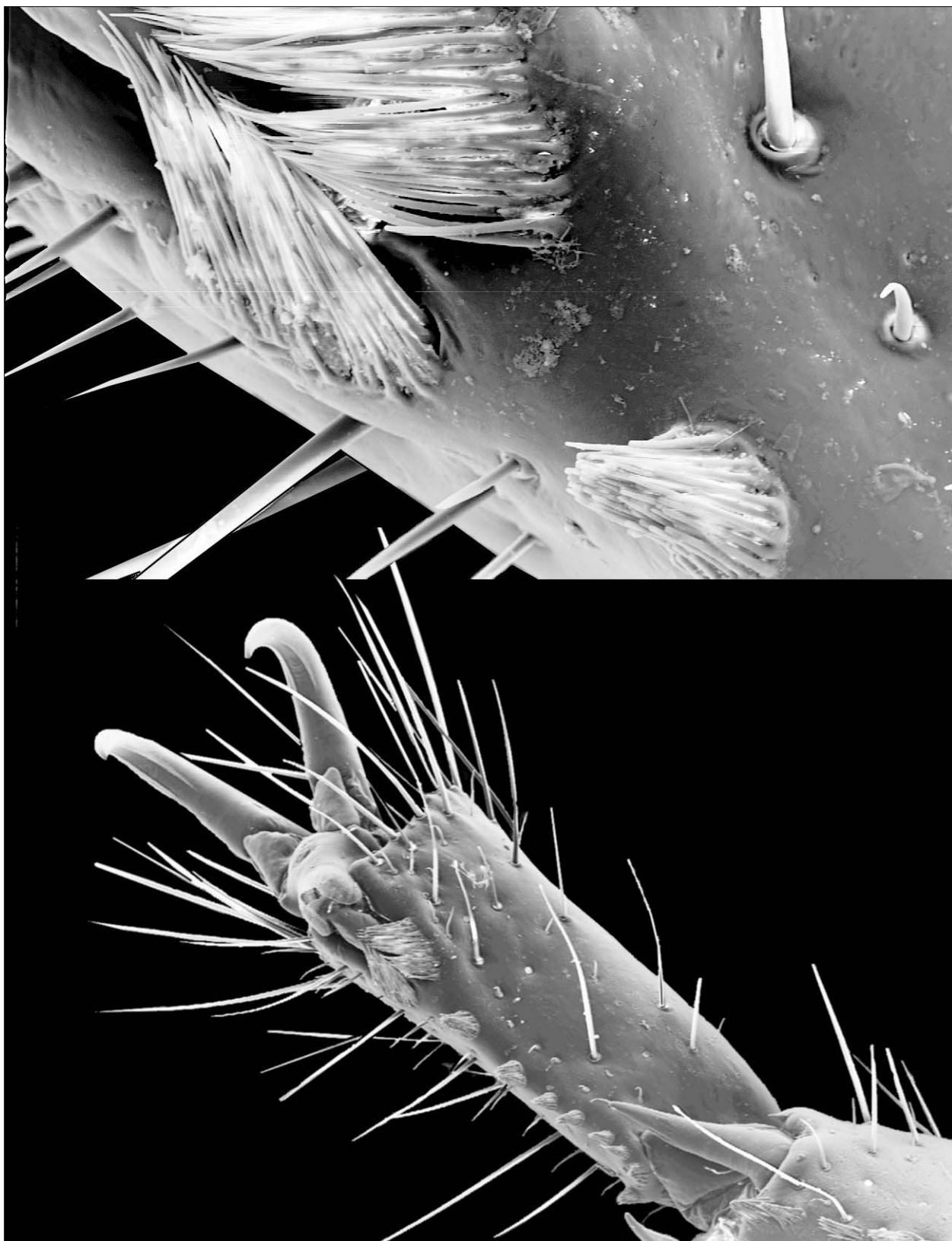


Figure 27: Leg I tarsus (35x) and its closeup (top, 200x), ventral view, showing characteristic spinule clusters. *Iurus asiaticus*, male, Kaşlıca, Adiyaman, Turkey.

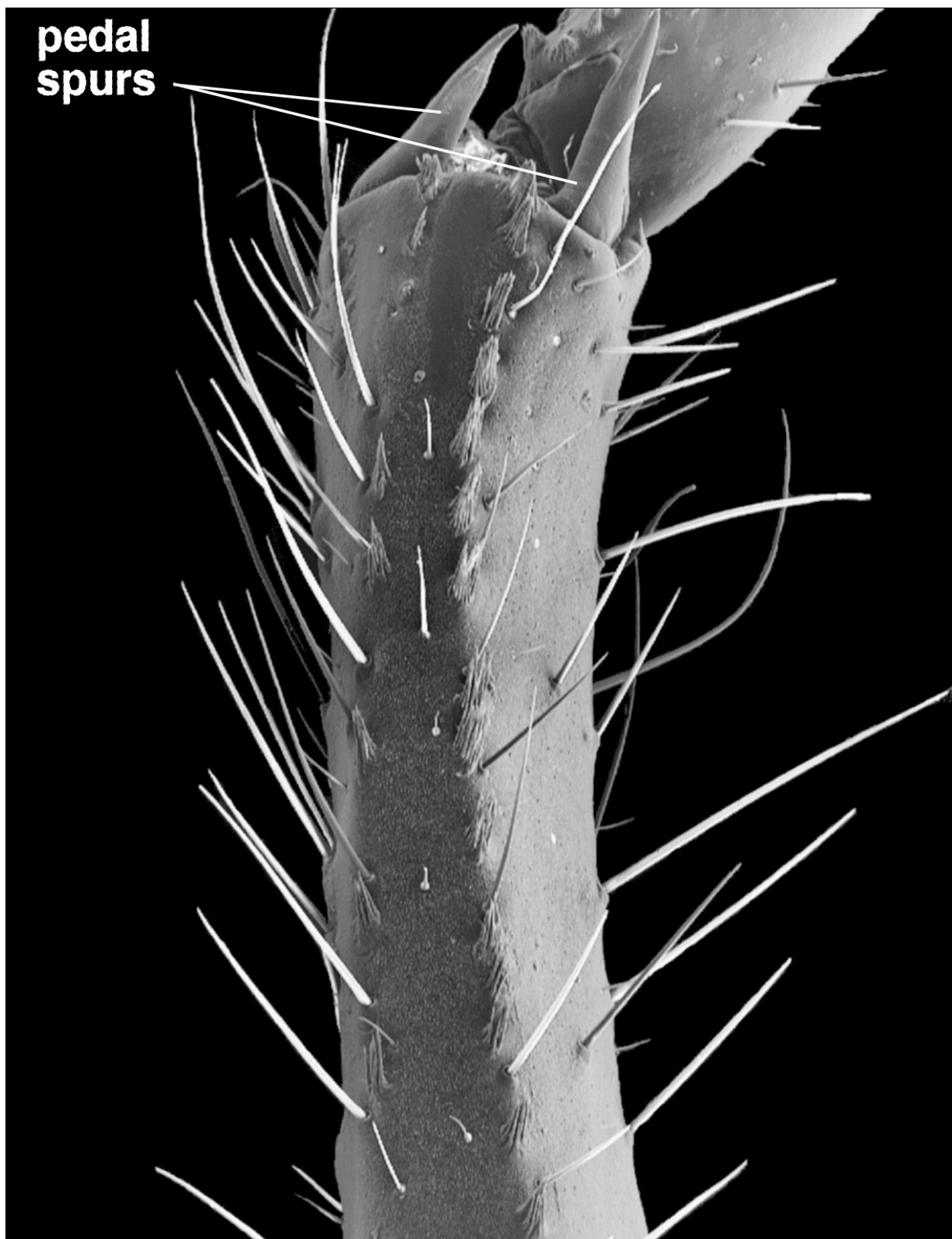


Figure 28: Leg I basitarsus (150x), ventral view, showing characteristic spinule clusters. *Iurus asiaticus*, male, Kaşlica, Adiyaman, Turkey.

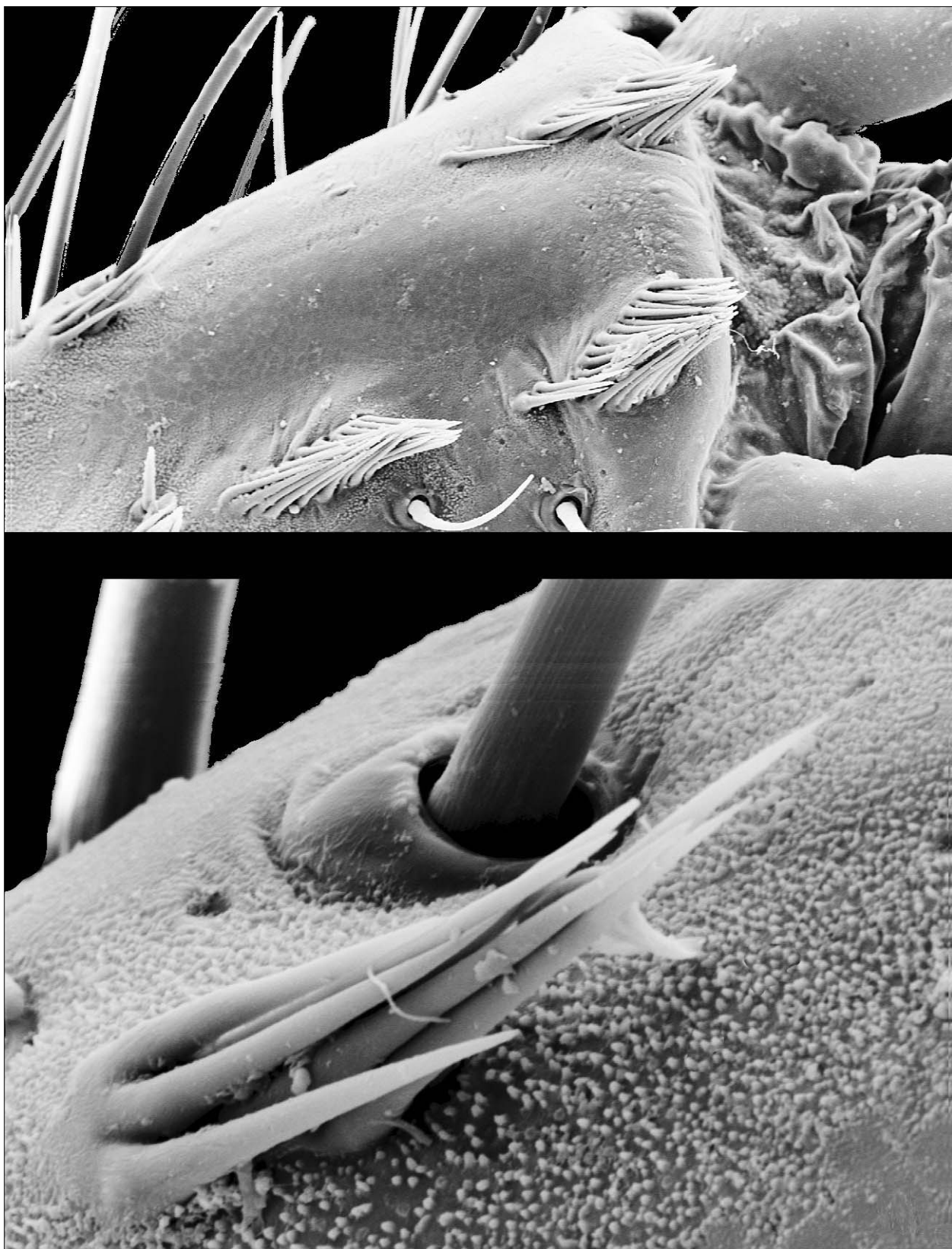


Figure 29: Leg I basitarsus, *Iurus kraepelini*, juvenile male, Akseki, Antalya, Turkey. **Top.** Distal aspect showing small spinule clusters (150x). **Bottom.** Close-up of spinule cluster (750x).

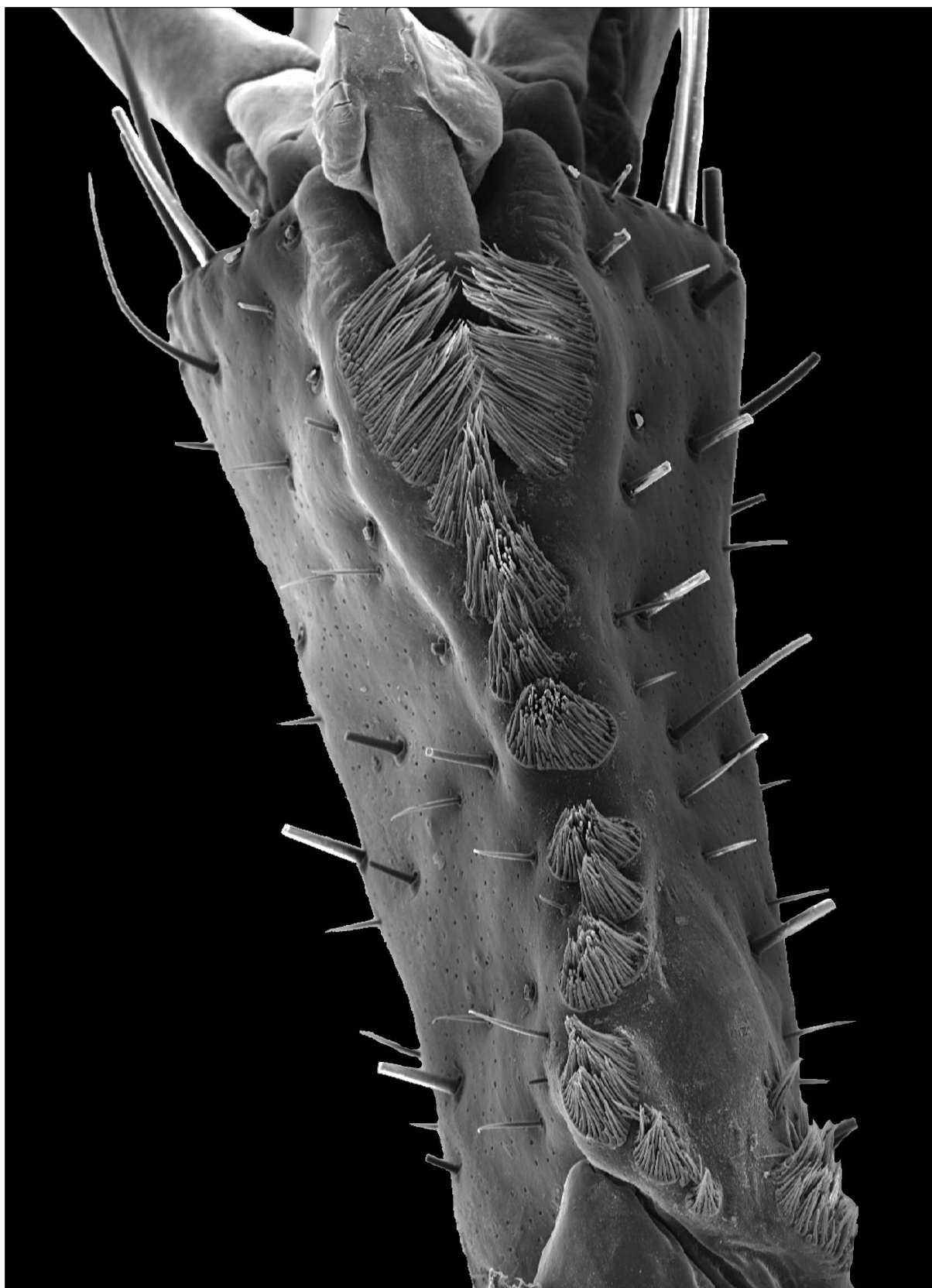


Figure 30: Leg I tarsus, adult *Iurus kraepelini*, Turkey, showing the well developed spinule clusters (50x) (after Fet et al., 2004: fig. 5, in part).

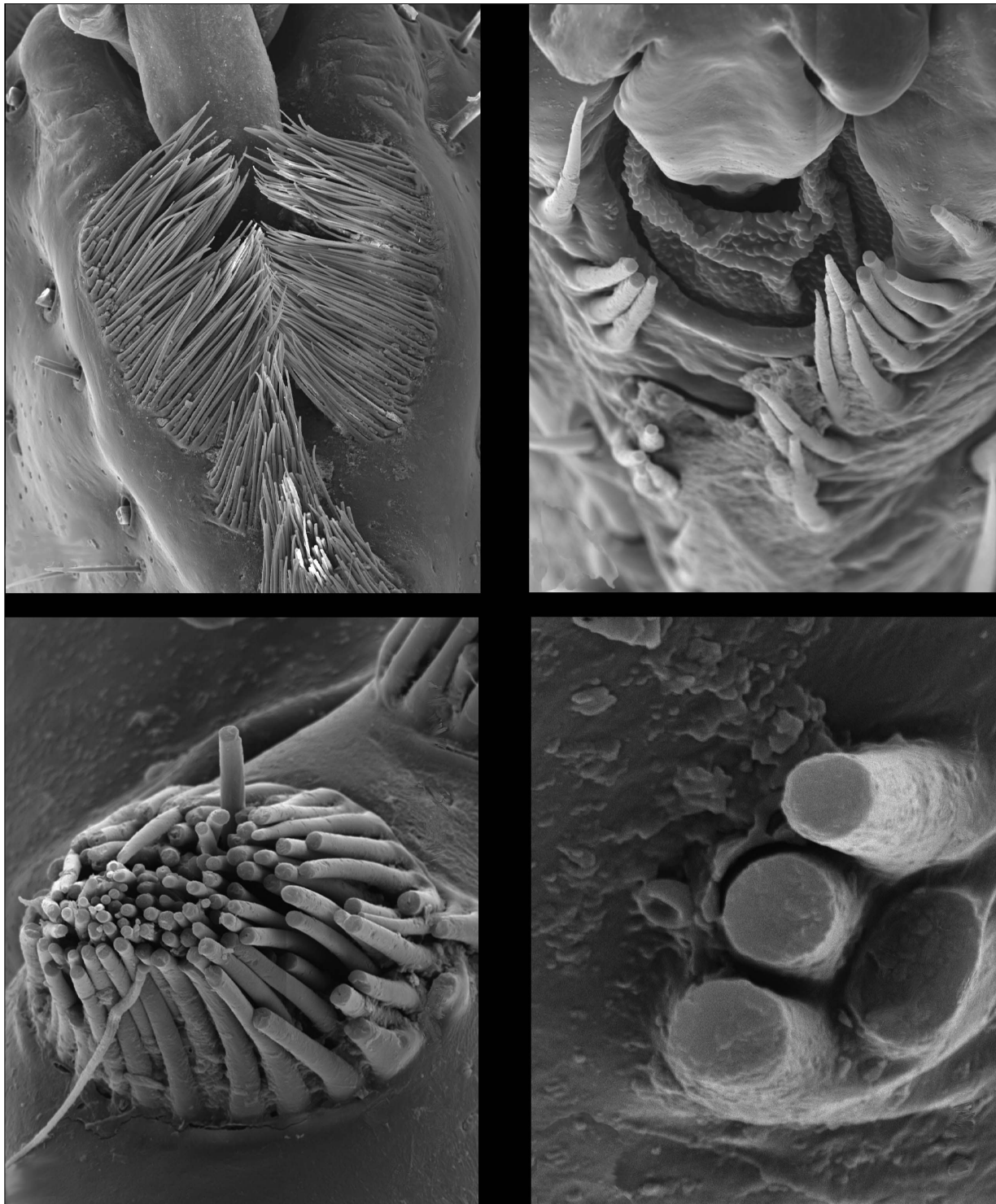


Figure 31: Closeup of leg tarsus showing significant differences in the development of the ventral spinule clusters between adult and juvenile *Iurus*. **Top.** Distal aspect of spinule clusters, adult male *I. kraepelini* (150x) (left), Turkey, compared to juvenile *I. dufoureius* (750x) (right), Crete, Greece. **Bottom.** Individual spinule cluster of *I. dufoureius*, adult female (750x) (left), Crete, Greece, compared to juvenile (3500x) (right), Crete, Greece. Note the distinctive blunted terminus of individual spinules, characteristic of *Iurus* (after Fet et al., 2004: figs. 6, 8, 38, 40).

vesicle, an extension of this sac, is found on the ventromedial section of the hemispermatophore with the vas deferens extending from its distal aspect (i.e., lamina

end). A hemispermatophore, when removed from its membranous sac, is yellowish in color with sclerotized substructures of a contrasting mahogany color. These

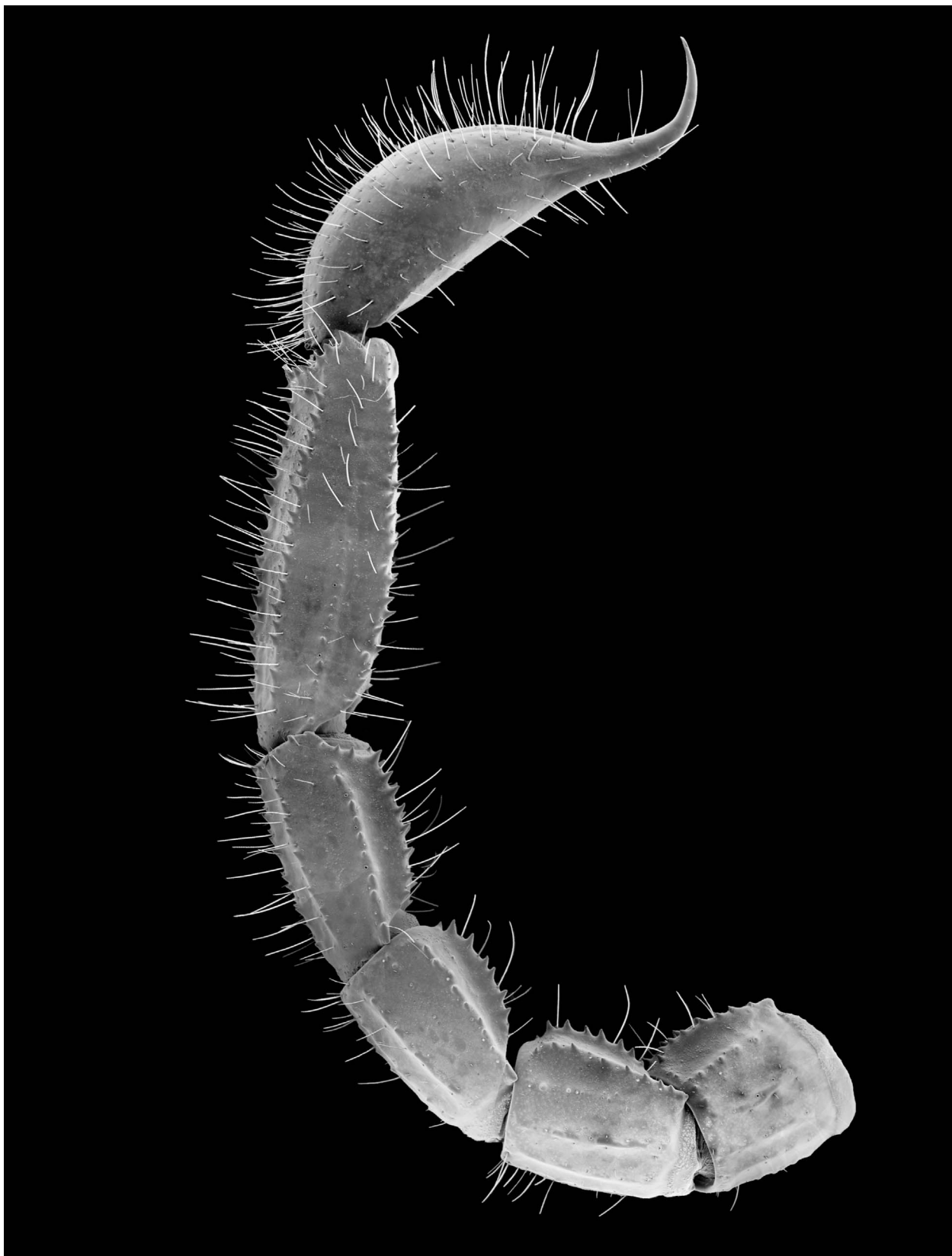


Figure 32: Metasoma and telson, lateral view (15x), *Iurus kraepelini*, juvenile male, Akseki, Antalya, Turkey.

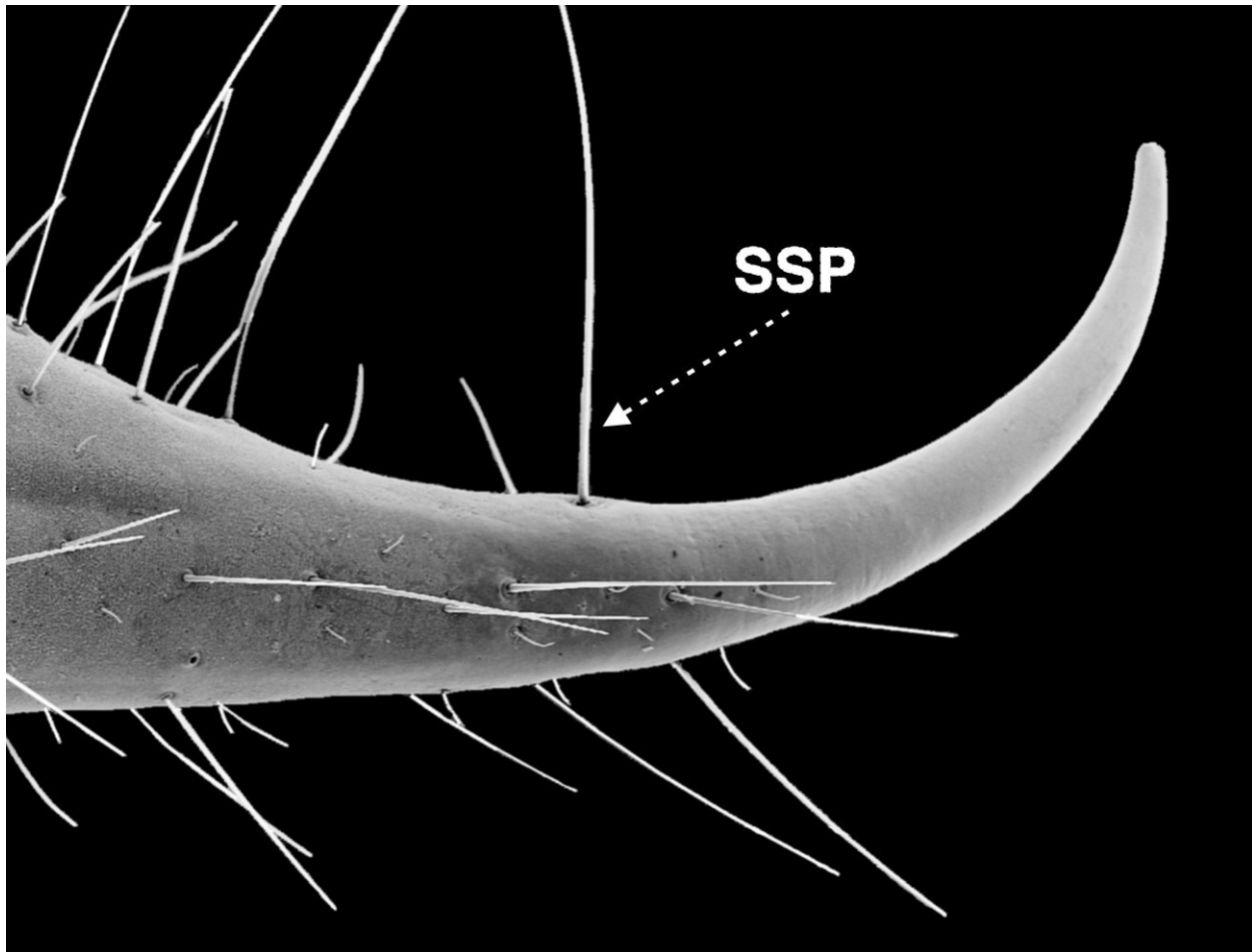


Figure 33: Aculeus, *Iurus dufourei*, subadult female, Krini, Gythio, Laconia, Greece, showing enlarged Subaculear Setal Pair (SSP) on aculeus midpoint (35x).

structures are 10–13 mm long. The hemispermatophore of *Iurus* is composed of three sections (Fig. 42): the *trunk*, the *median area*, and the *lamina*.

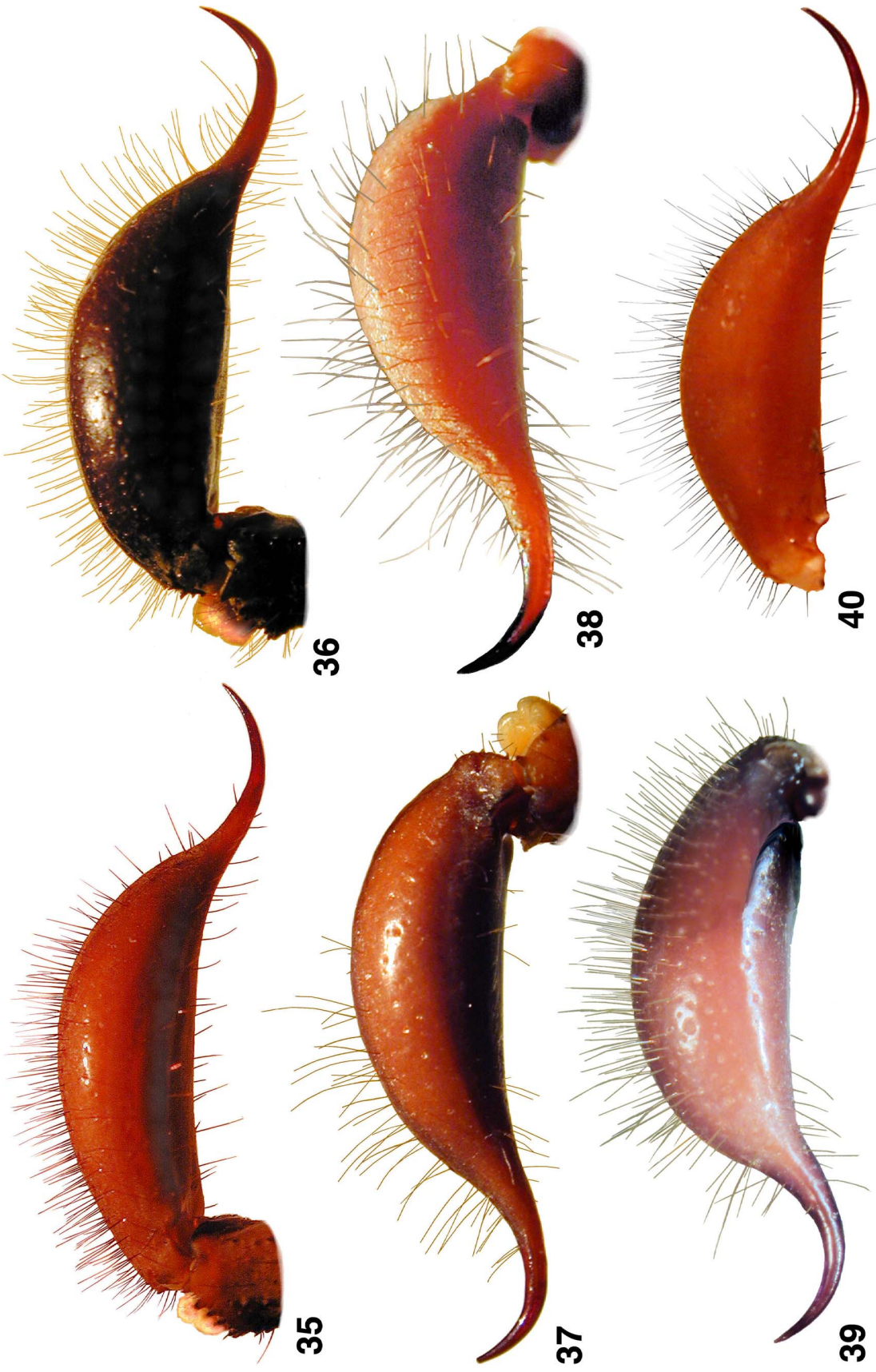
The **trunk** is a somewhat complex structure, wide and bulbous at the median area and tapering into a somewhat pointed “foot”. The bulbous section is highly convexed on the dorsal side and equally concaved ventrally. The actual walls of the trunk are thin slightly sclerotized cuticle supported by thickened bolsters (termed “ribs” by Lamoral, 1979). These bolsters are highly sclerotized, mahogany in color, thus contrasting with the lighter yellowish trunk walls. All hemispermatophores examined in this study exhibited at least two bolsters, a *primary bolster*, which traverses vertically from the base of the bulbous section to the foot’s external edge, and a *secondary bolster*, which extends down the internal edge from the base of the bulbous section to the trunk’s midpoint. In some *Iurus* species, *transverse bolsters* are also present. These bolsters extend horizontally from the medial area of the primary

bolster towards the internal edge. Two to four transverse bolsters have been observed in this study.

The **median area** is where the lamina connects to the trunk, formed by the *dorsal* and *ventral troughs*. The *acuminate process* and *seminal receptacle* are also located in the median area. On the external edge of the median area is a conspicuously developed *truncal flexure*. The **acuminate process** is a conspicuous mahogany colored highly sclerotized hook-like structure that originates from the internal edge of the median area, just above the dorsal/ventral troughs, curving in an upward/dorsal direction. The acuminate process tapers from its base to a somewhat pointed terminus, which is usually truncated, though a blunted terminus is found in one species. On the ventral side of the median area is the **seminal receptacle**, a sclerotized, mahogany-colored semicircular process found just above the ventral trough edge. Since most of the hemispermatophore is yellowish in color and translucent, highly sclerotized substructures such as the seminal receptacle or bolsters show through on the opposite surface. Therefore, this receptacle is



Figure 34: Telson, lateral view, showing subaculear setal pair (SSP) on *Iurus dufoureius*, juvenile female, Mystras, Laconia, Greece. Note location of SSP on midpoint of the aculeus.



Figures 35–40: Telson of *Iurus*, lateral view. 35. *I. kadleci*, sp. nov., adult male, Akseki, Antalya, Turkey. 36. *I. kraepelini*, adult male, Akseki, Antalya, Turkey. 37. *I. kinzelbachi*, sp. nov., adult male, Naldöken ("Narli Kioi"), Izmir, Turkey. 38. *I. difforensis*, adult male, Selinitsa, Greece. 39. *I. asiaticus*, adult male, Çamlıayla, Mersin, Turkey. 40. *I. kadleci*, subadult female, Düm Cave, Antalya, Turkey.

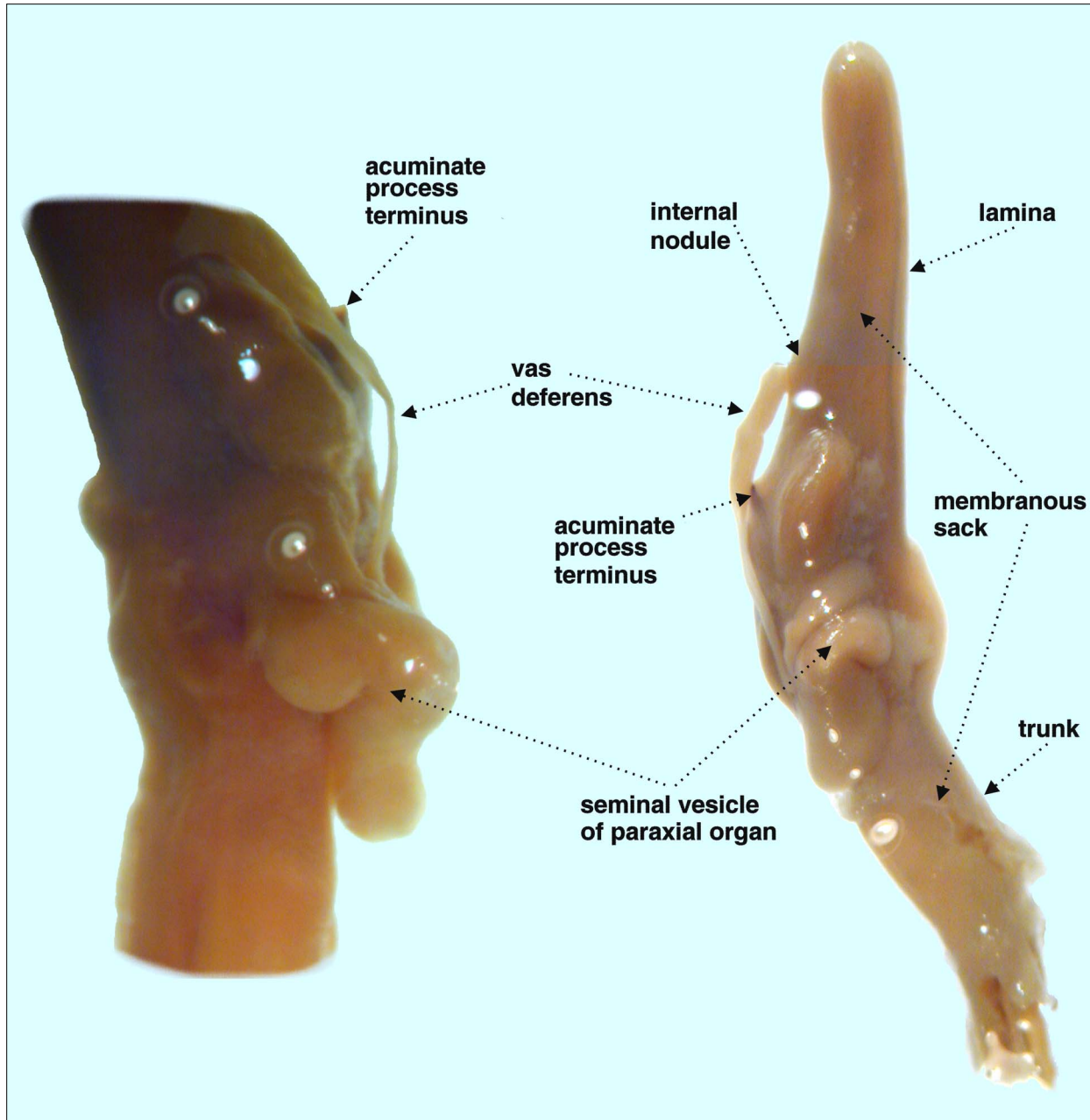


Figure 41: Right hemispermophore of *Iurus asiaticus*, ventrointernal view, showing membranous sack, and the attachment of the paraxial organ and severed vas deferens. **Right.** Yaylaüstü Village, Central District, Kahramanmaraş, Turkey, showing entire hemispermophore with major components identified. **Left.** Kaşlıca, Adiyaman, Turkey, showing a close-up of the paraxial organ seminal vesicle and vas deferens (this partial image is reversed for comparison). Note that the entire hemispermophore is enclosed in a sarcophagus-like membranous sack. The highly sclerotized terminus of the acuminate process is partially visible through the membrane in both photographs.

quite visible from the dorsal surface. This semi-circular receptacle ridge creates a hollow with the ventral trough edge (discussed further below). In many hemispermophores examined, a somewhat fragile transparent structure was found attached to the internal edge of the seminal receptacle, termed here the **paraxial organ**

sleeve. We hypothesize that this sleeve forms a conduit between the paraxial organ seminal vesicle and the seminal receptacle.

The **lamina** originates from the median area, its base formed by the dorsal and ventral troughs. With little sclerotization, the lamina is somewhat translucent.

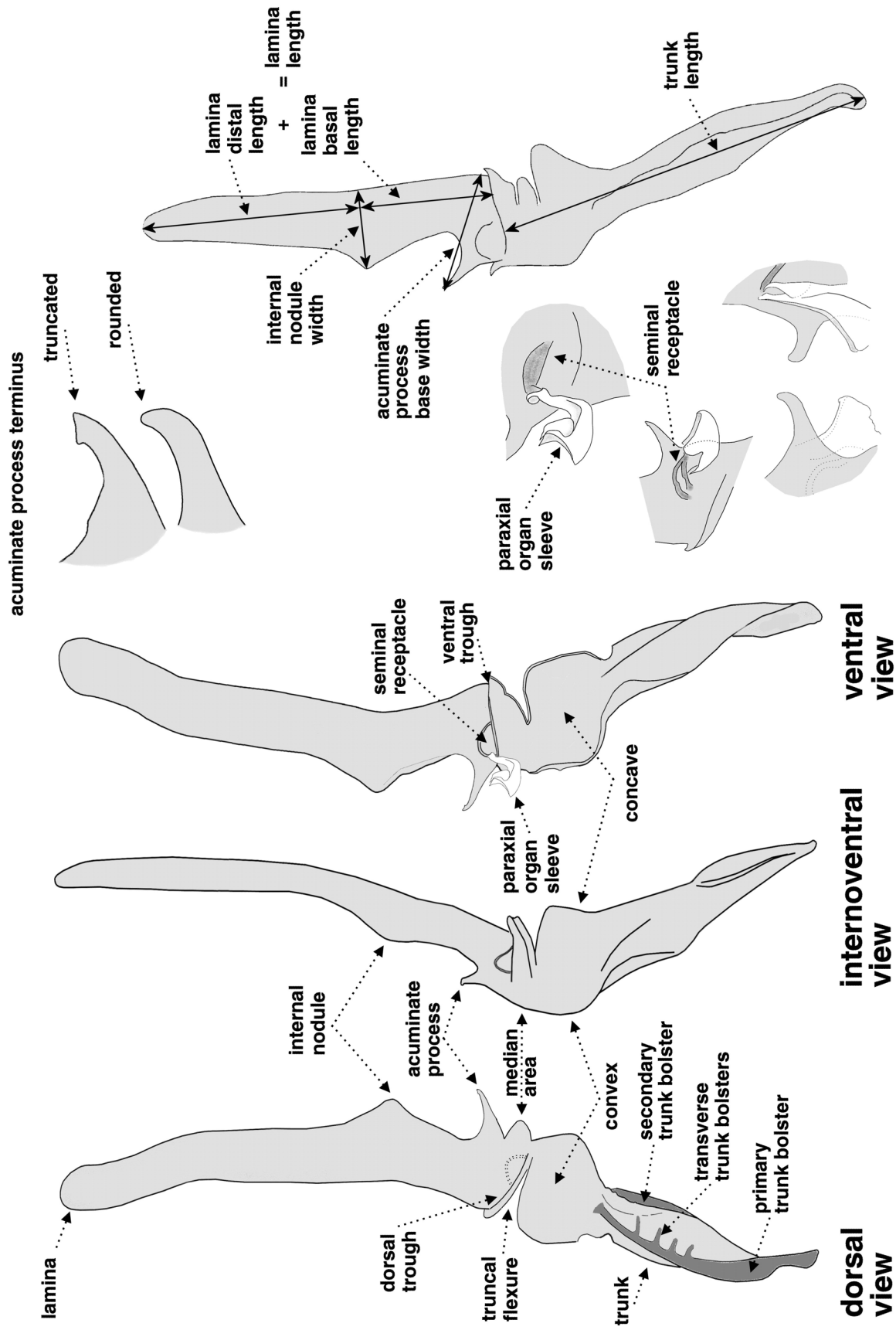


Figure 42: *Iurus* hemispermatophore. Terminology and method of measurement (from a right hemispermatophore perspective).

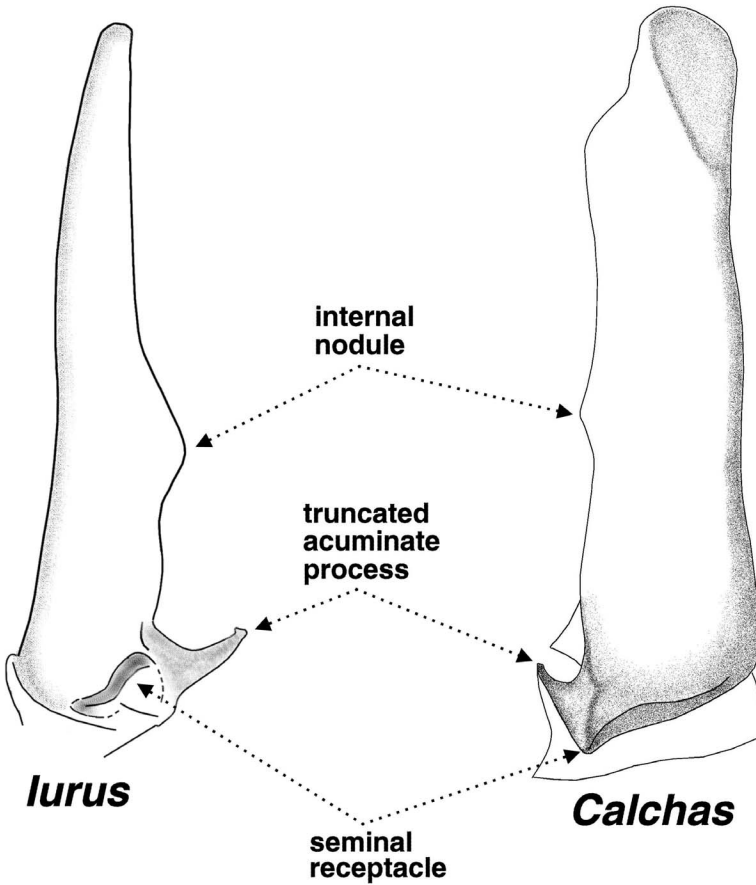


Figure 43: Hypothesized homologies for hemispermatophore morphology in genera *Iurus* and *Calchas*. Only lamina and median areas shown.

Though depending on the species, the lamina typically tapers distally, its terminus usually being narrower than the other areas. Present in all species examined is an **internal nodule** located on the internal edge, positioned on the proximal half of the lamina. The exact shape of this nodule and its relative position on the lamina is species-specific. The internal nodule extends the furthest on the internal edge, the lamina base and terminus subtly angling externally, the nodule forming the apex.

When viewing the hemispermatophore from either the internal or external edges, the median area angles outward in a dorsal direction, the lamina terminus and trunk foot pointing in a ventral direction, thus forming an obtuse angle roughly 135° (i.e., the median area as the apex).

Sperm transfer. From the above description of the *Iurus* hemispermatophore, it is clear that this is a somewhat simplistic and primitive form of the lamelliform type. There is no complex capsule as found in many lamelliform type scorpions, no mating plug as found in the vaejovids, or a multitude of complex lobe structures as identified in many scorpionoids, etc. The actual sequence of sperm transfer in this type of

hemispermatophore is not known. However, it appears that the sperm from the testes is transferred directly to the paraxial organ seminal vesicle via the vas deferens and then deposited into the seminal receptacle. There are two components of this receptacle, the outer sclerotized semi-circular ridge, and the hollow formed by this ridge and the ventral trough edge. As of now, we do not know where the sperm is actually deposited, but we can hypothesize two scenarios: 1) the semi-circular ridge is hollow and the sperm is injected into this sclerotized ridge (i.e., the ridge orifice would be the “sperm duct”); 2) the sperm is deposited into the hollow formed by the ridge and ventral trough. The latter scenario would only make sense if the two hemispermatophores (left and right) are “glued” together before the injection of sperm, thus forming an enclosed compartment to hold the sperm. The attachment of the paraxial organ sleeve can support either scenario of sperm transfer.

Comparison to *Calchas*. The hemispermatophore trunk is quite different between *Iurus* and *Calchas*. In the former, we have a sclerotized contorted structure exhibiting convoluted convex and concave contours whereas in the latter, the trunk is an evenly rounded membranous non-sclerotized component that tapers to a

point at its foot. A truncal flexure is found in both genera, moderately developed in *Calchas* and conspicuous in *Iurus*. The lamina in *Iurus* generally tapers from its base to a narrower distal tip, whereas in *Calchas* the lamina is spatulate in form, the lateral edges subparallel, the terminus abruptly truncated (Fig. 43). Both genera exhibit an **acuminate process** with a truncated terminus, unprecedented in Recent scorpions. In *Iurus*, this process is longer, protruding further from the median area. On the internal edge of the proximal half of the lamina is an **internal nodule** found in both genera. In *Iurus*, this nodule is variable in its relative location on the lamina, its width, size, and overall shape, species dependent. In *Calchas* (based on two species), the internal nodule is a subtle small pointed projection located just proximally of lamina midpoint. Both genera have a simplistic **seminal receptacle** located on the ventral surface just above the ventral trough. In *Iurus*, the receptacle is highly sclerotized, and therefore pigmented, forming a conspicuous semi-circle above the ventral trough. The receptacle in *Calchas* is not overly sclerotized or conspicuous; its upper edge forms a small slit-like hollow with the ventral trough edge. Unique to *Calchas* is a curious non-sclerotized triangular **internal protuberance** located on the internal edge of the lamina base. This protuberance is situated closer to the dorsal surface, thus not directly on the internal edge.

We consider the acuminate process (with truncated terminus), internal nodule, and the seminal receptacle to be *homologous structures* between these two genera and probable *synapomorphies* for family Iuridae (see Fig. 43). Of course, a detailed analysis of all iuroid hemispermatophore morphology and comparison to putative outgroup *Chaerilus* needs to be conducted in order to substantiate this hypothesis (Soleglad et al., in progress).

Species-Level Comparisons

In this section, major characters used to separate *Iurus* species are discussed in detail including an illustrated key. The major structures separating the five species currently recognized in *Iurus* include the morphology of the pedipalp chela and hemispermatophore, and several morphometrics. Other characters such as number of chelal finger inner denticles (*ID*), neobothriotaxy, and pectinal tooth counts are also discussed.

Illustrated key to species of *Iurus*

1 - Lobe position of chelal movable finger in adults basal of midfinger, lobe ratio 0.38–0.47 (Fig. 56); inner denticles (*ID*) of chelal movable finger number 14–16 (14.42) (Tab. 1); hemispermatophore transverse trunk bolsters present (Figs. 98, 216), lamina terminus rounded (Figs. 61–63), and lamina distal length / basal

length = 3.4–4.7 (Tab. 2); pectinal tooth counts 10–11 (10.63) males, 9–11 (9.58) females (Fig. 73) 2

■ - Lobe position of chelal movable finger in adults midfinger or distal, lobe ratio 0.44–0.64 (Fig. 56); inner denticles (*ID*) of chelal movable finger number 11–13 (12.45) (Tab. 1); hemispermatophore transverse trunk bolsters absent (Figs. 132, 168), lamina terminus pointed (Figs. 64–72), and lamina distal length / basal length = 1.7–2.6 (Tab. 2); pectinal tooth counts 11–14 (12.49) males, 10–12 (11.38) females (Fig. 73) 3

2 - Proximal gap lacking on chelal fixed finger in adult males (Fig. 59); hemispermatophore internal nodule conspicuous and knob-shaped, acuminate process terminus truncated (Fig. 61), and lamina length / internal nodule width = 6.8; chela fixed finger length / telson width = 2.62–2.73 males, 2.64–2.96 females, and movable finger length / telson width = 3.21–3.40 males, 3.31–3.68 females (Fig. C3) *I. dufourei* (Brullé, 1832)

■ - Proximal gap present on chelal fixed finger in adult males (Fig. 59); hemispermatophore internal nodule weak to obsolete, acuminate process terminus rounded (Fig. 62), lamina length / internal nodule width = 8.7; chela fixed finger length / telson width = 3.37–3.46 males, 3.41–3.65 females, and movable finger length / telson width = 4.14–4.34 males, 4.26–4.32 females (Fig. C3) *I. kinzelbachi* sp. nov.

3 - Proximal gap of chelal fixed finger vestigial to obsolete in adult females (Figs. 127, 163); metasomal segments stocky (Figs. C4–C5), segments I–III length / width = 0.81–0.92, 1.04–1.17, 1.24–1.37 males, 0.70–0.85, 0.97–1.11, 1.15–1.34 females; telson vesicle relatively wide (Fig. C3), telson length / vesicle width = 3.18–3.67 males, 3.27–3.49 females; dark grey to black in color (Figs. 110, 149) 4

■ - Proximal gap of chelal fixed finger large and conspicuous in adult females (Fig. 194); metasomal segments slender, all longer than wide (Figs. C4–C5), segments I–III length / width = 1.10–1.28, 1.35–1.45, 1.64–1.69 males, 1.11–1.12, 1.36–1.55, 1.55–1.71 females; telson vesicle narrow (Fig. C3), telson length / vesicle width = 4.34 males, 3.98–4.34 females; light reddish in color with darker chelae (Fig. 182) *I. kadleci* sp. nov.

4 - In adult males proximal gap of chelal fixed finger exaggerated, movable finger highly curved, and chelal palm short, noticeably vaulted (Figs. 121–126); chela depth / chela length = 0.41–0.46 males, 0.37–0.38 females (Fig. C2); hemispermatophore internal nodule widely rounded, located basally on lamina, lamina distal length / basal length = 2.16–3.07 (Tab. 2) *I. kraepelini* von Ubisch, 1922

■ - In adult males, proximal gap of chelal fixed finger not exaggerated, movable finger essentially straight with

a subtle curve, chelal palm elongated, not vaulted (Figs. 159–162); chela depth / chela length = 0.32–0.35 males, 0.32–0.34 females (Fig. C2); hemispermatophore internal nodule pointed, located suprabasally on lamina, lamina distal length / basal length = 1.61–1.80 (Tab. 2)

..... *I. asiaticus* Birula, 1903

(note that *standard error* ranges are stated in the above key)

Major morphological differences between *Iurus* species

The pedipalp chela and hemispermatophore provide major diagnostic characters for separating the five species we recognize in genus *Iurus*. However, it is important to note that the diagnostic characters derived from these two structures are based only on sexually mature males. Other important diagnostic characters, morphometrics in particular, also depend on mature specimens, but do include both genders. Fortunately, the morphometrics identified herein as diagnostic apply equally to both male and female. Lesser characters, such as the number of inner denticles (*ID*) of the movable finger, or number of pectinal teeth, are relevant for juvenile and subadult specimens as well as for adults.

Pedipalp chela morphology

Chelal finger lobe/socket and the proximal gap

Francke (1981), in a small but important paper on *Iurus*, was the first to observe the taxonomic value of the movable finger lobe in this genus. Although the material he studied was quite limited, Francke was able to identify some of the key issues concerning the lobe's structure, its bearing on sexual dimorphism, and allometric growth.

We examined the movable finger (MF) lobe of the chela from several perspectives: its relationship to the fixed finger socket and proximal gap if present; the relative position of the lobe on the movable finger; differences in form and location based on sexual dimorphism; development and relative finger lobe position with respect to allometric growth; and its overall importance to *Iurus* taxonomy. This examination of the MF lobe involved the study of over 200 specimens.

Lobe/socket relationships. Among Iuridae, a lobe on the denticle surface of the movable finger is present only in *Iurus* (this lobe is absent in its sister genus *Calchas*). This lobe increases in size and shape as the scorpion matures. Corresponding to this lobe is a socket (also called “notch” in literature) on the fixed finger which allows the denticle edges to meet when the fingers are closed. In Figures 44–55, we illustrate two basic configurations of chelal finger lobe/socket arrangement.

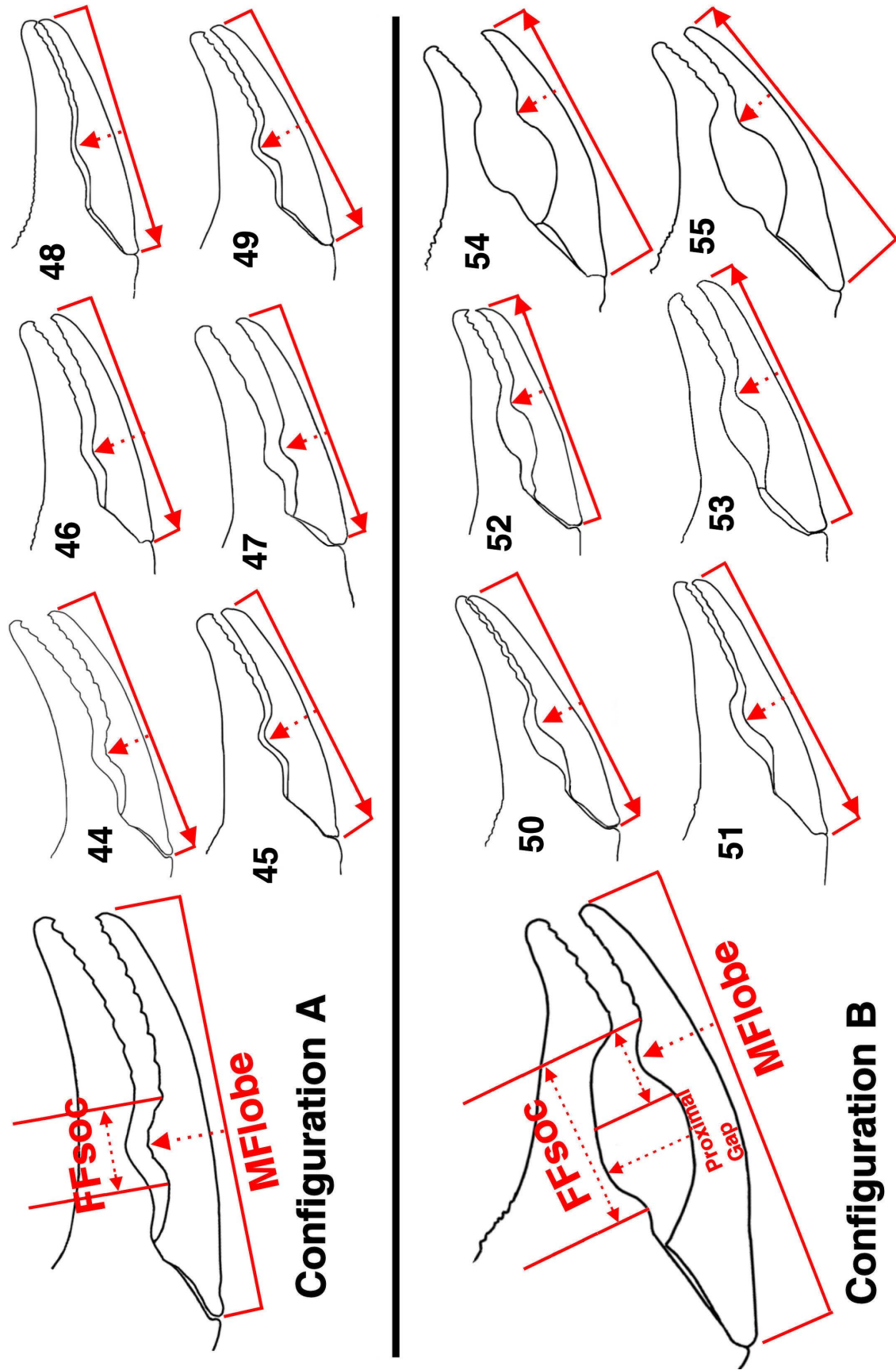
In configuration A, the socket and lobe have the same basal width, the lobe fitting exactly into the socket when the two fingers are closed. In configuration B, the socket base is wider than the lobe base, sometimes exceeding its width by a factor of two. The increase in socket width occurs proximally, the distal part of the socket matching up with the lobe when the fingers are closed. Therefore, when the fingers are closed there is a conspicuous gap between the fingers proximal of the MF lobe, termed in this paper a *proximal gap*. Figures 44–55 illustrates diagrammatically the lobe/socket relationship for both configurations, spanning all recognized *Iurus* species. In addition, a multitude of lateral views of chelae are presented under the individual species descriptions for all species examined in this study, for both males and females.

In general, configuration B is only detectable in large sexually mature males, and is not usually apparent in females. A notable exception is *I. kadlecii*, sp. nov., where the adult female exhibits a conspicuous proximal gap (this is discussed further below).

Lobe location on movable finger. Of particular interest for the MF lobe is its relative position on the finger. In the scatter chart shown in Fig. 56, the MF lobe ratio is analyzed with respect to the specimen's size, as represented by its carapace length. The ratio is the distance from the lobe to the external condyle divided by the movable finger length (see Fig. 57 for exact methods of measurement), thus representing its relative position on the finger; i.e., ratio < 0.5 = lobe proximal of midfinger, ratio > 0.5 = lobe distal of midfinger. Two attributes of this analysis are readily apparent directly from the scatter chart: 1) the lobe is found more distally on larger specimens within a species; 2) the species are partitioned into two groups, in part, by their lobe's relative position on the finger.

In Fig. 56 we see that the distribution of the various colored icons angles upwards as the MF lobe ratio increases (which means a lobe occurring further on the finger). This implies that the lobe does indeed occur further on the finger on larger specimens than it does on smaller specimens (as indicated by carapace length). For example, the smallest specimen of *I. dufourei* examined has a carapace of 6.9 mm and a lobe ratio of 0.317, also the smallest obtained in this species. In contrast, the largest specimen examined, with a carapace of 13 mm, exhibits the largest lobe ratio, 0.458. We see a similar condition in *I. kraepelini* (our largest dataset), where the smallest specimen has a carapace of 7.2 mm and a lobe ratio of 0.400, and nine specimens with the largest lobe ratios, 0.600 to 0.637, have carapaces ranging 11.85 to 14.65.

The separation of five species into two groups is clear in Fig. 56, as indicated by “red” + “blue”, and “green” + “black” + “white” icons, respectively. This can be verified by inspecting the histogram in Fig. 56



Figures 44–55: Movable finger lobe (MFlobe) and fixed finger socket (FFsoc) configurations in *Iurus*. *Iurus* species exhibit two distinct lobe/socket configurations: Species from the Peloponnese, Crete, Karpathos, and Rhodes comply to configuration A where the lobe and socket widths are approximately the same, exhibiting no proximal gap. Species from mainland Turkey conform to configuration B where the socket is wider than the lobe, sometimes exceeding the lobe width by a factor of two, as indicated by a conspicuous proximal gap. 44–46. *Iurus dufouriensis*, male, Peloponnese. 47. *I. dufouriensis*, female, Crete. 48. *I.* sp., subadult male, Karpathos. 49. *I.* sp., male, Rhodes. 50–51. *I. kinzelbachi*, male, Turkey. 52. *I. kadelci*, male, Turkey. 53. *I. astaticus*, male, Turkey. 54–55. *I. kraepelini*, male, Turkey.

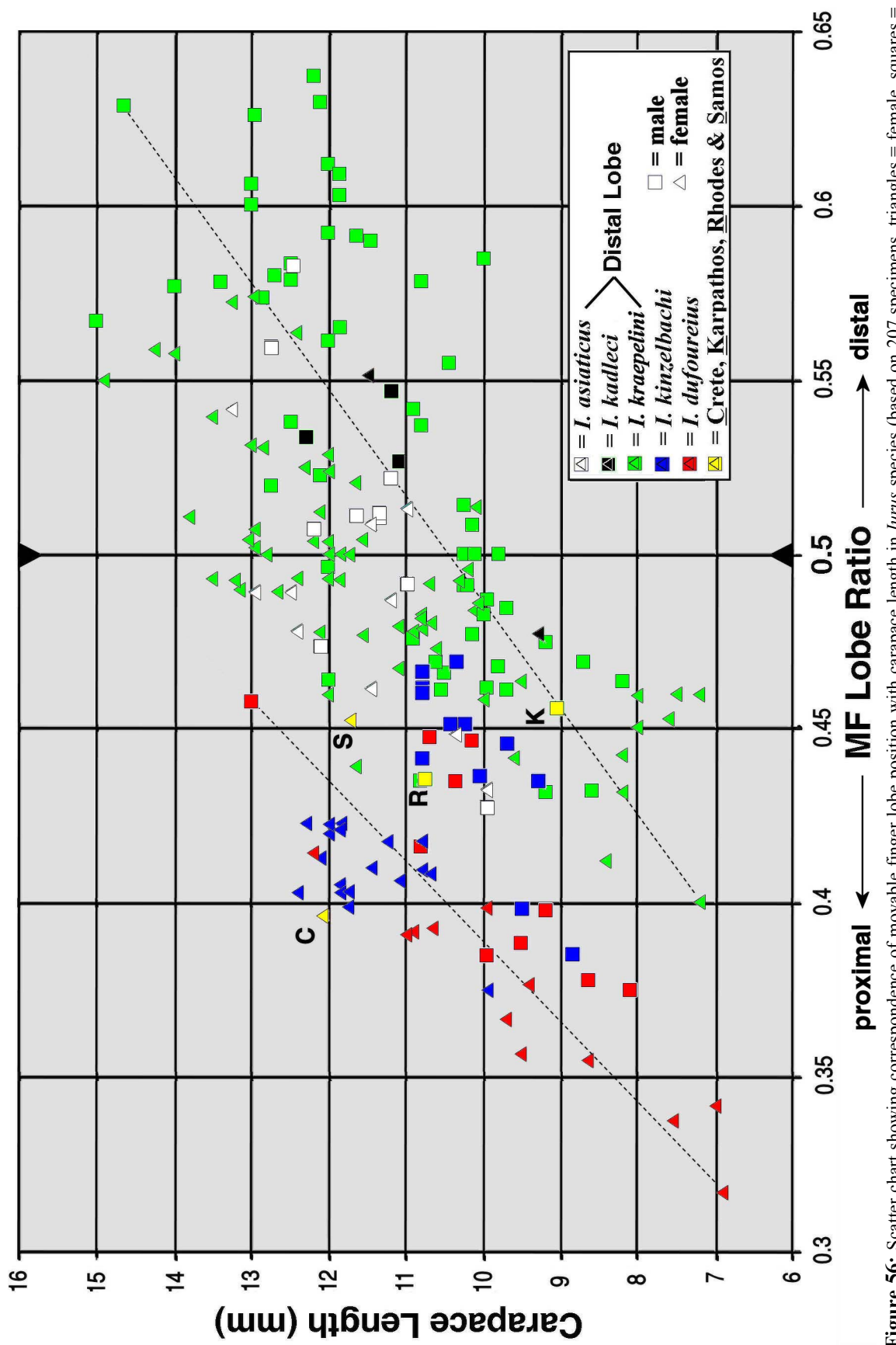


Figure 56: Scatter chart showing correspondence of movable finger lobe position with carapace length in *Iurus* species (based on 207 specimens, triangles = female, squares = male). MF lobe ratio = external condyle-to-lobe distance / MF length (i.e., a ratio of < 0.5 implies lobe is proximal of midfinger, 0.5 implies lobe is at midfinger, and > 0.5 implies lobe is distal of midfinger). Note, in particular, that the MF lobe moves distally as scorpions reach maturity in all five species (using carapace length as an indicator of maturity). Diagonal lines connecting small and large MF lobe ratios for *I. dufoureius* and *I. kraepelini* highlight this observation. In general, males of comparable size have a more distal MF lobe than corresponding females in all species. Also note that in mature *I. kraepelini*, *I. kradleci*, and *I. astaticus*, lobes are located distally, whereas *I. dufoureius* and *I. kinzelbachi* lobes are located proximally. Finally, *Iurus* sp. from Rhodes exhibit proximally placed lobes as in *I. dufoureius* and *I. kinzelbachi*, whereas in *I. sp.* from Karpatus (subadult) and Samos the lobe position is consistent with that in comparable specimens of *I. kraepelini*.

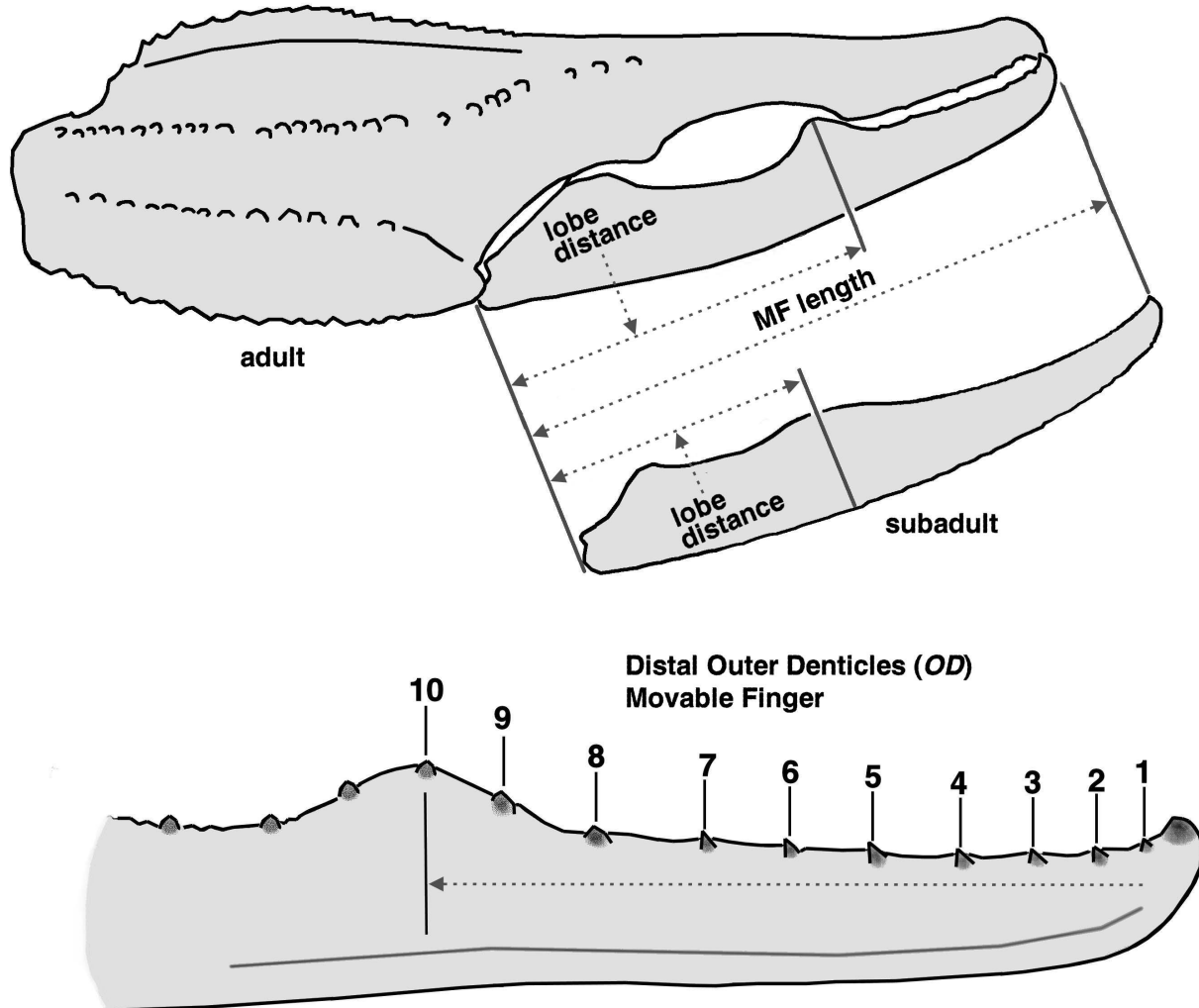


Figure 57: Conventions used in the analysis of the movable finger lobe in *Iurus*. **Top.** Method of measurement of the movable finger lobe. Lobe distance is measured from the external condyle to the center of the lobe. Movable finger lobe ratio is this distance divided by the movable finger length. Note that the finger lobe in juvenile to subadult specimens is more rounded and not as exaggerated as in adults (both are illustrated above). However, the lobe is detectable except only in the smaller juvenile specimens where the finger denticle edge is essentially straight. **Bottom.** Technique of counting the number of distal outer denticles (*OD*). *ODs*, which proximally terminate each median denticle (*MD*) group, are visible on the external edge of the movable finger (i.e., the *MD* denticle group proximal base slants externally). The “distal” *OD* count includes all *ODs* beginning from the distal denticle (*DD*) to the center of the movable finger lobe. By convention, if no *OD* occurs at the lobe center, then the closest *OD* occurring distally of the lobe is counted as the terminal *OD*.

horizontally for each carapace length partition: “red” and “blue” icons in most cases occur to the left of “green”, “black”, and “white” icons. There are very few exceptions in this 200+ sample set. *Iurus dufourei* and *I. kinzelbachi* in general exhibit a proximal MF lobe. Even the largest adults have lobe ratios less than 0.5. For example, *I. dufourei* (carapaces 12.2 and 13.0, female and male) have ratios of 0.414 and 0.458, respectively, and *I. kinzelbachi* (carapaces 12.0 to 12.4 mm, five females) exhibit ratios from 0.402 and 0.423. The largest ratios found in these two species are from male *I.*

kinzelbachi (carapaces 10.35 to 10.80), 0.460 to 0.470 (in general, males exhibit larger ratios than females, see discussion below). *Iurus kraepelini*, *I. kadleci*, and *I. asiaticus* exhibit MF lobe ratios exceeding 0.5 in most adults, especially in males. The larger specimens of *I. kraepelini* have lobe ratios exceeding 0.550 (29 specimens), nine of which exhibited 0.600 or larger. *Iurus kadleci*, sp. nov., a slightly smaller species (the largest known specimen is a male with a 12.2 mm carapace), reaches ratio values up to 0.550. *Iurus asiaticus*, with lobe ratios slightly smaller than the previous two

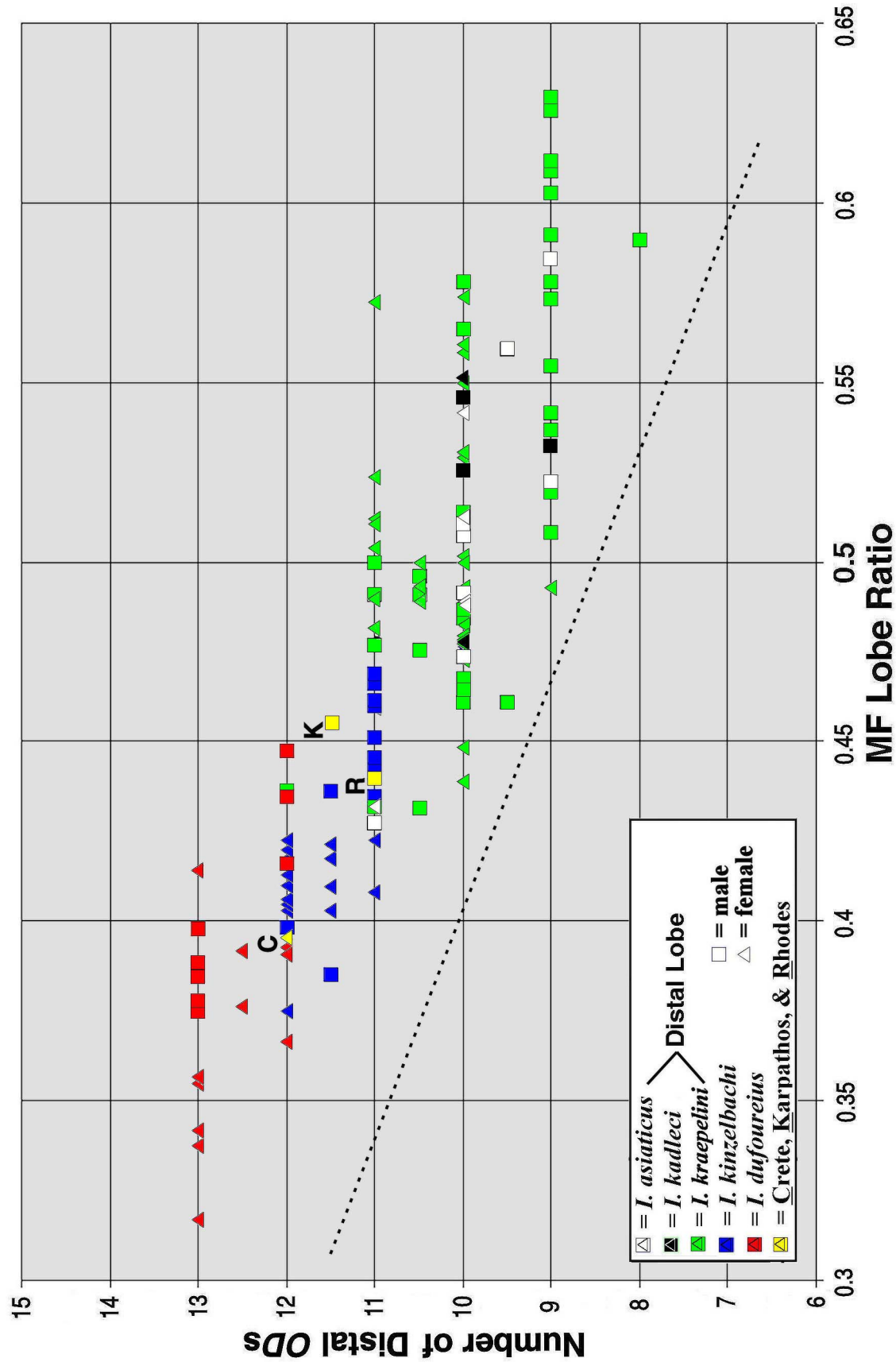


Figure 58: Scatter chart showing correspondence of movable finger lobe position with number of distal outer denticles (OD) in *Iurus* species (based on 149 specimens, triangles = female, squares = male). Number of distal ODs = number of ODs from distal denticle (DD) to lobe center (see Fig. 57); both fingers are tabulated and then averaged to produce count. Note, in particular, that the number of distal OD denticles decreases as the MF lobe moves distally. Diagonal arrow highlights this observation. See Fig. 56 for definition of MF lobe ratio.

species, ranges 0.474 to 0.584, with carapaces 12 mm or greater.

Sexual dimorphism in lobe/socket relationships.

As stated above, the proximal gap, which characterizes the two lobe/socket configurations, is almost exclusively found in sexually mature male specimens. This gap, in general, is not present, or at least is not conspicuous, in females. However, in *I. kadleci*, sp. nov., the proximal gap is quite conspicuous in the large female (carapace 11.5 mm) as it is in the males. The scatter chart in Fig. 56 delineates males and females. It is clear from this chart that, in general, male specimens of a species have greater lobe ratios than females of comparable size. Again, this can be determined by inspecting the scatter chart horizontally within carapace length brackets; i.e., “triangular” icons usually occur to the left of “rectangular” icons by species.

Allometric considerations in lobe location.

Above, we demonstrated that the movable finger lobe “migrates” distally on the finger as a specimen reaches successive ontogenetic stages. The question now arises as to the dynamics of this “migration”. The distal position of the lobe is based on a ratio using the movable finger length. Therefore, an expansion of the finger base, as suggested by the proximal gap seen in configuration B, is a possible cause of this “movement”. That is, the MF lobe does not actually move distally as indicated by the ratio, but instead the ratio is impacted by the expansion of the finger bases. The other alternative is that the lobe does indeed migrate down the finger, which would also equally impact the lobe ratio. The scatter chart shown in Fig. 58 contrasts the lobe ratio with the number of distal outer denticles (*OD*) (see Fig. 57 for method of counting distal *ODs*). It is clear from this analysis that as the lobe ratio increases the number of distal *ODs* decreases. For example, in *I. dufoureius*, the number of distal *ODs* ranges from 12 to 13, a count of 13 found on the specimens with the smallest lobe ratios. The same is also true of *I. kraepelini* where we see a range of 8 to 12 distal *ODs*. In most cases, counts of 8 or 9 were limited to sexually mature males only. This data implies that the MF lobe does indeed migrate distally on the finger, exhibiting less *ODs* between the lobe and the fingertip.

This same issue was discussed by Francke (1981) where he contrasted the fixed finger socket with the median denticle (*MD*) groups and finger trichobothria. We opted to use the MF lobe since it is an important taxonomic character observable in both genders throughout most ontogenetic stages.

Species differentiation based on lobe/socket

/proximal gap. Figure 59 presents a “graphic key” delineating all five *Iurus* species using chelal morphology. This key is based primarily on the analysis of chelal MF lobe and proximal gap discussed in detail above. The primary couplet is the presence/absence of a

proximal gap. Only *I. dufoureius* lacks a proximal gap on sexually mature males, being conspicuous in the other four species. The next key couplet is a relative position of the MF lobe, separating species by proximal or distal lobe positions. Only *I. dufoureius* and *I. kinzelbachi*, sp. nov., have basal lobes on sexually mature specimens; in the other three species the lobe is generally found midpoint or distally. The third couplet, curvature of the movable finger, separates *I. kraepelini* from *I. kadleci*, sp. nov., and *I. asiaticus*. In *I. kraepelini*, the movable finger is curved considerably, forming a 30+° angle from its base to the distal denticle. In the other four species, this angle is smaller, roughly 20°. *Iurus asiaticus* and *I. kadleci*, sp. nov., cannot be differentiated with these three characters alone (except that the proximal gap is also found in mature females in *I. kadleci*, sp. nov., unique in *Iurus*).

Francke (1981: 222, figs. 3–4) discussed morphometric size differences between two sexually mature males (both had hemispermatophores, dissected by Francke) from the “same” locality, stating that “... size differences of about 30 % between these two specimens strongly suggests ... sexual maturity at different instars ...”. We have examined both of these male specimens (NHW 11324 and NHW 11325; photographs, illustrations, and measurements are provided for both in this paper) and, as it turns out, the “small male” is *I. asiaticus* whereas the “large male” is *I. kraepelini*. Francke quotes both males as originating from “Namrum” in Turkey; however, this is an error since only the “small male” (NHW 11325, 16 May 1967, leg. F. Ressl) is from Namrun, now Çamlıayla, Mersin Province, Turkey, a plateau area high in the Taurus Mountains (1100 m). The “large male” (NHW 11324, 29 April 1967, leg. F. Ressl) is not from Çamlıayla (= Namrun), as stated by Francke (1981), but from Göksu Valley near Silifke, Mersin, Turkey. This is one of the easternmost localities of *I. kraepelini*, a coastal area ca. 100 km southwest of Çamlıayla, separated by a great wall of the Taurus Mts. Incidentally, these two males are easily distinguished by their chela and hemispermatophore morphology, both illustrated in the present paper.

Movable finger inner denticles (*ID*). As discussed elsewhere, determining the number of inner (*ID*) or outer (*OD*) denticles on the chelal fingers can be quite difficult in *Iurus*, especially when examining sexually mature specimens. First, the median denticle (*MD*) groups, which are oblique and highly imbricated, numbering 14 to 16, are grouped quite close to each other. On sexually mature specimens, this dentition is further obscured by movable finger lobe/fixed finger socket development. The proximal gap, if present, further complicates this issue. Typically, a precise dentition is difficult to determine at the lobe to proximal areas of the fingers. Having stated this, we still tabulated the number of *IDs*

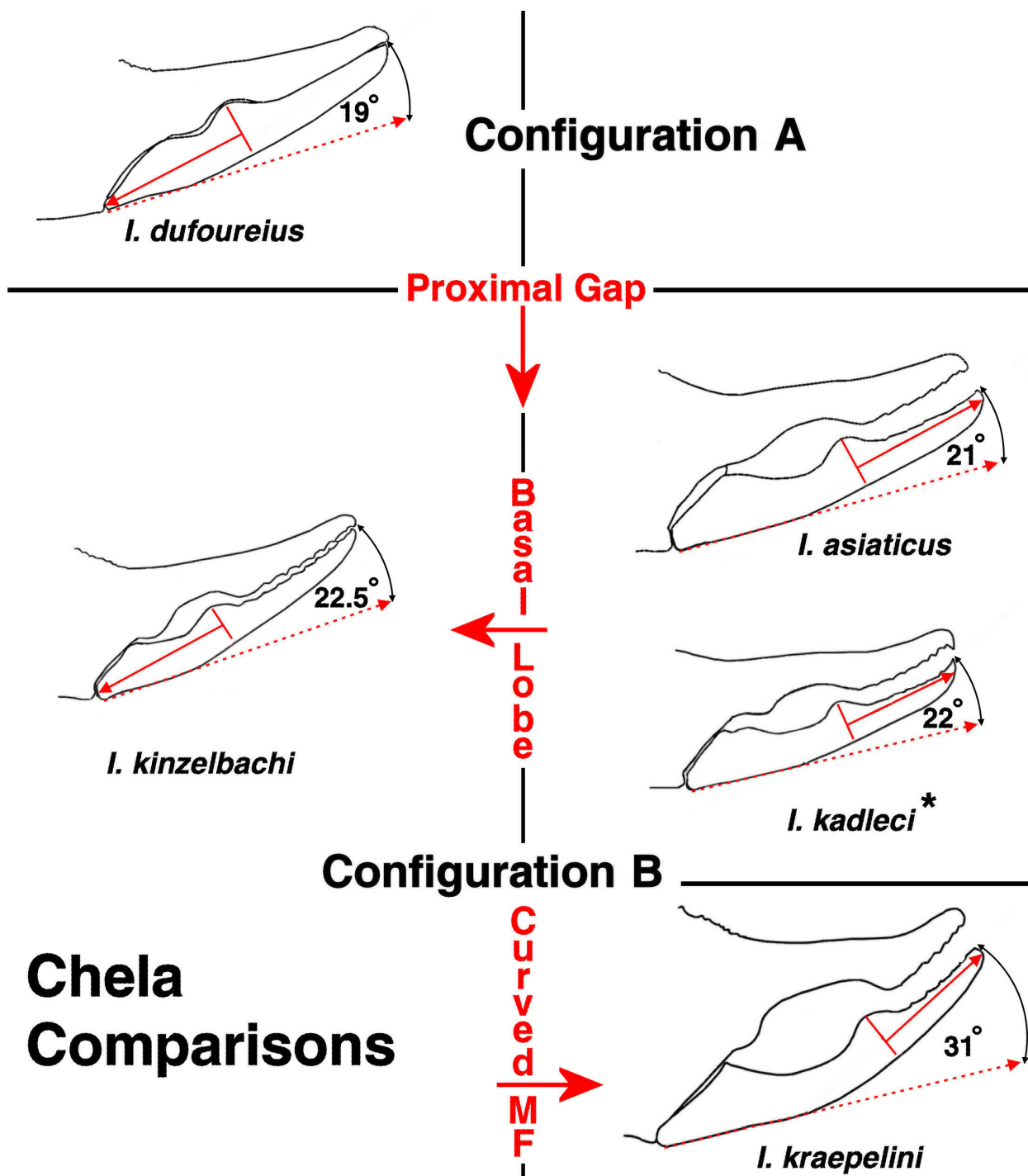


Figure 59: Chelal diagnostic differences in *Iurus* species (drawings rendered from adult males): presence/absence of proximal gap; basal/distal lobe; movable finger degree of curvature. See Figs. 44–55 for definition of terms. * Proximal gap conspicuously present in both male and female *I. kadleci* adults.

on the movable finger to establish a potential species-level diagnostic character. As can be seen from the data (Tab. 1), these ID counts are presented in ranges, and most data was derived from juvenile to subadult material, sexually mature specimens being ignored in

most cases for reasons just stated. We suspect that if only juvenile material was considered, the ID counts would be more stable, showing little variation. We also believe that the higher denticle counts probably most accurately depict the ID counts for the species.

	Number of IDs	MVD
<i>I. dufoureius</i>	14–16 (14.958) (± 0.550) [24] (14.408–15.508)	> 7.1 %, 19.0 %, 28.9 %, 36.0 %
<i>I. kinzelbachi</i>	13–15 (13.966) (± 0.325) [29] (13.640–14.291)	> 11.1 %, 20.4 %, 27.0 %
<i>I. kraepelini</i>	11–14 (12.568) (± 0.691) [88] (11.877–13.260)	> 8.3 %, 14.6 %
<i>I. asiaticus</i>	11–12 (11.600) (± 0.516) [10] (11.084–12.116)	> 5.5 %
<i>I. kadleci</i>	11–11 (11.000) (± 0.000) [1] (11–11)	-

Table 1: Statistical data showing number of inner denticles (*ID*) of the chelal movable finger. Mean Value Differences (MVD) contrast largest *ID* counts with smaller counts. Statistical data group = minimum–maximum (mean) (standard deviation) [number of samples] (standard error range).

Table 1 depicts movable finger *ID* counts for 150+ specimens. Clearly, *I. dufoureius* and *I. kinzelbachi* have the greater number of *IDs* within the genus, their combined means exceeding the other three species by 1.96 denticles. In the SEM micrographs of the movable fingers of *I. dufoureius* (Fig. 20) and *I. kraepelini* (Fig. 19), we see 16 and 12 *IDs*, respectively, based on juvenile to subadult specimens. Interestingly, in Vachon's (1966: figs. 15–16) illustrations of the movable fingers of two *Iurus* specimens, identified as *Iurus dekanum* (Röwer) (the type specimen) and *I. dufoureius*, depicted 16 and 12 *IDs*, respectively. Francke (1981), based on the chelal movable finger lobe, concluded that *I. dekanum* was probably from Greece and was *I. dufoureius*. We agree with Francke's conclusion, based on the basal MF lobe, the absence of a proximal gap, and, germane to this discussion, the presence of 16 *IDs* on the movable finger. We have examined Vachon's specimen of "*I. dufoureius*" from Tarsus, Mersin, Turkey, and have concluded that it belongs to *I. asiaticus* based on its chela and hemispermatophore morphology. In addition, the 12 *ID* shown in Vachon (1966: fig. 16) are consistent with our data in Table 1.

Hemispermatophore morphology

We examined 16 hemispermatophores from 13 specimens (see map in Fig. 60), representing four species. Currently, the hemispermatophore of *Iurus kadleci*, sp. nov., is unknown. With the exception of *I. dufoureius*, at least two specimens were examined per species, and in the case of *I. kraepelini*, six specimens. In the single studied male of *I. dufoureius*, both hemispermatophores were examined. The hemispermatophore is somewhat large in *Iurus*, measuring 10.00–13.15 (11.93) (based on 12 samples). In all cases, all hemispermatophores within a species were consistent in overall morphology and relative morphometrics used for ratio calculations. Of particular interest, we see considerable differences between the four species in hemispermatophore morphology. With these differences alone we can easily differentiate the species.

All three primary components of the hemispermatophore, the trunk, median area, and lamina, are used, in part, to differentiate four *Iurus* species (Fig. 42). The trunks are essentially the same across these species except for the presence/absence of the transverse trunk bolsters (see Fig. 42). *Iurus dufoureius* and *I. kinzelbachi*, sp. nov., exhibit two to four sclerotized transverse trunk bolsters, whereas they are absent in *I. asiaticus* and *I. kraepelini*, sp. nov. The acuminate process, located in the median area, terminates with a highly tapered truncated point in all species except *I. kinzelbachi*, sp. nov., whose process terminus is blunted. Since the acuminate process terminus of *Calchas* is also truncated (see discussion of this elsewhere), we hypothesize here that the blunted terminus is a derived autapomorphy for *I. kinzelbachi*, sp. nov. The hemispermatophore lamina provides several diagnostic differences between the four *Iurus* species. The distal portion of the lamina is either noticeably tapered forming a pointed terminus, as in *I. kraepelini* and *I. asiaticus*, or the lamina edges are essentially subparallel forming a somewhat blunted terminus, as in *I. dufoureius* and *I. kinzelbachi*, sp. nov. The lamina internal nodule is structured differently across all four species. In *I. kinzelbachi*, sp. nov., this nodule is quite subtle, rounded to obsolete. This appearance is further exaggerated by the overall elongation of the lamina and its somewhat subparallel edges. The internal nodule found in *I. dufoureius* is quite conspicuous, its terminus knoblike in appearance. Although the distal portion of the lamina has subparallel edges, the internal nodule is much wider than either the distal or basal portions of the lamina. *Iurus kraepelini* has a wide rounded internal nodule, the lamina tapering considerably distally. The internal nodule of *I. asiaticus* is quite conspicuous, much wider than the lamina base, and forming a point at its terminus. These features are further exaggerated by the highly tapered and somewhat shortened distal aspect of the lamina. Finally, the lamina in *I. asiaticus* is essentially straight on its external edge, with little angling at the internal nodule apex. In the other species, the distal and basal ends of the lamina angle in an external direction, with the distal aspect in *I. kraepelini* sometimes curving back in an internal direction.

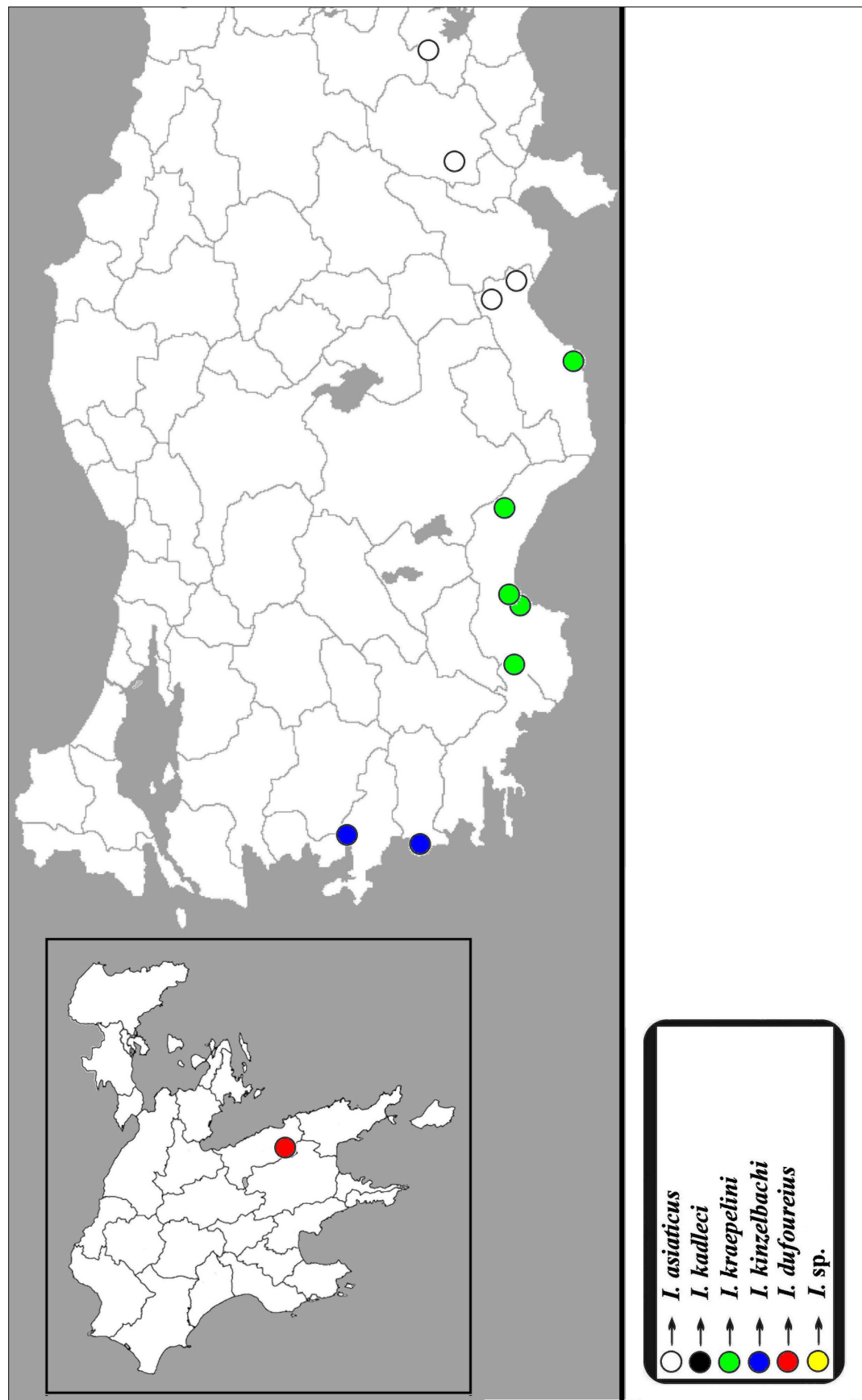


Figure 60: Map showing distribution of examined hemispermatophores across all five species of *Iurus*. As of now, only the hemispermatophore of *Iurus kadleci*, sp. nov., is unknown.

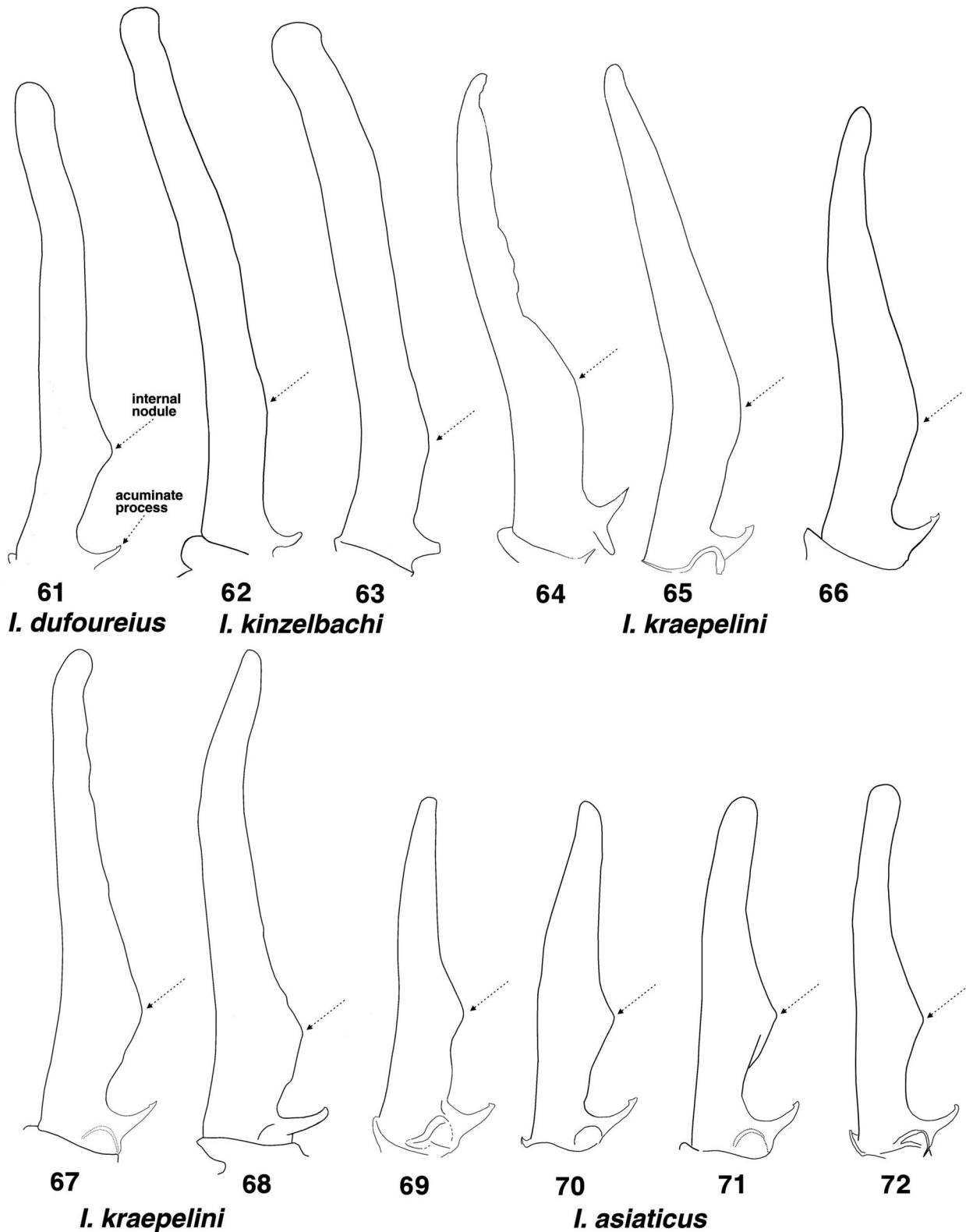


Figure 61–72: Diagrammatic illustrations of the hemispermophore lamina showing the significant differences across *Iurus* species. **61.** *Iurus dufoureius*, Parnon Mountains, Mani, Peloponnese, Greece. **62–63.** *I. kinzelbachi* sp. nov. **62.** Dilek Peninsula, Aydin, Turkey. **63.** Izmir, Izmir, Turkey. **64–68.** *I. kraepelini*. **64.** Antalya, Antalya, Turkey. **65.** Akseki, Antalya, Turkey. **66.** Silifke, Mersin, Turkey. **67.** Buyuk Calticak Village, Antalya, Turkey. **68.** “Taurus”, Turkey. **69–72.** *I. asiaticus*. **69.** Tarsus, Mersin, Turkey. **70.** Kaşlıca, Adiyaman, Turkey. **71.** Yaylaüstü Village, Kahramanmaraş, Turkey. **72.** Çamlıayyla, Mersin, Turkey.

	<i>I. kinzelbachi</i> (2/3)	<i>I. dufoureius</i> (1/2)	<i>I. kraepelini</i> (6/6)	<i>I. kadleci</i> (0/0)	<i>I. asiaticus</i> (4/5)
Acuminate Process Terminus	Rounded	Truncated	Truncated	?	Truncated
Internal Nodule	Weakly rounded to obsolete	Conspicuously developed, terminus knoblike	Widely rounded	?	Conspicuously developed, terminus pointed
Distal Lamina & Terminus	Subparallel, rounded	Subparallel, rounded	Tapered, pointed	?	Tapered, pointed
Transverse Bolsters	Present	Present	Absent	?	Absent
Lam_L / Trunk_L	1.513–1.571 (1.546) [3]	1.370 [1]	0.984–1.221 (1.122) [4]	?	0.884–0.965 (0.921) [5]
Lam_L / AP_W	5.343 [1]	4.255 [1]	3.667–4.362 (3.867) [4]	?	2.865–3.311 (3.130) [5]
Lam_L / Nod_W	8.111–9.293 (8.702) [2]	6.757 [1]	5.000–7.593 (6.315) [4]	?	4.500–5.429 (5.064) [5]
Lam_DL/ Lam_BL	4.313–5.107 (4.710) [2]	3.400	2.159–3.074 (2.564) [4]	?	1.614–1.802 (1.729) [4]
Hemi_L (mm)	12.95–13.15 (13.02) [3]	11.20	10.00–12.75 (11.20) [3]	?	10.90–13.15 (11.86) [5]

Table 2: Diagnostic characteristics of the hemispermatophore in *Iurus* species (hemispermatophore of *I. kadleci*, sp. nov., is unknown). Number pairs below species name are “number of specimens/number of hemispermatophores” examined. Minimum–maximum (mean) [number of samples]. Lam_L = lamina length, Lam_DL = lamina distal length, Lam_BL = lamina basal length, Trunk_L = trunk length, AP_W = acuminate process basal width, Nod_W = internal nodule width, Hemi_L = hemispermatophore length (mm). See Fig. 42 for further definition of terms.

	<i>I. asiaticus</i>	<i>I. kraepelini</i>	<i>I. dufoureius</i>	<i>I. kinzelbachi</i>
Lam_L/Trunk_L	<(21.8 %) kra <(48.8 %) duf <(67.9 %) kin	<(22.1 %) duf <(37.8 %) kin	<(12.8 %) kin	-
Lam_L/AP_W	<(23.8 %) kra <(35.9 %) duf <(70.7 %) kin	<(10.0 %) duf <(38.2 %) kin	<(25.6 %) kin	-
Lam_L/Nod_W	<(24.7 %) kra <(33.4 %) duf <(71.8 %) kin	<(7.0 %) duf <(37.8 %) kin	<(28.8 %) kin	-
Lam_DL/Lam_BL	<(48.3 %) kra <(96.6 %) duf <(172.4 %) kin	<(32.6 %) duf <(83.7 %) kin	<(16.5 %) kin	-

Table 3: Mean Value Differences (MVD) of hemispermatophore morphometrics between *Iurus* species (see Table 2). Species are ordered by smallest to largest ratio values. **kra** = *I. kraepelini*, **duf** = *I. dufoureius*, **kin** = *I. kinzelbachi*. See Table 2 for definition of terms.

Four morphometric ratios (see Tables 2 and 3) were constructed from measurements of the hemispermatophore. These ratios indicate proportions of the lamina length as it relates to trunk length, acuminate process width, internal nodule width, and the lamina distal length as it relates to its basal length. It is interesting to note that, for all four ratios, the species ordering with respect to largest/smallest ratio values are the same.

Ratio values in *I. kinzelbachi*, with the relatively longest lamina, exceeded the other species: 13 to 29 % as compared to *I. dufoureius*, 38 to 84 % as compared to *I. kraepelini*, and 68 to 172 % as compared to *I. asiaticus*. Ratio values in *I. asiaticus*, with the relatively shortest lamina, exceeded *I. kraepelini* by 22 to 48 % and *I. dufoureius* by 34 to 97 %. The shortened lamina, wide pointed internal nodule, and somewhat distally placed

nodule seen in *I. asiaticus* are supported by these ratios. In particular, when the lamina distal length is compared to its basal length, *I. asiaticus* ratio values were smaller by 48 to 172 %, truly significant differences.

Morphometrics

In Appendix C, we present a detailed analysis of the morphometrics of all five *Iurus* species, both males and females, based on 31 sets of measurements. Using these measurements, dominant morphometrics were established across all possible ratio combinations, contrasting each species pair by gender, a total of 20 sets of comparisons (i.e., 6500 ratio comparisons in all). Based on the results of these comparisons, eight morphometric ratios were established that best contrasted the five *Iurus* species (see histograms in Figs. C2–C7). Many of these ratios are used in this study as species diagnostic characters (see key above). We highlight the more important ratios here; refer to Appendix C for a complete discussion.

In the key above we use five morphometric ratios: 1) chelal fixed finger / telson width, 2) chelal movable finger / telson width, 3) metasomal segments I–III, length / width, 4) telson length / telson width, and 5) chela depth / chela length.

Iurus dufoureius and *I. kinzelbachi* can be easily separated by comparing chelal fingers to the width of the telson. These morphometric ratios differ due to the relatively elongated chelal fingers of *I. kinzelbachi* and the somewhat stocky telson vesicle of *I. dufoureius*. Mean Value Differences (MVD) between these species are 27.8 % (male) and 26.1 % (female), for the fixed finger, and 28.5 % (male) and 22.8 % (female), for the movable finger. Compare these MVDs with the histograms shown in Fig. C3.

Iurus kadleci can be separated from all other *Iurus* species by its slender metasoma, all segments longer than wide (male or female). This was even observed in a subadult female. The MVDs for all five metasoma segments are shown in Tab. 8 under the description of *I. kadleci*, and histograms of same are shown in Appendix C (Figs. C4–C5).

Morphometric ratio telson length / telson width is used in the key to separate *I. kadleci* from *I. kraepelini* and *I. asiaticus*. As with the metasoma, the telson in *I. kadleci* is quite slender, the most slender in the genus. The histogram for this ratio is shown in Fig. C6, representing all species. The MVDs for the above-mentioned species are 27.6 % (male) and 24.4 % (female), as contrasted with *I. kraepelini*, and 26.8 % (male) and 21.7% (female), as contrasted with *I. asiaticus*.

The chela in *I. kraepelini* is the most robust in *Iurus*, especially observable in the male. In the key above, the ratio chela depth / chela length is used to differentiate *I.*

kraepelini from *I. asiaticus*, although the histogram shown in Fig. C2 clearly indicates significant separation in this ratio for *I. kraepelini* when compared to all species for both genders. The MVDs when contrasted with *I. asiaticus* are 30.2 % (male) and 15.2 % (female). The large MVD difference between the male and female (i.e., the male difference by far the largest) further illustrates the exaggerated vaulted chelal palm found in sexually mature males of *I. kraepelini*.

Neobothriotaxy

In Appendix B, we summarize neobothriotaxy found in genus *Iurus*, a continuation of the study conducted by Soleglad, Kovařík & Fet (2009). All species, except *I. kadleci* (of which only five specimens have been studied) exhibit some form of neobothriotaxy. In *I. dufoureius* and *I. asiaticus*, neobothriotaxy is quite rare, occurring on only one pedipalp when observed, a total of four accessory trichobothria found in 54 specimens examined in this study. In *I. kraepelini*, neobothriotaxy is observable in many specimens (196 occurrences), and is represented by many neobothriotoxic types, in particular types 1 and 5. These occurrences are found scattered over much of the geographic range of *I. kraepelini*. They, however, do not form any specific pattern of neobothriotaxy that could be used as a definitive characteristic of this species. Only *I. kinzelbachi* exhibits neobothriotaxy that can be considered diagnostic. Four unique neobothrioxic types are exclusively found in *I. kinzelbachi*, one type or more being represented in 80 % of the specimens examined. The large majority of occurrences per specimen and the exclusivity of these occurrences to these four types certainly make it diagnostic for *I. kinzelbachi*. However, since many of these occurrences involve only a single pedipalp, all accessory trichobothria are petite, small petite, or vestigial, and they are absent altogether in 20 % of the specimens, we did not employ neobothriotaxy as a character in the key. Appendix B and the discussion under *I. kinzelbachi* provides additional details of this unique neobothriotaxy.

Pectinal tooth counts

Figure 73 presents pectinal tooth count statistics for all five *Iurus* species, representing over 250 specimens. *Iurus kinzelbachi* and *I. dufoureius* exhibit the lowest number of pectinal teeth, almost a two tooth difference from the other three species, including both genders; difference between means (combined) is 1.86 for male and 1.80 for female. *Iurus kraepelini* has the largest pectinal tooth counts in the genus, exceeding *I. asiaticus* by almost one tooth per gender, 0.96 for male and 0.90 for female. In general, the male exceeds the female by

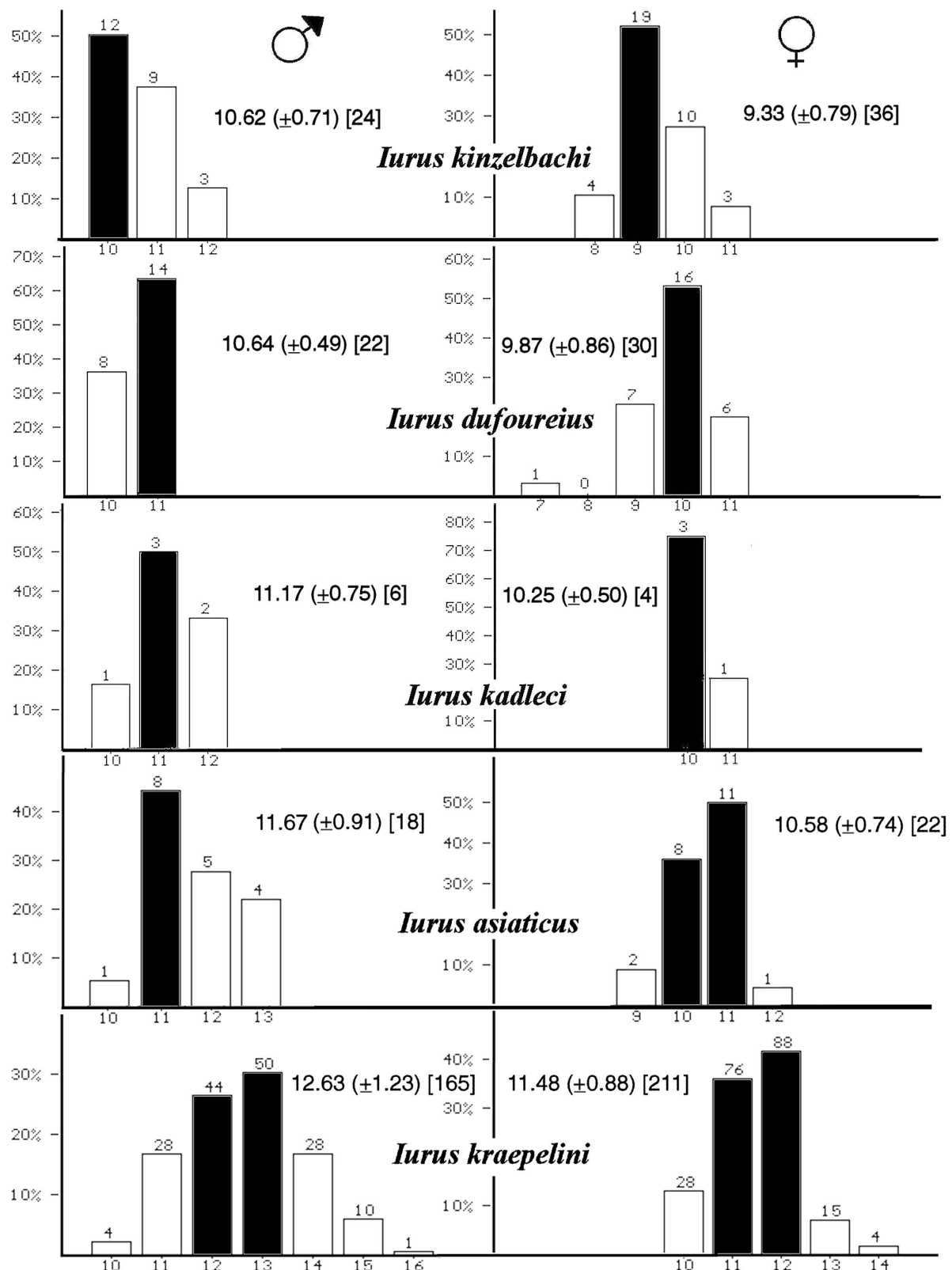


Figure 73: Pectinal tooth counts of *Iurus* based on 269 specimens (excludes specimens from the Greek islands of Karpathos, Rhodes, and Samos). Histograms are ordered by species with the least number of teeth to the largest. Data = mean, standard deviation and number of samples.

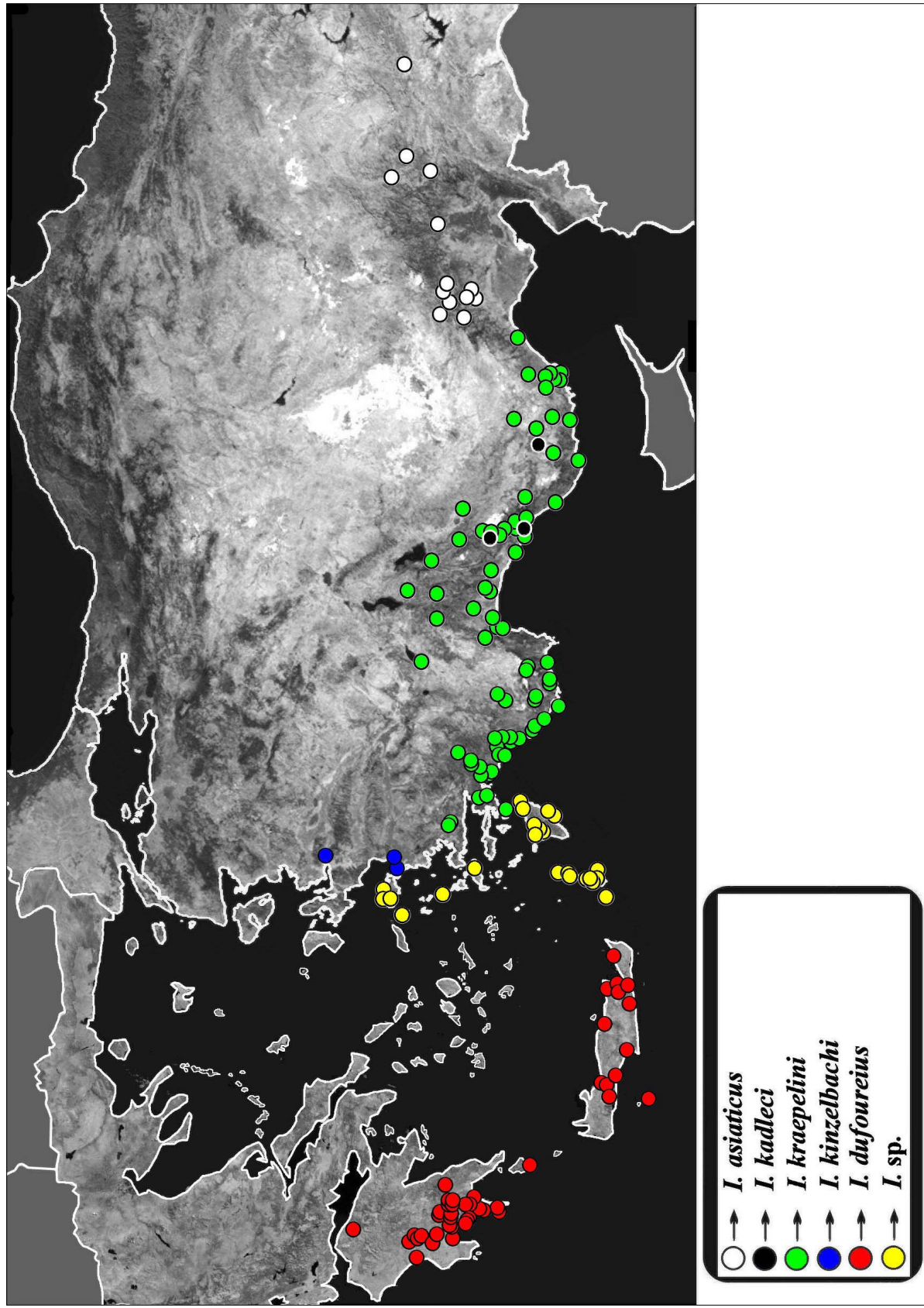


Figure 74: Distribution of genus *Iurus* based on material examined and literature. See Figs. 76, 109, 148, 181, and 201 for large-scale range of individual species and Appendix A for detailed locality data.

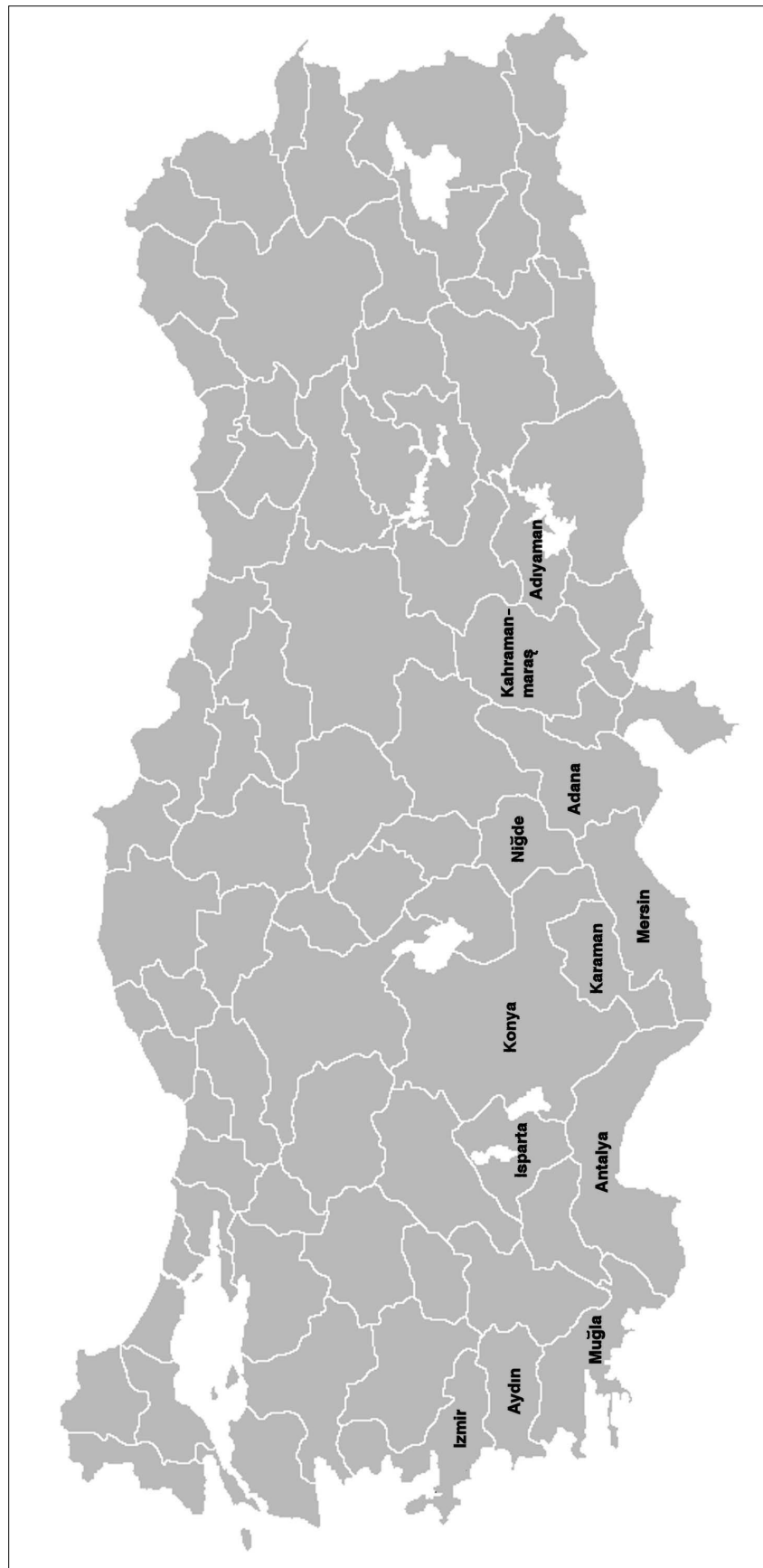


Figure 75: Map of Turkey showing provinces where *Iurus* has been reported. See Appendix A for detailed information.

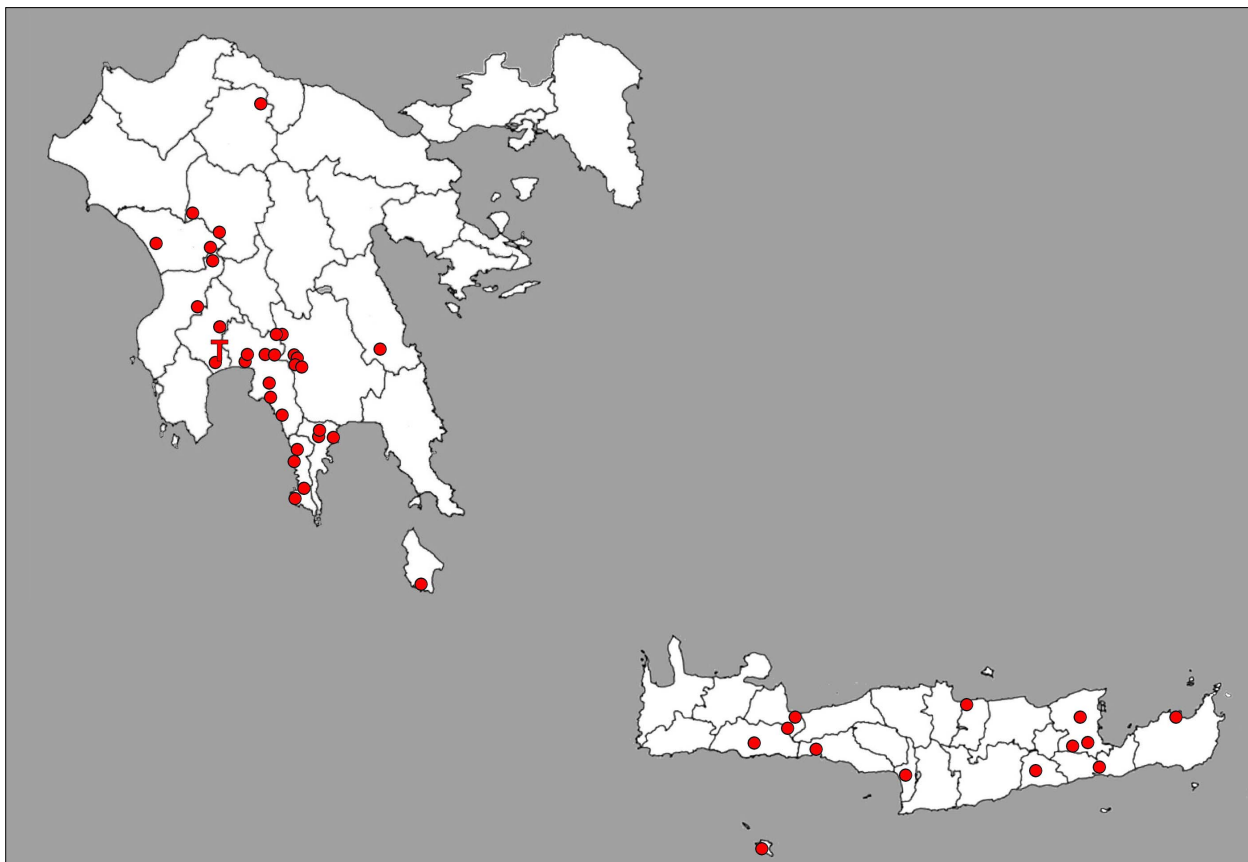


Figure 76: Large-scale map showing distribution of *Iurus dufoureius*. "T" marks type locality, Messini, Messini District, Peloponnese. See Fig. 74 for distribution of all species and Appendix A for detailed locality data.

approximately one tooth difference, from 0.77 in *I. dufoureius* to 1.29 in *I. kinzelbachi*.

Species Descriptions

In the map presented in Fig. 74, all reported localites (see Appendix A) of the five species of *Iurus* are plotted, as well as the eastern Greek island specimens, designated in this paper as *Iurus* sp. Under the individual species descriptions, large-scale maps are provided for each species. Fig. 75, which depicts the many provinces of Turkey, indicates the twelve provinces where *Iurus* has been reported.

Iurus dufoureius (Brullé, 1832)

(Figs. 1, 4, 9, 10, 11, 14, 16, 17, 20, 21, 31, 33, 34, 38, 44–47, 60, 61, 73, 74, 76–93, 97–101; Tabs. 1–4)

Buthus dufoureius Brullé, 1832: 57, tab. XXVIII, fig. 1; type locality: GREECE, Peloponnese ("Morée"), Messina (now Messini); holotype lost.

SYNONYMS:

Buthus granulatus C. L. Koch, 1837: 46–49, Taf. CXXII, fig. 279. Greece, Peloponnese ("Morea") (synonymized by Karsch, 1879: 102).

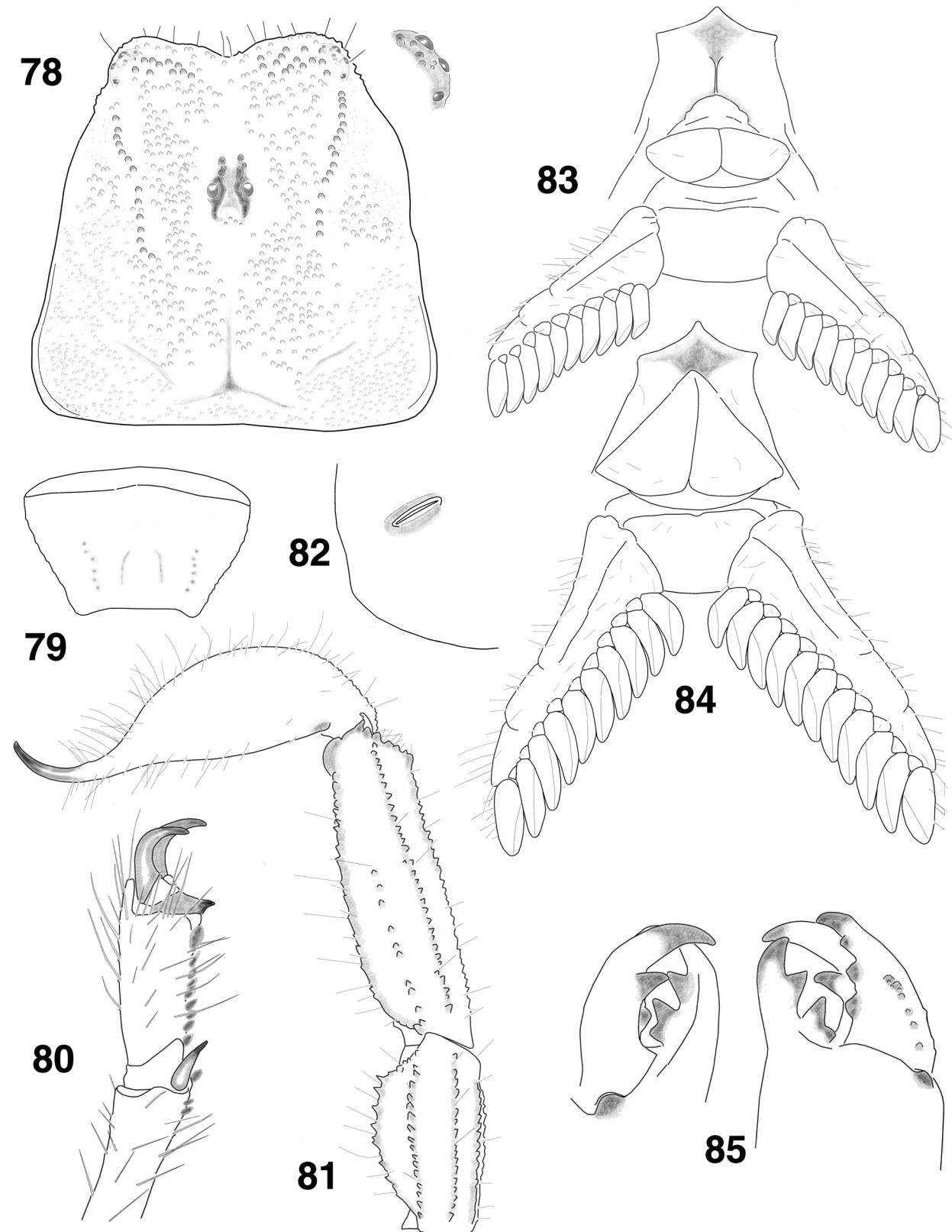
Chaerilomma dekanum Roewer, 1943: 238–240, pl. 6, fig. 11, 11a–e (synonymized by Francke, 1981: 222; genus *Chaerilomma* synonymized with *Iurus* by Vachon, 1966a). Holotype male, SMF RII/8895 ("Anamalai Hills, Deccan, India"; type locality incorrect).

REFERENCES:

- Androctonus dufoureius*: Gervais, 1844: 43.
- Buthus granulatus*: Gervais, 1844: 60; C. L. Koch, 1850: 88
- Scorpius gibbus* (nec *Buthus gibbosus* Brullé, 1832; incorrect subsequent spelling and misidentification): Lucas, 1853: 527.
- Iurus granulatus*: Thorell, 1876: 4; Thorell, 1877: 193–195 (in part; Greece).
- Buthus europaeus* (nec *Scorpio europaeus* Linnaeus, 1578; misidentification): Pavesi, 1877: 324.
- Iurus gibbosus* (nec *Buthus gibbosus* Brullé, 1832; misidentification): Pavesi, 1878: 360–361 (in part); Simon, 1879: 115.
- Iurus* (incorrect subsequent spelling) *dufoureius*: Karsch, 1879: 102 (in part); Karsch, 1881: 90; Simon, 1884: 351; Kraepelin, 1894: 183–185, fig. 79, 86, 89 (in part); Birula, 1898: 135 (in part); Birula, 1903: 297–298



Figure 77: *Iurus dufoureius*, female neotype. Nedontas River, between Artemisia and Kalamata, Peloponnese, Greece.



Figures 78–85: *Iurus dufoureius*. **78–83.** Female neotype, Nedontas River, Peloponnese, Greece. **84–85.** Male, Selinitsa, Peloponnese, Greece. **78.** Carapace and close-up of lateral eyes. **79.** Sternite VII. **80.** Tarsus and partial basitarsus, right leg IV. **81.** Telson and metasomal segments IV–V, lateral view. **82.** Stigma, right II. **83.** Sternopectinal area. **84.** Sternopectinal area. **85.** Right chelicera, ventral and dorsal views.

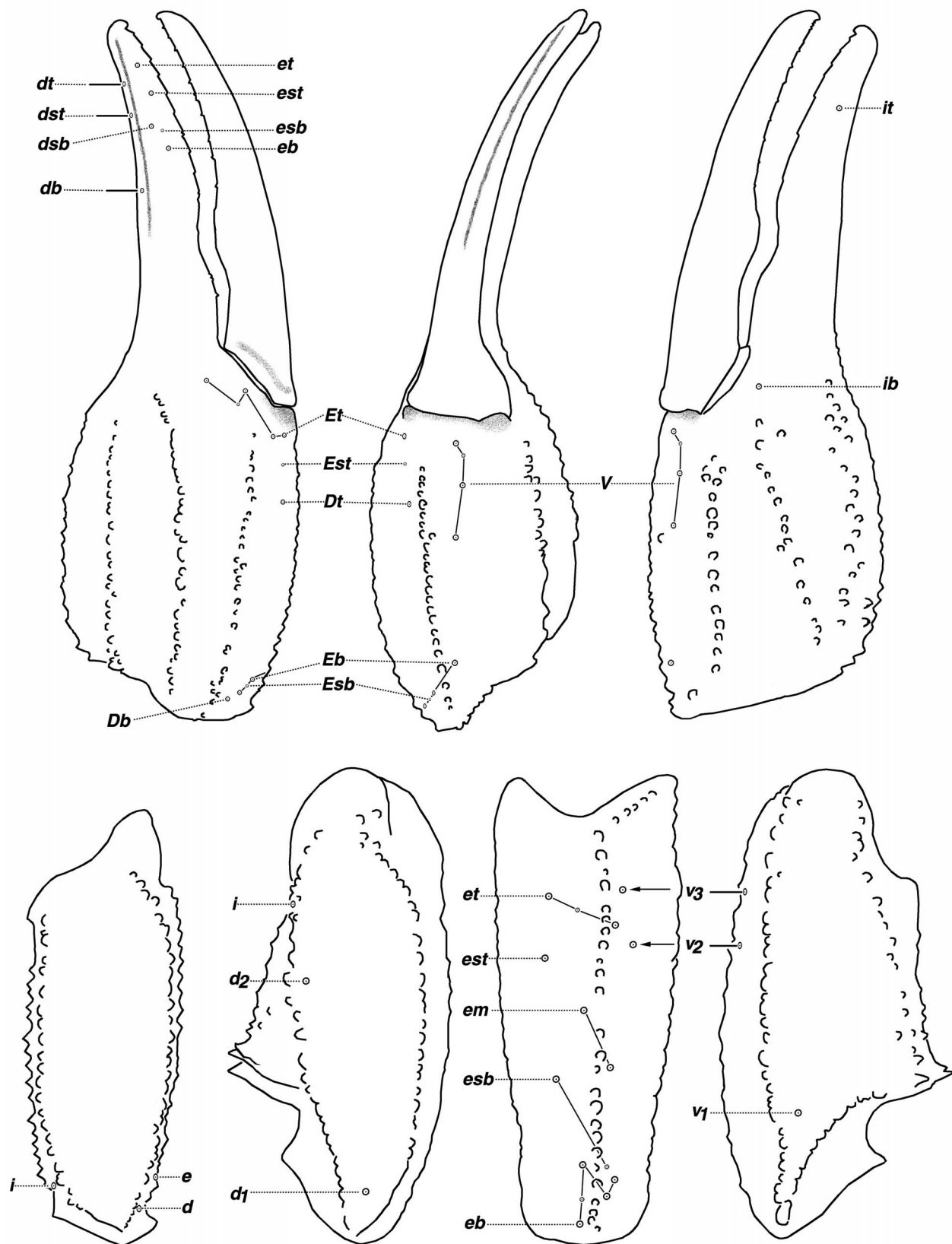


Figure 86: Trichobothrial pattern of *Iurus dusourei* sp. nov., female neotype. Nedontas River, Peloponnese, Greece.

(in part); Penther, 1906: 62–64; von Ubisch, 1922: 503; Werner, 1934a: 162 (in part); Werner, 1934b: 282; Werner, 1937: 136 (Kythira); Werner, 1938: 172 (in part); Vachon, 1948: 62–63 (in part); Vachon, 1953: 96–100 (in part).

Iurus dufoureius: Kraepelin, 1899: 179 (in part); Werner, 1902: 605 (in part?); Caporiacco, 1928: 240; Stahnke, 1974: 123 (in part); Vachon, 1974, fig. 141, 144, 151–153, 216–219 (in part?); Kinzelbach, 1975: 21–26 (in part); Francke, 1981: 221–224, fig. 1–2; Kinzelbach, 1982: 58 (in part); Kinzelbach, 1985: Map IV (in part); Kovařík, 1992: 185; Krtscher, 1993: 382; Crucitti, 1995a: 1–12, fig. 6–9; Crucitti, 1995b: 91–94, fig. 1–2; Crucitti, 1998: 31–43, fig. 2–5; Crucitti & Malori, 1998: 133; Kovařík, 1998: 136 (in part); Crucitti, 1999b: 251–256; Kovařík, 1999: 40; Fet, 2000: 49 (in part); Fet & Braunwalder, 2000: 18 (in part); Sissom & Fet, 2000: 419–420 (in part); Stathi & Mylonas, 2001: 290 (in part); Kovařík, 2002: 17; Fet et al., 2004: 18 (in part); Kovařík, 2005: 55 (in part); Peslier, 2005: 28–29; Glushkov et al., 2006: 290; Fet & Soleglad, 2008: 256 (in part); Kaltsas, Stathi & Fet, 2008: 228 (in part); Soleglad, Kovařík & Fet, 2009: 2–3 (in part), fig. 2, 10 (in part), 15 (in part); Fet, 2010: 8.

Iurus dekanum: Vachon, 1966a: 453–461, fig. 1–6, 13, 15, 17, 19–21.

Iurus asiaticus: Francke, 1981: 221–224 (in part; Crete).

Iurus dufoureus (incorrect spelling): Kučera, 1992: 175.

Iurus dufoureius dufoureius: Sissom & Fet, 2000: 420; Parmakelis et al., 2006: 253; Facheris, 2007a: 1–2; Facheris, 2007b: 1–2; Kamenz & Prendini, 2008: 43.

Iurus dufoureius asiaticus: Sissom & Fet, 2000: 420 (in part).

Neotype (designated here): ♀ (NHMW), GREECE, Peloponnese: Messinia Prefecture, Artemisia District, Nedontas River valley, between Artemisia and Kalamata, 29 July 1995, leg. P. Crucitti. The neotype is designated from the closest available locality to Messini. Its designation is warranted by a complicated taxonomic situation in *Iurus*, which is clarified in the present revision.

Diagnosis. Medium to large species, 90 mm. Dark gray to black in overall coloration. Pectinal tooth counts somewhat low, 10–11 (10.64) males, 7–11 (9.87) females. Chelal movable finger lobe in adults located on basal half, lobe ratio 0.38–0.46; proximal gap of fixed finger absent in males and females, juvenile or adult; movable finger of adult males essentially straight, not highly curved; number of inner denticles (*ID*) of chelal movable finger largest in genus, 14–16 (15); constellation array with six sensilla; hemispermatophore lamina with conspicuous knoblike internal nodule

positioned basally, transverse trunk bolsters present, lamina distal length / lamina basal length 3.4, terminus of acuminate process truncated. Dominant morphometrics are telson width and depth (see Appendix C).

Distribution. Greece: Peloponnese, Crete, Kythira, Gavdos. See map in Fig. 76 for large-scale distribution of this species.

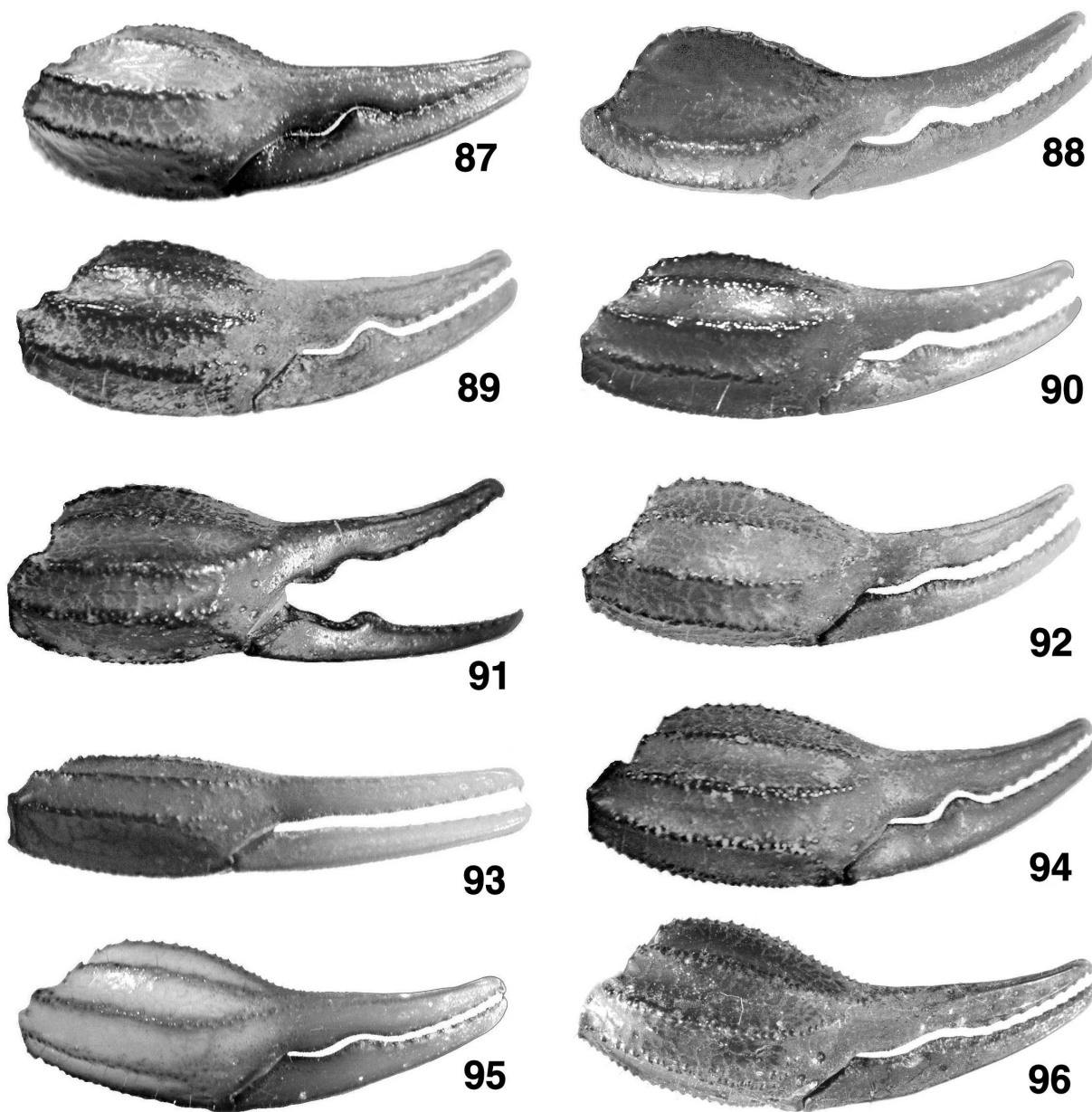
FEMALE. Description based on neotype female from Nedontas River, between Artemisia and Kalamata, Peloponnese, Greece. Measurements of the holotype plus two other specimens are presented in Table 4. See Figure 77 for a dorsal and ventral view of the female neotype.

COLORATION. Basic color of carapace, mesosoma, metasoma, telson, and pedipalp dark brown; legs lighter brown; carinae of metasoma and pedipalps dark gray to black; sternites, pectines, basal piece and genital operculum medium brown; cheliceral fingers dark brown, palms orange-yellow; eye tubercles black. Essentially void of patterns except for darker carinae on carapace.

CARAPACE (Fig. 78). Anterior edge with a conspicuous median indentation, approximately 14 irregularly sized and placed setae visible; anterior area between lateral eyes covered with enlarged granules; the most of the median area densely populated with smaller granules; smaller petite granules found on the posterior lateral areas. Mediolateral ocular carinae well-developed and with enlarged granules, extending to the lateral eyes; three lateral eyes are present, the posterior eye the smallest and somewhat removed from the others. Median eyes and tubercle somewhat small, positioned anterior of middle with the following length and width formulas: 481|1220 (anterior edge to medium tubercle middle |carapace length) and 142|1060 (width of median tubercle including eyes|width of carapace at that point).

MESOSOMA (Figs. 79, 82). Tergites I–VI densely populated with small granules; tergite VII densely granulose, lateral carinae serrated, median carinae not detectable or obscured by heavy granulation. Sternites III–VI smooth and lustrous; VII with one pair of weakly, irregularly granulated lateral carinae and one pair of smooth median carinae (Fig. 79). Stigmata (Fig. 82) are medium in size and slit-like in shape, angled 45° in an anterointernal direction.

METASOMA (Fig. 81). Segment I wider than long. Segments I–IV: dorsal and dorsolateral carinae serrated; dorsal carinae with 7/12, 9/13, 11/11, and 10/10 serrated



Figures 87–96: Chela, lateral view, adults unless stated otherwise. 87–93. *Iurus dufourei* and 94–96. *Iurus* sp. from Greek Islands. 87. Male, Parnon Mountains, Greece. 88. Male, Selinitsa, Greece. 89. Male, Gythio, Greece. 90. Subadult male, Krini, Greece. 91. Female, Crete, Greece. 92. Female neotype, Nedontas River, Greece. 93. Juvenile female, Mystras, Greece. 94. Male, Rhodes, Greece. 95. Subadult male, Karpathos, Greece. 96. Female, Samos, Greece. Note the movable finger lobe is positioned quite proximal of finger midpoint and the fixed finger proximal gap is absent in male and female, adult, subadult, or juvenile.

spines (left/right carina); dorsal (I–IV) and dorsolateral (I–III) carinae do not terminate with an enlarged spine; lateral carinae serrated on I, serrated on posterior one-third on II, traces of granulation on III, and absent on segments IV; ventrolateral carinae smooth to granulated on I–III and crenulated on IV; ventromedian carinae smooth to granulated on I–III, and crenulated on IV. Dorsolateral carinae of segment IV terminates at arti-

culation condyle. Segment V: dorsolateral carinae serrated; lateral carinae irregularly serrated for three-fifths of posterior aspect; ventrolateral and single ventromedian carinae serrated; ventromedian carina terminus irregular. Anal arch with 15 serrated granules. Intercarinal areas of segments I–V essentially smooth. Segments I–V with scatter setae ventrally, dorsally, and laterally.

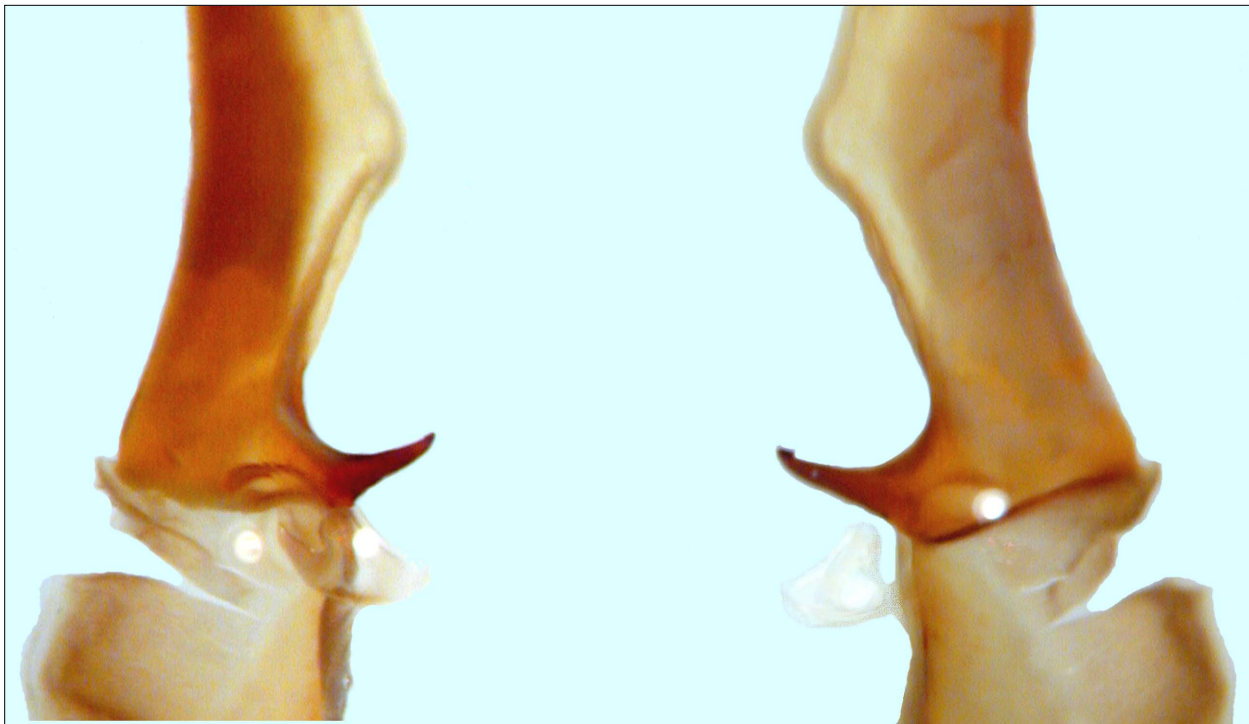


Figure 97: Close-up of median area of left hemispermatophore, ventral and dorsal views, *Iurus dufoureius*, Parnon Mountains, Peloponnese, Greece.

TELSON (Fig. 81). Vesicle somewhat bulbous with highly curved aculeus. Vesicle with slight granulation on ventral proximal area; ventral surface with several medium to long curved setae, dorsal setation less dense, irregularly scattered; base of aculeus with setation ventrally and dorsally, slightly enlarged setal pair located on aculeus midpoint, areolae area moderately swollen. Vesicular tabs smooth.

PECTINES (Fig. 83, 84). Well-developed segments exhibiting length|width formula 910|380 (length taken at anterior lamellae|width at widest point including teeth). Sclerite construction complex, three anterior lamellae and one large middle lamellae with slight indications of a smaller sclerite; fulcra of medium development. Teeth number 10/10. Sensory areas developed along most of tooth inner length on all teeth, including basal tooth. Scattered setae found on anterior lamellae and distal pectinal tooth. Basal piece large, with subtle swallow indentation along anterior edge, length|width formula 310|510.

GENITAL OPERCULUM (Fig. 83). Sclerites elongate, wider than long, connected for entire length except for a swallow medial indentation on proximal edge (see discussion on male below).

STERNUM (Fig. 83). Type 2, posterior emargination present, well-defined convex lateral lobes, apex visible but not conspicuous; conspicuous membranous plug situated proximally between lateral lobes; sclerite wider than long, length|width formula 280|325; sclerite tapers anteriorly, posterior-width|anterior-width formula 325|245 (see discussion on male below).

CHELICERAE (Fig. 85). Movable finger dorsal edge with one large subdistal (*sd*) denticle; ventral edge with one large pigmented accessory denticle at finger midpoint; ventral edge serrula not visible. Ventral distal denticle (*vd*) slightly longer than dorsal (*dd*). Fixed finger with four denticles, median (*m*) and basal (*b*) denticles conjoined on common trunk; no ventral accessory denticles present.

PEDIPALPS (Figs. 86, 92). Well-developed chelae, with medium length fingers, heavily carinated, inconspicuous scalloping on chelal fingers: weakly developed lobe on movable finger, positioned proximal of midpoint in ratio 0.414; proximal gap absent on fixed finger, socket matching movable finger lobe exactly. **Femur:** Dorsointernal, dorsoexternal and ventrointernal carinae serrated, ventroexternal serrated on basal one-half. Dorsal and ventral surfaces irregularly granulated, internal and external surface with line of 18 and 18+

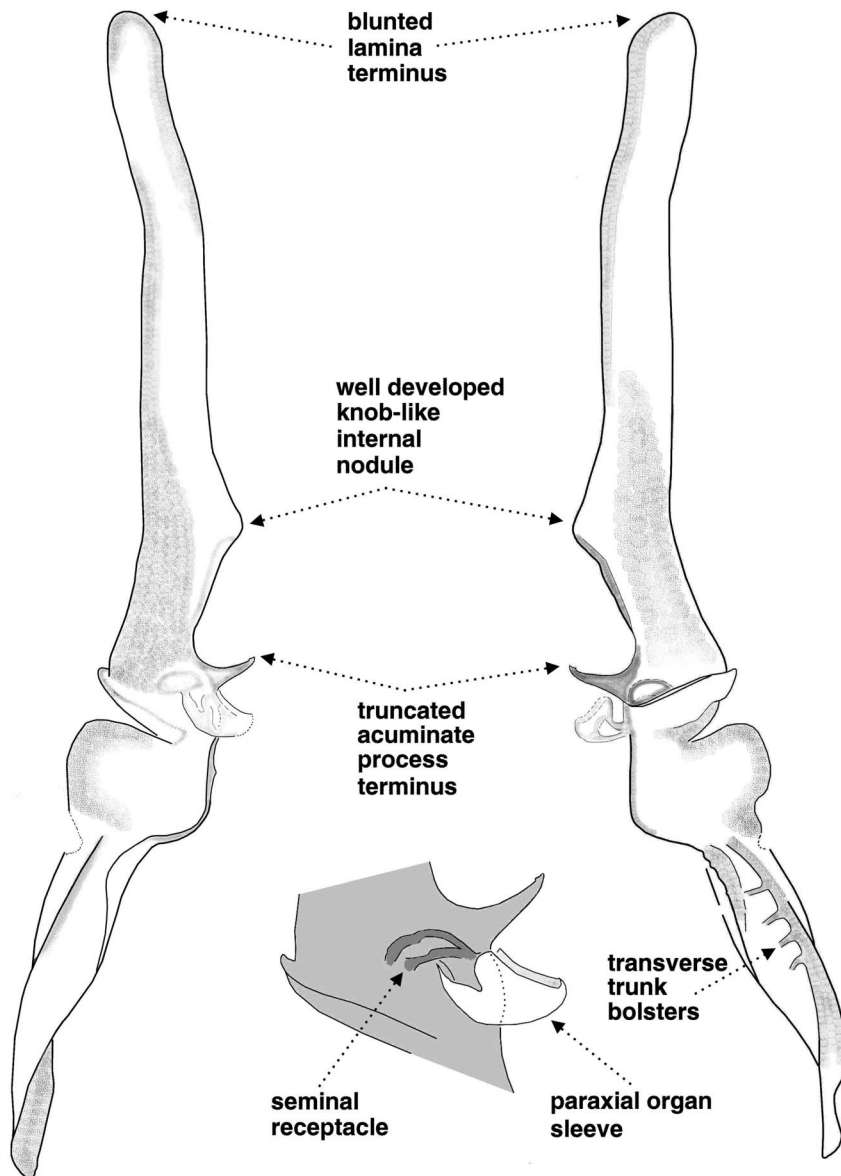


Figure 98: Left hemispermophore of *Iurus dufoureus*, Parnon Mountains, Peloponnese, Greece. **Left & Right.** Ventral and dorsal views. Diagnostic of this species is the blunted lamina terminus, a well developed knob-like internal nodule, transverse trunk bolsters, and a truncated acuminate process terminus. **Bottom.** Close-up of the attachment of the paraxial organ sleeve to the seminal receptacle.

serrated granules, respectively. **Patella:** Dorsointernal and dorsoexternal carinae serrated, ventrointernal and ventroexternal crenulated, and exteromedian carina strong, crenulated to serrated, and single. Dorsal surface rough with slight medial granulation and ventral surface smooth; external surface smooth with serrated exteromedian carina; internal surface smooth with well-developed, doubled DPS and VPS. **Chelal carinae:** Complies with the “8-carinae configuration”. Digital (*D1*) carina strong, granulated; dorsosecondary (*D3*) granulated; dorsomarginal (*D4*) serrated; dorsointernal (*D5*) irregularly serrated; ventroexternal (*V1*) strong, crenulated to serrated, terminating to external condyle of movable finger; ventrointernal (*V3*) serrated, continuous to internal condyle; external (*E*) strong, continuous, and crenulated to serrated; internal (*I*) serrated. **Chelal finger dentition:** Median denticle (*MD*) row groups

oblique and highly imbricated, numbering 16/16; 13/13 *IDs* on fixed finger and 15/15 *IDs* on movable finger; 14/14 *ODs* on fixed finger and 16/16 *ODs* on movable finger. No accessory denticles present. **Trichobothrial patterns** (Fig. 86): Type C, orthobothriotaxic, typical of genus.

LEGS (Fig. 80). Both pedal spurs present on all legs, lacking spinelets; tibial spurs absent. Tarsus with conspicuous spinule clusters in single row on ventral surface, terminating distally with a pair of enlarged spinule clusters. Unguicular spine well-developed and pointed.

HEMISPERMATOPHORE (Figs. 97–98). The hemispermophore description is based on a specimen from Parnon Mountains, Peloponnese, Greece. The hemi-

	<i>Iurus dufourei</i> (Brullé, 1832)		<i>Iurus</i> sp.	
	Nedontas River, Greece	Selinitsa, Greece	Crete, Greece	Rhodes, Greece
	Female Neotype	Male	Female	Male
Total length	86.50	75.45	72.85	72.80
Carapace length	12.20	10.35	11.85	10.70
Mesosoma length	27.95	20.50	17.80	22.85
Metasoma length	33.65	32.40	31.10	27.80
Segment I length/width	4.30/5.40	4.10/4.85	4.00/4.75	3.65/4.25
Segment II length/width	5.35/4.65	5.15/4.30	4.75/4.20	4.30/3.85
Segment III length/width	5.75/4.20	5.55/3.85	5.20/4.00	4.75/3.60
Segment IV length/width	6.80/3.70	6.80/3.60	6.35/3.60	5.60/3.25
Segment V length/width	11.45/3.85	10.80/3.65	10.80/3.35	9.50/3.00
Telson length	12.70***	12.20	12.10	11.45
Vesicle length	8.65	8.55	8.00	8.00
width/depth	4.10/3.55	3.85/3.40	4.10/3.80	3.45/3.10
Aculeus length	4.05***	3.65	4.10	3.45
Pedipalp length	45.50	40.50	44.95	40.37
Femur length/width	11.20/4.25	10.15/3.35	11.35/4.00	10.25/3.35
Patella length/width*	11.10/3.90 1.60	9.95/3.65 1.08	10.80/4.30 1.50	9.80/3.85 1.20
Chela length	23.20	20.40	22.80	20.32
Palm length width/depth	10.25 6.50/7.55	9.30 5.80/7.00	10.25 6.25/7.85	10.00 5.60/7.35
Fixed finger length	11.10	10.05	11.10	9.90
Movable finger length	14.00	12.30	13.80	11.10
Pectines teeth middle lamellae	10-10 5-5	11-10 6-5	9-7 4-4	11-11 1-1++
Sternum length/width	2.80/3.25	2.15/2.35	2.40/2.70	2.15/2.35

Table 4: Morphometrics (mm) of *Iurus dufourei* (Brullé, 1832). Note, male specimen from Rhodes is included because it shares many of the morphological diagnostic characters of *I. dufourei*. * Patella width is widest distance between the dorsointernal and externomedial carinae. ** DPS height is from tip of spines to dorsointernal carina center. *** Tip broken, length extrapolated.

spermatophore of *I. dufourei* is unique among *Iurus* species, exhibiting a rounded terminus on the lamina, a strong conspicuous knoblike internal nodule, presence of transverse trunk bolsters, and a truncated acuminate process terminus (see below for more data).

Male and female variability. As seen in Figures 87 and 92, the movable finger lobe in the adult female neotype is not as developed as in the male. Interestingly, however, this lobe is well-developed in the adult female from Crete. Whether this is indicative of this island population remains to be seen; additional material needs to be examined. There is no significant sexual dimorphism involving morphometrics. Though statistically the male has a thinner metasoma, the MVDs exhibited (L/W) were minimal, only ranging 0.0 to 3.6 %. Pectinal

tooth counts in males exceed those of females by less than one tooth (0.77), male 10–11 (10.64) [22], female 7–11 (9.87) [30] (see histograms in Fig. 73). The genital operculum of the male is significantly different from that found in the female (Figs. 83–84). The sclerites, subtriangular in shape, are as long as or longer than wide in the male, whereas in the female the sclerites are short and wide, more than twice as wide as long. Whereas the sclerites are fused medially in the female, they are separated along their entire length in the male, exposing significantly developed genital papillae. The enlarged genital operculum of the male extends distally between the lateral lobes of the sternum partially obscuring its proximal region. Figures 77 and 99 show dorsal and ventral views of both male and female specimens from the Peloponnese; Figure 100 shows the dorsal view of a female from the island of Crete, and Figure 101 a live



Figure 99: *Iurus dufoureius*, Adult male. Selinitsa, Gythio, Peloponnese, Greece.

female specimen from the Peloponnese. Figures 105–106 show collection localities of *I. dufoureius*.

Discussion

Unique to this species is the lack of a proximal gap in the adult male and female, the movable finger lobe fitting exactly into the fixed finger socket. The movable finger is slightly curved, forming an angle with its base of approximately 20°. *I. dufoureius* has the most proximally positioned movable finger lobe in the genus, slightly less than that seen in *I. kinzelbachi*. The

movable finger lobe ratio is slightly larger in the male than the female, 0.38–0.46 vs. 0.39–0.42 (ratios calculated from adults with carapaces 10 mm or larger; see scatter chart in Fig. 56 for a complete analysis of this character). It is important to note here that we were able to verify the sexual maturity of a male specimen lacking a proximal gap since it also contained hemispermatophores, which were dissected. The chela morphology of this male specimen is illustrated in Figs. 87–89, showing all the diagnostic characters just described.

I. dufoureius, statistically, has the second smallest number of pectinal teeth (Fig. 73); *I. kraepelini*, with the



Figure 100: *Iurus dufoureius*, adult female. Crete, Greece.

largest number of teeth, averaging roughly two more pectinal teeth per gender than *I. dufoureius*.

The hemispermatophore of *I. dufoureius* has been examined from a single specimen from the Parnon Mountains, Greece (see map in Fig. 60). Although only a single specimen was found with a hemispermatophore, both left and right structures were examined and complete consistency was found in both. The lamina is

quite elongated, at least 1.35 times longer than the trunk (see Table 2), the second longest lamina in the genus (only exceeded by *I. kinzelbachi*). The lamina terminus is somewhat blunted, not pointed due to the somewhat subparallel lamina edges. Unique in this hemispermatophore is the conspicuous knoblike internal nodule, which is situated basal on the lamina, in a ratio 3:4, exceeding other species hemispermatophores by at least



Figure 101: *Iurus dufoureius*, adult female, Areopolis, Peloponnese, Greece.



Figure 102: *Iurus* sp., Adult male. Rhodes, Greece.



Figure 103: *Iurus* sp., immature. Rhodes, Greece.

33 % (except for *I. kinzelbachi*, which has the most proximal nodule). The acuminate process terminus is truncated as in most other *Iurus* species. Transverse trunk bolsters are present, four in number. The paraxial organ sleeve was present (Fig. 97–98), its attachment to the seminal receptacle is as found in other species.

In Appendix C, we present a complete analysis of the morphometric trends across the five species of *Iurus*.

From this analysis, we see that the telson width and depth in *I. dufoureius* dominated in a large majority of morphometric ratio comparisons: averaging 17 and 20 comparisons out of 25 for the male and 23 and 22 for the female. To accompany this somewhat heavy telson is its relative shortness, only dominating between 7 and 11 ratio comparisons. Figure C6 in Appendix C presents the histograms of the telson width and depth as compared to



Figure 104: *Iurus* sp., dorsal and ventral views. Adult female (FKCP), Agios Nikolaos, 3 km west of Karlovasi, Samos, Greece.



Figure 105: Collection locality of *Iurus dufoureius*, Areopolis, Oitylo District, Laconia Prefecture, Mani Peninsula, Peloponnese, Greece.



Figure 106: Collection locality of *Iurus dufoureius*, Areopolis, Oitylo District, Laconia Prefecture, Mani Peninsula, Peloponnese, Greece.

its length. Although *I. dufoureius* exhibits the smallest ratio values in the genus (implying a stocky telson), it does cluster somewhat with species *I. kraepelini* and *I. asiaticus*. The relatively stocky telson seen in *I. dufoureius* is visible when compared to other *Iurus* species, see Figs. 35–40.

Soleglad, Kovařík & Fet (2009) reported two cases of neobothriotaxy in *I. dufoureius*. During this current study we isolated one more example of accessory trichobothria in this species. These three instances of neobothriotaxy are found in three different areas of the pedipalp, on the fixed finger internal surface, in the *E₁* series of the chelal palm, and on the patella external surface. These three cases are assigned unique neobothriotaxic types (types 3, 6, and 13) because their specific positions on the pedipalp are not matched in the other four species of *Iurus*. See Appendix B for details on this neobothriotaxy.

Material Examined (51 specimens). GREECE: Peloponnese: Arcadia Prefecture, Megalopolis District, Kastriti, Likosoura, 31 July 1995, 1 ♂, 1 ♀, leg. P. Crucitti (VFWV); Ilia Prefecture, Minthi Oros Mts., Zacharo District, Kurtaina (near Kalidona), 1 ♂, 13 August 1995, 1 ♂, 20 August 1995, leg. P. Crucitti (VFWV); Laconia Prefecture, Gythio District, Krini, 16 August 1995, 1 ♂, 1 ♂ sbad., 2 ♀, 14 August 1995, 1 ♀, leg. P. Crucitti (VFWV); Laconia Prefecture, Gythio District, Selinitsa, 1 ♂, 30 July 1995, 1 ♂, 1 ♀, 3 August 1995, 1 ♀, 9 August 1995, leg. P. Crucitti (VFWV); Laconia Prefecture, Mani Peninsula, Oitylo District, Areopolis, 30 April 1991, 1 ♂, leg. P. Rejsek (FKCP), June 1992, 1 juv., leg. P. Krásenský (FKCP); Laconia Prefecture, Mani Peninsula, Mina, 10 May 1965, 1 ♂, 1 ♂ juv., leg. E. Kristscher (NHMW 15920.1-2); Laconia Prefecture, Mani Peninsula, Parnon Mts., 10 September 2002, 1 ♂, leg. I. Stathi (MCNH 81.1.5.15, donated to MESB); Laconia Prefecture, Mystras District, Anavriti, 17 August 1995, 1 ♀, 1 ♂ juv., leg. P. Crucitti (VFWV); Laconia Prefecture, Mystras District, Kalivia Sohas, 10 August 1995, 2 ♀, 16 embryos; leg. P. Crucitti (VFWV); Laconia Prefecture, Mystras District, Mystras, 18 September 1983, 1 ♂, leg. P. Beron & S. Beshkov (SOFM 68); same locality, July 1990, 4 juv. (FKCP), 1 juv. (NMPC), leg. I. Šklíba; Messinia Prefecture, Artemisia District, Nedontas River, between Artemisia and Kalamata, 29 July 1995, 1 ♀, leg. P. Crucitti (**neotype**; NHMW); 1 ♀, leg. P. Crucitti (VFWV); Messinia Prefecture, Artemisia District, Nedontas River, 13 km from Kalamata, 10 August 1995, 1 ♂, leg. P. Crucitti (VFWV); Laconia Prefecture, Artemisia District, Taygetos Mts., 31 May 1984, 1 ♂ juv. leg. E. Kristscher (NHMW 15918). Crete: Vianos (=Viano), 25 April 1887, 1 ♀, leg. E. von Oertzen (ZMHB 8701); 1 juv., born in captivity from a ♀ collected in Mariou, 2001, leg. I. Stathi (MCNH 81.1.5.1, donated to

VFWV). Kythira: Agia Sofia Cave (Mylopotamos), 25 August 2001, 1 ♂, leg. I. Stathi (MCNH 81.1.5.3, donated to MESB).

Iurus kraepelini von Ubisch, 1922

(Figs. 2, 6, 8, 12, 14, 15, 17, 19, 22, 26, 29–32, 36, 54–55, 60, 64–68, 73, 74, 107–142; Tabs. 1–3, 5)

Iurus kraepelini von Ubisch, 1922: 503–515, text-figs. A–F, tab. 26, figs. 1–7; type locality: TURKEY, Antalya Province, Finike (“Fineka”), September 1902 (leg. J. Vosseler); holotype (female?) formerly in SMNS (Figs. 107–108), now lost (W. Schawaller, pers. comm., 2008).

REFERENCES:

Iurus dufoureius: Werner, 1902: 605 (Eskişehir; dubious locality); Werner, 1934a: 162 (in part); Werner, 1934b: 282 (in part); Werner, 1936a: 192 (Ovacık); Werner, 1938: 172 (in part); Vachon, 1948: 63 (in part); Vachon, 1951: 343 (in part); Vachon, 1953: 96–100 (in part).

Iurus dufoureius: Kraepelin, 1899: 178–179 (in part); Roewer, 1943: 235; Vachon, 1966b: 215 (in part); Kinzelbach, 1975: 21–26 (in part); Kinzelbach, 1982: 58 (in part); Kinzelbach, 1985: Map IV (in part); Fet & Braunwalder, 2000: 18 (in part); Soleglad & Fet, 2003: 8, fig. 20, 44, 53; Fet et al., 2004: 18 (in part); Fet & Soleglad, 2008: 256 (in part); Kaltsas, Stathi & Fet, 2008: 227–228 (in part); Soleglad, Kovařík & Fet, 2009: 2–3 (in part), fig. 10–15 (in part).

Iurus kraepelini: Werner, 1934a: 162; Werner, 1934b: 282; Werner, 1936a: 192; Vachon, 1948: 63.

Iurus dufoureius asiaticus: Vachon, 1947a: 162 (in part); Vachon, 1947b: 2 (in part); Vachon, 1948: 63 (in part); Vachon, 1951: 342 (in part).

Iurus kraepelini: Stahnke, 1974: 123 (in part; doubtful species).

Iurus asiaticus: Francke, 1981: 221–224 (in part), fig. 3 (“Namrun”, probably wrong locality), 5–6 (Antalya); Vachon & Kinzelbach, 1987: 102 (in part); Crucitti, 1995a: 2 (in part); Crucitti, 1998: 32 (in part); Kovařík, 1998: 136 (in part); Crucitti, 1999a: 87–88, fig. 2 (in part); Kovařík, 1999: 40 (in part); Crucitti & Cicuzza, 2001: 227, 229, fig. 7 (in part); Karataş, 2001: 14 (in part); Stathi & Mylonas, 2001: 290 (Megisti); Kovařík, 2002: 16–17 (in part); Kovařík, 2005: 55 (in part); Facheris, 2007a: 1 (in part); Facheris, 2007b: 1 (in part).

Iurus sp.: Francke & Soleglad, 1981: 252, fig. 53–56 (?Antalya; hemispermatophore).

Iurus dufoureius asiaticus: Kristscher, 1993: 383 (in part; Çakırlar); Sissom & Fet, 2000: 420 (in part); Parmakelis et al., 2006: 253 (in part); Francke & Prendini, 2008: 218 (in part); Kamenz & Prendini, 2008:

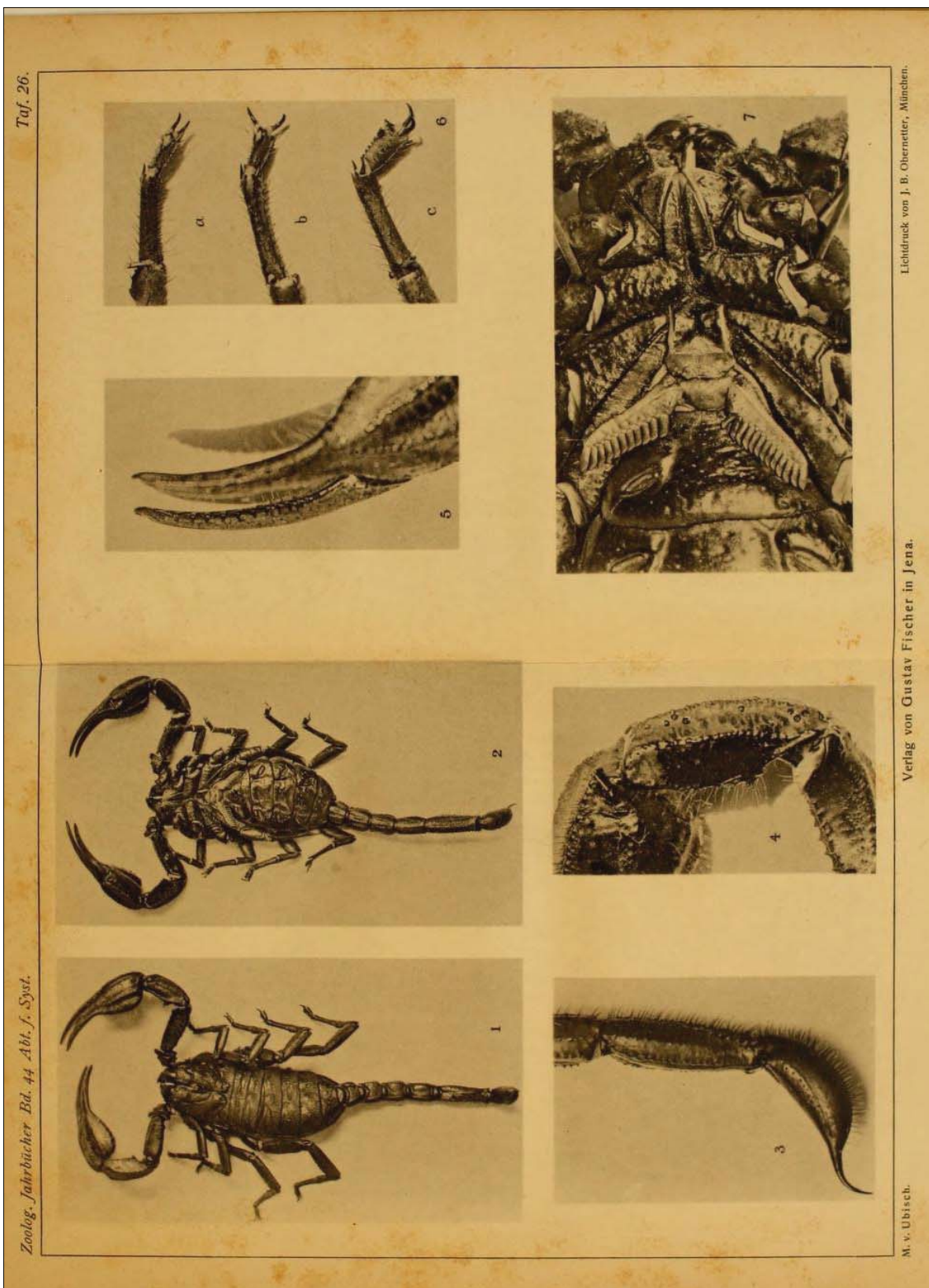


Figure 107: Illustrations of *Iurus kraepelini* from von Uebisch (1922).

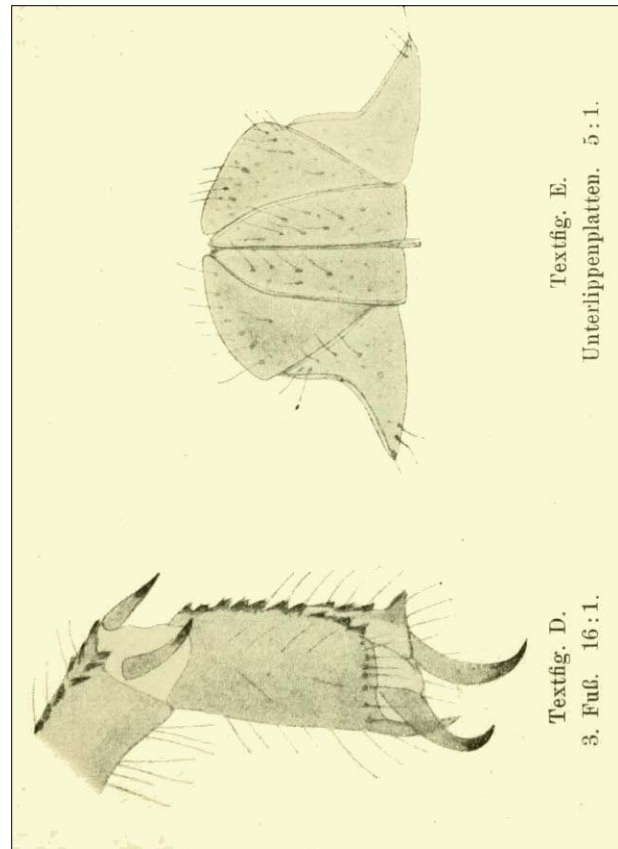
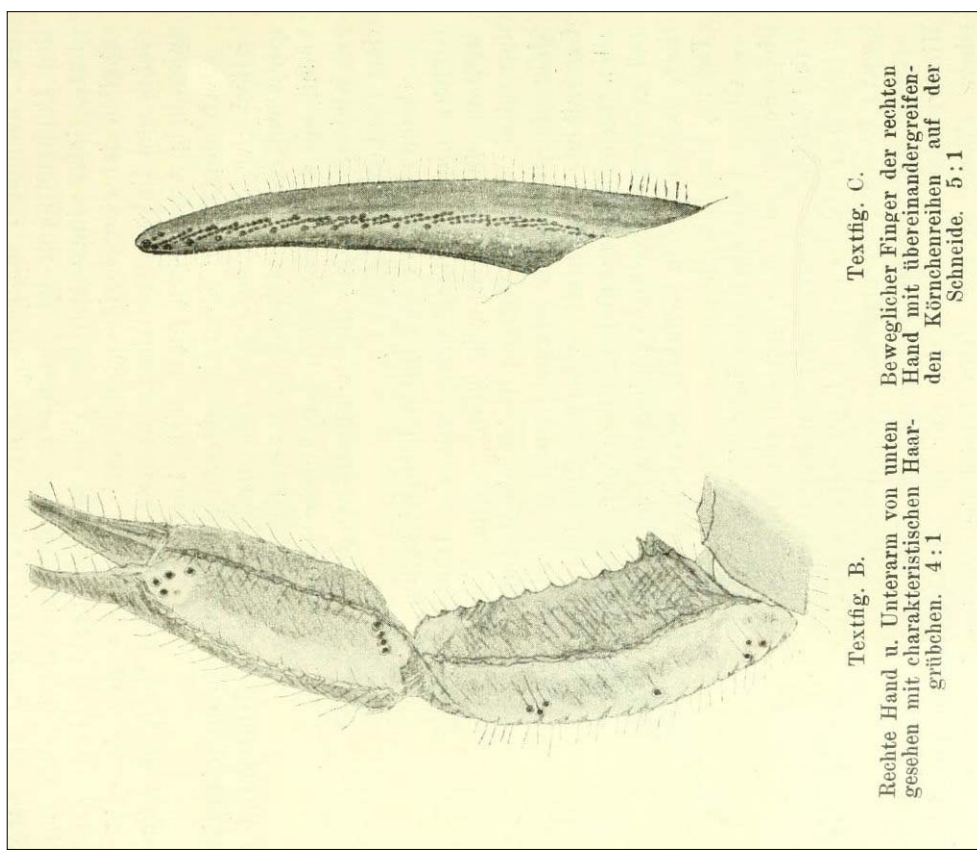


Figure 108: Illustrations of *Iurus kraepelini* from von Ubbisch (1922).

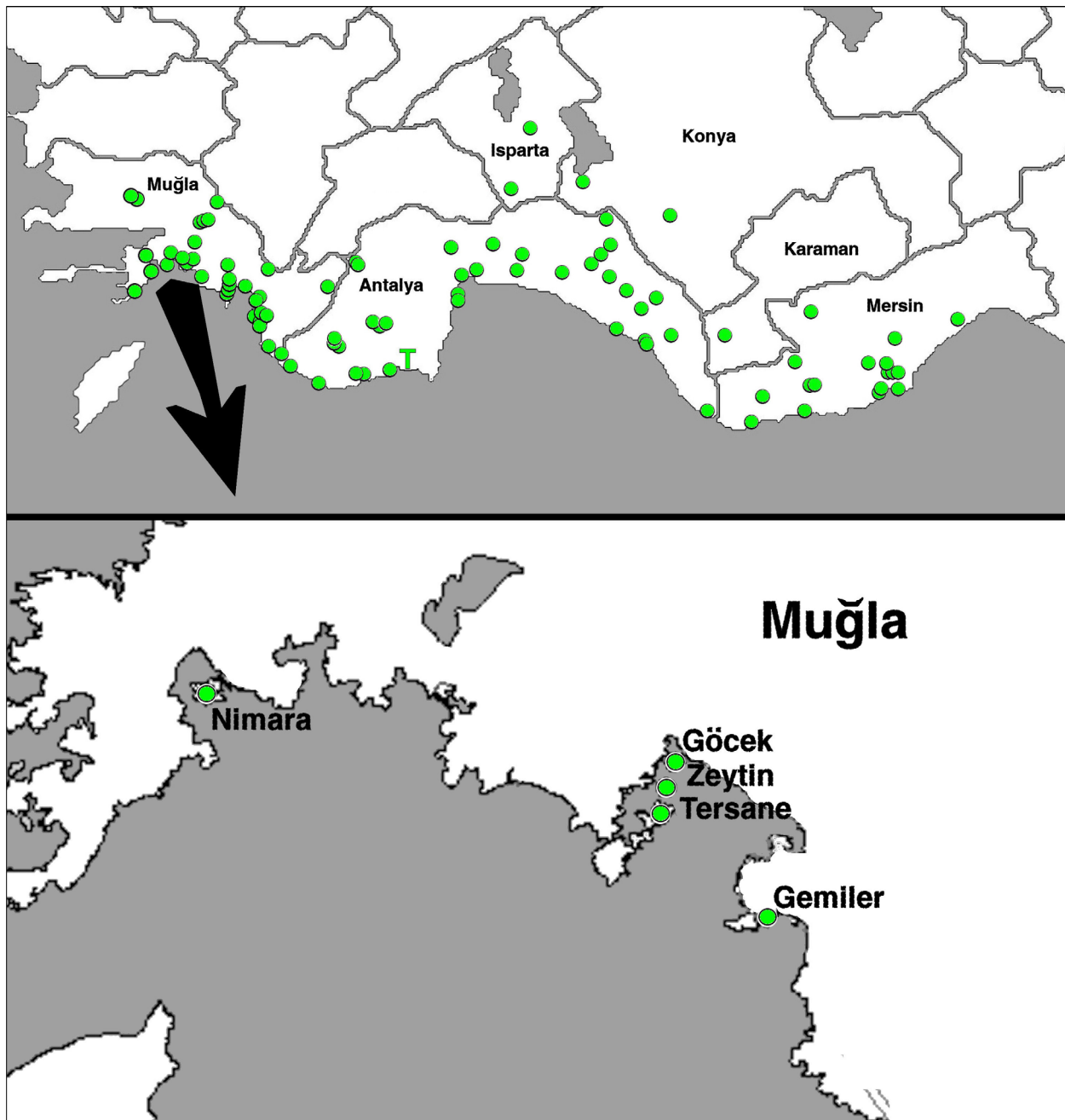


Figure 109: Large-scale map showing distribution of *Iurus kraepelini*. "T" marks type locality, Fineka, Antalya Province, Turkey. Bottom map shows close-up of Muğla Province island localities. See Fig. 74 for distribution of all species and Appendix A for detailed locality data.

43; Kaltsas, Stathi & Fet, 2008: 228 (in part); Yağmur, Koç & Akkaya, 2009: 154–159 (in part).

Neotype (designated here): ♀ (NMHW), TURKEY, Antalya Province: Kale District, 2nd km of the road from Demre to Kaş, 15 May 2008, leg. A. Akkaya & İ. H. Ugurtaş. The neotype is designated from the closest available locality to Finike. Its designation is warranted by a complicated taxonomic situation in Anatolian

species of *Iurus*, which is clarified in the present revision.

Diagnosis. Large species, up to 100 mm. Dark gray to black in overall coloration. Pectinal tooth counts largest in genus, 10–16 (12.63) males, 10–14 (11.48) females. Chelal movable finger lobe in adults located on mid-finger or distally, lobe ratio 0.44–0.64; proximal gap of fixed finger present in adult males; number of inner

denticles (*ID*) of chelal movable finger, 11–14 (12.5); chelal palm of adult males short, deep and highly vaulted, chela length/palm depth 2.21–2.49 (2.31) male, 2.62–2.69 (2.66) female; chelal movable finger of adult male conspicuously curved; constellation array with five sensilla; hemispermatophore lamina internal nodule widely rounded, positioned basally, lamina distal length/lamina basal length 2.159–3.074 (2.564), terminus of acuminate process truncated, transverse trunk bolsters are absent. Dominant morphometrics are chelal width and depth (see Appendix C).

Distribution. Turkey: Anatolia (south). Greece: Megisti (Kastelorizo). See map in Fig. 74 for large-scale distribution of this species.

FEMALE. Description based on neotype female collected in Kale District, Antalya Province, Turkey. Measurements of the neotype and four other specimens are presented in Table 5. See Figure 110 for dorsal and ventral views of the female neotype.

COLORATION. Basic color of carapace, mesosoma, metasoma, telson, and legs dark blackish, except for tarsus which is orange; carinae of metasoma and pedipalp black, barely distinguishable from background color. Sternites light brown; genital operculum, pectines, basal piece yellow. Essentially void of patterns.

CARAPACE (Fig. 111). Anterior edge with a conspicuous median indentation, with approximately 25–30 irregularly placed setae visible; anterior edge covered with large granules; interocular area delineated by mediolateral ocular carinae essentially smooth except for scattered sparse small granules; extreme lateral edges sparsely populated with medium-sized granules. Mediolateral ocular carinae, which are conspicuous due to the somewhat smooth interocular area, are well-developed and granulated, extending to the lateral eyes; there are three lateral eyes, the posterior eye the smallest, roughly half the size of the middle eye. Median eyes and tubercle somewhat small, positioned anteriorly of the middle with the following length and width formulas: 421|1185 and 166|1015.

MESOSOMA (Figs. 112, 115). Tergites I–VII coarsely granulated; tergite VII carinae not detectable due to heavy granulation on entire surface. Sternites III–VII smooth and lustrous; sternite VII with lateral carinae irregularly granulated, median carinae smooth proximally (Fig. 112). Stigmata (Fig. 115) are medium in size and slit-like in shape, angled 45° in an anterointernal direction.

METASOMA (Fig. 113). Segments I–II wider than long. Segments I–IV: dorsal and dorsolateral carinae serrated;

dorsal carinae with 10/9, 8/7, 8/8, and 10/9 serrated spines (left/right carina); dorsal (I–IV) and dorsolateral (I–III) carinae do not terminate with an enlarged spine; lateral carinae serrated on I, crenulated on two-thirds of II, irregularly crenulated on one-half of III, absent on segment IV; ventrolateral carinae crenulated on I–IV; ventromedian carinae irregularly granulated on I, irregularly crenulated on II, and crenulated on III–IV. Dorsolateral carinae of segment IV terminate at articulation condyle. Segment V: dorsolateral carinae serrated; lateral carinae serrated for three-fifths of their posterior portion; ventrolateral and single ventromedian carinae serrated; ventromedian carina terminus irregularly bifurcated. Anal arch with 16 serrated granules. Intercarinal areas of segments I–V essentially smooth. Metasomal segments with numerous long setae on all surfaces.

TELSON (Fig. 113). Vesicle of medium length with highly curved aculeus. Vesicle with slight traces of minute granules ventrally; ventral surface densely covered with medium-length, straight setae; dorsal setation much less dense, with shorter setae; base of aculeus with setation ventrally and dorsally, slightly enlarged setal pair located on aculeus midpoint, their areolae area slightly swollen. Vesicular tabs smooth.

PECTINES (Fig. 116, male Fig. 117). Well-developed segments exhibiting length/width formula 810|300. Sclerite construction complex, with three anterior lamellae and one large middle lamella; fulcra of medium development. Teeth number 11/10. Sensory areas developed along most of tooth inner length on all teeth, including basal tooth. Scattered setae found on anterior lamellae and distal pectinal tooth. Basal piece large, with subtle indentation along anterior edge, length/width formula 370|760.

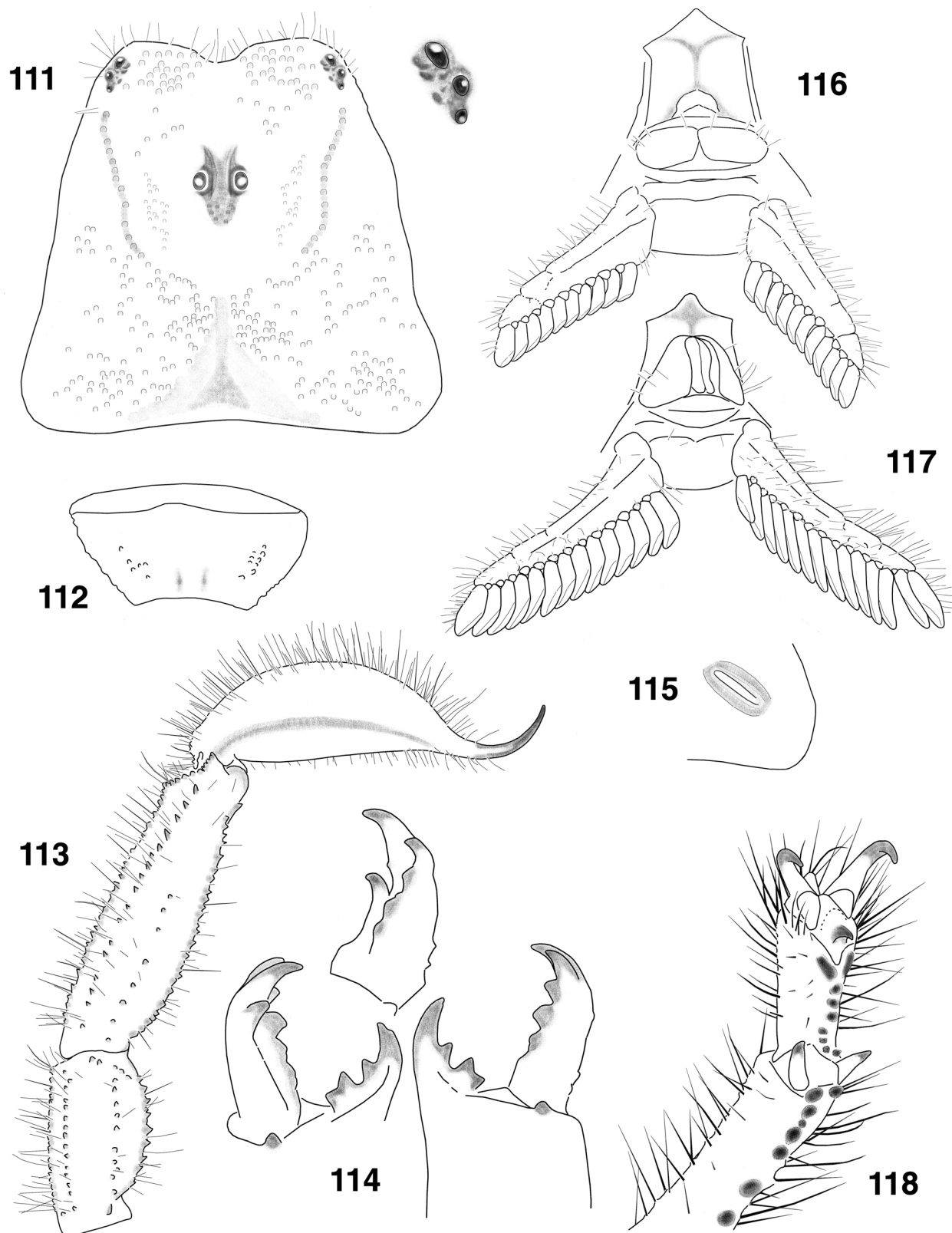
GENITAL OPERCULUM (Fig. 116). Sclerites elongate, wider than long, connected for entire length except for a shallow medial indentation on proximal edge (see discussion on male below).

STERNUM (Fig. 116). Type 2, posterior emargination present, well-defined convex lateral lobes, apex visible but not conspicuous; conspicuous membranous plug situated proximally between lateral lobes; sclerite longer than wide, length/width formula 300|280; sclerite slightly tapers anteriorly, posterior-width|anterior-width formula 280|245 (see discussion on male below).

CHELICERAE (Fig. 114). Movable finger dorsal edge with one large subdistal (*sd*) denticle; ventral edge with one large pigmented accessory denticle at finger midpoint and a small *va* denticle distal of this large denticle; ventral edge serrula not visible. Ventral distal



Figure 110: *Iurus kraepelini*, dorsal and ventral views. Female **neotype**, between Demre and Kaş, Kale District, Antalya Province, Turkey.



Figures 111–118: *Iurus kraepelini*. **111–116.** Female neotype, between Demre and Kaş, Antalya, Turkey. **117–118.** Male, 5 km south of Fethiye, Babadağ Mountains, Muğla, Turkey. **111.** Carapace and close-up of lateral eyes. **112.** Sternite VII. **113.** Telson and metasomal segments IV–V, lateral view. **114.** Right chelicera, ventral and dorsal views. **115.** Stigma II, left. **116.** Sternopectinal area. **117.** Sternopectinal area. **118.** Tarsus and partial basitarsus, right leg I.

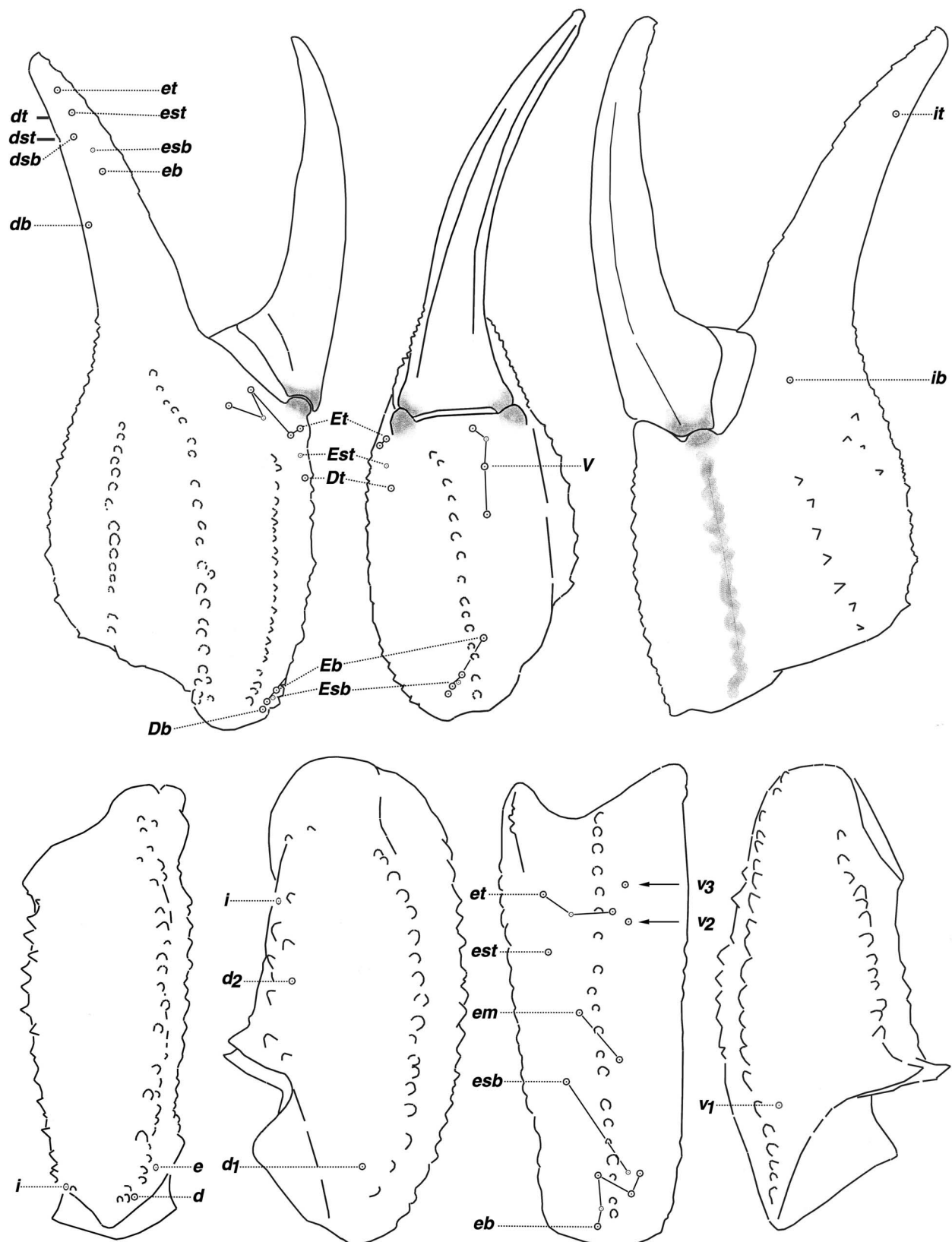


Figure 119: Trichobothrial pattern of *Iurus kraepelini*, female neotype. Between Demre and Kaş, Antalya, Turkey.

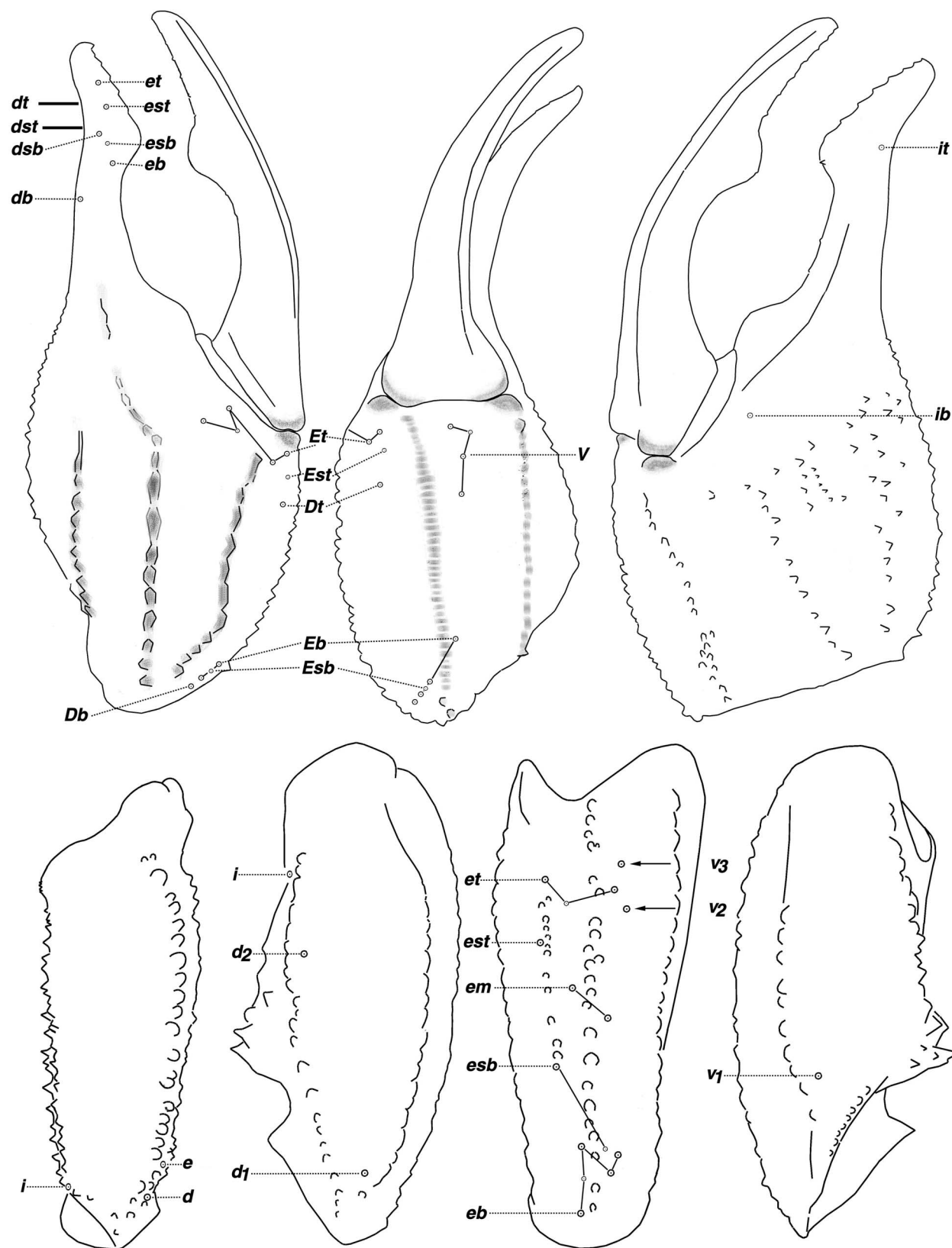
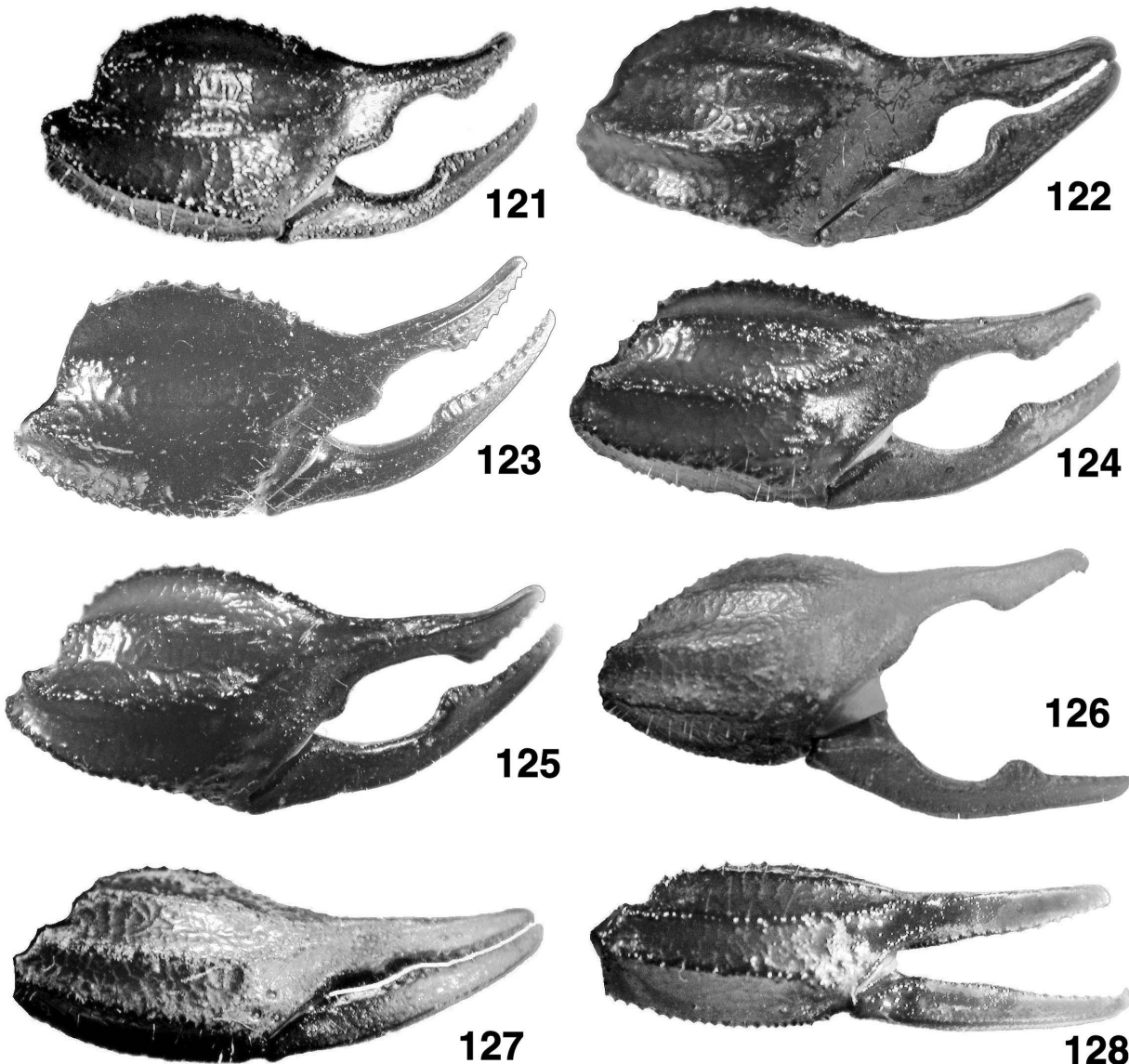


Figure 120: Trichobothrial pattern of *Iurus kraepelini*, male. Silifke, Mersin, Turkey.



Figures 121–128: Chela, lateral view, *Iurus kraepelini*, adults unless stated otherwise. **121.** Male, Akseki, Antalya, Turkey. **122.** Male, Gölbasi, Antalya, Turkey. **123.** Male, Akseki, Antalya, Turkey. **124.** Male, Uzuncaburg, Antalya, Turkey. **125.** Male, Silifke, Mersin, Turkey. **126.** Male, Fethiye, Mugla, Turkey. **127.** Female, Akseki, Antalya, Turkey. **128.** Juvenile male, Akseki, Antalya, Turkey. Note in adults, the movable finger lobe is positioned *distal* of finger midpoint and the fixed finger proximal gap is conspicuously *present* in adult males. Also, unique to this species, is the deep, vaulted chelal palm and highly curved movable finger in adult males.

denticle (*vd*) slightly longer than dorsal (*dd*). Fixed finger with four denticles, median (*m*) and basal (*b*) denticles conjoined on common trunk; no ventral accessory denticles present.

PEDIPALPS (Fig. 119). Well-developed chelae, with medium length fingers, heavily carinated, scalloping of chelal fingers essentially obsolete: lobe on movable finger barely visible, positioned at midpoint; proximal gap of fixed finger absent. **Femur:** Dorsointernal,

dorsoexternal and ventrointernal carinae serrated, ventroexternal rounded and granulated. Dorsal surface granulated, ventral scattered with minute granules, internal and external surface with line of 10 serrated granules each. **Patella:** Dorsointernal and ventrointernal carinae serrated, dorsoexternal crenulated, ventroexternal granulated; exteromedian carina strong, serrated, and single. Dorsal surface rough under 10x and ventral surface smooth; external surface smooth with serrated exteromedian carina; internal surface smooth



Figure 129: Close-up of median area of right hemispermatophore, *Iurus kraepelini*. **Top.** Dorsal, ventroexternal, and ventral views, Silifke, Mersin, Turkey. **Bottom.** Dorsal, internoventral, and ventral views, Antalya, Antalya, Turkey.

with well-developed, doubled DPS and VPS. **Chelal carinae:** Complies with the “8-carinae configuration”. Digital (*D1*) carina strong, granulated; dorsosecondary (*D3*) granulated; dorsomarginal (*D4*) serrated, doubled; dorsointernal (*D5*) irregularly serrated; ventroexternal

(*V1*) strong and serrated, terminating to external condyle of movable finger; ventrointernal (*V3*) rounded and rough, continuous to internal condyle; external (*E*) strong, continuous, and serrated; internal (*I*) serrated. **Chelal finger dentition:** Median denticle (*MD*) row

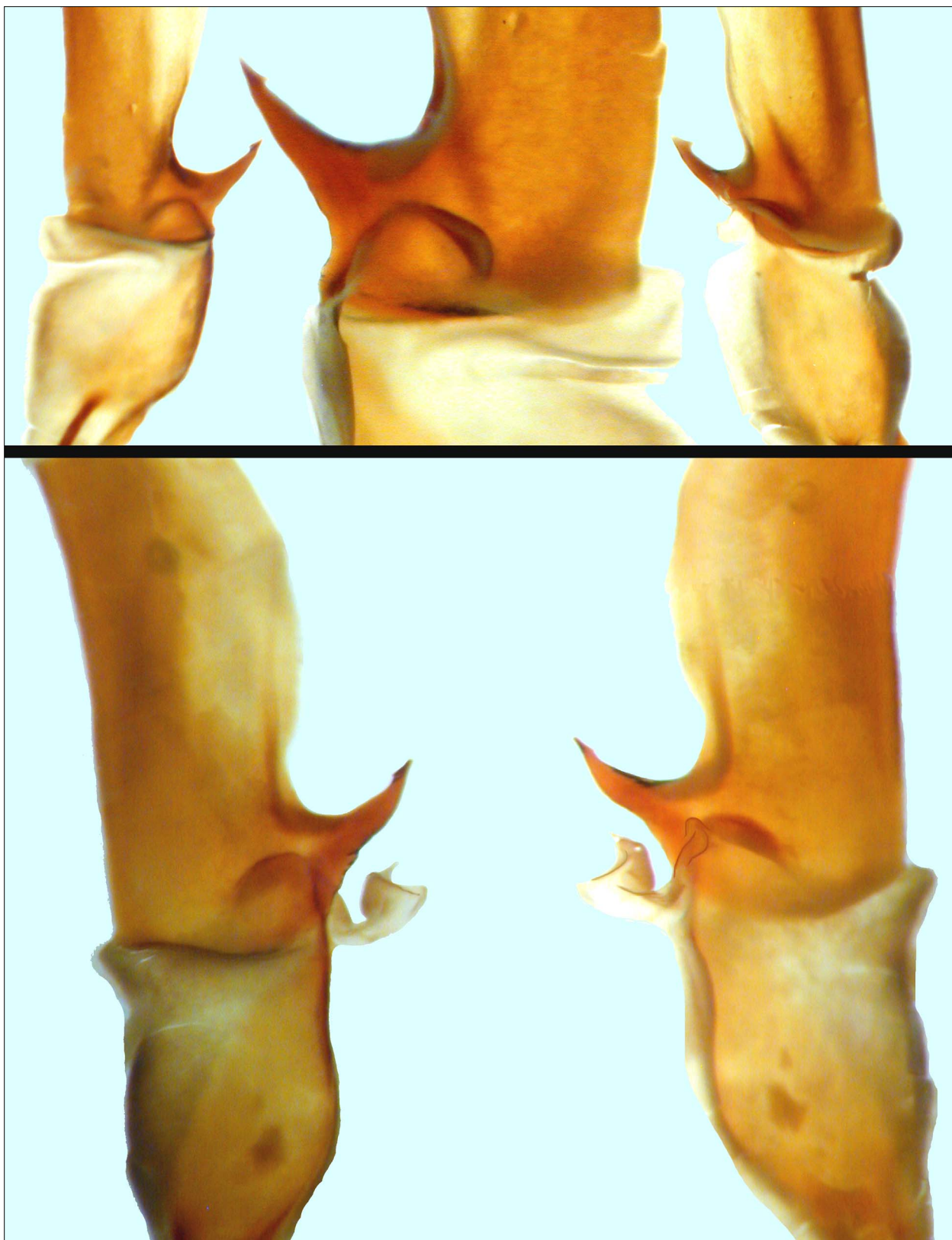


Figure 130: Close-up of median area of right hemispermatophore, *Iurus kraepelini*. **Top.** Dorsal, ventral, and internoventral views, Central District, Antalya Province, Turkey. **Bottom.** Dorsal and ventral views, Seki District, Muğla Province, Turkey. Note the fine detail of the paraxial organ sleeve emanating from the seminal receptacle on the ventral surface.

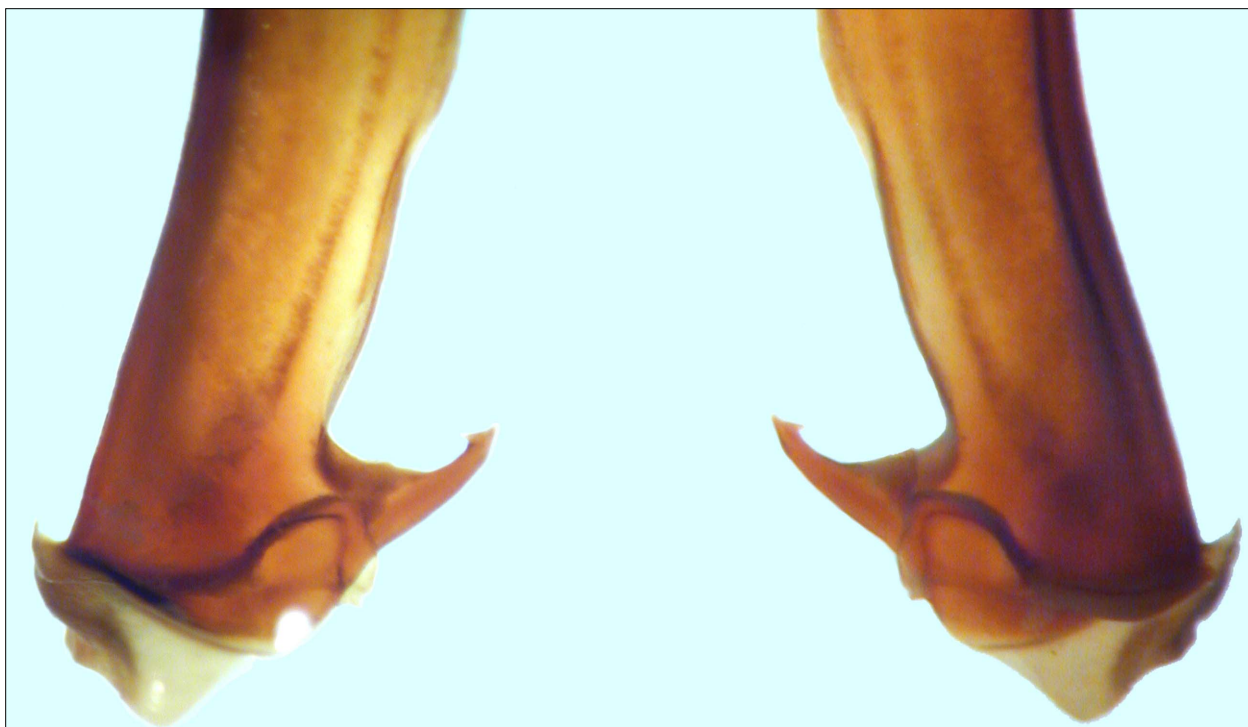


Figure 131: Close-up of median area of right hemispermophore, *Iurus kraepelini*, dorsal and ventral views, Akseki, Antalya, Turkey.

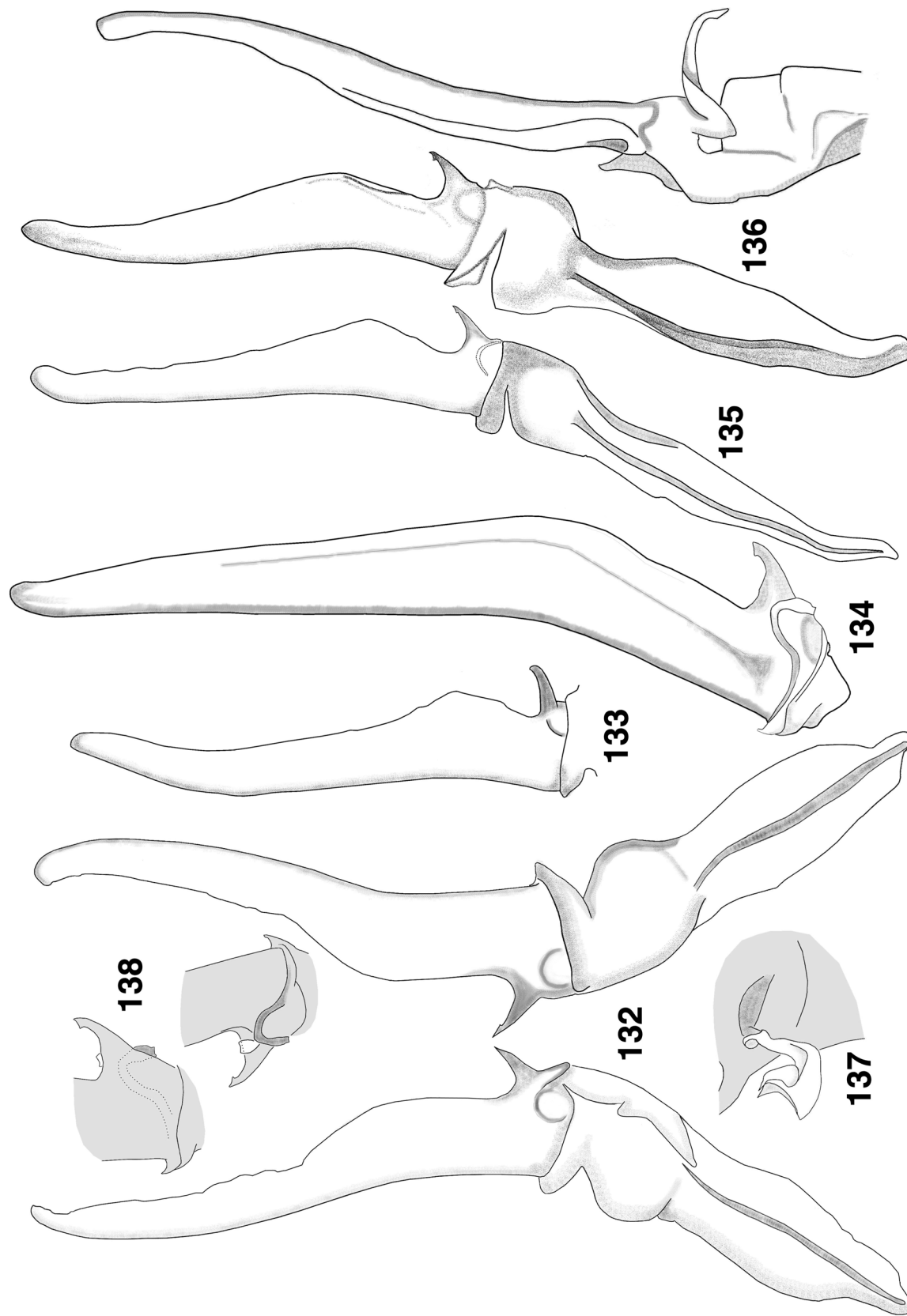
groups oblique and highly imbricated; 11/11 *IDs* on fixed fingers and 13/13 *IDs* on movable fingers; 14/14 *ODs* on fixed fingers and 15/15 *ODs* on movable fingers. No accessory denticles present. **Trichobothrial pattern (Fig. 119):** Type C, orthobothriotaxic, typical of genus (but see below on neobothriotaxy in this species).

LEGS (male, Fig. 118). Both pedal spurs present on all legs, lacking spinelets; tibial spurs absent. Tarsus with conspicuous spinule clusters in single row on ventral surface, terminating distally with a pair of enlarged spinule clusters. Unguicular spine well-developed and pointed.

HEMISPERMATOPHORE (Figs. 129–138). We have examined several hemispermophores of *I. kraepelini*, spanning major provinces of its distribution, Muğla, Antalya, and Mersin (see map in Fig. 60). The hemispermophore of *I. kraepelini* is unique among *Iurus* species, exhibiting a pointed terminus on the lamina, a rounded internal nodule, absence of transverse trunk bolsters, and a truncated acuminate process terminus (see below for more data).

Male and female variability. The overall morphology of the chela exhibits significant sexual dimorphism in this species (Figs. 123–127). In the sexually mature male, the pincer is very robust, the dorsal edge of the

palm quite vaulted. Its movable finger is quite curved, forming a 30° or larger angle (Fig. 59). The movable finger lobe is conspicuous in the male, fitting into an equally well developed fixed finger socket. The proximal gap on the fixed finger is greatly developed in the male. There is no significant sexual dimorphism in morphometrics except for the chelal depth which is relatively larger in the male (exhibiting a 14.8 % MVD with the female when compared to the chela length). The metasomal segments are relatively longer in the male, but the MVDs across all five segments only favored the male by 4.4 to 9.0 % when compared to the segment's width. Pectinal tooth counts in males exceed those of females by approximately one tooth (1.15), male 10–16 (12.63) [165], female 10–14 (11.48) [211] (see histograms in Fig. 73). The genital operculum of the male is dramatically different from that in the female (Figs. 116–117). The sclerites, subtriangular in shape, are as long as or longer than wide in the male, whereas in the female the sclerites are short and wide, more than twice as wide as long. Whereas the sclerites are fused medially in the female, they are separated along their entire length in the male, exposing significantly developed genital papillae. The enlarged genital operculum of the male extends distally between the lateral lobes of the sternum partially obscuring its proximal region. Figures 139–147 show dorsal and



Figures 132–138: Hemispermophore, *Lurus kraepelini* (right hemispermophore unless stated otherwise). **132.** Antalya, Antalya, Turkey, dorsal and ventral views. **133.** "Taurus", Turkey, dorsal view. **134.** Akseki, Antalya, Turkey, dorsal view. **135.** Central District, Antalya, Mersin, Turkey, dorsal and ventroexternal views. **137–138.** Close-up of paraxial organ sleeve showing its attachment to the seminal receptacle. **137.** Seki District, Muğla, Turkey. **138.** Akseki, Antalya, Turkey.

<i>I. kraepelini</i> von Ubisch, 1922					
	Between Demre and Kaş, Antalya, Turkey	Akseki, Antalya, Turkey		Silifke, Mersin, Turkey	
	Female Neotype	Male	Female	Male	Female
Total length	82.50	88.15	91.20	100.05	85.95
Carapace length	11.85	13.40	13.05	14.65	12.00
Mesosoma length	29.20	24.15	31.75	30.45	27.95
Metasoma length	28.80	35.50	32.90	39.10	31.95
Segment I length/width	3.55/5.20	4.55/5.50	4.20/5.70	4.95/5.95	4.10/5.20
Segment II length/width	4.35/4.50	5.40/4.80	5.00/4.90	6.00/5.20	4.75/4.55
Segment III length/width	4.75/4.15	5.85/4.60	5.40/4.60	6.60/4.80	5.20/4.05
Segment IV length/width	5.70/3.65	6.95/4.20	6.55/4.20	7.75/4.35	6.25/3.70
Segment V length/width	10.45/3.60	12.75/4.00	11.75/3.90	13.80/4.05	11.65/3.50
Telson length	12.65	15.10	13.50***	15.85	14.05***
Vesicle length	9.05	10.35	9.70	11.85	9.50
width/depth	3.80/3.35	4.60/4.15	4.15/3.55	4.70/4.15	4.15/3.45
Aculeus length	3.60	4.75	3.80***	4.00	4.55***
Pedipalp length	42.55	49.25	46.65	55.15	44.75
Femur length/width	10.80/3.90	12.50/4.20	11.75/4.30	13.80/4.65	11.10/4.30
Patella length/width*	10.25/4.25	12.65/4.75	11.35/4.45	13.15/5.30	10.80/4.45
DPS height**	1.20	1.75	1.10	1.75	1.40
Chela length	21.50	24.10	23.55	28.20	22.85
Palm length	9.70	11.55	10.70	13.15	10.80
width/depth	6.60/8.20	7.65/10.80	6.35/8.75	8.75/12.75	7.55/8.65
Fixed finger length	10.40	12.10	11.10	14.05	10.80
Movable finger length	13.70	16.20	14.90	18.80	14.25
Pectines teeth middle lamellae	11-10 1-1	13-14 1-1++	12-11 4-4++	12-12 2-2	11-11 1-1++
Sternum length/width	3.00/2.80	2.80/2.60	3.45/3.30	3.25/2.50	3.45/3.00

Table 5: Morphometrics (mm) of *Iurus kraepelini* von Ubisch, 1922, * Patella width is widest distance between the dorsointernal and externomedial carinae. ** DPS height is from tip of spines to dorsointernal carina center.

ventral views of both male and female specimens, and various collection localities for this species.

Discussion

Unique to this species is the extraordinarily developed chela of sexually mature males. The palm is highly vaulted, making it the deepest palm found in *Iurus*. The movable finger is highly curved, forming an angle with its base of approximately 30°, roughly 50 % greater than that found in other species. *I. kraepelini* has the most distally positioned movable finger lobe in the genus. The movable finger lobe ratio is larger in the male than the female, 0.465–0.640 vs. 0.440–0.575 (ratios calculated from adults with carapaces 11 mm long or larger; see scatter chart in Fig. 56 for a complete

analysis of this character). *I. kraepelini* also has the most exaggerated proximal gap in the genus (Figs. 121–126).

I. kraepelini has the highest number of pectinal teeth (Fig. 73), roughly one tooth more than found in *I. asiaticus*, the species with the next highest number of teeth. This species is also the largest in *Iurus*, males exceeding 100 mm in length (see measurements in Table 5).

The hemispermatophore of *I. kraepelini* (Figs. 129–138) has been examined from six specimens, each from a separate locality, spanning the provinces of Muğla, Antalya, and Mersin (see map in Fig. 60). The relative proportions of the hemispermatophore component in this species is situated between *I. asiaticus* with the smallest ratio values and *I. dufourei* and *I. kinzelbachi*, the species with the largest values (see Table 2). The lamina is of average length, slightly longer than its trunk, in a



Figure 139: *Iurus kraepelini*, dorsal and ventral views. Adult male (FKCP) (95 mm), 12 km S. Akseki, Antalya, Turkey.



Figure 140: *Iurus kraepelini*, dorsal and ventral views. Adult female (FKCP) (95 mm), 12 km S. Akseki, Antalya, Turkey.



Figure 141: *Iurus kraepelini*, male (100 mm), Silifke, Mersin, Turkey.

1.122 ratio (see Table 2). The lamina terminus is somewhat pointed, especially when compared to the wide and rounded internal nodule. The internal nodule is situated subbasally on the lamina, in a ratio 2.6. The acuminate process terminus is truncated as in most other *Iurus* species. Transverse trunk bolsters are absent. The paraxial organ sleeve was present in some hemi-

spermatophores (Fig. 130–131, 137–138), its attachment to the seminal receptacle is as found in other species. In particular, the sleeve is well represented in the specimen from Muğla (Figs. 130, 137).

In Appendix C, we present a complete analysis of the morphometric trends across the five species of *Iurus*. This analysis shows that the chela width and depth in *I.*

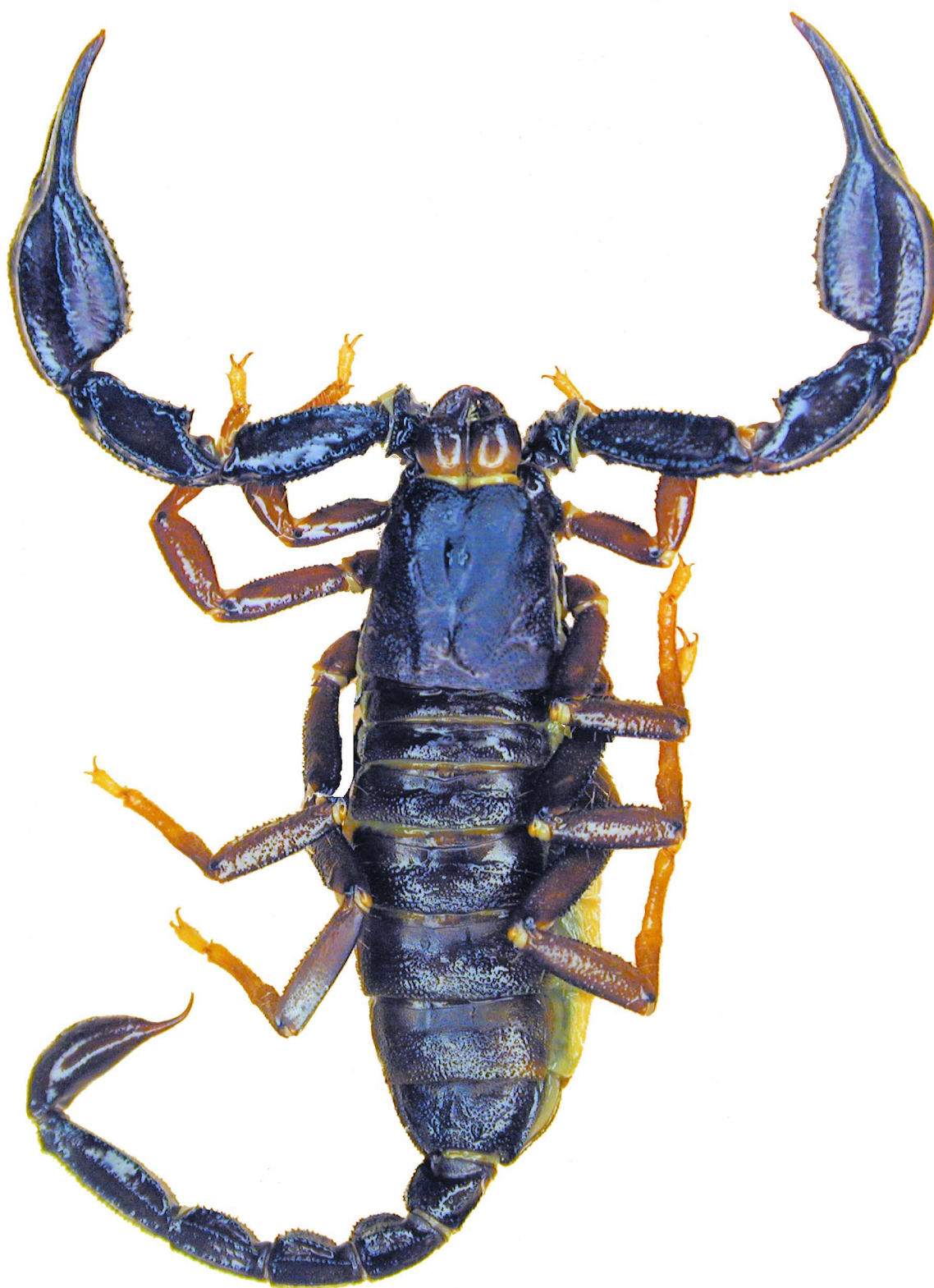


Figure 142: *Iurus kraepelini*, female, Gökböl Village, Ortaca Dist., Muğla, Turkey.

kraepelini dominated in a large majority of morphometric ratio comparisons: averaging 24 and 25 comparisons out of 25 for the male and 21 and 24 for the female. This somewhat stocky chela is accompanied by its relative shortness, only dominating 7 ratio comparisons on average. Figure C2 in Appendix C presents the histograms of the chela width and depth as compared to its length. These two morphometrics, consistent in both genders, provide excellent diagnostic separation characters for *I. kraepelini*. The MVDs for the chelal width ranged 7.6 to 27.2 % for the male and 7.9 to 23.2 % for the female; and the chelal depth ranged 24.6 to 47.3 % for the male and 15.2 to 24.9 % for the female.

Soleglad, Kovařík & Fet (2009) reported several cases of neobothriotaxy in *I. kraepelini* (referred to as *I. dusourei* from Turkey, without İzmir): out of 64 specimens, 37 instances of neobothriotaxy were reported, spanning 5 types, and representing 85 individual accessory trichobothria. During the current study we isolated one more type of neobothriotaxy in this species (type 7), eight instances, and eleven instances of the other five types. The majority of neobothriotaxy cases occurring in *Iurus* is found in *I. kraepelini* (six types), of which a couple of types might have taxonomic potential (types 1 and 5). These two types, which can occur together, are concentrated in Muğla, Antalya, and Konya Provinces (primarily in Antalya), and account for over 70 % of neobothriotaxy found in *Iurus*. Type 5, the most prevalent, occurs in Muğla, Antalya, Konya, and Mersin Provinces. See Appendix B for details on this neobothriotaxy.

Material Examined (217 specimens). TURKEY: *Antalya Province*: Akseki District, 12 km S of Akseki, 8–9 June 1993, 1 ♂, leg. J. Chaloupek (FKCP); Akseki District, 12 km S of Akseki, 11–12 May 2006, 2 ♂, 3 ♂ juv., 3 ♀, leg. F. Kovařík (FKCP); 5 ♂ juv., 3 ♀ juv. (born in captivity from one of the ♀) (FKCP); Alanya District, Alanya, 10 October 1998, 1 ♀ (E. Caraca) (NHW 19131); Alanya District, Alanya Castle, 36°31'59.8"N 31°59'28.8"E, 22 March 2009, 3 ♂ juv., leg. K.B. Kunt (MTAS); *Antalya Province*: Alanya District, 38 km NE Demirtaş, 11 August 1971, 1 ♀, leg. F. Spigenberger (NMHW); Alanya District, 2 km from Alanya-Taşatan Plateau fork in road, 24.04.2009, 36°38.498"N, 32°04.089"E, 1167 m asl, 2 ♂, leg. A. Kızıltuğ & K. B. Kunt (MTAS); Alanya District, Taşatan Plateau, 36°40.244"N 32°10.210"E, 1208 m asl, 9 June 2009, 1 ♀ sbad., 1 ♂ sbad., 1 juv., leg. A. Kızıltuğ & K. B. Kunt (MTAS); *Antalya*, 15 May 1965, 1 ♂, leg. F. Ressl (NHW 2066); *Antalya*, 19 May 1969, 1 ♂, leg. F. Ressl (NHW 11323); July 1996, 1 ♂ juv., leg. Hubert (FKCP); Central District, Büyük Çaltıcak Village, 36°47'06"N, 30°34'09"E, 14 m asl, 15 May 2008, 1 ♂, 2 ♀, leg. A. Akkaya & İ. H. Uğurtaş (MTAS); *Elmalı* District, Çiglikara Nature Reserve,

1680 m asl, 2 ♀, leg. Felten (SMFD 25890); *Elmalı* District, near *Elmalı*, 36°24'58"N, 29°40'18"E, 12 May 2007, 3 ♂ sbad., 1 ♂ juv., 2 ♀, 1 ♀ juv., leg. İ. H. Uğurtaş (MTAS); *Finike* District, ca. 25 km N of *Finike*, Avlanbeli Geçidi (=Pass), 1200 m asl, 36°32'N, 29°59'E, 13–16 May 2006, 1 ♀, 3 ♀ juv., leg. F. Kovařík (FKCP); *Gazipaşa* District, side valley near *Gazipaşa*, 17 May 1969, 1 ♀, leg. G. Pretzmann (NHW); *Kale* District, *Gölbaşı* (ancient Trysa, near Davazlar Village), ["Gölbakticke"], May 1882, 4 ♂, 5 ♀, leg. V. Luschan (NHW 11321), ["Gjölbanchi"], July 1882, 1 ♂, 2 ♀, leg. V. Luschan (NHW 11322); *Kale* District, 2nd km on the road from *Demre* to *Kaş*, 36°15'48.8"N, 29°56'37.7"E, 476 m asl, 15 May 2008, 1 ♀ (**neotype**) (NHW), 1 ♂ juv. (MTAS), leg. A. Akkaya & İ. H. Uğurtaş; *Kale* District, *Tersane* Island, 36°38'10"N, 29°5'19"E, 113 m asl, 14 May 2007, 1 ♀ sbad., leg. İ. H. Uğurtaş (MTAS); *Kaş* District, S of *Gömüçü* Village, 36°24'01"N, 29°41'56"E, 986 m asl, 15 May 2009, 1 ♀, leg. A. Akkaya (MTAS); *Kaş* District, 2nd km of the road from *Kalkan* to *Patara*, 36°17'01"N, 29°24'26"E, 242 m asl, 16 May 2008, 1 ♀ sbad., 1 ♀ juv., leg. A. Akkaya & İ. H. Uğurtaş (MTAS); *Kaş* District, *Kınık* (ancient Xanthos), 15–16 April 1990, 1 ♀, 1 ♀ juv. leg. R. Lízler (FKCP); *Manavgat* District, *İrmasan* Geçidi (= Pass), 1300 m asl, 2 June 1996, 2 ♀ sbad., leg. M. Snížek (FKCP); *Manavgat* District, *Oymapınar* Village, 36°53'52"N, 31°31'53"E, 65 m asl, 15 August 2005, 1 ♂ sbad., leg. E. A. Yağmur & A. Akkaya (MTAS), 5 September 2004, 1 ♂, 2 ♀, leg. A. Akkaya (MTAS); *Serik* District, *Catallar*, 14–15 May 2006, 1 juv., leg. F. Kovařík (FKCP); *Serik* District, 4 km N of *Serik*, *Belkis* (Aspendos), near ruins, 16 May 1965, 1 ♂, 1 juv., leg. F. Ressl (NHW 2067); *Serik* District, 4 km N of *Serik*, *Aspendos*, 1 ♂, 2 ♀ (NHW 11319); *Korkuteli* District, *Güllük* Mts ("Güllük-Dagh") [ancient Termessos on Mt Solymos], 2 ♂, leg. A. Gaheis (NHW 11320). *Isparta Province*: *Eğirdir* District, *Pazarköy* Village, SE of *Eğirdir* (now *Eğirdir*), 1400 m asl, 27 May 1966, leg. H. Felten, 1 ♀ (SMFD). *Konya Province*: *Beyşehir* District, *Bademli* Village, pasture, July 1998, 2 ♂, 2 ♀ (FKCP). *Mersin Province*: *Anamur* District, 20 km from *Anamur*, 22 April 1990, 1 ♀ juv., leg. Mertlik (FKCP); *Aydincık* District, *Aydincık*, 9 April 1990, 1 ♂, 19 April 1990, 1 ♀ juv., leg. R. Lízler (FKCP); *Erdemli* District, *Doğulu* Village, 36°44'58.9"N, 34°25'27.5"E, 161 m asl, 25 April 2007, 1 ♀, leg. M. Z. Yıldız (MTAS); *Gülnar* District, near *Gülnar*, July 2000, 1 ♂, leg. K. Werner & R. Lízler (FKCP); *Silifke* District, *Cennet* (=Korykos, Corycos) Cave, NE *Silifke*, 11 April 1981, 1 ♀, leg. Heinz (RKRO 367); same locality, "Corykische Grotte", 27 March 1966, 6 imm., 2 juv., leg. Dobat (SMFD 25893); same locality (?), rehydrated remnants of 2 ♀ (MNHN RS-5169); with a label, "Korikos" and note in M. Vachon's hand "types?" (their morphology does not match Brullé's type specimens, which we consider lost);



Figure 143: *Iurus kraepelini*. **Top.** Subadult, Finike, Antalya, Turkey, type locality of species. **Bottom.** Gügübeli Pass, Muğla, Turkey, specimen molting.

Silifke District, Değirmendere Village, 36°25'53"N, 33°45'21"E, 425 m asl, 13 May 2008, 1 ♀, 1 ♂ sbad., leg. A. Akkaya, İ. H. Uğurtaş (MTAS); Silifke District, Silifke, 27 April 1967, 1 ♂, 1 ♀ sbad., leg. F. Ressl

(NHMW); Silifke District, Göksu Delta Valley, 29 April 1967, 1 ♂, leg. F. Ressl (NHMW 11324); Silifke District, near Silifke, 37°08'19"N, 34°50'25"E, 425 m asl, 12 May 2008, 1 ♀, leg. A. Akkaya & İ. H. Uğurtaş



Figure 144: *Iurus kraepelini* collection localities. **Top.** Akdağ Mts., Fethiye District, Muğla, Turkey. The highest known altitude for the genus and family Iuridae (2130 m a.s.l.). **Bottom.** Avsallar, Alanya District, Antalya, Turkey.



Figure 145: Collection localities of *Iurus kraepelini*. **Top.** Avlanbeli Geçidi, 25 km S. Elmali, Antalya, Turkey, 1200 m., collected with *Mesobuthus gibbosus*. **Bottom.** Taşatan Plateau, Alanya, Antalya, Turkey.



Figure 146: Erdemli, Erdemli District, Mersin, Turkey. Near the most eastern locality of *Iurus kraepelini*.



Figure 147: Collection localities of *Iurus kraepelini*. **Top.** Çiçekbaba Mts., Muğla, Turkey. **Bottom.** Oymapınar, Manavgat District, Antalya, Turkey.

(MTAS); 1 ♀, Silifke District, 5 km NW Silifke, 1969, leg. G. Pretzmann (NHMW); Silifke District, Taşucu Village, 36°18'43"N, 33°51'41"E, 22 May 2007, 1 ♀, 1 ♂ sbad., leg. A. Avcı (MTAS); Silifke District, Uzun-caburç, 26 July 1986, 1 ♂ (RKRO 0732). *Muğla Province*: Bodrum District, Sarıot Island, 36°59'29"N, 27°13'26"E, 27 April 1985, 1 juv., leg. İ. Baran & H. Durmuş (MTAS); Dalaman District, Tersane Island, 36°40'4"N, 28°55'5"E, 178 m, 1 ♀, 13 February 1985, leg. İ. Baran & H. Durmuş (MTAS); Dalyan District, Dalyan, May 1999, 1 ♂, 1 ♀, 1 ♀ sbad (FKCP); Dalyan District, Dalyan, 36°51'14"N, 28°37'25"E, 28 m asl, 28 February 2004, 1 ♂ sbad., 1 ♀, 1 ♀ juv., leg. A. Avcı & K. Olgun (MTAS); Dalyan District, Gökbelen Village, 36°53'37"N, 28°15'22"E, 18 April 1991, 1 ♂, 2 ♀, leg. İ. Baran & H. Durmuş (MTAS); Dalyan District, Kışlak Village, 36°50'N, 28°37'E, 15 April 1991, 1 ♂, 2 ♀, leg. İ. Baran & H. Durmuş (MTAS); Fethiye, May 1989, 1 ♂, 1 ♀ (FKCP); Fethiye District, Kidirak, S of Fethiye, 24–28 May 1988, 1 ♀, leg. R. Kinzelbach (RKRO 1055); Fethiye District, 2 September 1985, 1 juv., leg. İ. Baran & H. Durmuş (MTAS); Fethiye District, 36°37' N, 29°07' E, 24 May 1970, 4 ♀, 2 ♂, 1 juv., leg. M. Başoğlu (MTAS); Fethiye District, Gemiler Island, 36°33'11"N, 29°04'10"E, 40 m asl, 7 June 1985, 2 ♀, leg. İ. Baran & H. Durmuş (MTAS); Fethiye District, Göcek, 36°45'25"N, 28°56'40"E, 38 m asl, 22 January 1965, 2 ♀, leg. M. Başoğlu (MTAS); Fethiye District, Göcek Island, opposite to Göcek, 36°43'35"N, 28°56'22"E, 12 February 1985, 1 ♀, leg. İ. Baran & H. Durmuş (MTAS); Fethiye District, 5 km S of Fethiye, Babadağ Mts, 36°33'39"N, 29°09'12"E, 499 m asl, 30 March 2007, 1 ♂, leg. A. Avcı (MTAS); Fethiye District, Domuz Island, 14.03.2008, 36°39'41"N, 28°53'59"E, 8 m asl, 14 March 2008, 2 ♂ sbad., leg. A. Avcı (MTAS); Fethiye District, Kelebekler Valley (Butterflies Valley), 36°29'48"N, 29°07'44"E, 24 November 2003, 1 ♀ sbad., leg. H. Koç (MTAS); Fethiye District, Ovacık Village, 6 km S of Fethiye, 1 ♀ (SMFD 6732/139); Fethiye District, Yeşilüzümlü Village, 36°48'03"N, 29°11'10"E, 990 m asl, 2 May 2008, 1 ♀ sbad., 16 May 2008, 3 ♂, 1 ♂ juv., 3 ♀, 1 ♀ juv., leg. A. Akkaya & İ. H. Uğurtaş (MTAS); Fethiye District, Zeytin Island, opposite to Göcek, 36°41'53"N, 28°55'36"E, 38 m asl, 4 August 1984, 1 ♀, leg. İ. Baran & H. Durmuş (MTAS); Köyceğiz District, 36°56' N, 28°44' E, 31 March 1991, 1 ♂, 3 ♀, 1 juv., leg. İ. Baran & H. Durmuş (MTAS); Köyceğiz District, Ekincik Village, 36°50'39"N, 28°33'10"E, 52 m asl, 17 April 1991, 1 ♂, 2 ♀, leg. İ. Baran & H. Durmuş (MTAS); Köyceğiz District, Kaunos Ruins, 36°49'34"N, 28°37'21"E, 20 m asl, 28 March 1991, 1 ♀, leg. İ. Baran & H. Durmuş (MTAS); Köyceğiz District, Sultanye Spring, 26 April 1991, 1 sbad. ♂, leg. E. Neubert (RKRO 1053); Marmaris District, 25 km N of Marmaris, 37°13' N, 28°14' E, 8 April 1984, 1 ♂, 2 ♀, leg. İ. Baran

& H. Durmuş (MTAS); Marmaris District, Nimara Island, 36°48'15"N, 28°17'15"E, 327 m asl, 8 April 1984, 4 ♀, 3 juv., leg. İ. Baran & H. Durmuş (MTAS); Ortaca District, Gökbelen Village, 15 February 2005, 36°47'04"N, 28°40'39"E, 145 m asl, 2 ♀, leg. K. Olgun & A. Avcı (MTAS); Seki District, Çiçekbaba Mts, 37°01'88"N, 28°45'73"E, 11 August 2005, 911 m asl, 2 ♂, 1 ♀, leg. E. A. Yağmur & H. Koç (MTAS); Seki District, Çiçekbaba Mts, near Kartal Lake, 37°03'66"N, 28°48'50"E, 1763 m, 11 August 2005, 1 ♂, 2 ♀, 1 ♀ sbad., leg. E. A. Yağmur & H. Koç (MTAS); Seki District, near Göögübelen Pass, 36°50'32"N, 29°45'16"E, 1807 m asl, 11 August 2005, 1 ♂, 1 ♀, 1 ♀ sbad., leg. E. A. Yağmur & H. Koç (MTAS); Seki District, Göögübelen Pass, 36°50'44"N, 29°44'76"E, 1830 m asl, 11 August 2005, 2 ♂, 1 ♂ sbad., leg. E. A. Yağmur & H. Koç (MTAS); Seki District, Göögübelen Pass, 1794 m asl, 12 August 2005, 2 ♂, 2 ♀, 3 ♀ sbad., 1 ♀ juv., leg. E. A. Yağmur & H. Koç (MTAS); Yatağan District, Bencik Mts, near fire watchtower, 37°14'14"N, 28°03'28"E, 1395 m asl, 19 June 2005, 2 ♂, 1 ♂ sbad., 2 ♀, 1 ♀ sbad., leg. E. A. Yağmur & H. Koç (MTAS). *No exact locality*: “Antalya, Adana, south Mersin”, 1 ♀, 1 ♀ juv., May 1991, leg. Nosek, 1 ♂, leg. Hašek (FKCP); Taurus [“Taurien”!], Kricheldorf [dealer’s name], 1 ♂, 3 ♂ sbad., 1 ♀ sbad. (ZMHB 15218); “Cilicien”, Rolle [dealer’s name], 1 ♂ (ZMHB 8315); Taurus, 1 ♀, leg. P. Niedieck (ZMHB 15219); Turkey, 1 ♂ (MESB).

Iurus asiaticus Birula, 1903

(Figs. 1, 3, 14, 23, 27, 28, 39, 41, 53, 60, 69–74, 148–176; Tabs. 1–3, 6)

Jurus dufourei *asiaticus* Birula, 1903: 297–298; type locality: TURKEY (southeast), Adana Province, Gülek Pass.

REFERENCES:

Jurus dufourei: Birula, 1898: 132, 135–136 (in part; Gülek); Werner, 1934a: 162 (in part); Werner, 1934b: 282 (in part); Werner, 1938: 172 (in part); Vachon, 1948: 63 (in part); Vachon, 1951: 343 (in part); Vachon, 1953: 96–100 (in part).

Iurus dufourei: Kraepelin, 1899: 178–179 (in part); Vachon, 1966a: 453–461, fig. 7–12, 14, 16, 18, 22 (Tarsus); Vachon, 1966b: 215 (in part); Stahnke, 1974: 123 (in part); Vachon, 1974, fig. 141, 144, 151–153, 216–219 (in part?); Kinzelbach, 1975: 21–26 (in part); Kinzelbach, 1985: Map IV (in part); Fet & Braunwalder, 2000: 18 (in part); Kaltsas, Stathi & Fet, 2008: 227–228 (in part); Soleglad, Kovařík & Fet, 2009: 2 (in part).

Iurus dufourei *asiaticus*: Borelli, 1913: 3; Sissom & Fet, 2000: 420 (in part); Kaltsas, Stathi & Fet, 2008: 228 (in part); Yağmur, Koç & Akkaya, 2009: 154–159 (in part), fig. 1.

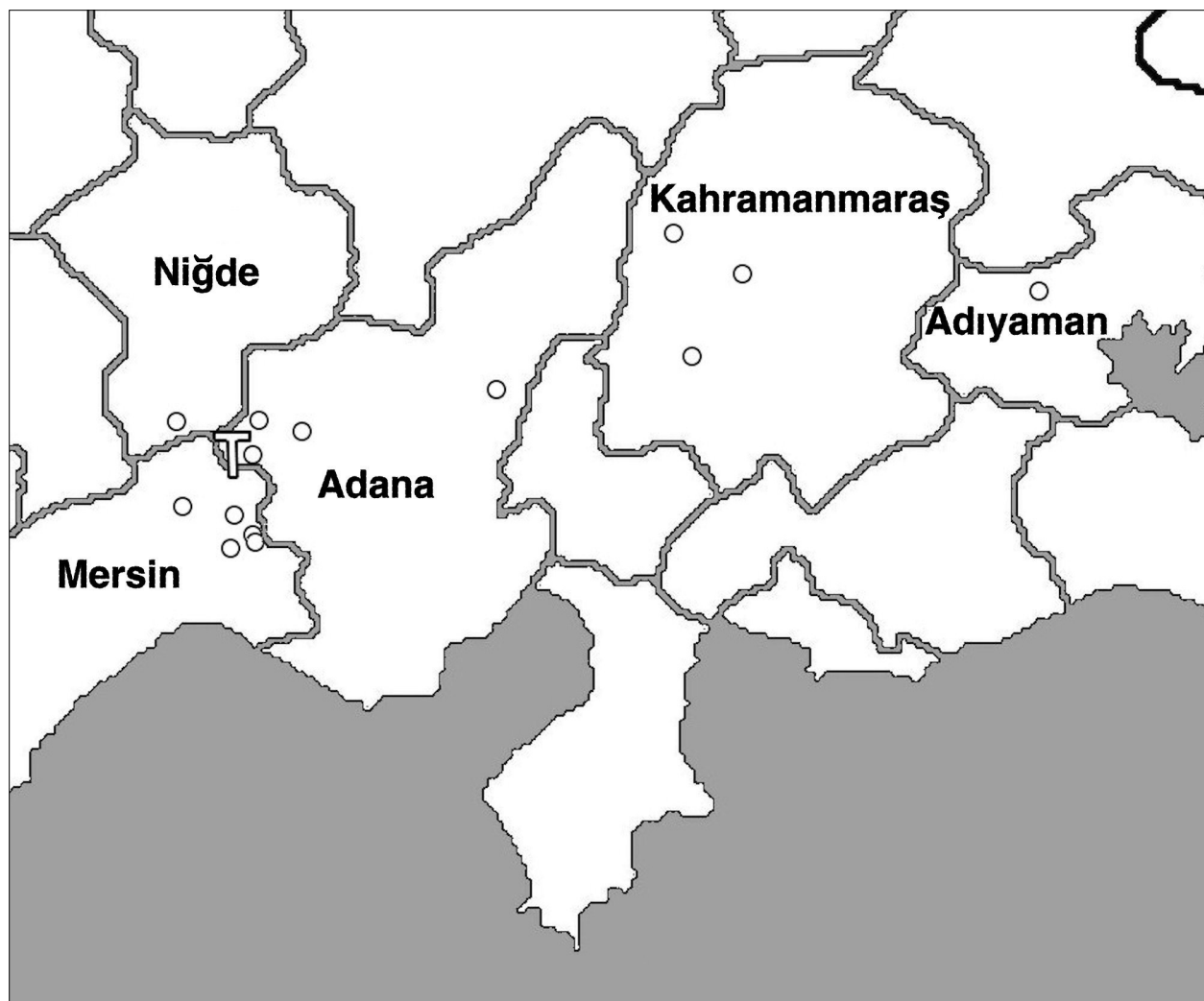


Figure 148: Large-scale map showing distribution of *Iurus asiaticus*. "T" marks type locality, Gülek Pass, Adana Province, Turkey. See Fig. 74 for distribution of all species and Appendix A for detailed locality data.

Jurus dufourieius asiaticus: Vachon, 1947a: 162 (in part); Vachon, 1947b: 2 (in part); Vachon, 1948: 63 (in part); Vachon, 1951: 342 (in part).

Iurus asiaticus: Francke, 1981: 221–224 (in part), fig. 4 (Namrun, in part); Vachon & Kinzelbach, 1987: 102 (in part); Crucitti, 1995a: 2 (in part); Crucitti, 1998: 32 (in part); Crucitti & Malori, 1998: 133–135; Kovařík, 1998: 136 (in part); Crucitti, 1999a: 87–88, fig. 2 (in part); Kovařík, 1999: 40 (in part); Crucitti & Cicuzza, 2001: 227, 229, fig. 7 (in part); Karataş, 2001: 14 (in part); Kovařík, 2002: 16 (in part; Belemedik); Kovařík, 2005: 55 (in part); Facheris, 2007a: 1 (in part); Facheris, 2007b: 1 (in part).

Lectotype: ♀ (designated here; see discussion below), TURKEY (southeast), *Adana Province*, Gülek Pass, 1300 m a.s.l., May-August 1897, leg. M. Holtz (see original label on Fig. 176) (ZISP 1066); **paralectotypes**:

1 subad. ♂, 1 subad. ♀, same label as lectotype (ZISP 1066).

Diagnosis: Medium to large species, 90 mm. Dark gray to black in overall coloration. Pectinal tooth counts, 10–13 (11.67) males, 9–12 (10.58) females. Chelal movable finger lobe in adults located mid-finger or distal, lobe ratio 0.47–0.58; proximal gap of fixed finger present in adult males; movable finger of adult males essentially straight, not highly curved; chelal palm of adult males elongate, not highly vaulted, chela length/palm depth 2.94–3.14 (3.01) male, 2.98–3.16 (3.06) female; number of inner denticles (*ID*) of chelal movable finger, 11–12 (11.5); constellation array with *two to four* sensilla; hemispermatophore lamina internal nodule conspicuously pointed, positioned suprabasally, lamina distal length/lamina basal length 1.614–1.802 (1.729), terminus of the acuminate process truncated, transverse trunk



Figure 149: *Iurus asiaticus*. Dorsal and ventral views. Adult male, Çamlıhayla (=Namrun), Mersin, Turkey.

bolsters absent. Dominant morphometric is palm length (see Appendix C).

Distribution. Turkey: Anatolia (southeast): Mersin, Niğde (south), Kahramanmaraş, Adana, and Adiyaman Provinces. See map in Fig. 74 for large-scale distribution of this species.

MALE. Description is based on a male from Çamlıayla (=Namrun), Mersin Province, Turkey, about 17 km from type locality. Measurements of the Çamlıayla male and five other specimens are presented in Table 6. See Figure 149 for dorsal and ventral views of the Çamlıayla male.

COLORATION. Basic color of carapace, mesosoma, metasoma, and pedipalps dark brown, telson a lighter orange; legs light yellowish-brown. Carinae of metasoma, pedipalp, and carapace dark brown. Sternites, pectines, and genital operculum yellowish. Cheliceral fingers dark brown, palms yellow-orange. Essentially void of patterns.

CARAPACE (Fig. 150). Anterior edge with a conspicuous median indentation; most setation missing; anterior edge between lateral eyes covered with large granules, less granulated with smaller granules in interocular area. Interocular area conspicuously delineated by mediolateral ocular carinae; extreme lateral edges sparsely populated with medium-sized granules; posterior half covered with small to medium sized granules. Mediolateral ocular carinae, which are conspicuous due to the somewhat smooth interocular area, are well-developed and granulated, extending to the lateral eyes. There are three lateral eyes, the posterior eye considerably smaller than middle eye. Median eyes and tubercle somewhat small, positioned anteriorly of the middle with the following length and width formulas: 456|1135 and 141|994.

MESOSOMA (Figs. 151, 153). Tergites I–VI rough to granulated; tergite VII coarsely granulated, lateral carinae detectable but median obscured by heavy granulation on entire surface. Sternites III–VII smooth and lustrous; sternite VII with lateral carinae irregularly granulated, median carinae smooth proximally (Fig. 153). Stigmata (Fig. 151) are medium in size and slit-like in shape, angled 45° in an anterointernal direction.

METASOMA (Fig. 152). Segment I wider than long. Segments I–IV: dorsal and dorsolateral carinae serrated; dorsal carinae with 7/6, 8/8, 8/8, and 8/9 serrated spines (left/right carina); dorsal (I–IV) and dorsolateral (I–III) carinae do not terminate with an enlarged spine; lateral carinae serrated on I, crenulated on one-half of II, absent on segments III–IV; ventrolateral carinae crenulated on

I–II, serrated on III–IV; ventromedian carinae smooth on I, irregularly granulated on II, crenulated on III, and serrated on IV. Dorsolateral carinae of segment IV terminate at articulation condyle. Segment V: dorsolateral carinae serrated; lateral carinae irregularly serrated for two-thirds of their posterior portion; ventrolateral and single ventromedian carinae serrated; ventromedian carina terminus slightly bifurcated. Anal arch with 16 serrated granules. Intercarinal areas of segments I–V essentially smooth. Metasomal segments moderately covered with long setae.

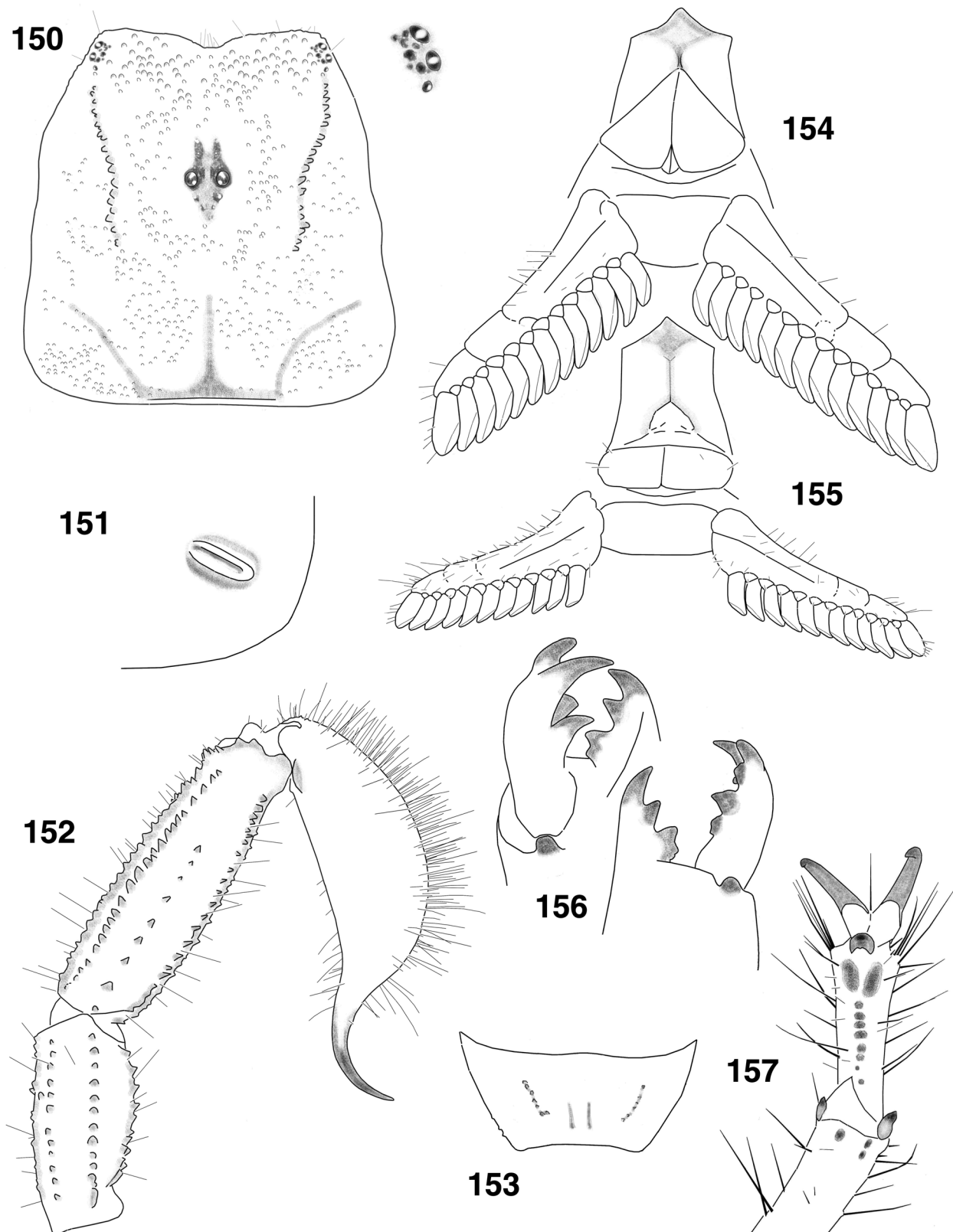
TELSON (Fig. 152). Vesicle elongated, with highly curved aculeus. Vesicle smooth ventrally; ventral surface densely covered with medium-length, straight setae; dorsal setation much less dense, with shorter setae; base of aculeus with setation ventrally and dorsally; areolae on aculeus base slightly swollen, setal pair broken off. Vesicular tabs with small granules.

PECTINES (Fig. 154, female Fig. 155). Well-developed segments exhibiting length|width formula 720|300. Sclerite construction complex, with three anterior lamellae and one large middle lamella, with slight traces of a smaller second sclerite; fulcra of medium development. Teeth number 13/13. Sensory areas developed along most of tooth inner length on all teeth, including basal tooth. Scattered setae found on anterior lamellae and distal pectinal tooth (many are broken off). Basal piece large, with subtle indentation along anterior edge, length|width formula 200|320.

GENITAL OPERCULUM (Fig. 154). Sclerites triangular in shape, longer than wide, separated for entire length; conspicuous genital papillae visible at posterior edge (see discussion on female below).

STERNUM (Fig. 154). Type 2, posterior emargination present, well-defined convex lateral lobes, apex visible but not conspicuous; anterior portion of genital operculum situated proximally between lateral lobes; sclerite longer than wide, length|width formula 275|250; sclerite slightly tapers anteriorly, posterior-width|anterior-width formula 250|188 (see discussion on female below).

CHELICERAE (female, Fig. 156). Movable finger dorsal edge with one large subdistal (*sd*) denticle; ventral edge with one large pigmented accessory denticle at finger midpoint; ventral edge serrula not visible. Ventral distal denticle (*vd*) slightly longer than dorsal (*dd*). Fixed finger with four denticles, median (*m*) and basal (*b*) denticles conjoined on common trunk; no ventral accessory denticles present.



Figures 150–157: *Iurus asiaticus*. 150–154. Male, Çamlıayla, Mersin, Turkey. 155–157. Female, 4 km E Kaşlıca Village, Adiyaman, Turkey. 150. Carapace and close-up of lateral eyes. 151. Stigma III, left. 152. Telson and metasomal segments IV–V, lateral view. 153. Sternite VII. 154. Stenopectinal area. 155. Stenopectinal area. 156. Right chelicera, ventral and dorsal views. 157. Tarsus and partial basitarsus, right leg IV.

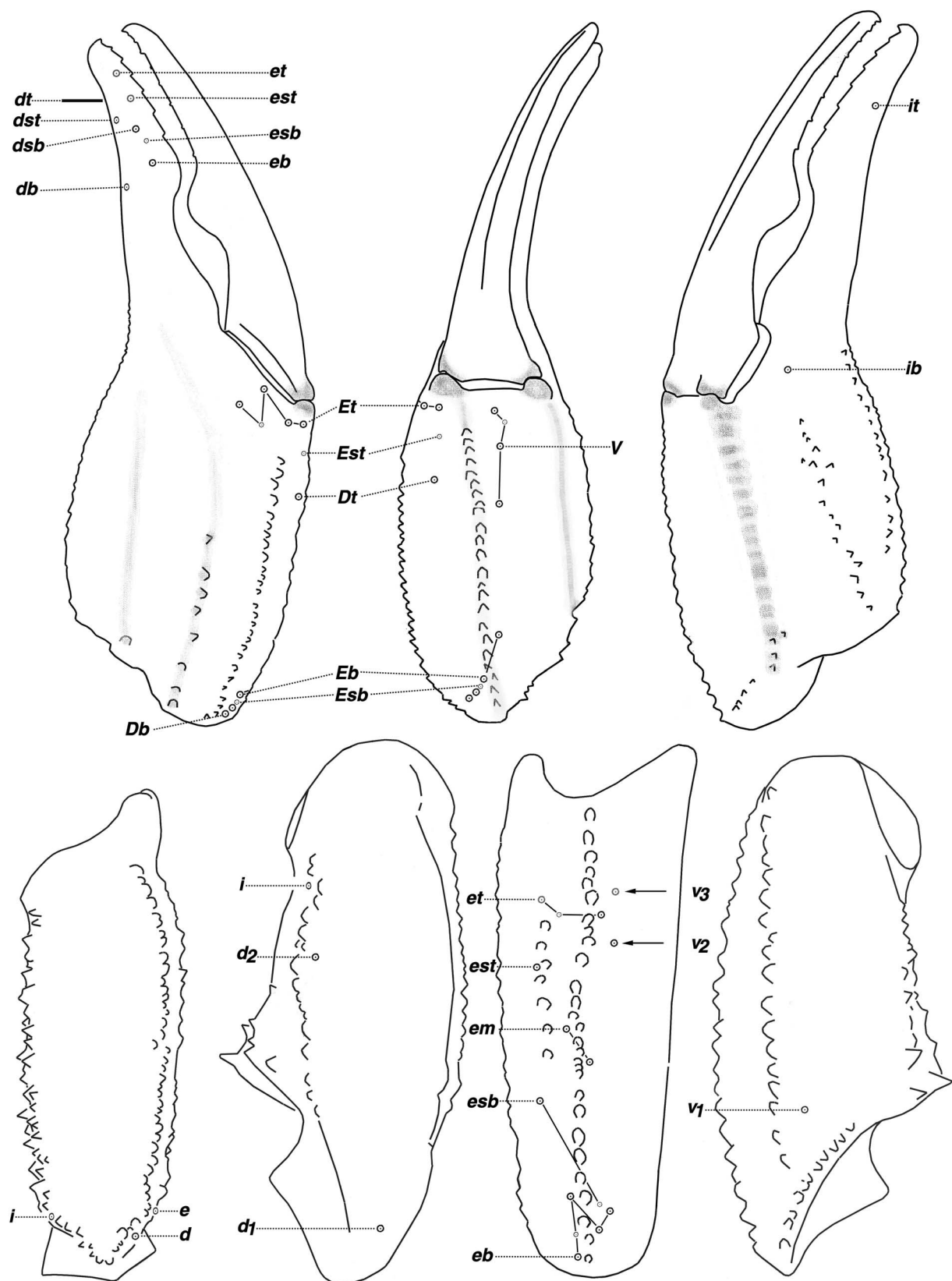
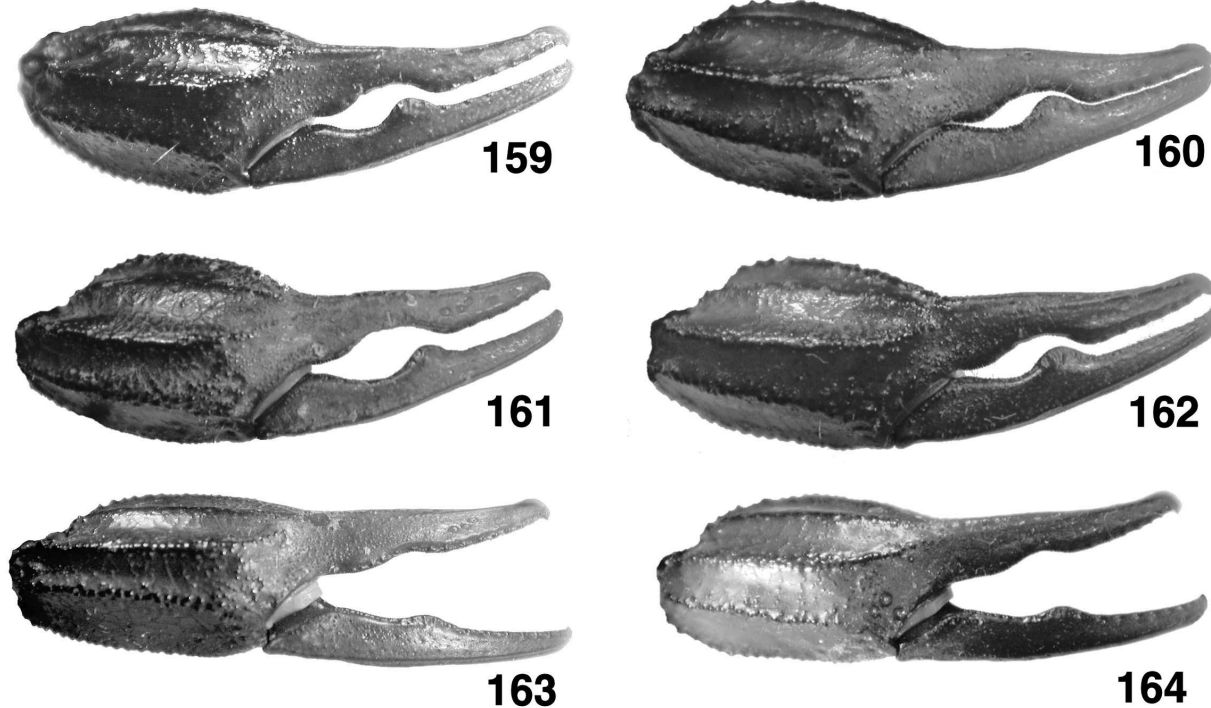


Figure 158: Trichobothrial pattern of *Iurus asiaticus*, male. Çamlıayyla, Mersin, Turkey.



Figures 159–164: Chela, lateral view, *Iurus asiaticus*, adults unless otherwise stated. **159.** Male, Kaşlıca, Adıyaman, Turkey. **160.** Male, Yaylaüstü Village, Kahramanmaraş, Turkey. **161.** Male, Eski Mantas Village, Adana, Turkey. **162.** Male, Çamlıayla, Mersin, Turkey. **163.** Female, Kaşlıca, Adıyaman, Turkey. **164.** Female, Yaylaüstü Village, Kahramanmaraş, Turkey. Note, in adults, the movable finger lobe is positioned distal of finger midpoint and the fixed finger proximal gap is conspicuously present in adult males.

PEDIPALPS (Fig. 158). Well-developed chelae, with long fingers, heavily carinated, scalloping of chelal fingers conspicuous: lobe on movable finger visible, positioned slightly beyond midpoint; proximal gap of fixed finger well-developed. **Femur:** Dorsointernal, dorsoexternal and ventrointernal carinae serrated, ventroexternal rounded. Dorsal and ventral surfaces irregularly granulated, internal and external surfaces with line of 12 and 17 serrated granules, respectively. **Patella:** Dorsointernal and ventrointernal carinae serrated, dorsoexternal and ventroexternal rounded and crenulated; exteromedian carina strong, serrated, and doubled medially. Dorsal surface sparsely granulated; ventral surface smooth; external surface smooth with serrated exteromedian carina; internal surface smooth, with well-developed, doubled DPS and VPS. **Chelal carinae:** Complies with the “8-carinae configuration”. Digital (*D1*) carina strong, smooth to granulated; dorsosecondary (*D3*) smooth with subtle granulation; dorsomarginal (*D4*) serrated, doubled; dorsointernal (*D5*) serrated; ventroexternal (*V1*) strong and serrated, terminating to external condyle of movable finger; ventrointernal (*V3*) rounded, smooth to granulated, continuous to internal condyle; external (*E*) strong, continuous, and serrated; internal (*I*) irregularly serrated. **Chelal finger dentition:** Median

denticle (*MD*) row groups oblique and highly imbricated; 10/10 *IDs* on fixed fingers and 12/12 *IDs* on movable fingers; 10/10 *ODs* to socket on fixed fingers and 15/15 *ODs* on movable fingers. No accessory denticles present. **Trichobothrial pattern (Fig. 158):** Type C, orthobothriotaxic, typical of genus (but see below on neobothriotaxy in this species).

LEGS (female, Fig. 157). Both pedal spurs present on all legs, lacking spinelets; tibial spurs absent. Tarsus with conspicuous spinule clusters in single row on ventral surface, terminating distally with a pair of enlarged spinule clusters. Unguicular spine well-developed and pointed.

HEMISPERMATOPHORE (Figs. 165–171). We have examined several hemispermophores of *I. asiaticus*, spanning major parts of its distribution range (Mersin, Kahramanmaraş, and Adıyaman Provinces; see map in Fig. 60). The hemispermophore of *I. asiaticus* is unique among *Iurus* species, exhibiting a short lamina with a pointed terminus, a wide pointed medially positioned internal nodule, absence of transverse trunk bolsters, and a truncated acuminate process terminus (see below for more data).

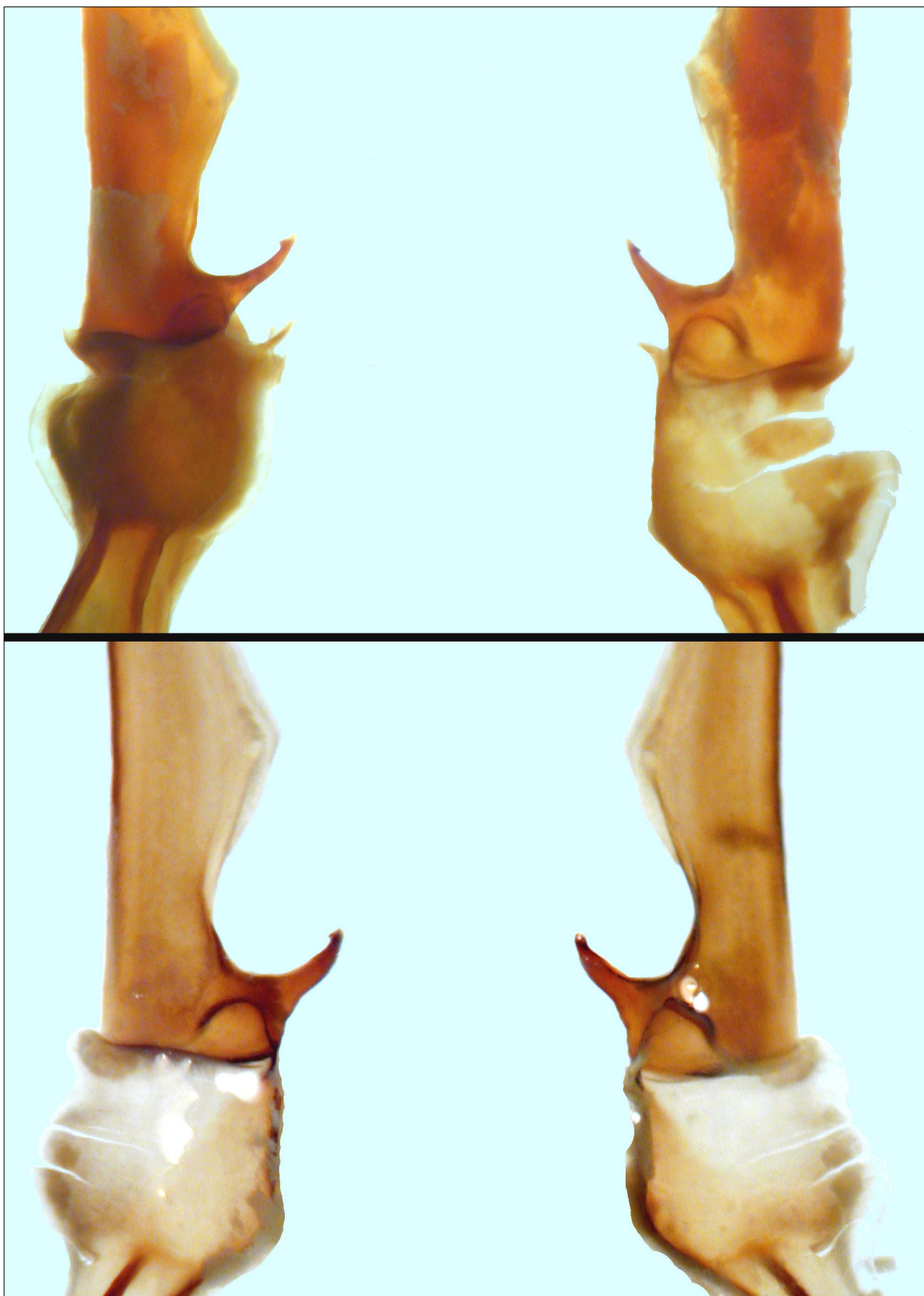


Figure 165: Close-up of median area of hemispermatophore, *Iurus asiaticus*. **Top.** Right hemispermatophore, dorsal and ventral views, Tut District, Adiyaman, Turkey. **Bottom.** Right hemispermatophore, dorsal and ventral views, Central District, Kahramanmaraş, Turkey.



Figure 166: Close-up of median area of right hemispermatophore, *Iurus asiaticus*, Çamlıayla, Mersin, Turkey. **Top.** Externodorsal, internoventral, and ventrointernal views. Note, a lightly sclerotized fragment has peeled away from median area. **Bottom.** Dorsal and ventral views.

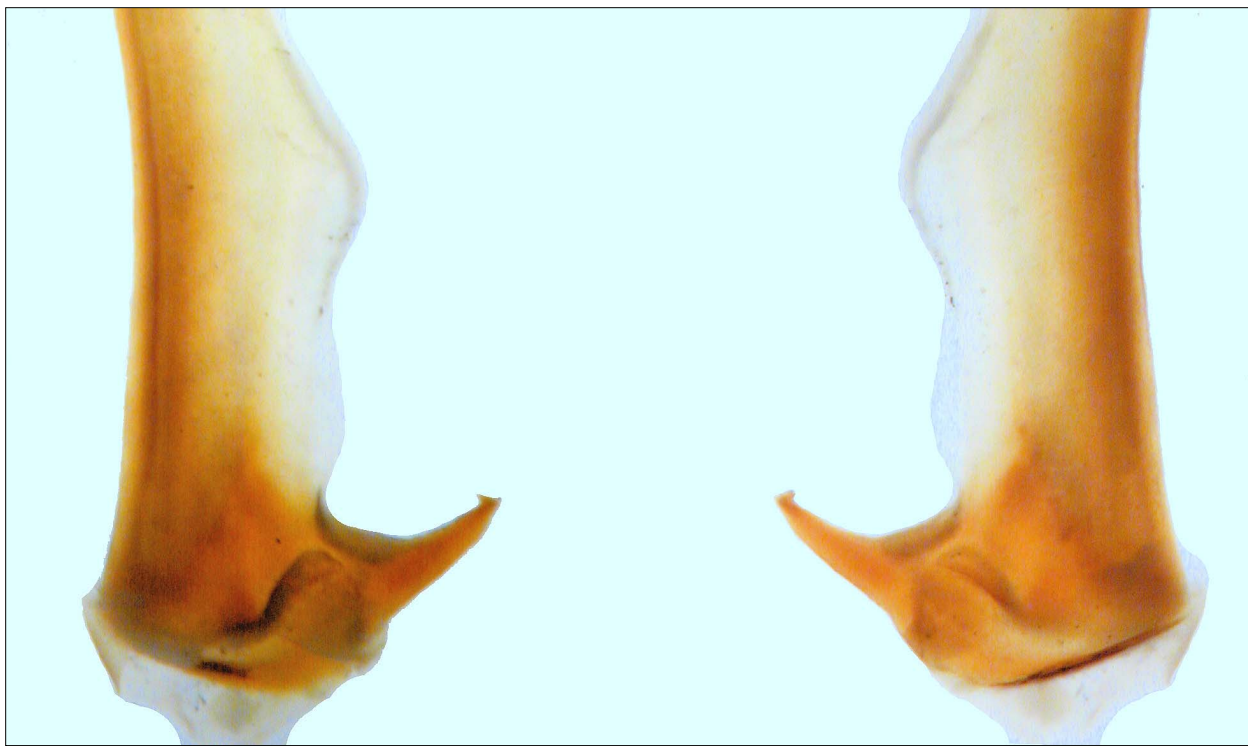


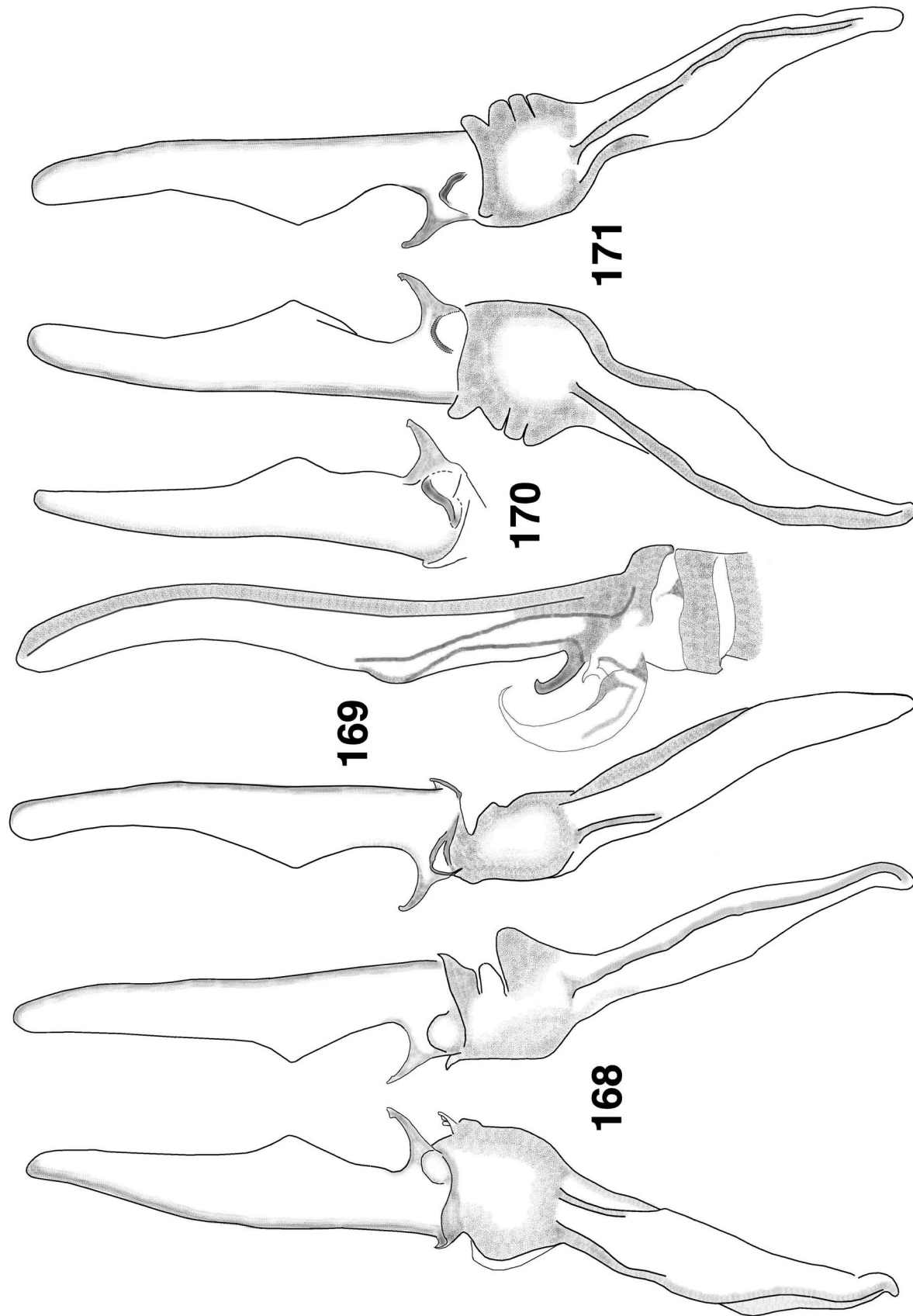
Figure 167: Close-up of median area of left hemispermatophore, *Iurus asiaticus*, ventral and dorsal views. Tarsus, Mersin, Turkey. Note a well developed internal nodule, a truncated acuminate process terminus, and a seminal receptacle in ventral view (reflection of receptacle is visible in dorsal view).

Male and female variability. The overall morphology of the chela exhibits significant sexual dimorphism (Figs. 159–164). In the sexually mature male, the movable finger lobe is conspicuous, fitting into an equally well developed fixed finger socket with a proximal gap. In the female, the lobe and socket are not as developed and the proximal gap is missing. There is no significant sexual dimorphism in morphometrics. The metasomal segments are relatively longer in the male, but the MVDs across all five segments only favored the male by 4.6 to 9.0 % when compared to the segment's width. Pectinal tooth counts in males exceed those of females by approximately one tooth (1.09), male 10–13 (11.67) [18], female 9–12 (10.58) [22] (see histograms in Fig. 73). The genital operculum of the male is different from that in the female (Figs. 154–155). The sclerites, subtriangular in shape, are as long as or longer than wide in the male, whereas in the female the sclerites are short and wide, more than twice as wide as long. Whereas the sclerites are fused medially in the female, they are separated along their entire length in the male, exposing significantly developed genital papillae. The enlarged genital operculum of the male extends distally between the lateral lobes of the sternum partially obscuring its proximal region. Figures 172–173 and 177–180 show dorsal and ventral views of both male and female specimens, and various collection localities for this species.

Lectotype analysis

Three specimens from Gülek were first mentioned by Birula (1898) as *Iurus dufoureius*; these were likely the first Anatolian specimens of *Iurus* available to researchers. The subspecies *Iurus dufoureius asiaticus* was described, however, only five years later when Birula had a chance to compare it to the Crete and mainland Greece specimens. In a very brief comparative paragraph, Birula (1903) wrote (talking about a population of *Iurus dufoureius* from Crete) (Figs. 174–176):

[p. 297:] [p. 297:] "Two good specimens from the vicinity of the town of Candia [now Iraklio, Crete] - one female with 9 pectinal teeth, about 82 mm long, another, probably male, with larger pectines (also with 9 teeth) and a triangular genital plate, 74 mm long. Both of these specimens do not differ from specimens found in [mainland] Greece (10–11 pectinal teeth); however, the Anatolian (Gülek specimens) somewhat differ from the typical ones (from Greece) in the following: the larger female from Gülek is dark-brown with strong green shine; telson ventrally strongly hirsute; chela dorsally with distinct but smooth carinae; carapace coarsely granulated, but with smooth spaces between the rows of granules; metasomal segment I somewhat rough between ventral carinae; [p. 298:] also pectines with 12 teeth. Thus Anatolian specimens can be, not without a jus-



Figures 168–171: Hemispermatophore, *Iurus asiaticus* (right hemispermatophore unless stated otherwise). **168.** Tut District, Adiyaman, Turkey, dorsal and ventral views. **169.** Çamlıayla, Mersin, Turkey, left, ventral view, right, ventrointernal view. Note, a lightly sclerotized fragment has peeled away from median area. **170.** Tarsus, Mersin, Turkey, left hemispermatophore, ventral view. **171.** Central District, Kahramanmaraş, Turkey, dorsal and ventral views.

<i>Iurus asiaticus</i> Birula, 1903						
	Çamhiyaya, Mersin, Turkey	Kaşlıca Village, Adıyaman, Turkey				Yaylaüstü Village, Kahramanmaraş, Turkey
	Male	Male	Female	Female	Male	Female
Total length	72.90	84.05	82.60	88.15	83.50	80.80
Carapace length	11.35	12.10	12.15	12.75	11.65	11.45
Mesosoma length	20.30	25.40	27.95	30.45	28.95	30.50
Metasoma length	29.20	33.70	30.30	32.30	30.80	27.30
Segment I length/width	3.95/4.55	4.45/4.80	4.20/4.95	4.30/5.20	4.30/4.85	3.65/4.65
Segment II length/width	4.55/4.00	5.20/4.50	4.70/4.30	4.90/4.55	4.90/4.30	4.20/4.25
Segment III length/width	4.95/3.70	5.50/4.10	5.20/3.90	5.40/4.20	5.30/4.00	4.60/3.80
Segment IV length/width	6.00/3.35	6.70/3.70	6.05/3.50	6.60/3.75	6.15/3.55	5.45/3.45
Segment V length/width	9.75/3.15	11.85/3.55	10.15/3.30	11.10/3.55	10.15/3.30	9.40/3.25
Telson length	12.05	12.85	12.20	12.65	12.10	11.55
Vesicle length width/depth	8.45 3.25/3.10	9.20 3.95/3.50	8.40 3.60/3.35	9.15 3.75/3.50	8.65 3.65/3.35	7.90 3.30/3.00
Aculeus length	3.60	3.65	3.80	3.50	3.45	3.65
Pedipalp length	43.20	50.45	48.00	49.70	48.60	42.55
Femur length/width	11.40/3.90	12.95/4.05	12.40/4.20	12.85/4.40	12.10/4.10	10.80/3.35
Patella length/width* DPS height**	10.45/4.10 1.35	12.10/4.30 1.60	11.45/4.20 1.30	12.10/4.55 1.70	11.10/4.25 1.70	10.15/3.90 1.40
Chela length	21.35	25.40	24.15	24.75	25.40	21.60
Palm length width/depth	10.25 5.60/7.25	11.85 6.60/8.65	11.60 5.95/7.65	11.85 6.40/8.30	11.00 6.30/8.10	10.40 6.15/7.10
Fixed finger length	10.20	11.85	11.35	12.10	11.10	10.05
Movable finger length	13.05	14.90	14.35	15.30	14.25	-
Pectines teeth middle lamellae	13-13 2-2++	11-10 3-4	11-11 3-3	12-11 2-2	11-11 3-3	11-11 1-2
Sternum length/width	2.75/2.50	3.15/2.25	3.25/2.60	3.45/2.70	2.90/2.15	3.25/2.80

Table 6: Morphometrics (mm) of *Iurus asiaticus* Birula, 1903. * Patella width is widest distance between the dorsointernal and externomedial carinae. ** DPS height is from tip of spines to dorsointernal carina center.

tification, separated as a subspecies of *Jurus dufourei* (Brullé), which I name here *Jurus dufourei* *asiaticus* Birula, 1903." (transl. from German).

We received photographs (courtesy of Viktor Krivochatsky, November 2008) of all three Birula's original syntypes (ZISP 1066; see log sheet in Fig. 175): dorsal and ventral views of a subadult female, pectinal teeth 10; dorsal and ventral views of a subadult male; and dorsal views of an adult female (presumably with 12 pectinal teeth). Fig. 174 shows this adult female, which we designate here as a lectotype of *Iurus asiaticus*. Fig. 176 shows the original type series label for this species.

In the photograph of the female lectotype, we can observe the following: the movable finger lobe of the chela is positioned distally on the finger, in a ratio of 0.517; a proximal gap is not present on the fixed finger;

and the interocular area of the carapace is somewhat smooth, delineated by the strongly developed mediolateral ocular carinae. Morphometric ratios derived from the pedipalp chela of the female lectotype (the chelal length as compared to the palm depth, movable finger length, and palm length) are consistent with those of three adult females of *I. asiaticus* measured in this study (see Table 6). Finally, the movable finger lobe ratio of the female lectotype is consistent with that for *I. asiaticus* (see scatter chart in Fig. 56).

Discussion

I. asiaticus has the second most distally positioned movable finger lobe in the genus, only exceeded by that



Figure 172: *Iurus asiaticus*. Dorsal view. Adult male, 2 km W Yaylaustu Village, Kahramanmaraş, Turkey.

of *I. kraepelini*. The movable finger lobe ratio is larger in the male than in the female, 0.475–0.580 vs. 0.460–0.540 (ratios calculated from adults with carapaces 11 mm long or larger; see scatter chart in Fig. 56 for a complete analysis of this character).

The hemispermatophore of *I. asiaticus* (Figs. 165–171) has been examined from four specimens, each from a separate locality (see map in Fig. 60). Unique to this species is the relatively short lamina. As can be seen in Tables 2 and 3, *I. asiaticus* exhibits the smallest morpho-

metric ratio values across all species in *all* four ratios. In part, this is due to the relatively short lamina: when the lamina length is compared to the trunk length, *I. asiaticus* shows a 22 to 68 % in MVD; and in the ratio that compares the lamina distal length to its basal length, we see MVDs of 48 to 172 %, a very significant value. The lamina terminus is somewhat pointed, especially when compared to its wide and pointed internal nodule. The internal nodule is situated suprabasally on the lamina, in a ratio 1.7. The acuminate process terminus is



Figure 173: *Iurus asiaticus*. Dorsal view. Adult female, 4 km E Kaşlıca Village, Adiyaman, Turkey.

truncated as in most other *Iurus* species. Transverse trunk bolsters are absent. The paraxial organ sleeve was not detected in the five hemispermatophores examined.

In Appendix C, we present a complete analysis of the morphometric trends across the five species of *Iurus*. This analysis shows that the palm length of *I. asiaticus* dominated in a large majority of morphometric ratio comparisons: averaging 20 comparisons out of 25 for

males and 24 for females. This dominant morphometric was combined with the telson length, a measurement with the least dominance in ratio comparisons (it only dominated in five to six morphometric comparisons), to form a diagnostic character for *I. asiaticus*. Figure C7 in Appendix C presents the histograms of the chela palm length as compared to the telson length. This morphometric, consistent in both genders, provides decent



Figure 174: *Iurus asiaticus* Birula, 1903, female lectotype, Gülek Pass (Gülek Boğazı, Cilician Gates), Taurus Mts., Adana, Turkey (photograph courtesy of Viktor Krivochatsky, St. Petersburg, Russia). The left pedipalp is situated closer to the photographic plane and therefore is somewhat out of focus.

diagnostic separation for *I. asiaticus* from the species closest geographically, *I. kraepelini*, exhibiting 12.2 and 18.8 % MVDs for the male and female, respectively.

Only once was neobothriotaxy encountered among the 20 specimens of *I. asiaticus* examined, in a male

from Çamlıayla District, Mersin Province. See Appendix B for more information.

Material Examined (31 specimens). TURKEY: Adana Province: Kozan District, Eski Mantaş Village, Beşiktaş

Наземн. жив.							
<i>Iurus dufourii</i> (Boulenger)							
Лист №							
№ входящего в журн.	Число экз.	Место сбора.	Время сбора.	Коллекторъ.	Кто определил.	ОТМЕНА.	
1066	♂	Греция, Каппадокия Г - VIII		M. Holtz	A. Birula	126-97	
1067	♀	Малор - Гатун (1300 м) 897					
1068	?	о-в Крит: Гакоди 242/1898 фр бородатый					
1068.VI	♂	Месинес (Крит)		M. Holtz	"		
		Маньчжур.					
Registration number	Number of specimens	Gender	Locality	Date "old calendar"	Collector	Who identified	Notes
	in alcohol	dry	microscope slides				
1066 (654)	3		♀ + 2 pul.	Asia Minor, Cilician Taurus - Gulek (1300 m)	May - August 1897	M. Holtz	A. Birula No 126-97
1067	2		?	Crete Island, Candia	24 October 1898	Dr. Bogolyubov	"
1068	1	♀	Peloponnes (Greece), Taygetos		M. Holtz	"	

Figure 175: *Iurus* specimens from Birula's collection deposited in ZISP (St. Petersburg, Russia). **Top.** the original handwritten (in Birula's hand) collection list in the museum journal from ZISP (courtesy V. A. Krivochatsky, ZISP). **Bottom.** Translation from Russian. The first entry (ZISP 1066) is the type series of *Iurus asiaticus* (see vial label at Fig. 176) while two other entries refer to *I. dufourii*; the specimen from Crete (ZISP 1067) collected by Bogolyubov was mentioned by Birula (1903).

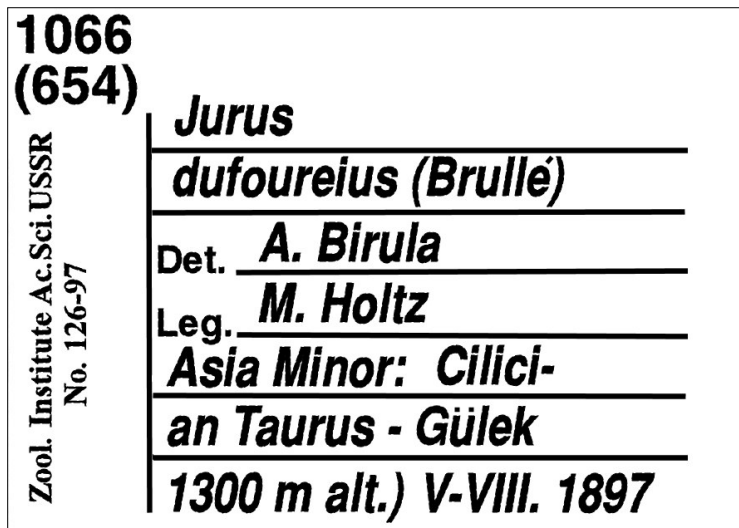
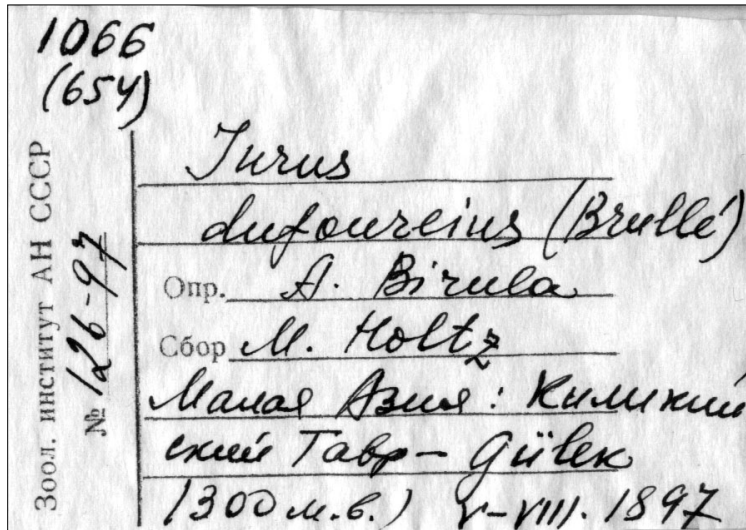


Figure 176: Locality label for original type series of *Jurus asiaticus*. **Top.** Original label. **Bottom.** English translation.

area, 37°30'43"N, 35°52'31"E, 29 August 2004, 450 m asl, 1 ♂, leg. E. A. Yağmur & H. Karaoğlu (MTAS); Pozanti District, Belemedik ("Belemedek Mara, Barakken"), 1914, 1 ♂, 1 ♀, 2 imm. (SMFD 24518); Pozanti District, E of Pozanti, 37°26'02"N, 34°53'57"E, 8 June 2007, 1 ♂ sbad., 1 ♂ juv., leg. E. A. Yağmur & A. V. Gromov (MTAS). *Adiyaman Province*: Tut District, 4 km E of Kaşlıca Village, southern slopes of Akdağ Mts, 37°48'34.6"N, 37°59'21.9"E, 1183 m asl, 8 June 2007, 1 ♂, 1 ♂, 5 ♀, 1 ♀ juv. (MTAS), 1 ♂, 1 ♀ sbad. (FKCP), leg. E. A. Yağmur & G. Çalışır. *Kahramanmaraş Province*: Central District, Süleymanlı Village, 23 April 1966, 1 ♂, 1 ♀ sbad. (NHMW); Central District, 2 km W of Yaylaüstü Village fork in the road to Andırın, 37°34'33"N, 36°35'6"E, 1237 m asl, 21 June 2007, 1 ♀ sbad., leg. M. Z. Yıldız (MTAS), 23

June 2007, 1 ♂, 1 ♂ juv., 3 ♀ sbad., leg. E. A. Yağmur, M. Yalçın & S. Dudaklı (MTAS). *Mersin Province*: Çamlıayyla District, Namrun (now Çamlıayyla), 16 May 1967, 1 ♂, leg. F. Ressl (NHW 11325); Çamlıayyla District, near Çamlıayyla Village, 1100–1200 m, 9 May 1998, 1 ♀ sbad., leg. A. Plutenko (FKCP); Çamlıayyla District, Çamlıayyla Plateau, 37°08'19"N, 34°50'25"E, 425 m asl, 12 May 2008, 1 ♀, leg. A. Akkaya & İ. H. Uğurtaş (MTAS); Tarsus District, "Haci Hamfal" (?Haci Hamzali), 1 ♂ (MNHN RS 3007); Tarsus District, 1 km from Taşobası Village, 37°05'55"N, 34°55'40"E, 209 m asl, 24 April 2009, 1 ♂ sbad., leg. M. Z. Yıldız (MTAS). *Niğde Province*: Ulukışla District, Madenköy Village, 1710 m asl, 27 July 1970, 1 ♀, leg. F. Spigenberger (NHW 70/282).



Figure 177: Collection locality of *Iurus asiaticus*. Taşobası Village, Mersin, Turkey.



Figure 178: Collection locality of *Iurus asiaticus*. **Top.** Çamlıayla Plateau, Çamlıayla District, Mersin, Turkey. **Bottom.** Kaşlıca Village area, Tut District, Adıyaman, Turkey, 1183 m a.s.l. Most eastern locality of *Iurus asiaticus*.



Figure 179: Collection locality of *Iurus asiaticus*, Yaylaüstü Village fork in the road to Andırın, Kahramanmaraş, Turkey.



Figure 180: Collection locality of *Iurus asiaticus*. Maden Village, Bolkar Mts, Niğde, Turkey, 1710 m a.s.l.

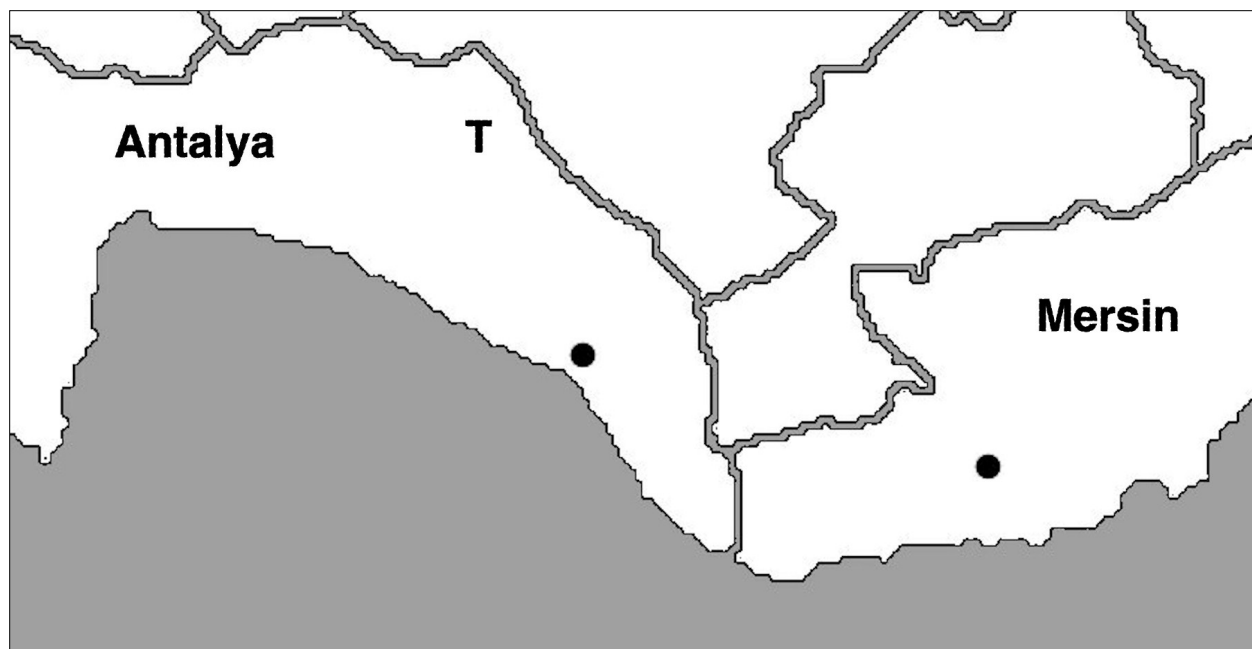


Figure 181: Large-scale map showing distribution of *Iurus kadleci*, sp. nov. "T" marks type locality, Akseki, Antalya Province, Turkey. See Fig. 74 for distribution of all species and Appendix A for detailed locality data.

***Iurus kadleci* Kovařík, Fet, Soleglad et Yağmur, sp. nov.**

(Figs. 7, 24, 35, 40, 52, 60, 73, 74, 181–197;
Tabs. 1, 7–9)

REFERENCES:

Iurus dufourei: Soleglad, Kovařík & Fet, 2009: 2 (in part; Akseki).

Holotype: ♀ (FKCP), TURKEY, Antalya Province: Akseki District, 12 km S Akseki, 11–12 May 2006, leg. F. Kovařík. **Paratypes**, see list below.

Diagnosis. Medium to large species, 90 mm. Red in overall coloration, chelae darkened. Pectinal tooth counts 10–12 (11.17) males, 10–11 (10.25) females. Chelal movable finger lobe in adults located on mid-finger or distally, lobe ratio 0.53–0.56; conspicuous proximal gap of fixed finger present in both adult males and females; movable finger of adult males essentially straight, not highly curved; number of inner denticles (ID) of chelal movable finger 11; most slender species in the genus, as exhibited in the metasoma, telson, and chela: metasomal segments thin, all longer than wide in both genders, subadults as well as adults (see Table 8 for morphometrics); chelal palm thin, chela length/palm depth (3.40) male, (3.32) female; telson thin, telson length/telson width (4.34) male, (4.29) female; constellation array with nine sensilla; hemispermatophore unknown. Tergites I–VI smooth; lateral carinae of

metasomal segments II–IV obsolete. Dominate morphometrics are metasoma segment and telson lengths (see Appendix C).

Distribution. Turkey (south): Antalya and Mersin Provinces. See map in Fig. 181 for large-scale distribution of this species.

Etymology. Named after the Czech coleopterist Stanislav Kadlec (27.12.1948–31.12.2008), who visited Turkey with FK and helped in collecting the type specimens.

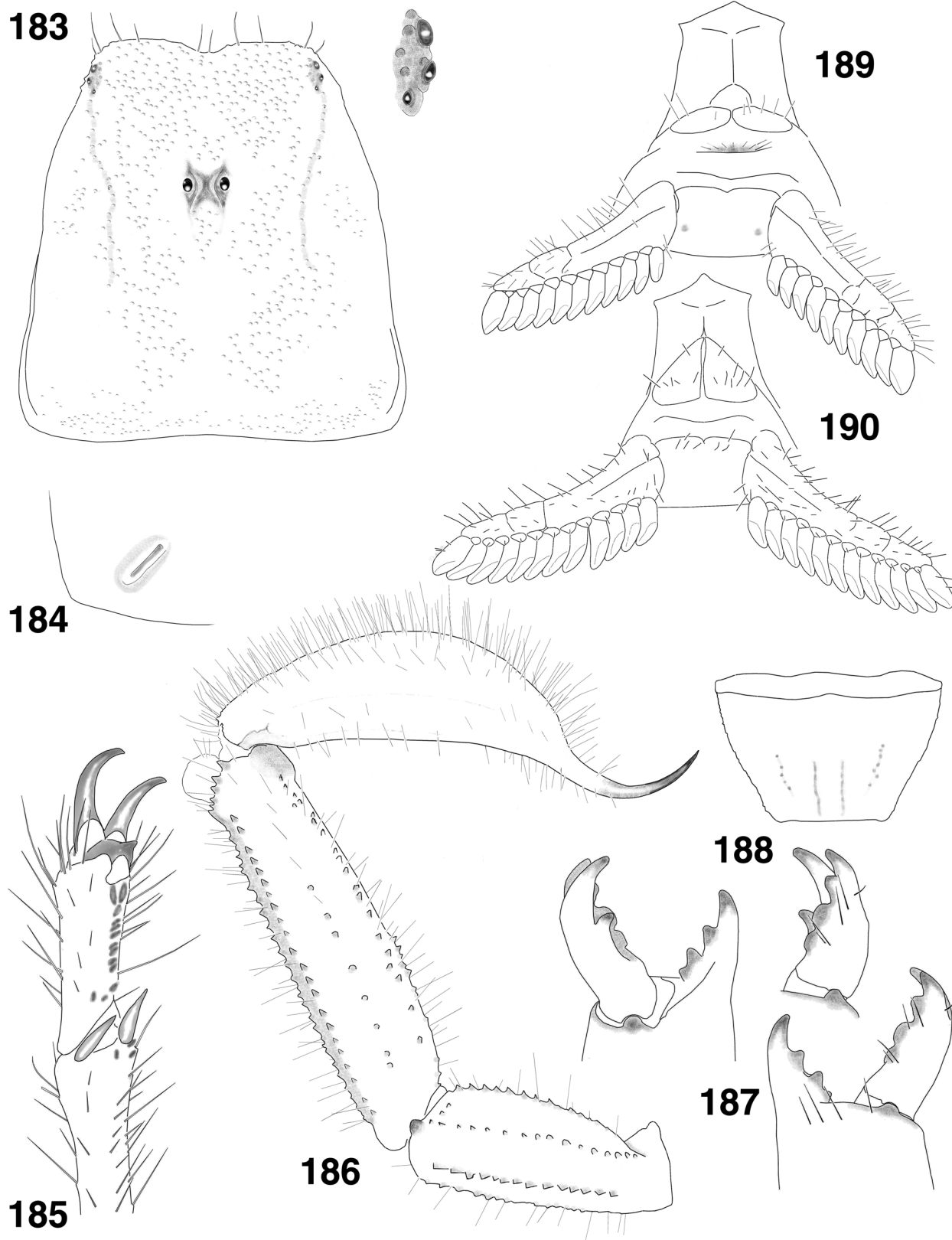
FEMALE. Description based on holotype female from Akseki, Antalya, Turkey. Measurements of the holotype plus two other specimens are presented in Table 7. See Figure 182 for a dorsal and ventral view of the female holotype.

COLORATION. Basic color of carapace, mesosoma, metasoma, telson, pedipalpal femur and patella reddish-brown; legs slightly lighter; chelae much darker, carinae dark gray to black, intercarinal areas dark red; leg condyles, chelal finger dentition, and telson aculeus dark brown; median and lateral eyes black. Essentially void of patterns except for lighter areas between carapace carinae.

CARAPACE (Fig. 183). Anterior edge with a conspicuous median indentation, approximately ten irregularly placed setae visible; entire surface densely covered with small



Figure 182: *Iurus kadleci*, sp. nov., dorsal and ventral views. Adult female holotype (FKCP) (97 mm), 12 km S. Akseki, Antalya, Turkey.



Figures 183–190: *Iurus kadleci*, sp. nov., Akseki, Antalya, Turkey. 183–189. Female holotype. 190. Male paratype. 183. Carapace and close-up of lateral eyes. 184. Stigma. 185. Tarsus and partial basitarsus, left leg IV. 186. Telson and metasomal segments IV–V, lateral view. 187. Right chelicera, dorsal and ventral views. 188. Sternite VII. 189. Sternopectinal area. 190. Sternopectinal area.

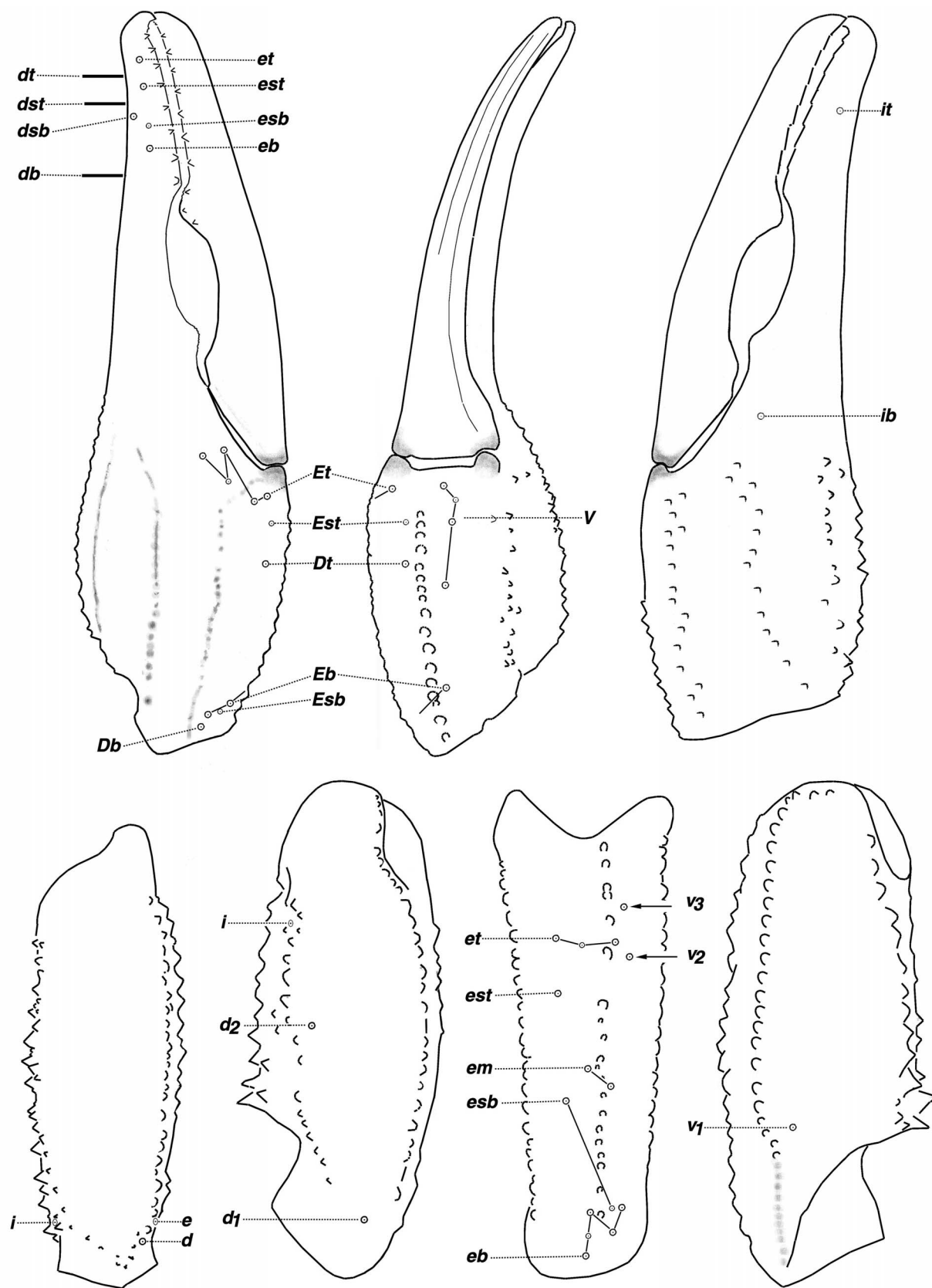
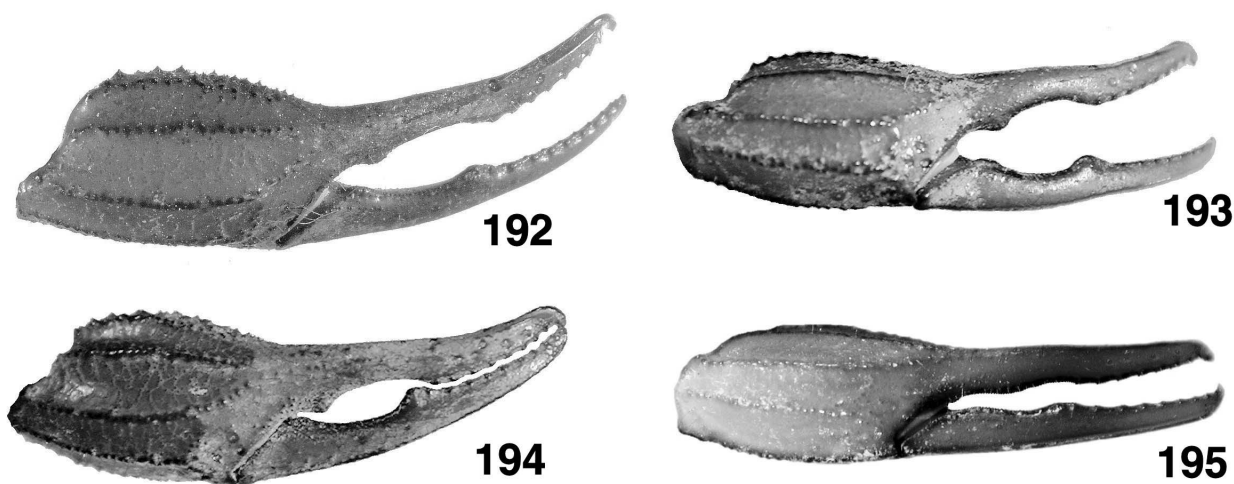


Figure 191: Trichobothrial pattern of *Iurus kadleci* sp. nov., female holotype. Akseki, Antalya, Turkey.



Figures 192–195: Chela, lateral view, *Iurus kadleci* sp. nov. 192–194. Adults, Akseki, Antalya, Turkey. 192–193. Male. 194. Female. 195. Subadult female, Dim Cave, Antalya, Turkey. Note in the adults, Figs. 192–194, the distally position movable finger lobe and exaggerated fixed finger proximal gap. In particular, Fig. 194, the proximal gap is also conspicuous in the adult female, unpredicated in *Iurus*.

granules, except for extreme lateral edges which are sparsely populated with granules. Mediolateral ocular carinae well-developed and granulated, extending to the lateral eyes; there are three lateral eyes, the posterior eye the smallest and facing inward. Median eyes and tubercle somewhat small, positioned anterior of middle with the following length and width formulas: 398|1150 and 133|958.

MESOSOMA (Figs. 184, 188). Tergites I–VI lacking granulation, but appearing somewhat rough at 10 \times ; tergite VII covered with minute granules, lateral carinae serrated, median carinae not detectable. Sternites III–VI smooth and lustrous; VII with one pair of irregularly granulated lateral carinae and one pair of smooth median carinae (Fig. 188). Stigmata (Fig. 184) are medium in size and slit-like in shape, angled 45° in an anterointernal direction.

METASOMA (Fig. 186). All segments are longer than wide. Segments I–IV: dorsal and dorsolateral carinae serrated; dorsal carinae with 12/13, 13/12, 14/14, and 15/14 serrated spines (left/right carina); dorsal (I–IV) and dorsolateral (I–III) carinae do not terminate with an enlarged spine; lateral carinae irregularly serrated on I, absent on segments II–IV; ventrolateral carinae crenulated on I–III and crenulated to serrated on IV; ventromedian carinae irregularly granulated on I–II, crenulated on III, and crenulated to serrated on IV. Dorsolateral carinae of segment IV terminates at articulation condyle. Segment V: dorsolateral carinae serrated; lateral carinae sparsely serrated for two-thirds of posterior aspect; ventrolateral and single ventro-

median carinae serrated; ventromedian carina not bifurcated, terminating in straight line. Anal arch with 14 serrated granules. Intercarinal areas of segments I–IV essentially smooth; segment V rough ventrally. Segments I–III with few setae ventrally; IV with dorsal and ventral setation; V with light to medium setation.

TELSON (Fig. 186). Vesicle extremely elongated with highly curved aculeus. Vesicle essentially void of granules; ventral surface densely covered with medium length straight reddish setae, dorsal setation much less dense, irregularly scattered; base of aculeus with setation ventrally and dorsally, slightly enlarged setal pair located on aculeus midpoint, areolae area not noticeably swollen. Vesicular tabs with small serrated granules ventrally.

PECTINES (Fig. 189, paratype male Fig. 190). Well-developed segments exhibiting length|width formula 970|345. Sclerite construction complex, three anterior lamellae and one large middle lamellae with slight indications of a smaller distal sclerite; fulcra of medium development. Teeth number 10/11. Sensory areas developed along most of tooth inner length on all teeth, including basal tooth. Scattered red setae found on anterior lamellae and distal pectinal tooth. Basal piece large, with subtle swallow indentation along anterior edge, length|width formula 330|490.

GENITAL OPERCULUM (Fig. 189). Sclerites elongate, wider than long, connected for entire length except for a swallow medial indentation on proximal edge (see discussion on male below).

<i>Iurus kadleci</i> sp. nov.			
	Akseki, Antalya, Turkey	Dim Cave, Antalya, Turkey	
	Female Holotype	Male Paratype	Subadult Female Paratype
Total length	97.00	92.20	74.85
Carapace length	11.50	11.10	9.30
Mesosoma length	33.50	28.45	25.35
Metasoma length	37.20	37.45	28.70
Segment I length/width	5.10/4.60	4.90/4.50	3.80/3.40
Segment II length/width	5.95/3.90	5.80/4.00	4.80/3.45
Segment III length/width	6.40/3.80	6.60/3.95	4.65/2.95
Segment IV length/width	7.35/3.45	7.65/3.40	5.45/2.70
Segment V length/width	12.40/3.20	12.50/2.95	10.00/2.60
Telson length	14.80	15.20	11.50
Vesicle length	10.25	10.80	7.55
width/depth	3.45/3.25	3.50/3.30	2.85/2.75
Aculeus length	4.55	4.40	3.95
Pedipalp length	46.55	45.65	38.00
Femur length/width	12.10/4.00	11.85/3.55	9.90/3.25
Patella length/width*	10.90/3.80	10.60/3.65	9.20/3.25
DPS height**	1.20	1.30	1.05
Chela length	23.55	23.20	18.90
Palm length	9.40	9.30	7.90
width/depth	5.60/7.10	5.30/6.50	4.35/5.40
Fixed finger length	12.20	11.90	10.00
Movable finger length	14.90	14.30	11.70
Pectines teeth middle lamellae	10-11 1-1++	12-12 3-4	10-10 2-2
Sternum length/width	3.00/2.45	2.75/2.15	2.60/2.10

Table 7: Morphometrics (mm) of *Iurus kadleci* sp. nov. * Patella width is widest distance between the dorsointernal and externomedial carinae. ** DPS height is from tip of spines to dorsointernal carina.

STERNUM (Fig. 189). Type 2, posterior emargination present, well-defined convex lateral lobes, apex visible but not conspicuous; conspicuous membranous plug situated proximally between lateral lobes; sclerite longer than wide, length|width formula 300|245; sclerite slightly tapers anteriorly, posterior-width|anterior-width formula 530|490 (see discussion on male below).

CHELICERAE (Fig. 187). Movable finger dorsal edge with somewhat worn dentition, with one large subdistal (*sd*) denticle; ventral edge with one large pigmented accessory denticle at finger midpoint; ventral edge serrula not visible. Ventral distal denticle (*vd*) slightly longer than dorsal (*dd*). Fixed finger with four denticles, median (*m*) and basal (*b*) denticles conjoined on common trunk; no ventral accessory denticles present.

PEDIPALPS (Fig. 191). Well-developed chelae, with medium to long fingers, heavily carinated, conspicuous

scalloping on chelal fingers: well-developed lobe on movable finger, positioned beyond midpoint in ratio 0.55; conspicuous proximal gap present on fixed finger.

Femur: Dorsointernal, dorsoexternal and ventrointernal carinae serrated, ventroexternal obsolete. Dorsal and ventral surfaces sparsely granulated, internal and external surface with line of 13 and 15 serrated granules, respectively. **Patella:** Dorsointernal and ventrointernal carinae serrated, dorsoexternal and ventroexternal crenulated, and exteromedian carina strong, serrated, and doubled on anterior median area. Dorsal surface with sparse rounded granules and ventral surface smooth; external surface with serrated exteromedian carina; internal surface smooth with well-developed, doubled DPS and VPS. **Chelal carinae:** Complies with the “8-carinae configuration”. Digital (*D1*) carina strong, crenulated; dorsosecondary (*D3*) crenulated; dorso-marginal (*D4*) roughly serrated, doubled; dorsointernal (*D5*) irregularly serrated; ventroexternal (*V1*) strong and

	<i>I. kraepelini</i>	<i>I. asiaticus</i>	<i>I. kinzelbachi</i>	<i>I. dufoureius</i>
Meta-I (L/W)	♂ 45 % 47 %	33 % 35 %	42 % 42 %	40 % 35 %
	♀			
Meta-II (L/W)	♂ 27 % 47 %	22 % 45 %	22 % 44 %	20 % 32 %
	♀			
Meta-III (L/W)	♂ 27 % 38 %	25 % 32 %	18 % 30 %	20 % 23 %
	♀			
Meta-IV (L/W)	♂ 26 % 32 %	20 % 26 %	14 % 21 %	16 % 16 %
	♀			
Meta-V (L/W)	♂ 20 % 22 %	25 % 28 %	13 % 11 %	30 % 25 %
	♀			
Tel_L / Tel_W	♂ 28 % 28 %	27 % 25 %	18 % 18 %	34 % 36 %
	♀			
Che_L/Che_D	♂ 47 % 25 %	13 % 8 %	16 % 5 %	18 % 8 %
	♀			

Table 8: Morphometric ratio Mean Value Differences (MVD) between *Iurus kadleci* sp. nov. and the other four species of *Iurus*. This data illustrates the relative slenderness of *I. kadleci* in metasomal segments, the telson, and the chelal depth. In particular, sympatric species *I. kraepelini* exhibits the largest MVDs, ranging from 20 to 47 percent. See Appendix C for a detailed discussion of the dominant morphometrics for all five *Iurus* species and histograms of important morphometrics.

	Average Number of Spines on Metasomal Dorsal Carinae *	MVD % with <i>I. kadleci</i>
<i>I. kadleci</i>	10.50–13.38 (12.200) (± 1.077) [005] {11.12–13.28}: 0.088	-
<i>I. dufoureius</i>	9.38–12.75 (10.548) (± 0.808) [021] { 9.74–11.36}: 0.077	15.7 %
<i>I. kinzelbachi</i>	8.12–10.00 (9.030) (± 0.487) [026] { 8.54–9.52}: 0.054	35.1 %
<i>I. asiaticus</i>	7.38–9.00 (8.175) (± 0.445) [018] { 7.73–8.62}: 0.054	49.2 %
<i>I. kraepelini</i>	6.00–9.12 (7.807) (± 0.719) [062] { 7.09–8.53}: 0.092	56.3 %

Table 9: Statistical data on the number of spines found on the metasomal dorsal carinae (segments I–IV) based on 132 samples. This data clearly shows that *I. kadleci* has the largest number of spines on the dorsal carinae, exhibiting 16 to 56 percent MVDs with the other species. * Counts are based on the average number of spines for segments I–IV, including both left and right carina. Statistical data group includes absolute range (mean) (\pm standard deviation) [number of samples] {standard error range}: coefficient of variability. MVD % = mean value difference percentage.

serrated, terminating slightly internal to external condyle of movable finger; ventrointernal (*V3*) irregularly serrated, continuous to internal condyle; external (*E*) strong, continuous, and serrated; internal (*I*) irregularly serrated. **Chelal finger dentition:** Number of median rows, internal denticles (*ID*), and outer denticles (*OD*) are difficult to determine due to conspicuous scalloping of the fingers. Median denticle (*MD*) row groups oblique and highly imbricated; 9 *IDs* to socket beginning on fixed finger and 10 *IDs* to lobe center on movable finger; 8 *ODs* to socket beginning on fixed finger and 10 *ODs* to lobe center on movable finger. No accessory denticles present. **Trichobothrial patterns (Fig. 191):** Type C, orthobothriotaxic, typical of genus.

LEGS (Fig. 185). Both pedal spurs present on all legs, lacking spinelets; tibial spurs absent. Tarsus with con-

spicuous spinule clusters in single row on ventral surface, terminating distally with a pair of enlarged spinule clusters. Unguicular spine well-developed and pointed.

HEMISPERMATOPHORE. Unknown in this species.

Male and female variability. Unique to this species is the conspicuous proximal gap present in the adult female. Its development is as strong as that in the male (Figs. 192–194). There is no significant sexual dimorphism in morphometrics except for the telson which is relatively longer in the male. For the metasomal segments all are longer than wide in both genders. Pectinal tooth counts in males exceed those of females by approximately one tooth, male 10–12 (11.17) [6], female 10–11 (10.25) [4] (see histograms in Fig. 73).



Figure 196: *Iurus kadleci*, sp. nov., dorsal and ventral views. Adult male paratype (FKCP) (90 mm), 12 km S. Akseki, Antalya, Turkey.



Figure 197: *Iurus kadleci*, sp. nov., dorsal view. Subadult paratype female, Dim Cave, Antalya, Turkey.



Figure 198: *Iurus kadleci*, sp. nov. Subadult paratype female shown 25 vertical meters deep inside Dim Cave, Antalya, Turkey.



Figure 199: *Iurus kadleci*, sp. nov. Adult male paratype (FKCP) (90 mm), 12 km S. Akseki, Antalya, Turkey.



Figure 200: 12 km S. Akseki, Antalya, Turkey. Collection locality of *Iurus kadleci*, sp. nov., and *I. kraepelini*, together with *Calchas gruberi* and *Mesobuthus gibbosus*.

The genital operculum of the male is dramatically different from that in the female (Figs. 189–190). The sclerites, subtriangular in shape, are as long as or longer than wide in the male, whereas in the female the sclerites are short and wide, more than twice as wide as long. Whereas the sclerites are fused medially in the female, they are separated along their entire length in the male, exposing significantly developed genital papillae. The enlarged genital operculum of the male extends distally between the lateral lobes of the sternum partially obscuring its proximal region. Figures 196–200 show dorsal and ventral views of both male and female specimens, and collection localities for this species. A subadult female collected deep inside the Dim Cave (Fig. 198) also exhibited a slender metasoma, all segments longer than wide.

Discussion. The chela is quite unique in *I. kadleci*. It has an exaggerated proximal gap in both male and female adults. The size of this gap is only matched in its sympatric species *I. kraepelini*. However, unique in *I. kadleci* is the presence of this gap in the female, unprecedented in *Iurus* (i.e., in other *Iurus* species the gap, if present, is only well-developed in adult males).

The gap size is further exaggerated due to the slenderness of the chela, in particular its somewhat narrow depth (see discussion below). We can hypothesize here, when contrasted to the highly vaulted, deep chelal palm of *I. kraepelini*, that the somewhat thin palm of *I. kadleci* might contribute to the enlarged proximal gap seen in the female.

I. kadleci is considerably thinner than the other species of *Iurus*. This is exhibited in the metasomal segments, the telson, and the chela. The slender metasoma is even evident in a subadult female from the Dim Cave, with all segments longer than wide. As shown in the histograms in Appendix C (Figs. C4–C5), morphometric ratios constructed from the five metasomal segments, the telson length as compared to its width, and the chelal length as compared to its depth, exhibit complete standard error separation from the other four species in both genders. Mean value differences (MVD) between *I. kadleci* and the other four species are shown in Table 8.

Accompanying the thin metasoma of *I. kadleci* is the relatively large number of serrated spines comprising the dorsal carinae of segments I–IV, the largest in the genus. Table 9 compares average spine numbers across

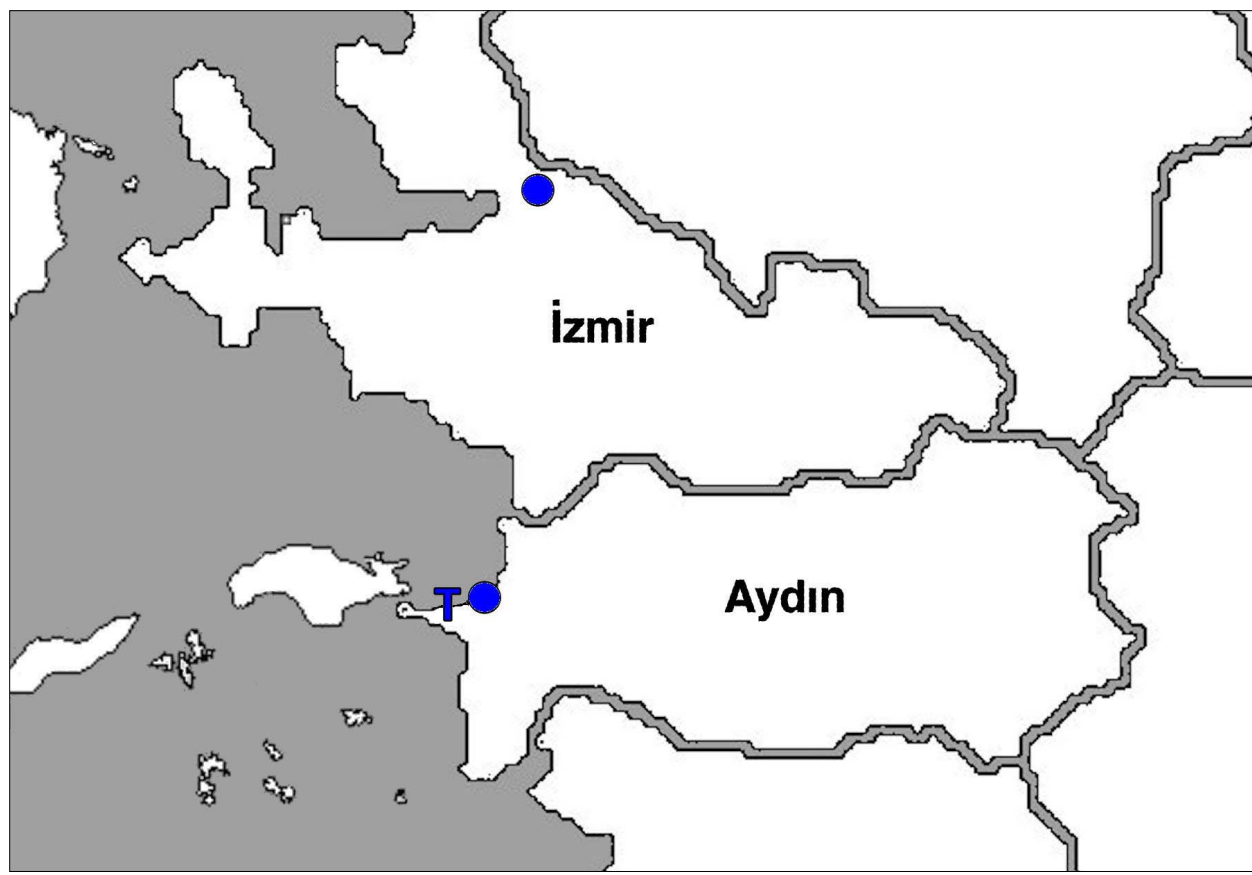


Figure 201: Large-scale map showing distribution of *Iurus kinzelbachi*, sp. nov. "T" marks type locality, Dilek Peninsula, Aydin Province, Turkey. See Fig. 74 for distribution of all species and Appendix A for detailed locality data.

the five species of *Iurus*. *I. dufourei* has spine numbers approaching *I. kadleci* showing some standard error overlap, but still exhibiting a 16 percent mean value difference. The other species show no overlap with *I. kadleci*, including absolute ranges. *I. kraepelini* has the smallest number of spines on the dorsal carinae in the genus, with over a 55 % MVD from *I. kadleci*.

The mesosomal tergites of *I. kadleci* are essentially smooth on segments I–VI, the other *Iurus* species exhibit heavily granulose plates. The lateral carinae of metasomal segments I–IV are only developed on segment I in *I. kadleci*, whereas they occur on segments I–II to I–III in the other species.

Unfortunately, the hemispermatophore is unknown in *I. kadleci*. As seen in this paper, the hemispermatophore has proved to be an excellent diagnostic character, exhibiting major structural and morphometric differences across the four species where it has been examined. We suspect the hemispermatophore of *I. kadleci* when finally examined will be similar in structure to its sympatric species *I. kraepelini*, which is also its proposed sister taxon.

Thus far, not much is known about the habitat or microhabitat preferences of *I. kadleci*. In Akseki, two

specimens were found in the same general habitat as *I. kraepelini*, and therefore are sympatric if not syntopic with the latter species. Presence of this species deep in Dim Cave, where it has been found hiding in a rock crevice (Fig. 198) might indicate its lithophilic and/or troglophilic nature. Its much lighter coloration than in all other *Iurus* species as well as its relative slenderness could indicate a specialized adaptation. We are currently attempting to locate more specimens with careful attention to their specific microhabitats. Detailed ecological information on Dim Cave and its fauna are presented in Kunt, Yağmur & Elverici (2008).

Material Examined (= type material, 5 specimens).

Holotype: ♀ (FKCP), TURKEY, Antalya Province: Akseki District, 12 km S Akseki, 11–12 May 2006, leg. F. Kovařík. **Paratypes:** 1 ♀ (FKCP), 1 ♂ (VFWV), same label as holotype; Alanya District, Dim Cave, 11 km E of Alanya, 36°32'21"N, 32°06'33"E, cave entrance at 221 m asl, vertical depth 25 m, 22 April 2007, 1 ♂ sbad., leg. K. B. Kunt, G. Tunsley & R. Gabriel (MTAS). Mersin Province: Gülnar District, Gülnar, July 2000, 1 ♂, leg. R. Werner & R. Lízler (FKCP).

***Iurus kinzelbachi* Kovařík, Fet, Soleglad
et Yağmur, sp. nov.**

(Figs. 5, 13, 25, 37, 50–51, 60, 62–63, 73–74, 201–224;
Tabs. 1–3, 10–11)

REFERENCES:

Iurus dufourei: Kinzelbach, 1975: 25 (in part; “Marli Kioi”); Crucitti & Cicuzza, 2001: 227, 229, fig. 7 (in part; map plot near İzmir); Soleglad, Kovařík & Fet, 2009: 2–3 (in part; “Narlı Kioi”), fig. 13–15 (in part).

Iurus dufourei *asiaticus*: Koç & Yağmur, 2007: 57, fig. 4; Francke & Prendini, 2008: 218 (in part; Davutlar); Yağmur, Koç & Akkaya, 2009: 154–159 (in part; Aydin: Dilek).

Holotype: ♂ (NHMW), TURKEY, *Aydin Province*: Söke District, Dilek Peninsula National Park, Canyon, 37°41'37"N, 27°09'37"E, 82 m asl, 18 June 2005, leg. H. Koç. **Paratypes**, see list below.

Diagnosis. Medium sized species, 85 mm. Dark gray to black in overall coloration. Pectinal tooth counts lowest in genus, 10–12 (10.62) males, 8–11 (9.33) females. Chelal movable finger lobe in adults located on basal half, lobe ratio 0.38–0.47; proximal gap on fixed finger present in adult males; movable finger of adult males essentially straight, not highly curved; number of inner denticles (*ID*) of chelal movable finger, 13–15 (14); constellation array with *four* to *six* sensilla; hemispermatophore lamina internal nodule vestigial to obsolete, positioned very basally due to elongated lamina, lamina distal length / lamina basal length 4.313–5.107 (4.710), lamina terminus blunted, not pointed, terminus of acuminate process truncated, transverse trunk bolsters are present. Four unique types of neobothriotaxy found on external aspects of chela and patella, although not on all specimens or both pedipalps; at least one neobothriotoxic type has been detected on 80 % of specimens examined. Dominant morphometrics (see Appendix X) are chelal movable and fixed finger lengths.

Distribution. Turkey (west): İzmir (extinct?) and Aydin Provinces. See map in Fig. 201 for large-scale distribution of this species.

Etymology. We are honored to name this new species after our esteemed colleague Dr. Ragnar Kinzelbach (Rostock, Germany) who pioneered modern studies of scorpions from Greece and Turkey (Kinzelbach, 1975, 1982, 1985, etc.).

MALE. The following description is based on holotype male from Dilek Peninsula National Park, Aydin, Turkey. Measurements of the holotype plus two other

specimens are presented in Table 10. See Figure 202 for a dorsal and ventral view of the male holotype.

COLORATION. Basic color of carapace, mesosoma, metasoma, telson, and pedipalp blackish-brown; legs a lighter mahogany color, tarsus yellowish; cheliceral fingers and distal aspect of palm purplish, proximal aspect of palm yellowish; pedipalp and dorsal metasomal carinae blackish; sternites mahogany; genital operculum, basal piece and pectines yellow-tan. Eyes and tubercles black, leg condyles and aculeus tip dark brown. No patterns present.

CARAPACE (Fig. 203). Anterior edge with a conspicuous median indentation, approximately twelve irregularly placed setae visible; entire surface densely covered with small to medium granules. Mediolateral ocular carinae well-developed and granulated, extending to the lateral eyes; there are three lateral eyes, the posterior eye the smallest. Median eyes and tubercle of medium size, positioned anterior of middle with the following length and width formulas: 394|1040 and 143|917.

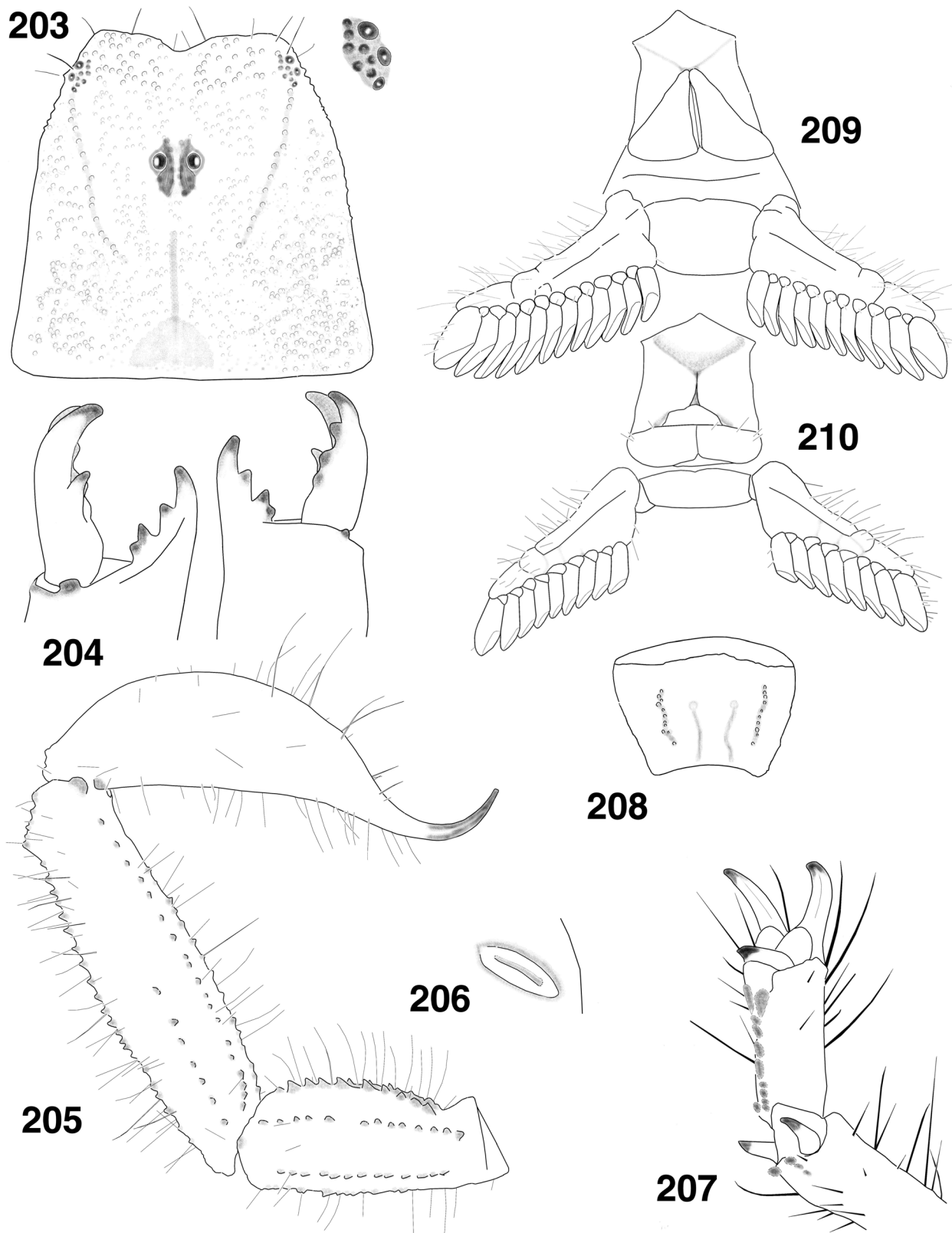
MESOSOMA (Figs. 206, 208). Tergites I–VII densely populated with minute granules; tergite VII lateral carinae serrated, median carinae obsolete, essentially obscured by coarse granulation. Sternites III–VI smooth and lustrous; VII with scattered lateral granulation, one pair of irregularly granulated lateral carinae and one pair of smooth median carinae (Fig. 208). Stigmata (Fig. 206) are medium in size and slit-like in shape, angled 45° in an anterointernal direction.

METASOMA (Fig. 205). Segment I wider than long. Segments I–IV: dorsal and dorsolateral carinae serrated; dorsal carinae with 10/12, 10/10, 9/10, and 10/9 serrated spines (left/right carina); dorsal (I–IV) and dorsolateral (I–III) carinae do not terminate with an enlarged spine; lateral carinae serrated on I, weakly crenulated on posterior half of II; absent on segments III–IV; ventrolateral carinae crenulated on I–III and serrated on IV; ventromedian carinae smooth on I, irregularly granulated on II, granulated on III, and crenulated on IV. Dorsolateral carinae of segment IV terminate at articulation condyle. Segment V: dorsolateral carinae serrated; lateral carinae irregularly crenulated for two-fifths of posterior aspect; ventrolateral and single ventromedian carinae serrated; ventromedian carina not bifurcated, terminating in straight line. Anal arch with 13 small serrated granules. Intercarinal areas of segments I–V essentially smooth. Segments I–V with numerous long setae on ventral, lateral and dorsal aspects.

TELSOM (Fig. 205). Vesicle elongated, with highly curved aculeus. Vesicle essentially void of granules; distal half of ventral surface with scattered elongated



Figure 202: *Iurus kinzelbachi*, sp. nov., dorsal and ventral views. Holotype male, Aydin Province, Dilek Peninsula National Park, Turkey.



Figures 203–210: *Iurus kinzelbachi*, sp. nov., Dilek Peninsula National Park, Aydin, Turkey. 203–209. Male holotype. 210. Female paratype. 203. Carapace and close-up of lateral eyes. 204. Right chelicera, ventral and dorsal views. 205. Telson and metasomal segments IV–V, lateral view. 206. Stigma. 207. Tarsus and partial basitarsus, left leg IV. 208. Sternite VII. 209. Sternopectinal area. 210. Sternopectinal area.

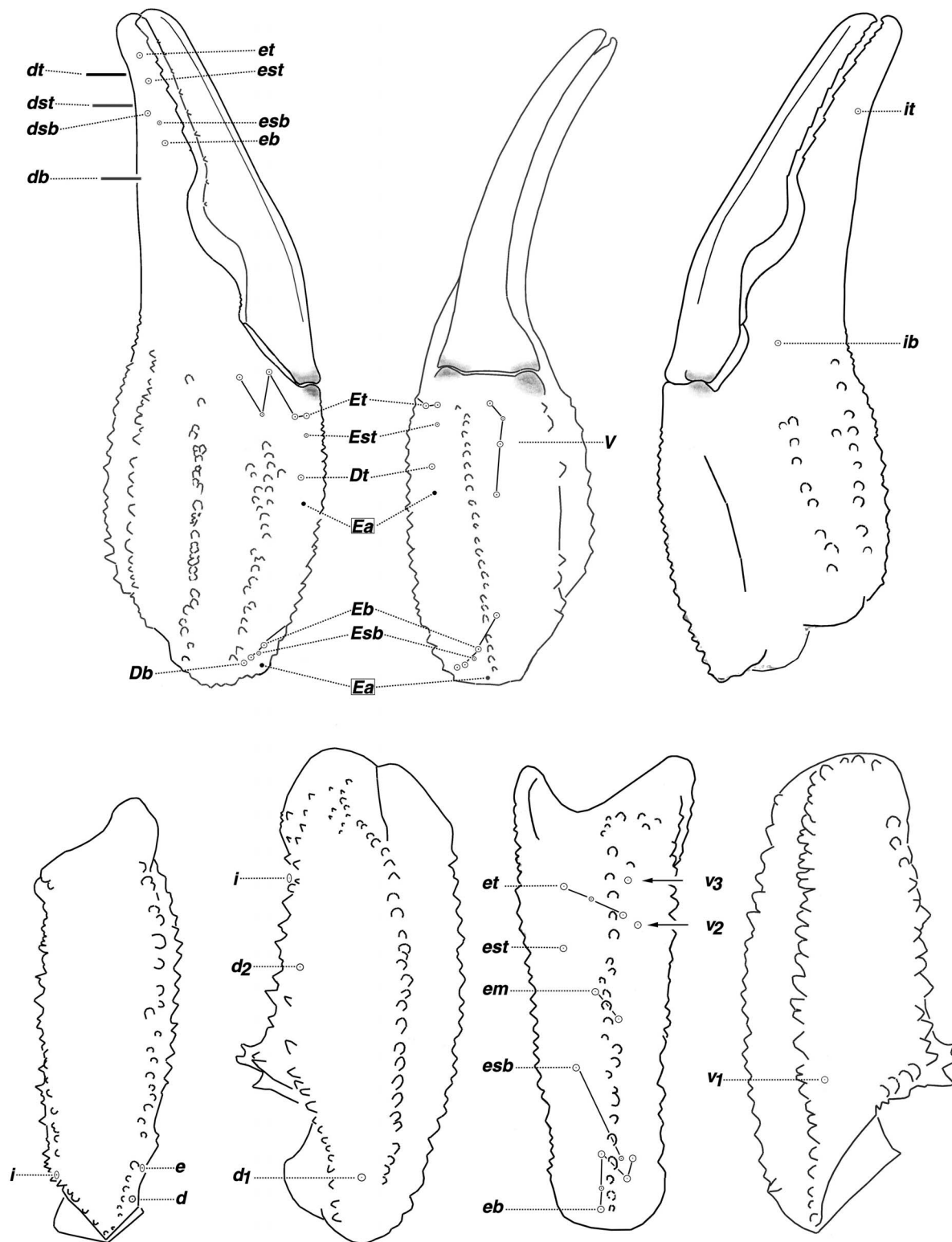
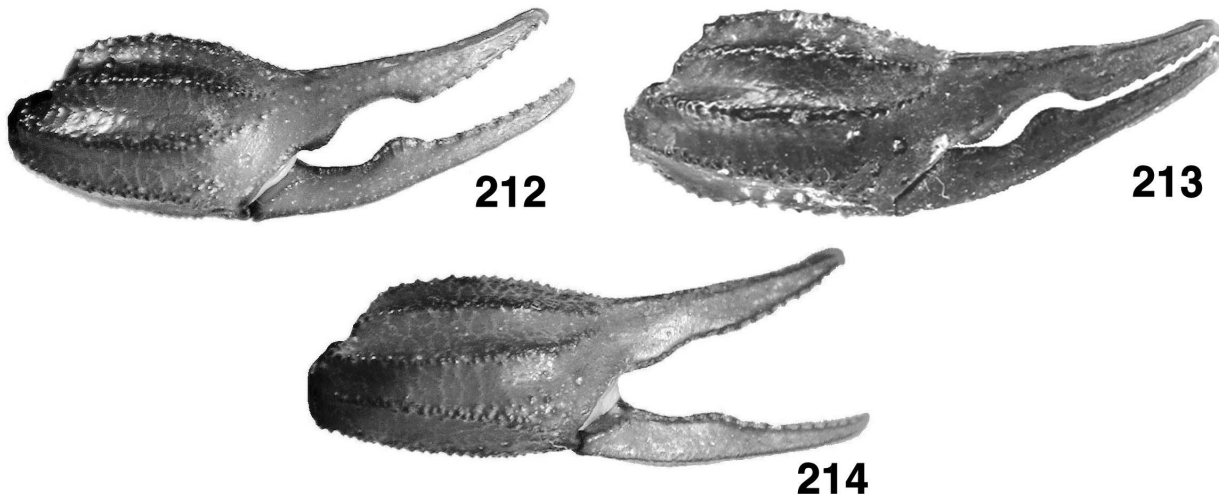


Figure 211: Trichobothrial pattern of *Iurus kinzelbachi* sp. nov., male holotype. Dilek Peninsula National Park, Aydin, Turkey. Note presence of two external petite accessory trichobothria (*Ea* inside rectangle) on the chela representing types 8 and 9, exclusively found in *I. kinzelbachi*.



Figures 212–214: Chela, lateral view, *Iurus kinzelbachi* sp. nov. **212.** Male, Naldöken (“Narli Kioi”), İzmir, Turkey. **213.** Male, Dilek Peninsula, Aydin, Turkey. **214.** Female, Naldöken (“Narli Kioi”), İzmir, Turkey. Note, in the adults the movable finger lobe is positioned proximal of finger midpoint, and a moderate fixed finger proximal gap exists in the males.

curved setae, basal half essentially void of setation; dorsal surface irregularly scattered with short to medium length setae; base of aculeus with setation ventrally and dorsally. Vesicular tabs with small rounded granules ventrally.

PECTINES (Fig. 209, paratype female Fig. 210). Well-developed segments exhibiting length|width formula 916|505. Sclerite construction complex, three anterior lamellae and one large middle lamella with slight indications of a smaller distal sclerite; fulcra of medium development. Teeth number 11/12. Sensory areas developed along most of tooth inner length on all teeth, including basal tooth. Scattered setae found on anterior lamellae and distal pectinal tooth. Basal piece large, with subtle swallow indentation along anterior edge, length|width formula 335|505.

GENITAL OPERCULUM (Fig. 209). Sclerites triangular, longer than wide, separated for entire length. Genital papillae visible between sclerites but do not extend beyond genital operculum posterior edge (see discussion on female below).

STERNUM (Fig. 209). Type 2, posterior emargination present, well-defined convex lateral lobes, apex visible but not conspicuous; anterior portion of genital operculum situated proximally between lateral lobes; sclerite longer than wide, length|width formula 290|260; sclerite slightly tapers anteriorly, posterior-width|anterior-width formula 485|415 (see discussion on female below).

CHELICERAE (Fig. 204). Movable finger dorsal edge with one large subdistal (*sd*) denticle; ventral edge with

one large pigmented accessory denticle at finger midpoint; ventral edge serrula not visible. Ventral distal denticle (*vd*) slightly longer than dorsal (*dd*). Fixed finger with four denticles, median (*m*) and basal (*b*) denticles conjoined on common trunk; no ventral accessory denticles present.

PEDIPALPS (Fig. 211). Well-developed chelae, with long fingers, heavily carinated, conspicuous scalloping on chelal fingers: well-developed lobe on movable finger, positioned proximal of midpoint in ratio 0.47; proximal gap present on fixed finger. **Femur:** Dorsointernal, dorsoexternal and ventrointernal carinae serrated, ventroexternal irregularly serrated. Dorsal surface smooth, ventral surface with minute granules medially, internal and external surface with line of 11 and 14 serrated granules, respectively. **Patella:** Dorsointernal and ventrointernal carinae serrated, dorsoexternal crenulated and ventroexternal serrated, and extero-median carina strong, serrated, and singular. Dorsal and ventral surfaces smooth; external surface with serrated exteromedian carina; internal surface smooth with well-developed, doubled DPS and VPS. **Chelal carinae:** Complies with the “8-carinae configuration”. Digital (*D1*) carina strong, granulated; dorsosecondary (*D3*) and dorsomarginal (*D4*) rounded, heavily granulated; dorsointernal (*D5*) irregularly serrated; ventroexternal (*V1*) strong and serrated, terminating at external condyle of movable finger; ventrointernal (*V3*) rounded, smooth to granulated, continuous to internal condyle; external (*E*) heavily granulated, irregular distally; internal (*I*) irregularly serrated. **Chelal finger dentition:** Number of median rows, internal denticles (*ID*), and outer denticles (*OD*) are difficult to determine due to conspicuous scal-

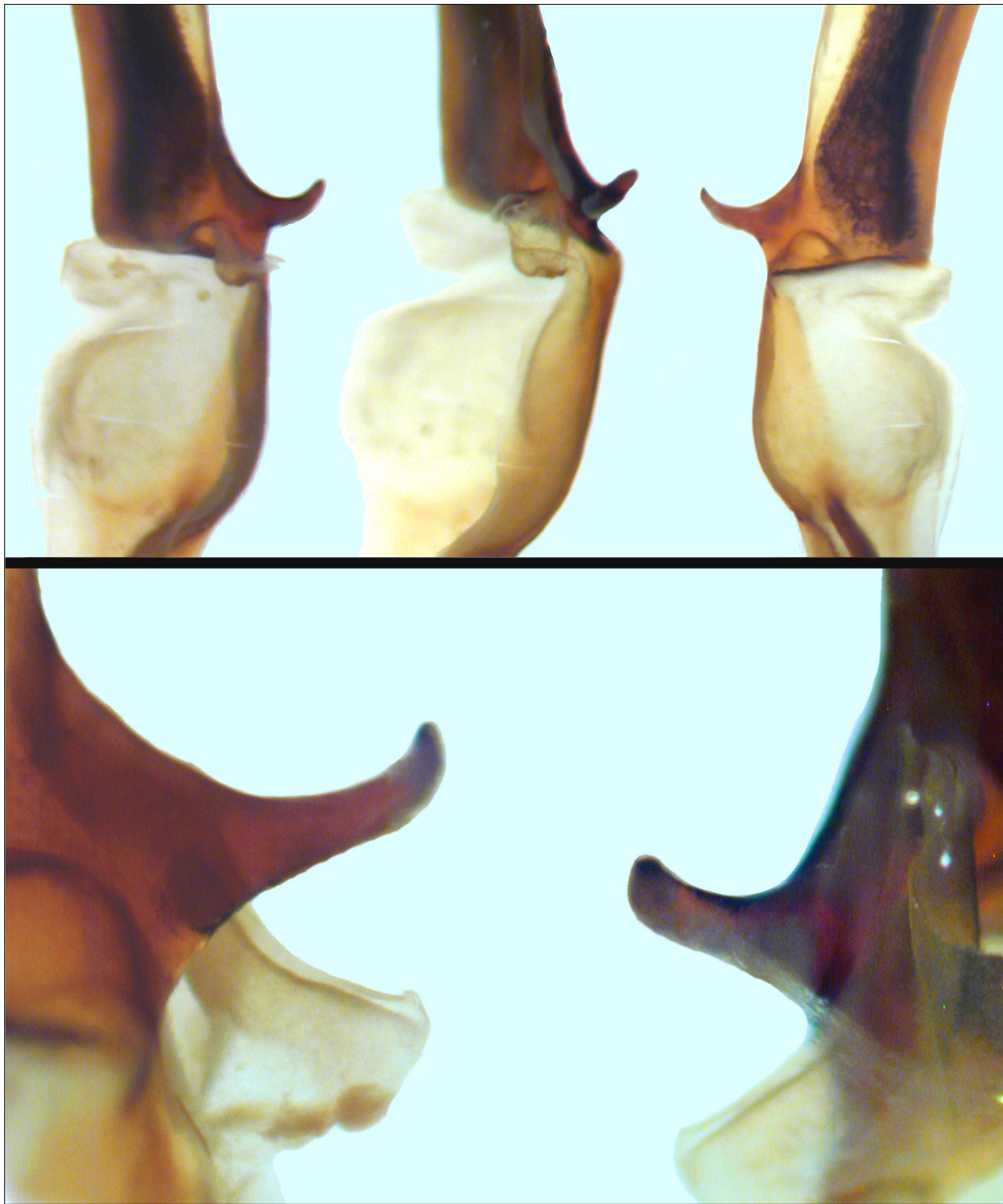


Figure 215: Close-up of median area of hemispermatophore, *Iurus kinzelbachi*, sp. nov., paratype, Dilek Peninsula National Park, Aydin, Turkey. **Top.** Left hemispermatophore, ventral, ventrointernal, and dorsal views. **Bottom.** Right hemispermatophore, close-up of acuminata process showing the blunt terminus. The paraxial organ sleeve attachment to the seminal receptacle is visible in the ventral view of these photographs.

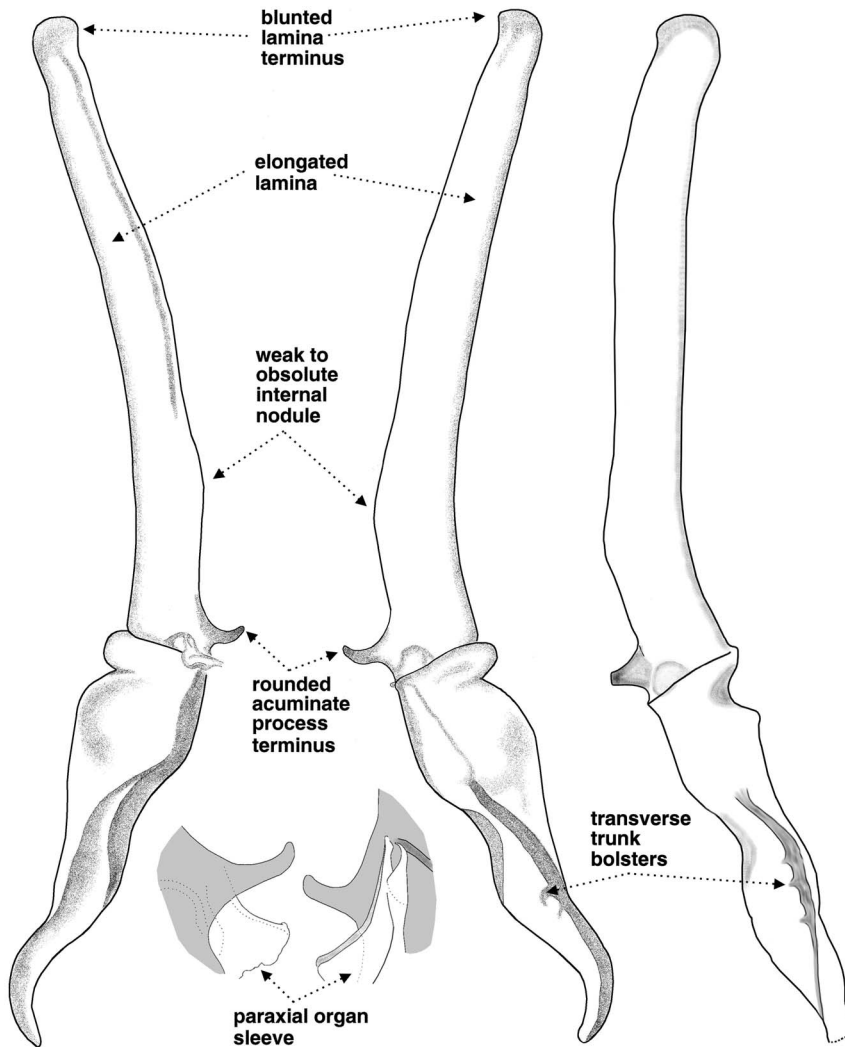


Figure 216: Hemispermatophore of *Iurus kinzelbachi*, sp. nov., paratype. **Left & Center.** Ventral and dorsal views, Dilek Peninsula National Park, Aydin, Turkey. **Right.** Dorsal view, Naldöken (“Narli Kioi”), Izmir, Turkey, paratype; note that tip of acuminate process is missing. Diagnostic of this species is the elongated lamina with blunted terminus, shown in both hemispermatophores, a somewhat weak to obsolete internal nodule, transverse trunk bolsters, and a rounded acuminate process terminus. **Bottom.** Close-up of the attachment of the paraxial organ sleeve to the seminal receptacle (right hemispermatophore).

loping of the fingers. Median denticle (*MD*) row groups oblique and highly imbricated; 11/11 *IDs* to socket beginning on fixed finger and 14/14 *IDs* on movable finger; 14/14 *ODs* on fixed finger and 11/11 *ODs* to lobe center on movable finger. No accessory denticles present. **Trichobothrial patterns (Fig. 211):** Type C, neobothrioxic, a single petite accessory trichobothrium in *Est* series (type-8), both chelae, and *Esb* series (type-9), right chela only.

LEGS (Fig. 207). Both pedal spurs present on all legs, lacking spinelets; tibial spurs absent. Tarsus with conspicuous spinule clusters in single row on ventral surface, terminating distally with a pair of enlarged spinule clusters. Unguicular spine well-developed and pointed.

HEMISPERMATOPHORE (Figs. 215–216). The hemispermatophore of the holotype has not been examined, therefore this description is based on two paratype

specimens from Izmir and Dilek Peninsula. The hemispermatophore of *I. kinzelbachi* is unique among *Iurus* species, exhibiting the most elongated lamina, rounded terminus, weak to obsolete internal nodule, presence of transverse trunk bolsters, and a round acuminate process terminus (more data below).

Male and female variability. As seen in Figures 212–214, the adult female does not exhibit a proximal gap and the movable finger lobe is not as developed as in the male. There is no significant sexual dimorphism in morphometrics. Though the male has a thinner metasoma, the MVDs (L/W) only ranged from 7.1 to 9.2 %. Pectinal tooth counts in males exceed those of females by approximately 1.3 teeth, male 10–12 (10.62) [24], female 8–11 (9.33) [36] (see histograms in Fig. 73). The genital operculum of the male is dramatically different from that in the female (Figs. 209–210). The sclerites, subtriangular in shape, are as long as or longer than wide in the male, whereas the sclerites

<i>Iurus kinzelbachi</i> sp. nov.			
Dilek Peninsula, Adyin, Turkey	Naldöken, İzmir, Turkey		
	Male Holotype	Male Paratype	Female Paratype
Total length	78.35	75.05	80.55
Carapace length	10.40	10.80	12.30
Mesosoma length	25.35	20.55	22.85
Metasoma length	30.20	31.30	32.55
Segment I length/width	3.95/4.60	3.95/4.70	4.10/5.20
Segment II length/width	4.55/3.90	4.70/4.10	4.90/4.45
Segment III length/width	5.05/3.70	5.20/3.70	5.35/4.00
Segment IV length/width	6.10/3.35	6.35/3.30	6.50/3.60
Segment V length/width	10.55/3.00	11.10/3.15	11.70/3.25
Telson length	12.40	12.40***	12.85***
Vesicle length width/depth	8.20 3.30/3.05	8.65 3.50/3.20	9.40 3.65/3.35
Aculeus length	4.20	3.75***	3.45***
Pedipalp length	44.15	44.55	49.25
Femur length/width	11.20/3.65	11.25/3.45	12.65/4.00
Patella length/width* DPS height**	10.70/2.80 1.40	10.45/4.05 1.35	11.20/4.30 1.55
Chela length	22.25	22.85	25.40
Palm length width/depth	10.40 5.70/7.50	10.45 6.00/7.65	11.55 6.30/8.00
Fixed finger length	11.10	12.00	13.25
Movable finger length	14.15	14.45	15.65
Pectines teeth middle lamellae	11-12 3-2	10-10 3-3	9-9 1-1++
Sternum length/width	2.90/2.60	2.35/2.80	3.45/3.35

Table 10: Morphometrics (mm) of *Iurus kinzelbachi* sp. nov. * Patella width is widest distance between the dorsointernal and externomedial carinae. ** DPS height is from tip of spines to dorsointernal carina center.

are short and wide, more than twice as wide as long. Whereas the sclerites are fused medially in the female, they are separated along their entire length in the male, exposing significantly developed genital papillae. The enlarged genital operculum of the male extends distally between the lateral lobes of the sternum partially obscuring its proximal region. Figures 223–226 show dorsal and ventral views of both male and female specimens, the map of distribution for this species, and photographs of its type locality.

Discussion

Unique in this species is the combination of a proximal gap in the adult male and a proximally positioned movable finger lobe. All other *Iurus* species that exhibit a proximal gap also have a distally placed

lobe in adults. The movable finger lobe ratio is larger in the male than the female, 0.44–0.47 vs. 0.40–0.42 (ratios calculated from adults with carapaces 10 mm or larger; see scatter chart in Fig. 56 for a complete analysis of this character).

I. kinzelbachi, statistically, has the overall smallest number of pectinal teeth (Fig. 73), but *I. dufoureius* is quite close, exhibiting only a small fractional difference; *I. kraepelini*, with the largest number of teeth, averages roughly two more pectinal teeth per gender than *I. kinzelbachi*.

The hemispermatophore of *I. kinzelbachi* has been examined from material representing both of its major reported localities (see map in Fig. 60), Aydin and İzmir provinces. The unique and unusual morphology of this hemispermatophore is consistent in the three examined for this study (Figs. 215–216). The lamina is quite elong-

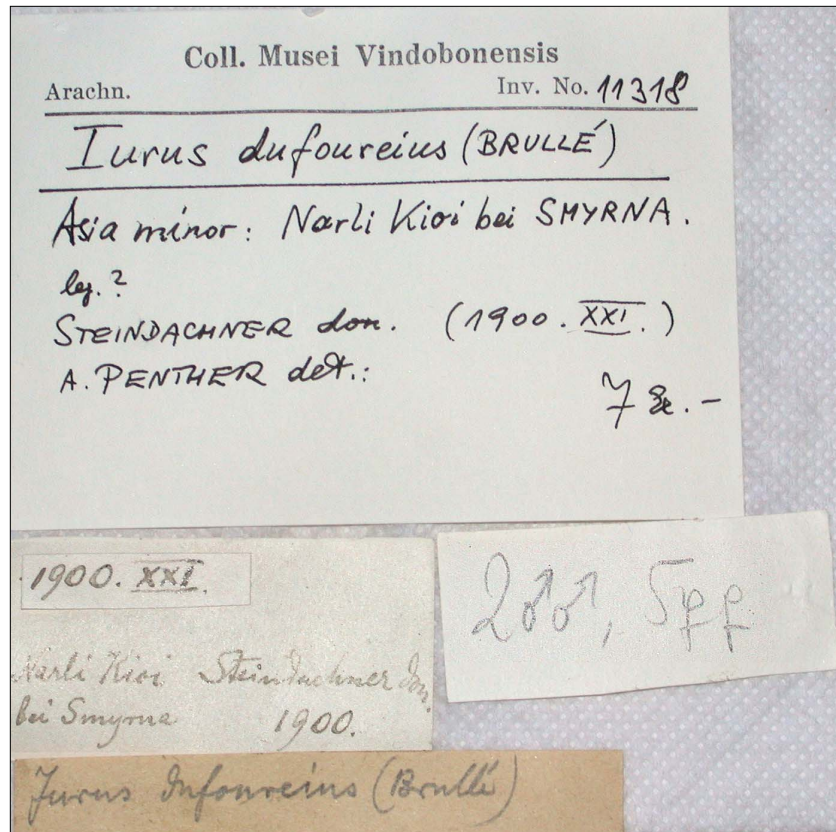


Figure 217: Set of labels for seven specimens of *Iurus kinzelbachi*, sp. nov., from Narli Kioi (= Naldöken), Izmir, Turkey. Collected in 1900.

gated, at least 1.5 times longer than the trunk with the ratio 1.513–1.571 (1.546) [3] (see Table 2), the relatively longest lamina in the genus. The lamina terminus is somewhat blunted, not pointed, though this appearance is due, in part, to the somewhat subparallel and narrow lamina base edges. Also unique in this hemispermatophore is the rounded or near obsolete internal nodule. This vestigial nodule is situated quite basal on the lamina, in a ratio 4.313–5.107 (4.710) [2], exceeding other species hemispermatophores by at least 39 %. As depicted in Table 3, *I. kinzelbachi* exceeds the other species in all four morphometric ratios, all indicators of the elongated lamina found in this species. Finally, the acuminate process terminus is rounded not truncated as in the other *Iurus* species, and transverse trunk bolsters are present. The paraxial organ sleeve was present in two of the three hemispermatophores examined (Figs. 215–216); its attachment to the seminal receptacle is as found in other species.

In Appendix C we present a complete analysis of the morphometric trends across the five species of *Iurus*. From this analysis, we see that the chelal finger lengths in *I. kinzelbachi* dominated in a large majority of morphometric ratio comparisons: averaging 21 and 22 comparisons out of 25 for the male and 20 and 23 for the female. Of equal importance, this analysis also indicates

morphometrics that dominated the *least* in ratio comparisons. In *I. kinzelbachi* the telson width dominated only 5–6 morphometrics out of 25 (i.e., *I. kinzelbachi* has a relatively thin telson vesicle). We constructed two ratios, the movable finger and fixed finger lengths divided by the telson width, comparing *I. kinzelbachi* to the other four species for both genders. These two ratios provide excellent diagnostic characters separating *I. kinzelbachi* from *I. dufoureius* and *I. kraepelini*, the species closest geographically to *I. kinzelbachi*: MVDs for *I. dufoureius* are 26.1–27.8 % and 22.8–28.5 % for fixed and movable fingers, respectively, and for *I. kraepelini* are 23.0–28.4 % and 12.9–19.3 for fixed and movable fingers, respectively (note, ranges represent both genders). These ratios also provide separation from *I. asiaticus* but the MVDs were considerably smaller, ranging 11.6–12.4 % and 6.4–8.8 % for fixed and movable fingers. The ratios were essentially equal when compared with *I. kladeli*, another species with a thin telson.

Soleglad, Kovařík & Fet (2009) reported for the first time neobothriotaxy in genus *Iurus*. Although nine types and 77 occurrences of neobothriotaxy were reported in their study, spanning 101 specimens, they occurred sparingly, many times only on a single pedipalp, and many trichobothria were petite in size. In

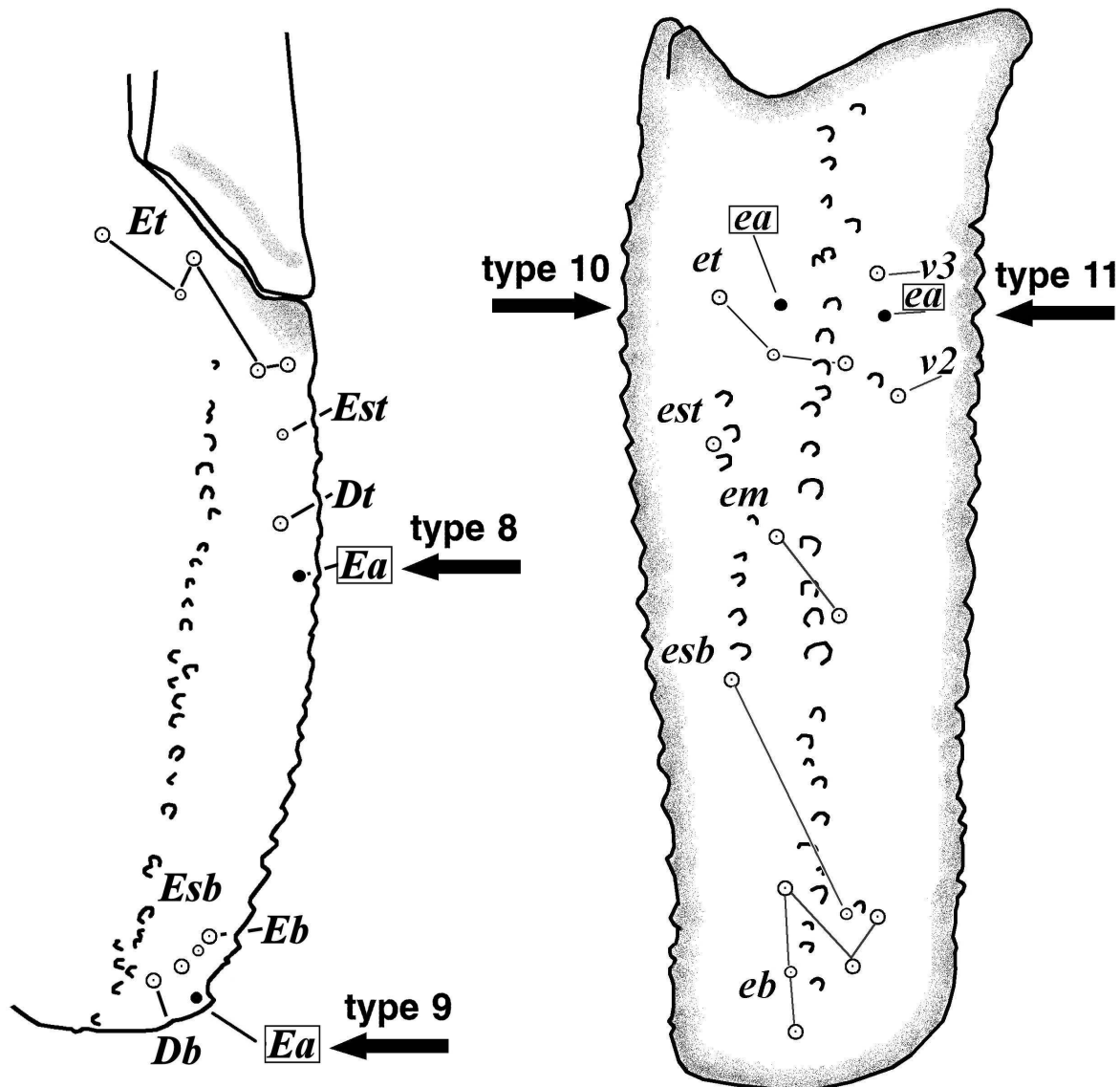


Figure 218: Partial trichobothrial pattern illustrating neobothriotaxy in *Iurus kinzelbachi*, sp. nov. **Left.** Chelal *Est* series, one accessory trichobothrium (*Ea*); *Eb* series, one accessory trichobothrium (*Ea*). **Right.** Patellar *et* series, two types of accessory trichobothria (*ea*). Note that all accessory trichobothria are *petite* in size and in some cases may be vestigial. Accessory trichobothria are represented by closed circles. See Appendix B for a complete synopsis of neobothriotaxy in *Iurus*.

this study, two types of neobothriotaxy were reported, unique in the genus, found in an isolated population of seven specimens from the western coast of Turkey, near İzmir. We have examined an additional series of 23 specimens from the Dilek Peninsula National Park, Aydin, Turkey, and discovered they also exhibited these two specific types of neobothriotaxy. We concluded from the analysis of neobothriotaxy alone that the two populations belonged to the same species that also is a new one, *I. kinzelbachi*. In addition, two more neobothriotic types were detected in the Dilek population,

making a total of four types unique to *I. kinzelbachi*. Figure 218 illustrates the four types of neobothriotaxy diagnostic of *I. kinzelbachi*: two accessory trichobothria found on the chela, one each in the *Est* and *Esb* series, and two accessory trichobothria on the external aspect of patella, both in the *et* series. These accessory trichobothria are petite in size, some on the chela are reduced in size to be classified as "small petite" while others, at best, can be described only as vestigial. Figures 219–222 present close-up photographs of these four neobothriotic types representing both populations

Locality	Specimen	Chela		Patella		Patella	
		Types 8 & 9 <i>Esb Series, Eb Series</i>		Type 11 <i>et series</i>		Type 10 <i>et series</i>	
		left	right	left	right	left	right
İzmir, İzmir, Turkey	A ♂	vestigial*, -	petite*, -	-	-	-	-
	A ♀	sm. petite*, petite	petite*, -	petite*	-	-	-
	SA ♂	vestigial, -	vestigial, -	-	-	-	-
	J ♀	vestigial, -	vestigial, -	-	petite*	-	-
	SA ♀	vestigial, vestigial	petite*, -	-	-	-	-
	SA ♀	petite*, -	petite*, vestigial	-	petite*	-	-
	A ♀	vestigial*, -	vestigial, -	-	petite*	-	-
Dilek Peninsula, Aydin, Turkey	A ♂	-, -	-, -	-	-	petite*	-
	A ♀	-, -	-, -	-	petite*	-	-
	A ♂	petite*, -	petite, petite	-	-	-	-
	A ♀	vestigial, -	-, -	-	-	-	-
	A ♂	-, -	petite, -	-	-	-	-
	A ♀	-, -	-, -	-	-	-	-
	A ♂	-, -	-, -	-	-	-	-
	SA ♂	-, petite	petite, -	-	-	-	-
	SA ♂	-, -	-, vestigial	-	-	-	-
	A ♂	vestigial, -	-, vestigial	-	-	-	-
	SA ♂	vestigial, -	-, small petite*	-	-	-	-
	A ♀	-, -	-, petite	-	-	-	-
	A ♀	-, -	-, -	-	-	-	-
	A ♀	-, -	-, petite	-	-	-	-
	A ♀	-, petite	petite, petite	-	-	-	-
	SA ♂	-, -	-, -	-	-	-	-
	SA ♂	-, -	-, -	-	-	petite	-
	SA ♀	-, small petite	-, -	-	-	-	-
	SA ♂	vestigial, -	petite, sm. petite	-	-	-	-
	A ♂	-, -	-, -	-	-	-	-
	A ♀	-, -	-, -	-	-	-	-
	A ♀	-, -	-, small petite	-	-	-	-
	A ♀	-, -	-, -	petite	-	-	-
♂ petite: 7 (12) 58 % ♂ vestigial: 3 (12) 25 % ♂ total: 10 (12) 83 %	<u>Esb:</u> petite: 12 (60) 20 % vestigial: 12 (60) 20 % total: 24 (60) 40 %	total: 6 (60) 10 %	total: 2 (60) 3 %				
♀ petite: 13 (18) 72 % ♀ vestigial: 1 (18) 6 % ♀ total: 14 (18) 78 %	<u>Eb:</u> petite: 11 (60) 18 % vestigial: 4 (60) 7 % total: 15 (60) 25 %						
♂ & ♀: 24 (30) 80 %							

Table 11: Statistics on four types of neobothriotaxy found exclusively in *Iurus kinzelbachi*, sp. nov. These accessory trichobothria are classified as petite, small petite, and vestigial. This data shows that 80 % of the 30 specimens examined exhibited at least vestigial to petite accessory trichobothria, 70 % of which were petite. Neobothriotaxy in the *Esb* series was the most prevalent, occurring in 40 % of the specimens, whereas patellar type 10 was the rarest, only detected in 3 %. * indicates neobothriotaxy illustrated in Figures 219–222. See Appendix B for overview of all neobothriotic types across all species of *Iurus*.

of *I. kinzelbachi*, both left and right pedipalps, and full and small petite, as well as vestigial types. Table 11 presents a complete analysis of the occurrence of neobothriotaxy in all 30 specimens of *I. kinzelbachi* examined. We see that 80 % of the specimens exhibited at least one accessory trichobothrium; only six spec-

imens, all from Aydin, lacked accessory trichobothria. All specimens from İzmir had at least one accessory trichobothrium on each pedipalp, though in three specimens only vestigial. Six specimens from Aydin showed neobothriotaxy on both pedipalps. Neobothriotaxy on the chela was the most prevalent, being found

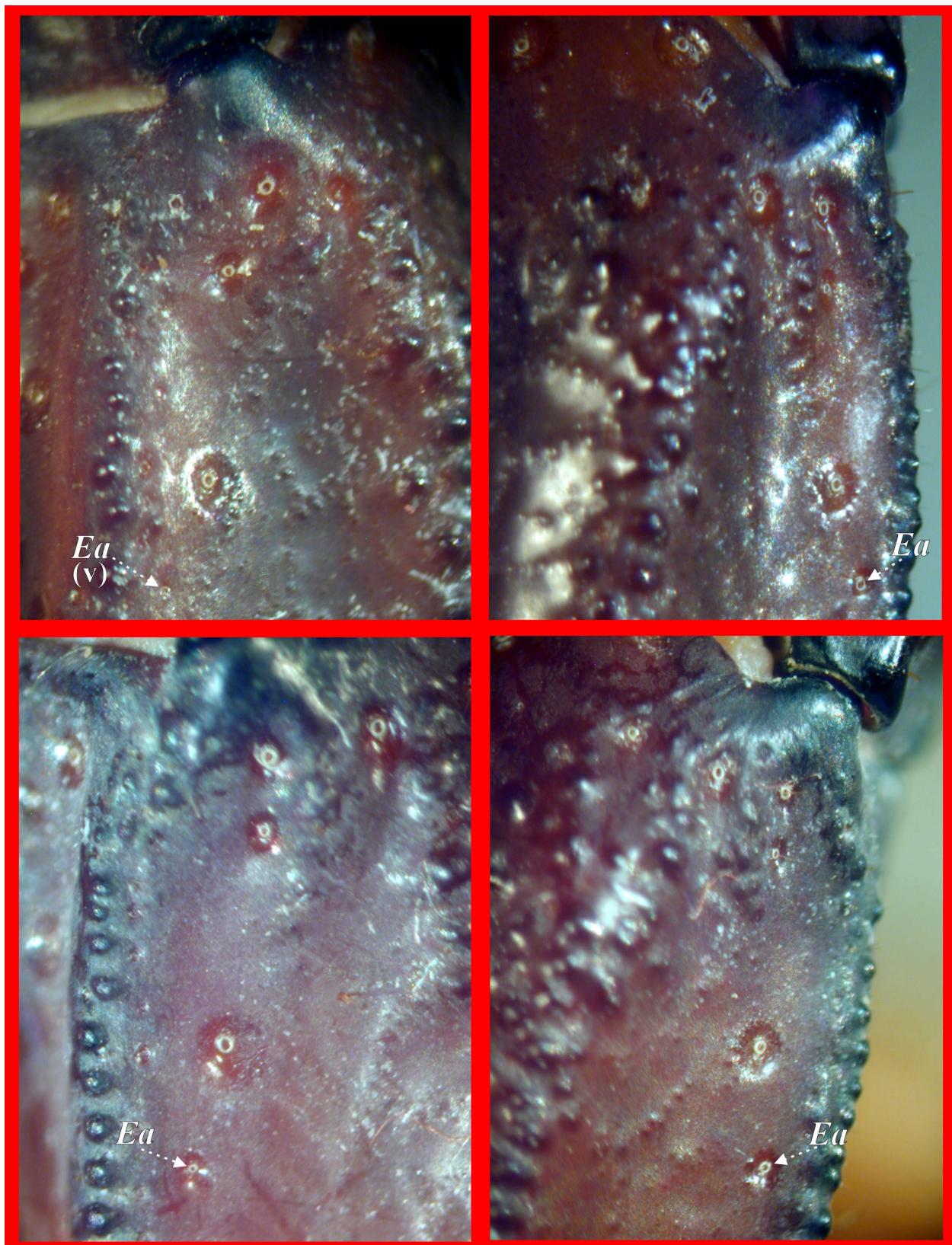


Figure 219: Neobothriotaxy on chela in *Iurus kinzelbachi*, sp. nov., Naldöken, İzmir, Turkey, type 8. **Top-Left.** Adult male, left chela, showing vestigial (v) *Ea*. **Top-Right.** Adult male, right chela. **Bottom-Left.** Adult female, left chela, showing small petite *Ea*. **Bottom-Right.** Adult female, right patella. Solitary accessory trichobothrium (*Ea*, marked in white) located in *Est* series.

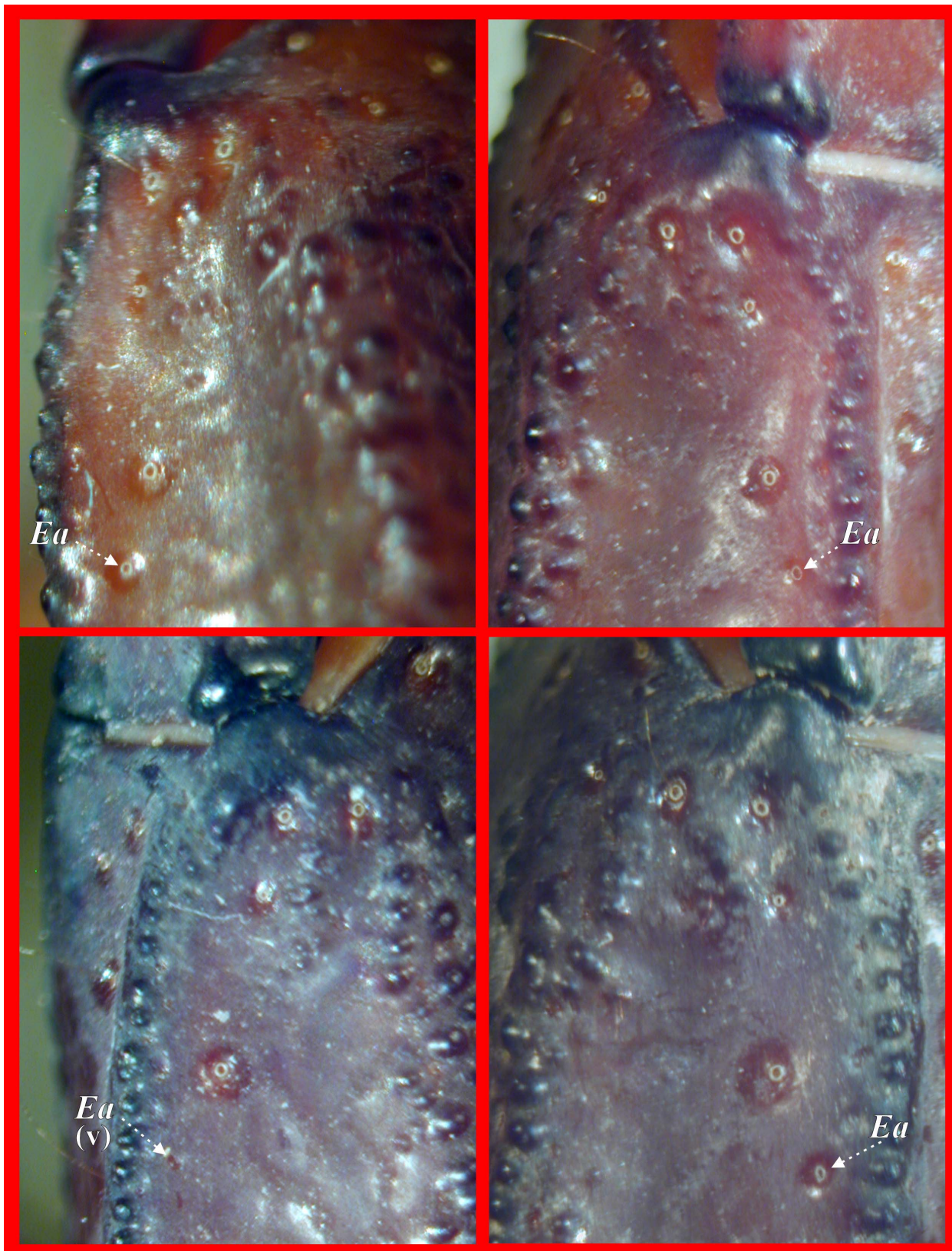


Figure 220: Neobothriotaxy on chela in *Iurus kinzelbachi*, sp. nov., Naldöken, İzmir, Turkey, type 8. **Top-Left.** Subadult female, left chela. **Top-Right.** Subadult female, right chela. **Bottom-Left.** Adult female, right chela, showing vestigial (v) Ea. **Bottom-Right.** Subadult female, right chela. Solitary accessory trichobothrium (*Ea*, marked in white) located in *Est* series.

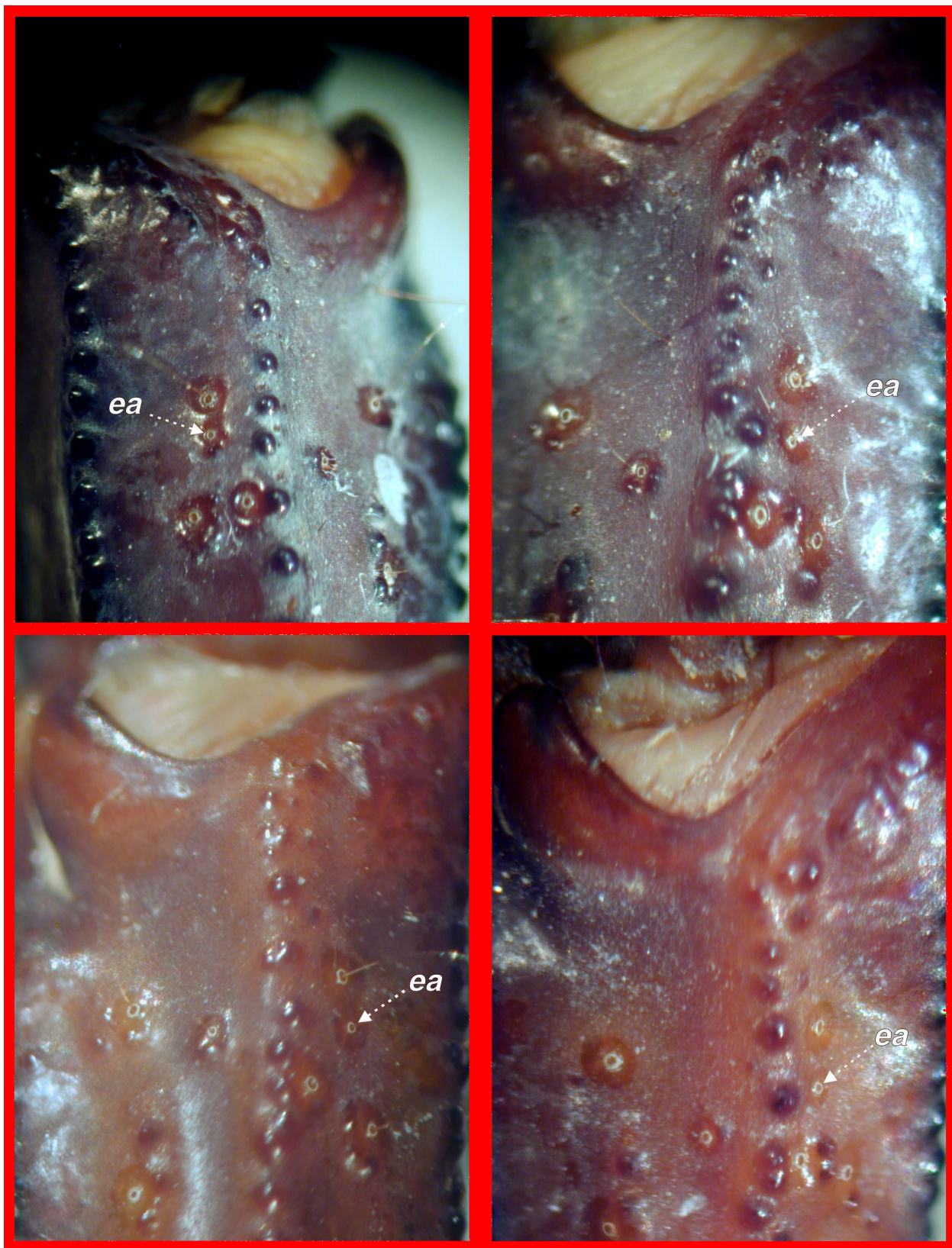


Figure 221: Neobothriotaxy on patella in *Iurus kinzelbachi*, sp. nov., Naldöken, İzmir, Turkey, type 11. **Top-Left.** Adult female, left patella. **Top-Right.** Adult female, right patella. **Bottom-Left.** Juvenile female, right patella. **Bottom-Right.** Subadult female, right patella. Solitary accessory trichobothrium (*ea*, marked in white) is located in *et* series.

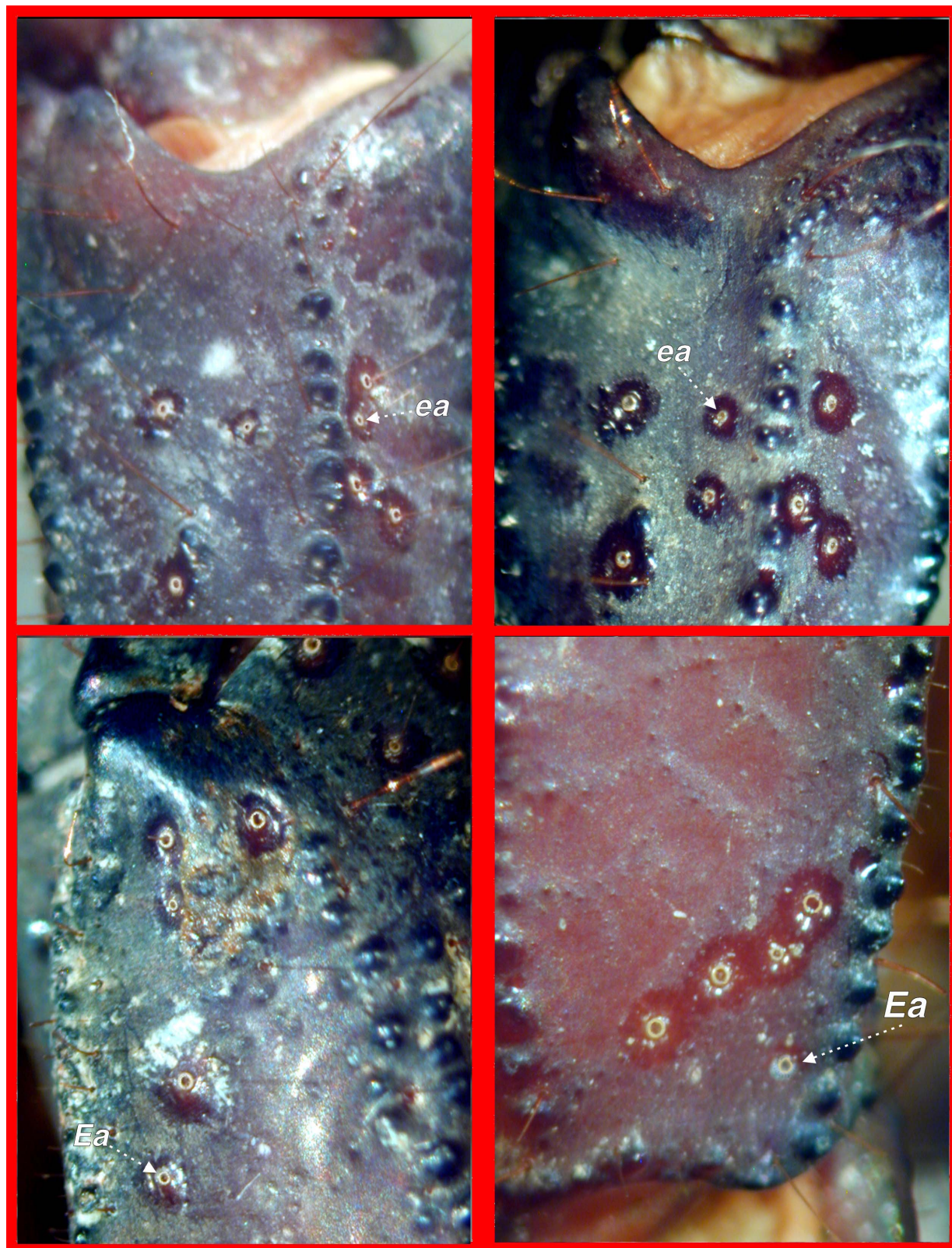


Figure 222: Neobothriotaxy on patella and chela in *Iurus kinzelbachi*, sp. nov., Dilek Peninsula, Aydin, Turkey, types 8, 9, 10, 11. **Top-Left.** Adult female, right patella, type 11. **Top-Right.** Adult male, right patella, type 10. **Bottom-Left.** Adult male, left chela, type 8. **Bottom-Right.** Subadult male, right chela, type 9. Solitary accessory trichobothria (*ea* and *Ea*, marked in white) are located in *et* and *Est* and *Eb* series, respectively.



Figure 223: *Iurus kinzelbachi*, sp. nov., dorsal and ventral views. Paratype female, Aydin Province, Dilek Peninsula National Park, Turkey.

on 67 % of the specimens; neobothriotaxy on the patella was present only in 13 %. Although we consider this unique neobothriotaxy diagnostic of *I. kinzelbachi* and important in serious discussions of the overall evolution of the genus, we did not include it in the key since it is not found in all specimens or both chela.

Material Examined (= type material, 30 specimens).

Holotype: ♂ (NHMW), TURKEY, Aydin Province: Söke District, Dilek Peninsula National Park, Canyon, 37°41'37"N, 27°09'37"E, 82 m asl, 18 June 2005, leg. H. Koç. **Paratypes:** Turkey, same label as holotype, 1 sbad. ♂, 1 ♀ (FKCP), 5 sbad. ♂, 9 ♀, 1 sbad. ♀, leg. H.



Figure 224: *Iurus kinzelbachi*, sp. nov., dorsal view. Adult male, Aydin Province, Dilek Peninsula National Park, Turkey.



Figure 225: Dilek Peninsula National Park, Aydin, Turkey, type locality of *Iurus kinzelbachi*, sp. nov. Ersen Yağmur pictured in foreground.



Figure 226: Dilek Peninsula National Park, Aydin, Turkey, type locality of *Iurus kinzelbachi*, sp. nov. Ersen Yağmur pictured in foreground.

	Time of ecdyses counted in days from date of birth				
	First	Second	Third	Fourth	Fifth
<i>Iurus kraepelini</i>	15	104–265	219–403	371–406	609♀ 605♂ 609♂ 622♂ 623♂ 639♂ -
				179	250
					465–493
					776♂ 793♂ 793♀ 797♀
					605
					793♀ 800♀
					610
					785♂
					621

Table 12: Breeding statistics for *Iurus kraepelini*, showing time of ecdyses.

Koç (MTAS); same locality, 7 June 2009, 1 ♂ (VFWV), 1 sbad. ♂, 1 ♀ (MESB), leg. K. B. Kunt & A. Kızıltuğ; same locality, 94 m, 13 August 2009, 1 ♂, 1 ♀, leg. E. A. Yağmur & V. Ülgezer (FKCP). *İzmir Province*: Bornova District, Naldöken, formerly Narlıköy ("Narlı Kioi", "Marli Kioi"), 1900, 2 ♂, 5 ♀ (NHMW 11318).

NOTE. An old NHMW label first published by Kinzelbach (1975: 25; misspelled as "Marli Kioi") mentions "Narlı Kioi bei Smyrna." This refers to a historical Levantine settlement near İzmir (Oban, 2007) that corresponds to the modern suburb of İzmir called Naldöken (formerly Narlıköy). Figure 217 shows these labels. No specimens of *Iurus* have been currently (2009) discovered during repeated field trips by one of the authors (EAY) in Naldöken, or anywhere between İzmir and Dilek Peninsula. It is likely that populations of *Iurus kinzelbachi* in İzmir Province are now extinct due to the enormous urban growth of the metropolis of İzmir in the last 100 years.

Biology

Breeding of *Iurus*

One of the authors (FK) conducted long-term observations on breeding *Iurus* in captivity, and obtained the data listed below. All specimens of different ontogenetic development shown in Figures 227–234 were bred from a female *Iurus kraepelini* collected in Akseki, Turkey.

Specimens were kept together in sibling groups at temperatures ranging from 22 to 30°C, on a substrate of moistened lignocel and pieces of bark added for hiding.

Food consisted exclusively of crickets *Acheta domesticus* of suitable size. As soon as a specimen underwent an ecdysis, it was transferred into another similarly furnished enclosure. In this way each of the sibling groups was split into two to three enclosures with a different frequency/volume of feeding (as an ecdysis approaches, the intake of food declines). Individuals were marked with acetone-based paints that beekeepers use to mark queens. Four colors were used on different body parts, most often on the legs. In each group, only those juveniles that were the first and last to undergo an ecdysis were marked, whereas in mature specimens we marked every individual whose life parameters (longevity, number, and periodicity of clutches) were followed.

Table 12 contains data on the development of captive specimens. Males of *I. kraepelini* reach adulthood after the fourth (age of 637 days) or fifth (age of 605–785 days) ecdysis, whereas females reach adulthood always after the fifth ecdysis (age of 402–800 days).

Specimens born in captivity measured ca. 26–30 mm after the first ecdysis, ca. 34–44 mm after the second, ca. 47–56 mm after the third, 58–74 mm after the fourth and 76–86 mm after the fifth ecdysis.

Since some specimens collected in the wild are nearly 100 mm long, it is likely that they have undergone an additional (sixth) ecdysis. Unusual is the relatively wide size range of specimens that underwent the same number of ecdyses, which includes siblings kept in identical conditions in the same enclosure, and the widely differing amounts of time that captive specimens kept in identical conditions require to reach



Figure 227: *Iurus kraepelini*, female with juveniles. **Top.** Shortly after delivery. **Bottom.** Shortly after first ecdysis.



Figure 228: *Iurus kraepelini*. **Top.** Female with juveniles one week after first ecdysis. **Bottom.** Juveniles after first ecdysis.



Figure 229: *Iurus kraepelini*. **Top.** At bottom left a juvenile before the second ecdysis, at top right a juvenile just after the second ecdysis, still with exuvium. **Bottom.** Juveniles after second ecdysis.



Figure 230: *Iurus kraepelini*, juveniles after the third and one during the fourth ecdysis.



Figure 231: *Iurus kraepelini*. **Top.** A juvenile after second ecdysis. **Bottom.** A juvenile after third ecdysis



Figure 232: *Iurus kraepelini*. **Top.** A juvenile shortly after the fourth ecdysis. **Bottom.** An immature specimen before the fifth ecdysis.



Figure 233: *Iurus asiaticus*. **Top.** An adult male shortly after the fifth ecdysis. **Bottom.** An adult male well after the fifth ecdysis.



Figure 234: *Iurus kraepelini*, an adult male immediately after the fourth ecdysis and its exuvium.

maturity, with the first female undergoing the fifth ecdysis at the age of 402 days and the last female undergoing the fifth ecdysis at the age of 800 days.

Observations on *Iurus* Embryos

Among a large collection of *Iurus dufourei* from Peloponnese, Greece, given to the authors by Pierangelo Crucitti were two gravid females from Kalivia Sohas (Mystras District, Laconia Prefecture) with their embryos removed. We obtained 16 fully formed, late-stage embryos, contained in the vials with these two females (seven and nine embryos, respectively). Since *Iurus* embryos have not been previously observed and described in the literature, we offer here a pilot study of their morphology. Five embryos were prepared for SEM imaging (see Methods) with the kind help of David P. A. Neff. In the photographs and micrographs presented in Figures 235–246, we illustrate several of these embryos.

For the information on scorpion embryonic development, the reader is addressed to the most recent reviews by Farley (1999, 2001a) and to other important works by the same author (Farley, 2001b, 2005, 2008). The overall arrangement of the *Iurus* embryo and detail of structure development is similar to late-stage embryos of the apoikogenic *Smeringurus mesaensis* (Vaejovidae) and *Hadrurus arizonensis* (Caraboctonidae, the sister family of Iuridae) illustrated by Farley (1999, 2001a). The late-stage embryos of *Iurus* are formed in a typical “supine position” (such as depicted for *Hadrurus arizonensis* in Farley, 1999: fig. 23); i.e., the metasoma and telson as well as the legs and pedipalps are folded over the ventral aspect of the mesosoma (Fig. 235). The studied embryos were not the same size, some considerably smaller than others. The total length of a large embryo is 14.55 mm for the body (prosoma and mesosoma) and 7.65 for metasoma and telson.

As confirmed and discussed by Farley (2005), the so-called first stadium (= first instar, pronymph, newborn, pullus) in scorpions is a continuation and extension of embryological development. Its first ecdysis (molt) results in a drastic transformation of an embryo-like newborn to an adult-like second instar (= second stadium, nymph); see Farley (2005: figs. 9–10). The late-stage embryo in scorpions is generally very similar to the newborn animal. An interesting feature of this observed stage is a marked heterochrony: advanced embryonic development of some morphological features combined with the delayed development of others.

Mesosoma. The *carapace* is formed, exhibiting a wide anterior emargination, which is also found on adults; this emargination is much wider in the embryo. The lateral and median eye tubercles are developed and pigmented black, but no trace of median eyes are present. The developing three lateral eyes are definitely visible in Fig. 236 but are below the surface (as

confirmed by SEM). The *chelicerae* are present; both movable and fixed fingers are developed, the movable finger slightly longer than the fixed; some setae are present. No cheliceral dentition is visible, but a beginning of the movable finger dorsal edge is visible due to a slight bifurcation distally (Fig. 237). The maxillary lobes are visible in Figs. 236 and 239, their distal portions extending somewhat outward. The sternum and genital operculum are well-developed and resemble what is seen in adults, except the sternum is considerably wider in the embryo (Fig. 236). The *pectines* are well-developed with their teeth, fulcra, and lamellae clearly formed, with visible setation. Even the sensorial areas are delineated, and a number of developing peg sensilla in various stages of development are well-visible (Figs. 237, 240). The elongated *stigmata* are developed (Fig. 241), located approximately at their adult position, not close to the posterior edge of the sternite.

Metasoma and telson. All five segments of the metasoma are present, but their proportions are considerably different than those found in post-embryonic stages. Typical of adult *Iurus*, we see that the metasomal segments are the widest basally on segment I and then narrowing successively through segments II–V. However, the segments of the embryo do not exhibit the successive lengthening as in post-embryonic stages; on the contrary, segment I in the embryo is by far the longest, II is longer than III, and so forth. Slight indications of dorsal carinae are visible on segments III–V, presented as wide longitudinal raised areas on the segment surface (Fig. 238). Large setae are present on metasoma (Fig. 242). The telson is present, formed as a short triangular-shaped segment with a blunt tip. There is no indication of a vesicle-aculeus juncture or a formed aculeus, although setae are definitely visible (Fig. 243).

Pedipalps. All five segments, as well as the chelal movable finger, are developed in the embryo (Fig. 235). The relative proportions of these segments are not abnormally different from post-embryonic stage, as seen in the metasoma. However, carinae are not developed, and finger dentition is not present. No *trichobothria* are found on any of examined aspects of all three pedipalp segments (confirmed by SEM imaging of five embryos). Definitely socketed, large setae (but *not* trichobothria) are present on the fixed finger. Farley (2005, for *Centruroides vittatus*) commented on the fact that trichobothria and other sensory organs appear *en masse* after the first ecdysis (molt) to the second instar.

An interesting find is a somewhat well-developed *constellation array* (Fet et al., 2006), which is easily recognizable, with as many as five of its characteristic sensilla visible (Figs. 244–245). The adult *Iurus dufouri* has six sensilla (see Fig. 21). This is the first time that the *constellation array* is documented for an embryonic stage.



Figure 235: Embryo of *Iurus dusourei*, Kalivia Sohas, Mystras, Greece. **Top.** Embryo, ventral view, showing typical “fetal position”, metasoma, legs, and pedipalps folded tightly against the mesosoma. **Bottom.** Close-up, ventral view, showing chelicerae, pedipalps, and legs.



Figure 236: Embryo of *Iurus dufoureius*, Kalivia Sohas, Mystras, Greece. **Top.** Close-up, ventral view, showing pectines, basal piece, genital operculum, and an enlarged sternum. At the top, coxosternal lobes appear as protruding plugs (some leg portions were removed for this picture). **Bottom.** Close-up, chelicerae and anterior edge of carapace showing darkened eye tubercles. Three lateral eye positions are visible.

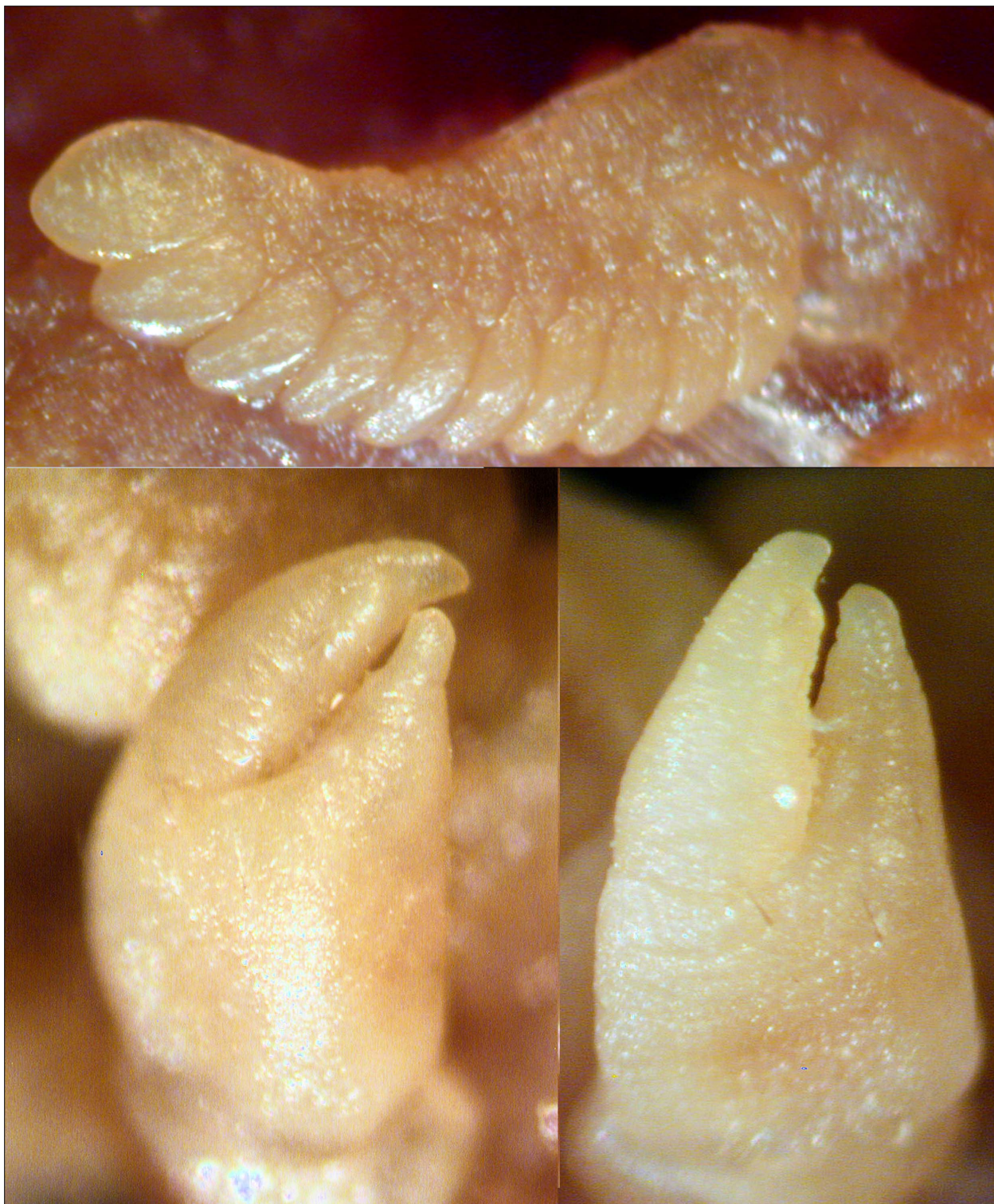


Figure 237: Embryo of *Iurus dufoureius*, Kalivia Sohas, Mystras, Greece. **Top.** Close-up, right pecten, showing anterior lamellae, fulcra, and teeth. **Bottom.** Close-up of left chelicera, dorsal view (left) and external view (right). In dorsal view, the movable finger connection to the palm is visible, and in the external view, a slight bifurcation is visible on movable finger terminus showing the initial development of the dorsal edge.

Legs. Seven of the eight segments are developed: coxa, trochanter, femur, patella, tibia, basitarsus, and a fused tarsus-epitarsus. The proportions of the leg seg-

ments are not as in adult specimens; in particular, the femur and patella are much shorter in the embryo. The characteristic *Iurus* leg spination (spinule tufts) is not



Figure 238: Embryo of *Iurus dufoureius*, Kalivia Sohas, Mystras, Greece. **Top.** Close-up of ventral view of metasoma and telson. **Middle.** Close-up of left chela, ventral view, showing connection of movable finger to palm. **Bottom.** Close-up of chelal fixed finger showing development of setae.

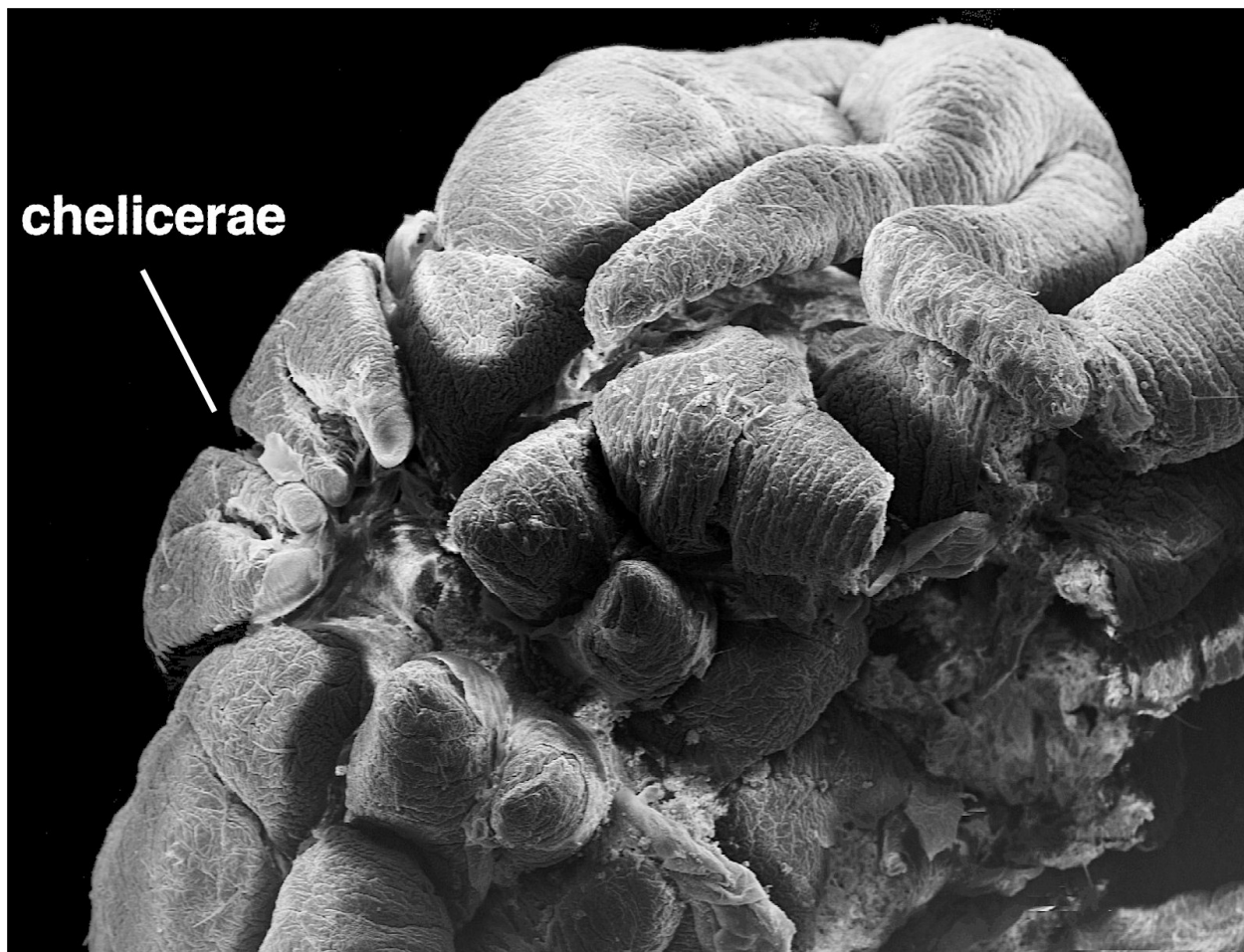


Figure 239: Embryo of *Iurus dufoureius*, Kalivia Sohas, Mystras, Greece. General ventroanterior view, coxae and chelicerae (35x).

developed in the embryo, and the fused tarsus-epitarsus does not exhibit pedal spurs, unguis or an unguicular spine (dactyl). However, strong, disproportionately long socketed setae are visible on the tarsus.

The distal aspect of the embryonic tarsus is quite interesting (Fig. 246). All surfaces are “tucked” into the tarsus tip, forming a pad-like structure, which does not become a developed distal epitarsus (= unguis + dactyl) until the first ecdysis. Millot & Vachon (1949: fig. 191) have a schematic illustration, for *Parabuthus capensis* (Buthidae), of an “adhesive organ” which newborn legs have instead of unguis, “resembling those in *Thelyphonida pulli*.” Similar structures in other arachnids are discussed by Dunlop (2002). Farley (2005, figs. 11, 16) for the first time illustrated this structure in detail for the newborn of *Centruroides vittatus*, providing SEM micrographs. According to Farley (2005: 7), “The tip of the pronymphal leg may function like a suction cup, since pronymphs removed from the mother’s dorsum are able to climb a vertical glass slide and cling to the underside of a glass slide on a microscope stage. When

viewed in this position, the leg tips are somewhat spread out and pressed against the glass as though forming a seal. Second and subsequent instars with distal claws are unable to climb a vertical glass wall but usually have no difficulty with a roughened surface.”

Ecology and Biogeography

Throughout the genus range, most of *Iurus* species are found from the sea level to high mountains. The highest altitudinal record for this genus (and also for the family Iuridae) is for *Iurus kraepelini*, 2130 m asl in Akdağ Mts (Muğla Province, Fethiye District; Yağmur, Koç & Akkaya, 2009). For *I. asiaticus*, the record altitude is 1600 m asl (Adana Province: Karaisalı District, Kızıldağ Plateau) (Karataş, 2001); *I. dufoureius* was found at 1200 m asl on Crete, Mt. Lefka Ori (Stathi & Mylonas, 2001). At the same time, *I. kinzelbachi* was so far found only at 84–92 m asl.

Preference of humid environment seems to be constant in all species of *Iurus*, although they seem to



Figure 240: Embryo of *Iurus dufoureius*, Kalivia Sohas, Mystras, Greece. Left pecten, showing peg sensilla. Full view (bottom, 100x) and close-up of peg sensilla (top, 350x).

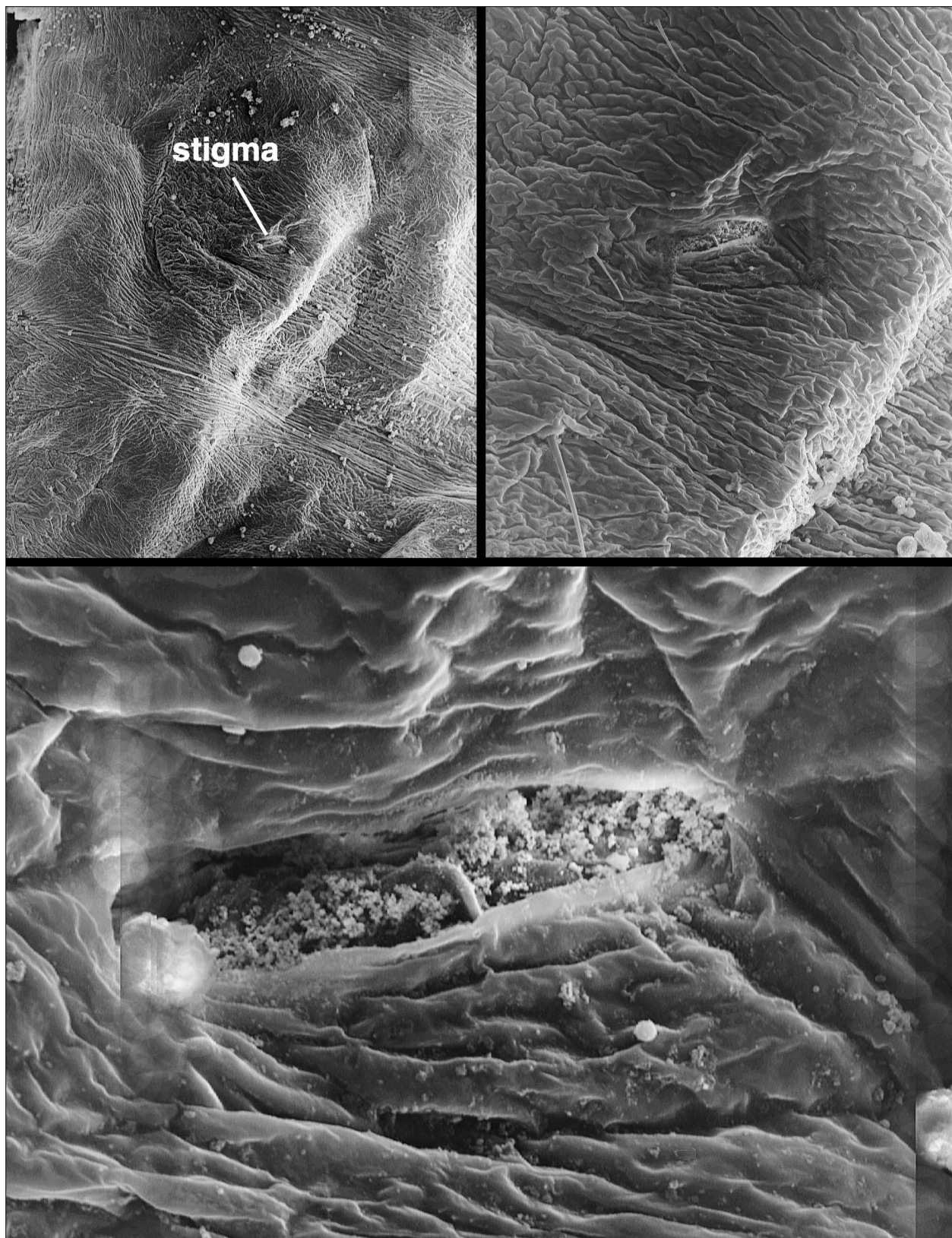


Figure 241: Embryo of *Iurus dufoureius*, Kalivia Sohas, Mystras, Greece. Right stigma IV; three successively magnified images (50x, 200x, 500x).

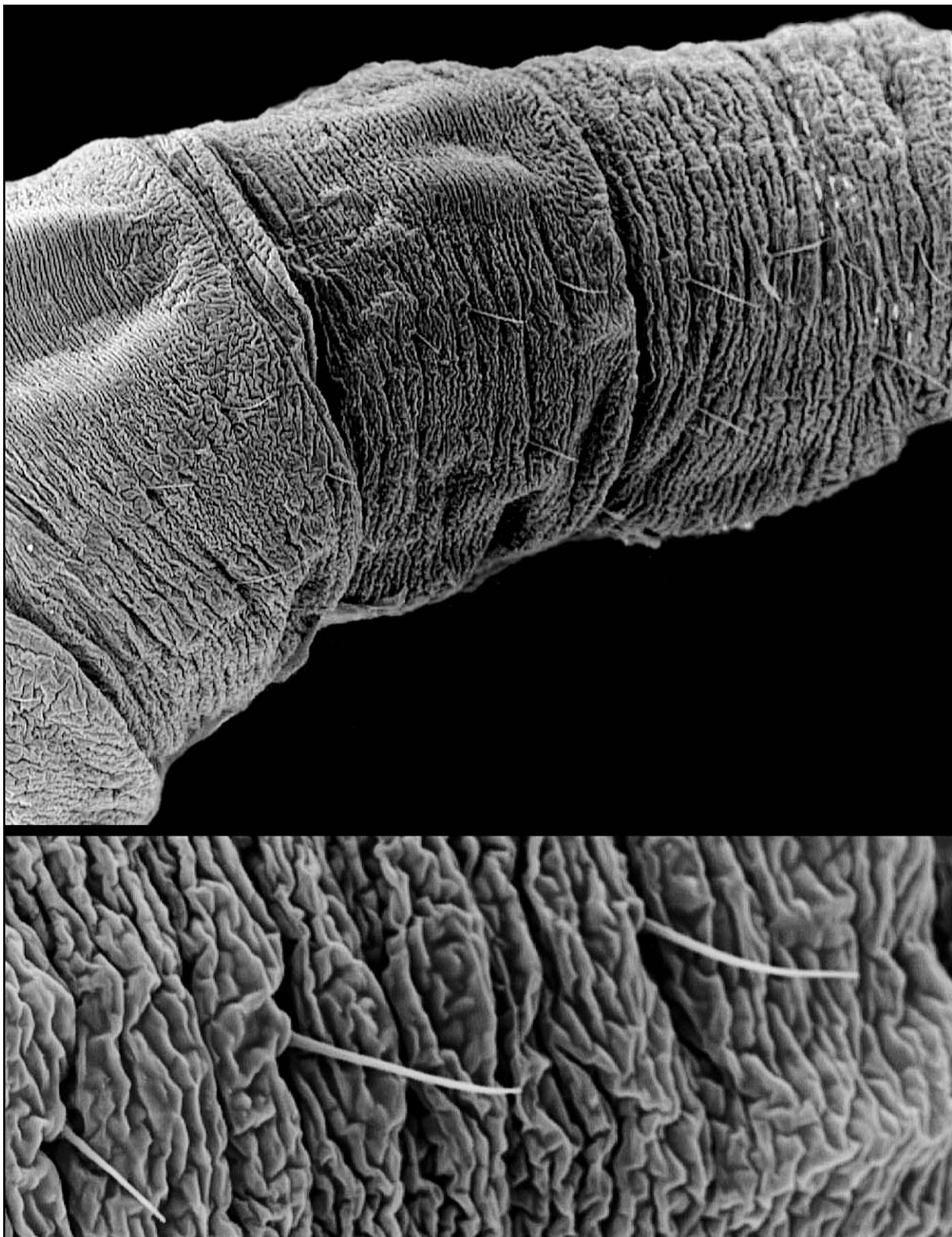


Figure 242: Embryo of *Iurus dufourei*, Kalivia Sohas, Mystras, Greece. Metasoma, ventral view, showing setae. Large view (top, 50x) and close-up of three setae (bottom, 200x).

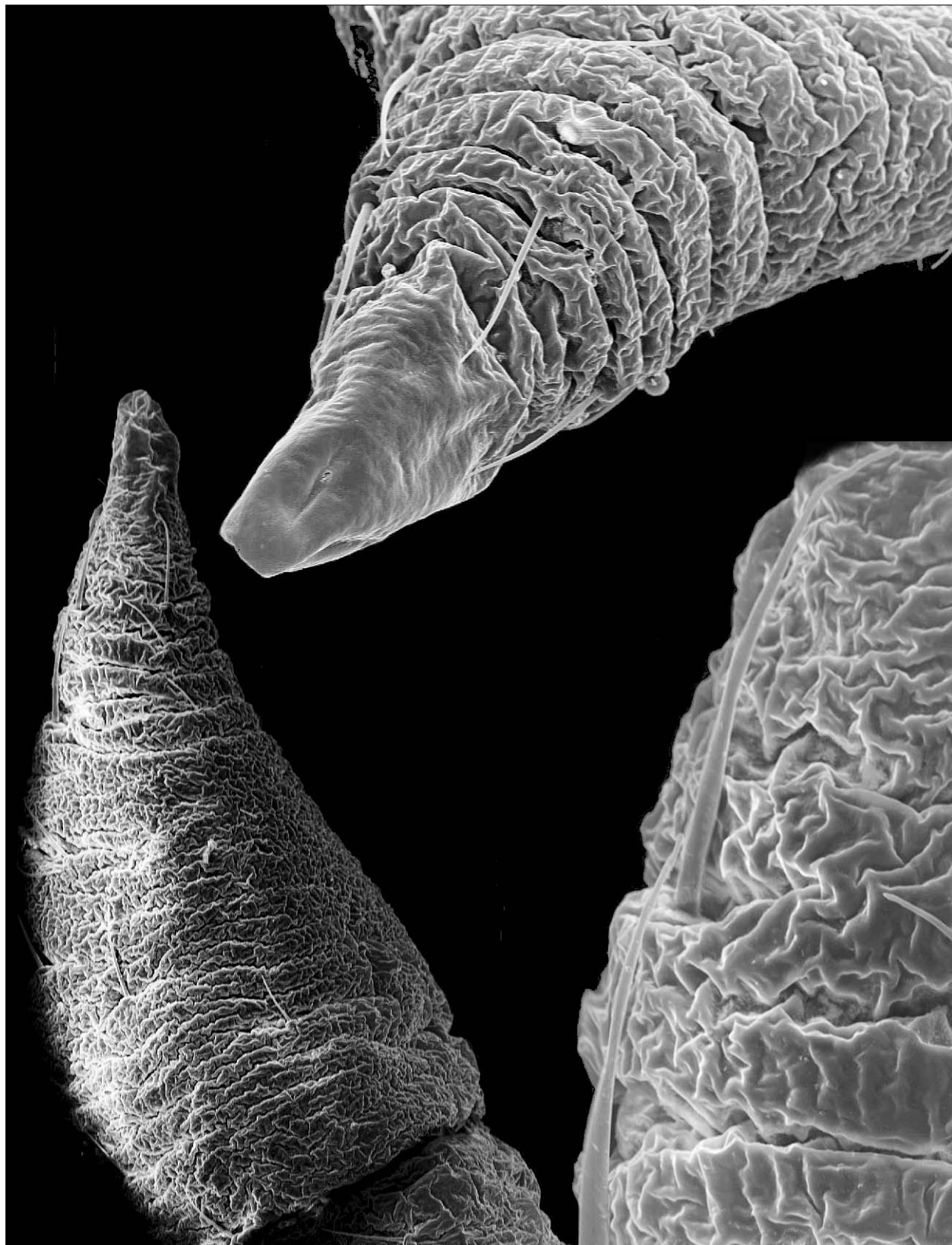


Figure 243: Embryo of *Iurus dufoureius*, Kalivia Sohas, Mystras, Greece. Telson, full lateral view on left (75x); aculeus view on top (150x); and close-up of setation on the vesicle (350x).

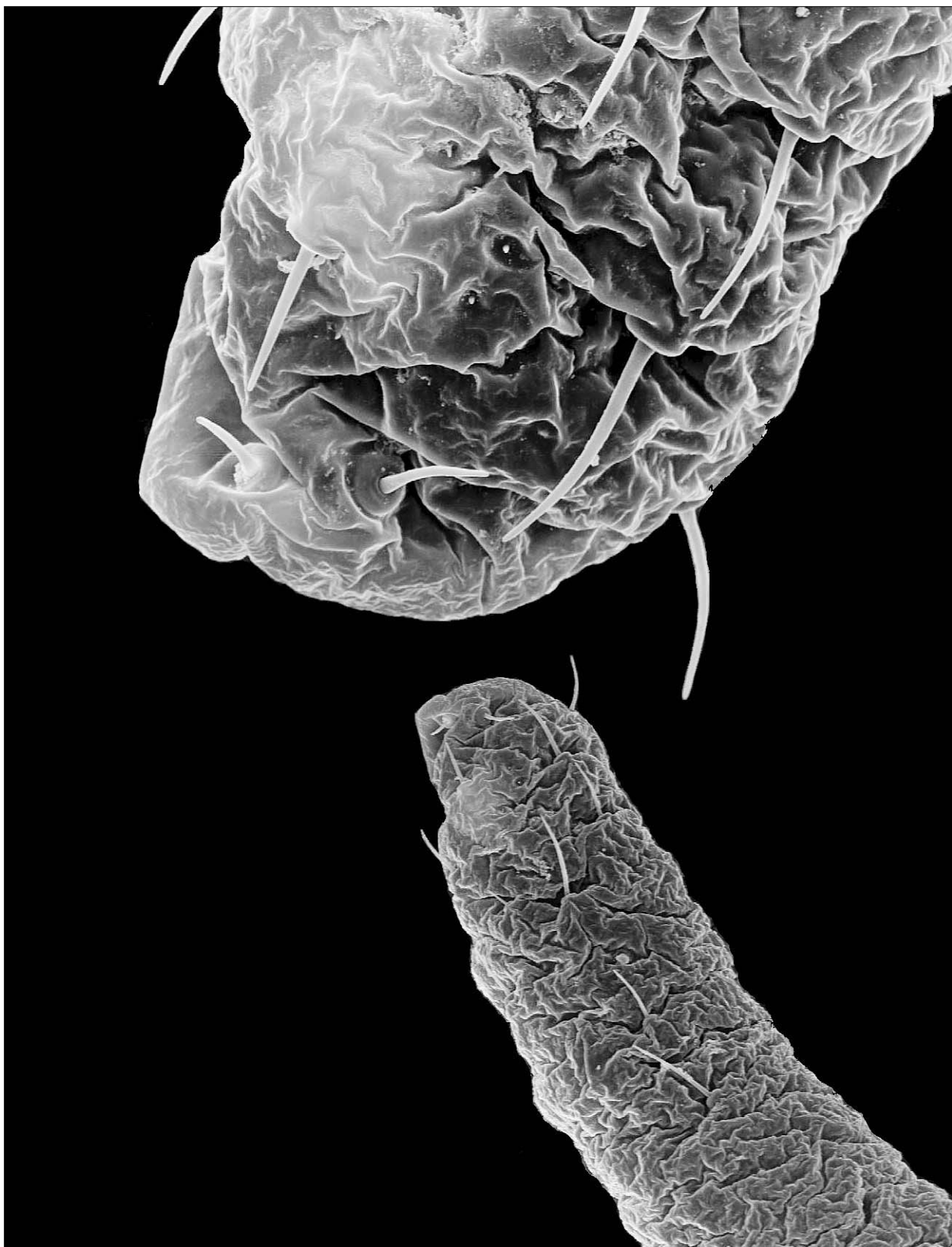


Figure 244: Embryo of *Iurus dusourei*, Kalivia Sohas, Mystras, Greece. **Bottom.** Left chelal fixed finger showing socketed setae (100x). **Top.** Close-up of distal aspect of fixed finger showing socketed setae and three constellation array sensilla (350x).

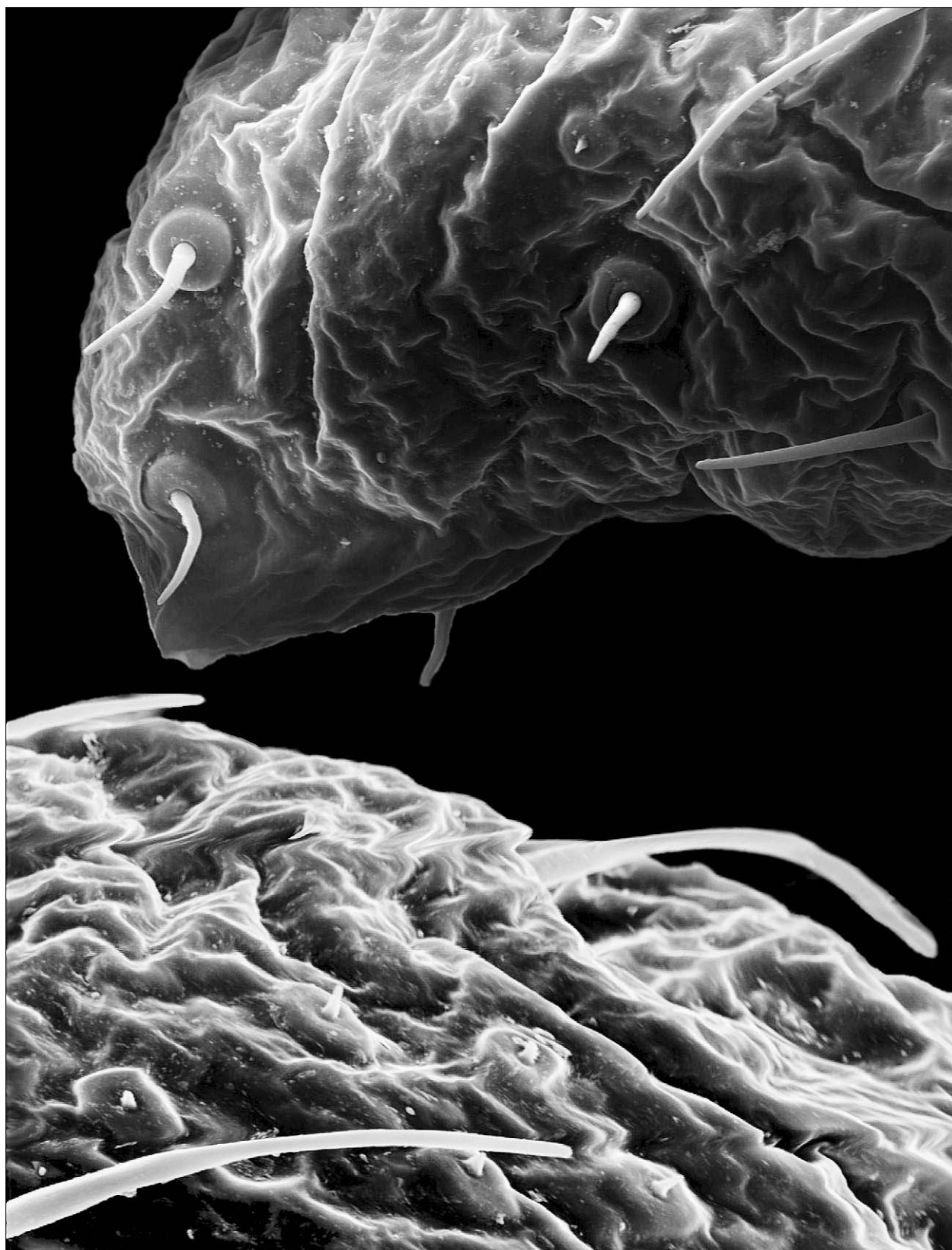


Figure 245: Embryo of *Iurus dusfourieus*, Kalivia Sohas, Mystras, Greece. **Top.** Close-up of left chelal fixed finger showing socketed setae and constellation array (500x). **Bottom.** Close-up of right fixed finger showing five constellation array sensilla (750x).



Figure 246: Embryo of *Iurus dusourei*, Kalivia Sohas, Mystras, Greece. **Top.** Right leg II showing socketed setae (200x). **Bottom.** Close-up of right leg II distal tip (350x).

tolerate a large range of temperatures. In Anatolia, *Iurus* is “a strictly hygrophilic scorpion that lives in dense fir and maple, forests and oak groves, where it is fairly common” (Crucitti, 1999a). One of the authors (EAY) observed and collected three Anatolian species of *Iurus* (*I. kinzelbachi*, *I. kraepelini*, and *I. asiaticus*) in dozens of localities and various natural habitats. According to these observations, *I. kinzelbachi* prefers rocky areas covered with pine forest. Both *I. kraepelini* and *I. asiaticus* prefer rocky areas covered with pine forest and also with shrub vegetation; *I. asiaticus* favors open areas as well. All three Anatolian species hide under large stones and inside cracks in the rocks. The rare Anatolian species *I. kadleci* was found both in the open habitats as well as deep in the Dim Cave, thus some of its populations could be cave dwelling; for the details on ecology and fauna of this cave see Kunt, Yağmur & Elverici (2008). For detailed characteristics of the habitats, see also Crucitti (1995a, 1995b, 1998) for *I. dufoureius* in the Peloponnese, and Crucitti & Malori (1998) for *I. kraepelini* and *I. asiaticus*.

The western Anatolian species with a limited range, *Iurus kinzelbachi* is geographically separated from the southern *I. kraepelini* by the Menderes River (Fig. 247). Localities where *I. kinzelbachi* is found are not as warm as those of *I. kraepelini*. Both *I. kinzelbachi* and *I. kraepelini* do not penetrate further north into Anatolia although there are no mountain barriers to prevent this. It is likely that *Iurus* here is limited by arid climatic conditions.

Although *Iurus kraepelini* penetrates into the slopes of the Taurus Mountains up to 2130 m asl, it clearly prefers low elevations with hot and humid habitats, and is very common in the southern (Mediterranean) coast of Anatolia. In the east, the Göksu River in Mersin Province along with the Bolkar Mountains appear to limit the range of *I. kraepelini*, which does not penetrate further east along the coast to the southern Mersin and Hatay Provinces. The Göksu River also provides the isolation between *I. kraepelini* and *I. asiaticus*. The role of Taurus Mountains in providing zoogeographic barriers for the Anatolian fauna is well-known (Crucitti & Malori, 1998; Çiplak, 2003).

The eastern Anatolian species, *Iurus asiaticus*, clearly prefers higher elevations and cooler places than *I. kraepelini*; however, it also favors humid habitats. All records of *I. asiaticus* from Kahramanmaraş, Adiyaman, Mersin and Adana Provinces always belong to cool, high-altitude places. On the east, the range of *I. asiaticus* appears to be limited by a combination of temperature and humidity: south of Adana, Mersin and Hatay are humid but warm, while Gaziantep and south of Adiyaman are very hot and dry.

Kaltsas, Stathi & Fet (2008) outlined two contrasting published historical scenarios that exist for the dating of *Iurus* vicariance. Francke and Soleglad

(1981) followed Vachon (1953) and Kinzelbach (1975) in attributing the distribution pattern of the genus *Iurus* to a vicariant process resulting from the recent tectonic events that occurred between the Turkish Plate and the Anatolian Fault during the Quaternary period (1.8 Mya). On the other hand, the first pilot DNA phylogeny of Parmakelis et al. (2006), and its molecular clock calibration interpreted *Iurus* as a much older taxon that has been differentiating in the studied region at least since the middle Miocene, with a split between major clades ca. 8 Mya. Similar ancient divergence between eastern and western Aegean populations and taxa is known for other terrestrial animals in this area such as lizards and land snails (Schmitt, 2007); it is dated back to the formation of the mid-Aegean trench (12 to 9 Mya).

Assuming a hypothetical dispersal of *Iurus* from east to west (Parmakelis et al., 2006), we expect the populations of *I. asiaticus* Birula, 1903, to be most basal in the genus. Our discovery of two new species in Anatolia (allopatric *I. kinzelbachi* and sympatric *I. kadleci*) revealed an additional local speciation that took place independently on the periphery of the main Anatolian species, *I. kraepelini*. Moreover, *I. kinzelbachi* appears to be closer to the Greek *I. dufoureius* than to the three other Anatolian species.

Within the most widespread *Iurus* species, the Anatolian *I. kraepelini*, we describe for the first time the intraspecific geographic variation reflected in neobothriotaxy patterns (Figs. B1–B2); see also Soleglad, Kovařík & Fet, 2009) provides an evidence for intensive local diversification. Therefore, *Iurus* emerges as a promising model genus for the study of speciation and microevolution, and needs to be tested further with modern techniques in genetics using multiple markers and numerous populations, especially from Anatolia.

Acknowledgments

We are first of all grateful to Pierangelo Crucitti who donated to us an extensive and important series of *Iurus* from Peloponnese. We are very grateful to Petar Beron, Christoph Hörweg, Jason Dunlop, Jürgen Gruber, Petr Kabátek, Ragnar Kinzelbach, Pavel Krásenský, Robert Lízler, Marcello Malori, Verena Stagl, Iasmí Stathi, Valerio Vignoli, Sarah Whitman, and the late Gary A. Polis for the loans or gifts of specimens; and to Julia Altmann, Janet Beccaloni, Gernot J. Bergthaler, Matt E. Braunwalder, Marco Colombo, Benjamin Gantenbein, Peter Jäger, Viktor Krivochatsky, Serge Peslier, Wolfgang Schawaller, Peter J. Schwendinger, and the late Jean-Bernard Lacroix for the information on museum holdings and geographic distribution. Wilson R. Lourenço helped to obtain a loan of Paris specimens, including an important Vachon’s “Tarsus male.” Michal Hoskovec kindly provided photographs of Greek habitats (Figs. 105–106). E.A.Y. is grateful for their help

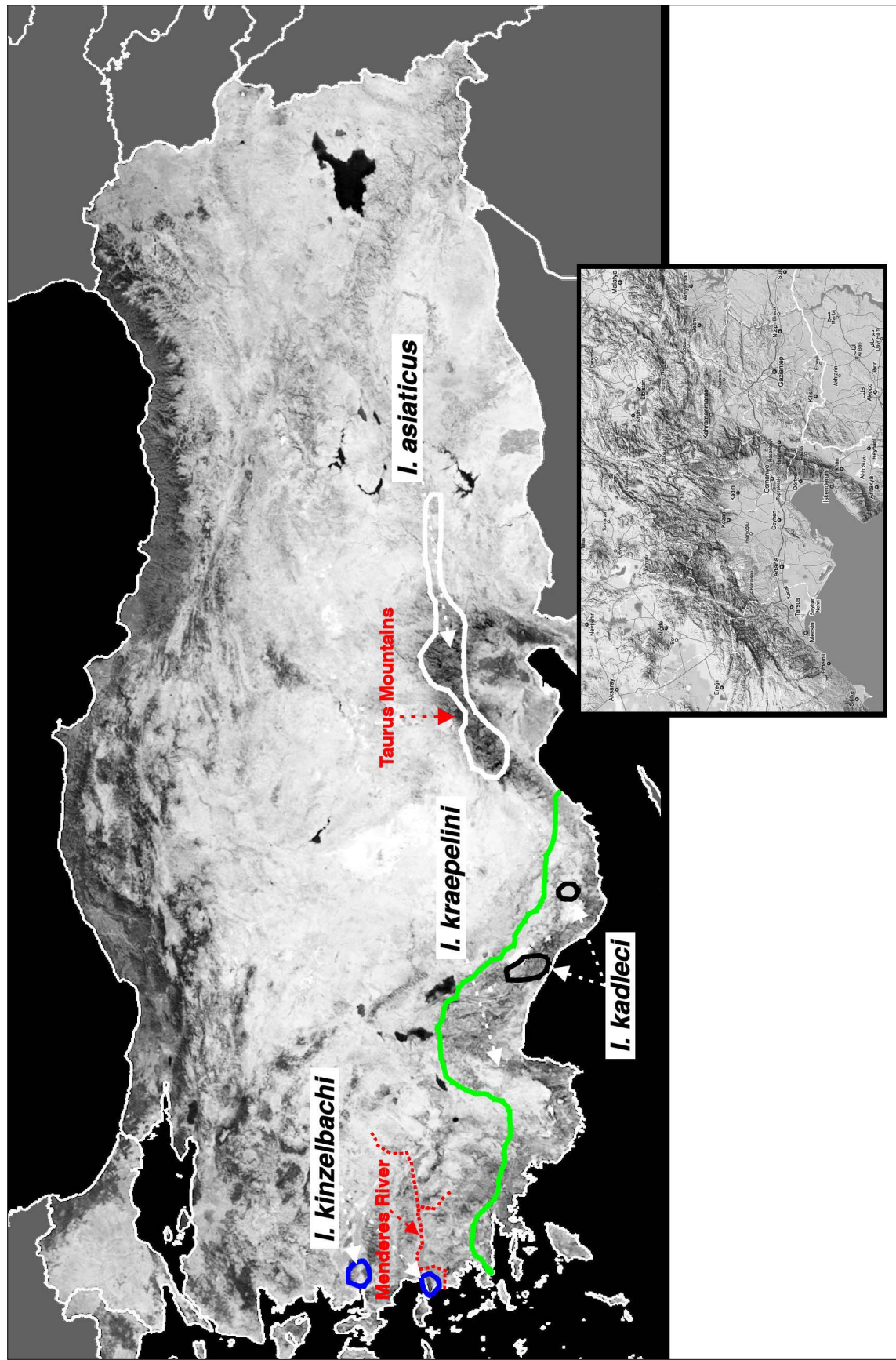


Figure 247: Two natural boundaries separate *Iurus kraepelini* (outlined in green) from *I. kinzelbachi* (outlined in blue), the Menderes River, and *I. asiaticus*, the Taurus Mountains. *I. kadleci* (outlined in black) occurs sympatrically with *I. kraepelini*. SE Taurus mountains shown in inset.

in field collections and gifts of specimens and/or photographs to Abdulmuttalip Akkaya (Fig. 143), Aziz Avci, Gökhan Çalışır, Salim Dudaklı, Hakan Durmuş, Alexander V. Gromov, Hakan Karaoglu, Altuğ Kızıltuğ, Halil Koç (Figs. 143–144, 147), Kadir Boğaç Kunt (Figs. 144–145), Kurtuluş Olgun, Mehmet Özkarük, İsmail Hakkı Uğurtaş, Volkan Ülgezer, Mehmet Yalçın, and Mehmet Zülfü Yıldız (Figs. 146, 177–179). Roger Farley generously advised us on embryo morphology. David P. A. Neff was instrumental in embryo fixation and SEM help; SEM microscopy was supported by Marshall University. Finally, we thank two anonymous reviewers for their valuable and expedient review of this paper.

References

- ARNETT, H. R. JR., G. A. SAMUELSON & G. M. NISHIDA. 1993. *The Insect and Spider Collections of the World*. Flora & Fauna Handbook No. 11, 2nd ed. Gainesville: Sandhill Crane Press, 308 pp.
- BIRULA, A. 1898. Ein Beitrag zur Kenntnis der Skorpionsfauna Kleinasiens. *Horae Societatis Entomologicae Rossicae*, 33: 132–140.
- BIRULA, A. 1903. Miscellanea scorpilogica V. Ein Beitrag zur Kenntnis der Scorpionenfauna der Insel Kreta. *Annuaire du Musée zoologique de l'Académie impériale des sciences de St.-Pétersbourg*, 8: 295–299.
- BORELLI, A. 1913. Escurzioni zoologiche del Dr. Enrico Festa nell'Isola di Rodi. Scorpioni. *Bollettino dei Musei di Zoologia ed Anatomia Comparata della Reale Università di Torino*, 28(675): 1–3.
- BRULLÉ, A. 1832. Des Animaux articulés. Scorpions. In: Baron J. B. G. M. Bory de Saint Vincent (ed.), *Expédition scientifique de Morée. Section des sciences physiques. Zoologie*. Paris, 3(1): 57–60.
- CAPORIACCO, L. di. 1928. Ricerche faunistiche nell'isole Italiane dell'Egeo. Aracnidi. *Archivio Zoologico Italiano*, 13: 221–242.
- ÇIPLAK B. 2003. Distribution of Tettigoniinae (Orthoptera: Tettigoniidae) bush-crickets in Turkey: the importance of the Anatolian Taurus Mountains in biodiversity and implications for conservation. *Biodiversity and Conservation*, 12(1): 47–64.
- CRUCITTI, P. 1995a. *Iurus dufoureius* del Peloponneso meridionale: Osservazioni ecologiche e biometriche (Scorpiones, Iuridae). *Bollettino dell'Associazione Romana di entomologia*, 49(3–4) (1994): 1–14.
- CRUCITTI, P. 1995b. *Iurus dufoureius* (Brullé) nel Peloponneso occidentale e considerazioni sulla scorpiofauna dei Minthi Óros (Grecia). *Bollettino della Società Entomologica Italiana*, 127 (2): 91–98.
- CRUCITTI, P. 1998. Ricerche bio-ecologiche su *Iurus dufoureius* (Brullé, 1832) del Peloponneso sud-occidentale (Scorpiones, Iuridae). *Annali del Museo Civico di Storia Naturale di Ferrara*, 1: 31–43.
- CRUCITTI, P. 1999a. The scorpions of Anatolia: Biogeographical patterns. *Biogeographia*, 20: 81–94.
- CRUCITTI, P. 1999b. Scorpion species diversity in southwestern Peloponnese, Greece (Scorpiones). *Contributions to the Zoogeography and Ecology of the Eastern Mediterranean Region*, 1: 251–256.
- CRUCITTI, P. & D. CICUZZA. 2001. Scorpions of Anatolia: Ecological patterns. Pp. 225–234 in: Fet, V. & P. A. Selden (eds.). *Scorpions 2001. In memoriam Gary A. Polis*. Burnham Beeches, Bucks: British Arachnological Society.
- CRUCITTI, P. & M. MALORI. 1998. Gli Scorpioni (Scorpiones) del Tauro (Turchia). *Giornale Italiano di Entomologia*, 9: 131–136.
- DUNLOP, J. A. 2002. Character states and evolution of the chelicerate claws. Pp. 345–354 in: Toft, S. & N. Scharff (eds.), *Proceedings of the 19th European Colloquium of Arachnology*, Aarhus, 17–22 July 2000. Aarhus: Aarhus University Press.
- FACHERIS, D. 2007a. New localities of *Iurus dufoureius dufoureius* (Brullé, 1832) in the Peloponnese, Greece (Scorpiones: Iuridae). *Euscorpius*, 52: 1–4.
- FACHERIS, D. 2007b. Nuove stazioni di *Iurus dufoureius dufoureius* (Brullé, 1832) (Scorpiones: Iuridae) nel Peloponneso (Grecia). *Rivista del Museo Civico di Scienze Naturali "E. Caffi"*, Bergamo, 2005(2006), 24: 125–128.
- FARLEY, R. D. 1999. Scorpiones. Pp. 117–222 in: Harrison, F.W. & R.F. Foelix (eds.), *Microscopic Anatomy of Invertebrates. Chelicerate Arthropods*, vol. 8A. New York: Wiley-Liss.

- FARLEY, R. D. 2001a. Structure, reproduction, and development. Pp. 13–78 in: Brownell, P.H. & Polis G.A. (eds.), *Scorpion Biology and Research*. Oxford University Press: Oxford.
- FARLEY, R. D. 2001b. Development of segments and appendages in embryos of the desert scorpion *Paruroctonus mesaensis* (Scorpiones: Vaejovidae). *Journal of Morphology*, 250(1): 70–88.
- FARLEY, R. D. 2005. Developmental changes in the embryo, pronymph, and first molt of the scorpion *Centruroides vittatus* (Scorpiones: Buthidae). *Journal of Morphology*, 265(1): 1–27.
- FARLEY, R. D. 2008. Development of respiratory structures in embryos and first and second instars of the bark scorpion, *Centruroides gracilis* (Scorpiones: Buthidae). *Journal of Morphology*, 269(9): 1134–1156.
- FET, V. 2000. Scorpions (Arachnida, Scorpiones) from the Balkan Peninsula in the collections of the National Museum of Natural History, Sofia. *Historia Naturalis Bulgarica*, 11: 47–60.
- FET, V. 2010. Scorpions of Europe. *Acta Zoologica Bulgarica*, 62(1): 3–12.
- FET, V. & M. E. BRAUNWALDER. 2000. The scorpions (Arachnida: Scorpiones) of the Aegean area: current problems in taxonomy and bio-geography. *Belgian Journal of Zoology*, 130 (Supplement): 17–22.
- FET, V., M. S. BREWER, M. E. SOLEGLAD & D. P. A. NEFF. 2006. Constellation array: a new sensory structure in scorpions (Arachnida: Scorpiones). *Boletín de la Sociedad Entomológica Aragonesa*, 38: 269–278.
- FET, V. & M. E. SOLEGLAD. 2002. Morphology analysis supports presence of more than one species in the “*Euscorpius carpathicus*” complex (Scorpiones: Euscorpiidae). *Euscorpius*, 3: 1–51.
- FET, V. & M. E. SOLEGLAD. 2005. Contributions to scorpion systematics. I. On recent changes in high-level taxonomy. *Euscorpius*, 31: 1–13.
- FET, V. & M. E. SOLEGLAD. 2008. Cladistic analysis of superfamily Iuroidea, with emphasis on subfamily Hadrurinae (Scorpiones: Iurida). *Boletín de la Sociedad Entomológica Aragonesa*, 43: 255–281.
- FET, V., M. E. SOLEGLAD & F. KOVAŘÍK. 2009. Etudes on iurids, II. Revision of genus *Calchas* Birula, 1899, with the description of two new species (Scorpiones: Iuridae). *Euscorpius*, 82: 1–72.
- FET, V., M. E. SOLEGLAD, D. P. A. NEFF & I. STATHI. 2004. Tarsal armature in the superfamily Iuroidea (Scorpiones: Iurida). *Revista Ibérica de Aracnología*, 10: 17–40.
- FRANCKE, O. F. 1981. Taxonomic and zoogeographic observations on *Iurus* Thorell (Scorpiones, Iuridae). *Bulletin of the British Arachnological Society*, 5(5): 221–224.
- FRANCKE, O. F. & L. PRENDINI. 2008. Phylogeny and classification of the giant hairy scorpions, *Hadrurus* Thorell (Iuridae Thorell): a reappraisal. *Systematics and Biodiversity*, 6(2): 205–223.
- FRANCKE, O. F. & M. E. SOLEGLAD. 1981. The family Iuridae Thorell (Arachnida, Scorpiones). *Journal of Arachnology*, 9: 233–258.
- GLUSHKOV, S., O. NOVIKOVA, A. BLINOV & V. FET. 2006. Divergent non-LTR retrotransposon lineages from the genomes of scorpions (Arachnida: Scorpiones). *Molecular Genetics and Genomics*, 275: 288–296.
- GRAHAM, M. R. & V. FET. 2006. Serrula in retrospect: a historical look at scorpion literature (Scorpiones: Orthosterni). *Euscorpius*, 48: 1–19.
- GRUBER, J. 1963. Ergebnisse der von Dr. O. Paget und Dr. E. Kritscher auf Rhodos durchgeföhrten zoologischen Exkursionen. VII. Scorpiones und Opiliones. *Annalen des Naturhistorischen Museums in Wien*, 66: 307–316.
- GRUBER, J. 1966. Ergebnisse der von Dr. O. Paget und Dr. E. Kritscher auf Rhodos durchgeföhrten zoologischen Exkursionen. VII. Scorpiones und Opiliones (2.Teil). *Annalen des Naturhistorischen Museums in Wien*, 69: 423–426.
- HJELLE, J. T. 1990. Anatomy and morphology. Pp. 9–63 in Polis, G. A. (ed.). *The Biology of Scorpions*. Stanford, CA: Stanford University Press.
- KALTAS, D., I. STATHI & V. FET. 2008. Scorpions of the Eastern Mediterranean. Pp. 209–246 in Makarov, S. E. & R. N. Dimitrijević (eds.). *Advances in Arachnology and Developmental Biology*. Papers dedicated to Prof. Dr. Božidar Ćurčić. Vienna–Belgrade–Sofia, 517 pp.

- KAMENZ, C., J. A. DUNLOP & G. SCHOLTZ. 2005. Characters in the book lungs of Scorpiones (Chelicerata, Arachnida) revealed by scanning electron microscopy. *Zoomorphology*, 124: 101–109.
- KAMENZ, C. & L. PRENDINI. 2008. An atlas of book lung fine structure in the order Scorpiones (Arachnida). *Bulletin of the American Museum of Natural History*, 316: 1–359.
- KARATAŞ, A. 2001. *Doğu Akdeniz Akrep (Scorpiones) Faunası* [Eastern Mediterranean Scorpion Fauna]. E.Ü. Fen Bilimleri Enstitüsü. Doktora Tezi [Ph.D. Dissertation]. 93 pp. (in Turkish; unpublished).
- KARSCH, F. 1879. Scorpionologische Beiträge. Part II. *Mitteilungen des Münchener Entomologischen Vereins*, 3: 97–136.
- KARSCH, F. 1881. Uebersicht der europäischen Skorpione. *Berliner Entomologische Zeitschrift*, 25: 89–91.
- KINZELBACH, R. 1966. Über das Waschen von *Iurus dufourei* Brullé (Scorpiones, Arachnida). *Zoologischer Anzeiger*, 176(1): 12–23.
- KINZELBACH, R. 1975. Die Skorpione der Ägäis. Beiträge zur Systematik, Phylogenie und Biogeographie. *Zoologische Jahrbücher. Abteilung für Systematik, Ökologie und Geographie der Tiere*, 102: 12–50.
- KINZELBACH, R. 1982. Die Skorpionssammlung des Naturhistorischen Museums der Stadt Mainz. Teil I: Europa und Anatolien. *Mainzer naturwissenschaftliches Archiv*, 20: 49–66.
- KINZELBACH, R. 1985. Vorderer Orient. Skorpione (Arachnida: Scorpiones). *Tübinger Atlas der Vorderer Orients (TAVO), Karte Nr. A VI 14.2*.
- KOÇ, H. & E. A. YAĞMUR. 2007. Dilek Yarımadası Milli Parkı (Söke-Kuşadası, Aydın) akrep faunası. [The scorpiofauna (Scorpiones) of Dilek Peninsula National Park (Soke-Kusadasi, Aydin)]. *Ekoloji*, 17(65): 52–59 (in Turkish).
- KOCH, C. L. 1837. *Die Arachniden*. Nürnberg: C. H. Zeh'sche Buchhandlung, 4(1–5): 1–108.
- KOCH, C. L. 1850. Skorpionen. Scorpiones. In: *Uebersicht des Arachnidensystems*, J. L. Lotzbeck, Nürnberg, 5: 86–92.
- KOVAŘÍK, F. 1992. A check list of scorpions (Arachnida: Scorpiones) in the collections of the zoological department, National Museum in Prague. *Acta Societatis Zoologicae Bohemoslovenicae*, 56 (3): 181–186.
- KOVAŘÍK, F. 1998. *Štíři [Scorpions]*. Madagaskar, Jihlava. 175 pp. (in Czech).
- KOVAŘÍK, F. 1999. Review of European scorpions with a key to species. *Serket*, 6 (2): 38–44.
- KOVAŘÍK, F. 2002. A checklist of scorpions (Arachnida) in the collection of the Forschungsinstitut und Naturmuseum Senckenberg, Frankfurt am Main, Germany. *Serket*, 8(1): 1–23.
- KOVAŘÍK, F. 2005. *Iurus dufourei* Brullé – Štířecký. *Akva Tera Fórum*, 1(9): 55 (in Czech).
- KOVAŘÍK, F. & S. WHITMAN. 2005. Cataloghi del Museo di Storia Naturale dell'Università di Firenze – sezione di zoologia “La Specola”. XXII. Arachnida Scorpiones. Tipi. Addenda (1998–2004) e checklist della collezione (Euscorpiinae esclusi). *Atti della Società Toscana di Scienze Naturali, Memorie*, serie B, 111 (2004): 103–119.
- KRAEPELIN, K. 1894. Revision der Skorpione. II. Scorpionidae und Bothriuridae. *Beiheft zum Jahrbuch der Hamburgischen Wissenschaftlichen Anstalten*, 11(1): 1–248.
- KRAEPELIN, K. 1899. Scorpiones und Pedipalpi. In F. Dahl (ed.), *Das Tierreich*. Herausgegeben von der Deutschen Zoologischen Gesellschaft. Berlin: R. Friedländer und Sohn Verlag, 8 (Arachnoidea): 1–265.
- KRITSCHER, E. 1993. Ein Beitrag zur Verbreitung der Skorpione im Östlichen Mittelmeerraum. *Annalen des Naturhistorischen Museums in Wien. Serie B. Botanik und Zoologie*, 94/95, B: 377–391.
- KUČERA, J. 1992. A contribution to the knowledge of scorpion species *Iurus dufourei* habitat in Greece. *Ziva*, 40(4): 175 (in Czech, English summary).
- KUNT, K. B., E. A. YAĞMUR & M. ELVERICI. 2008. The cave dwelling arthropods of Dim cave (Turkey: Antalya: Alanya). *Munis Entomology & Zoology*, 3 (2): 682–690.
- LAMORAL, B. H. 1979. The scorpions of Namibia (Arachnida: Scorpionida). *Annals of the Natal Museum*, 23(3): 497–784.

- LUCAS, H. 1853. Essai sur les animaux articulés, qui habitent l'île de Crète. *Revue et Magasin de Zoologie*, (2), 5: 527–528.
- MENOZZI, C. 1941. Nuovi contributi alla conoscenza della fauna delle Isole Italiane dell'Egeo. *Bollettino del Laboratorio di Zoologia Generale e Agraria della Reale Scuola Superiore d'Agricoltura in Portici*, 31: 230–237.
- MILLOT, J. & M. VACHON. 1949. Ordre des Scorpions. Pp. 386–436 in: Grassé, P.P. (ed.). *Traité de Zoologie*. Paris: Masson, 6.
- OBAN, R. (ÇAKICIOĞLU). 2007. Levanten kavramı ve Levanteler üzerine bir inceleme [Examination on the concept of Levantine and Levantines]. *Türkiyat Araştırmaları Dergisi*, 22: 337–356 (in Turkish).
- PARMAKELIS, A., I. STATHI, L. SPANOS, C. LOUIS & M. MYLONAS. 2006. Phylogeography of *Iurus dufourei* (Brullé, 1832) (Scorpiones, Iuridae). *Journal of Biogeography*, 33(2): 251–260.
- PAVESI, P. 1877. Sugli Aracnidi di Grecia. *Rendiconti Reale Istituto Lombardo di Scienze e Lettere*, (2), 10: 323–327.
- PAVESI, P. 1878. Aracnidi: aggiunto un Catalogo sistematico delle specie di Grecia, in: Risultati zoologici, Crociera del Violante, ii. *Annali del Museo Civico di Storia Naturale di Genova*, 11: 337–396.
- PENTHER, A. 1906. Bemerkungen über einige Scorpione aus Kreta. *Verhandlungen der zoologisch-botanischen Gesellschaft in Wien*, 56: 60–64.
- PESLIER, S. 2005. Observation du grand Scorpion européen *Iurus dufourei* (Brullé, 1832). *Revue de l'Association Roussillonnaise d'Entomologie*, 14 (91): 28–29.
- RAULIN, V. 1869. Description zoologique de l'île de Crète. *Actes de la Société Linnéenne de Bordeaux*, 24(6): 643–708.
- ROEWER, C. F. 1943. Über eine neuerworbene Sammlung von Skorpionen des Natur-Museums Senckenberg. *Senckenbergiana*, 26(4): 205–244.
- SCHMITT, T. 2007. Molecular biogeography of Europe: Pleistocene cycles and postglacial trends. *Frontiers in Zoology*, 4: 11 doi:10.1186/1742-9994-4-11.
- SIMON, E. 1879. 3e Ordre. - Scorpiones. Pp. 79–115 in *Les Arachnides de France*. VII. Contenant les Ordres des Chernetes, Scorpiones et Opiliones. Paris: Roret.
- SIMON, E. 1884. Études arachnologiques. 16e Mémoire (1), XXIII. Matériaux pour servir à la faune des Arachnides de la Grèce. *Annales de la Société Entomologique de France*, (6), 4: 305–356.
- SISSOM, W. D. & V. FET. 2000. Family Iuridae. Pp. 409–420 in Fet, V., W. D. Sissom, G. Lowe & M.E. Braunwalder. *Catalog of the Scorpions of the World (1758–1998)*. New York: New York Entomological Society, 690 pp.
- SOLEGLAD, M. E. & V. FET. 2001. Evolution of scorpion orthobothriotaxy: a cladistic approach. *Euscorpius*, 1: 1–38.
- SOLEGLAD, M. E. & V. FET. 2003a. The scorpion sternum: structure and phylogeny (Scorpiones: Orthosterni). *Euscorpius*, 5: 1–34.
- SOLEGLAD, M. E. & V. FET. 2003b. High-level systematics and phylogeny of the extant scorpions (Scorpiones: Orthosterni). *Euscorpius*, 11, pp. 1–175.
- SOLEGLAD, M. E. & V. FET. 2008. Contributions to scorpion systematics. III. Subfamilies Smeringurinae and Syntropinae (Scorpiones: Vaejovidae). *Euscorpius*, 71: 1–115.
- SOLEGLAD, M. E., F. KOVÁŘÍK & V. FET. 2009. Etudes on iurids, I. The orthobothriotaxic pattern of Iuridae, with observations on neobothriotaxy in genus *Iurus* (Scorpiones: Iuroidea). *Euscorpius*, 79: 1–21.
- SOLEGLAD, M. E. & W. D. SISSOM. 2001. Phylogeny of the family Euscorpiidae Laurie, 1896: a major revision. Pp. 25–111 in Fet, V. & P. A. Selden (eds.). *Scorpions 2001. In memoriam Gary A. Polis*. Burnham Beeches, Bucks: British Arachnological Society.
- STAHNKE, H. L. 1974. Revision and keys to the higher categories of Vejovidae. *The Journal of Arachnology*, 1(2): 107–141.
- STATHI, I. & M. MYLONAS. 2001. New records of scorpion from central and eastern Mediterranean area: biogeographical comments, with special reference to the Greek species. Pp. 287–295 in Fet,

- V. & P. A. Selden (eds.). *Scorpions 2001. In memoriam Gary A. Polis.* Burnham Beeches, Bucks: British Arachnological Society.
- STOCKWELL, S. A. 1989. *Revision of the Phylogeny and Higher Classification of Scorpions (Chelicerata).* Ph.D. Dissertation, University of Berkeley, Berkeley, California. 319 pp. (unpublished). University Microfilms International, Ann Arbor, Michigan.
- THORELL, T. 1876. On the classification of scorpions. *Annals and Magazine of Natural History*, 4(17): 1–15.
- THORELL, T. 1877. Études Scorpionologiques. *Atti della Società Italiana di Scienze Naturali*, 19: 75–272.
- TOLUNAY, A. 1959. Zur Verbreitung der Skorpione in der Türkei. *Zeitschrift für angewandte Entomologie*, 43(4): 366–370.
- UBISCH, M. von. 1922. Über eine neue *Jurus*-Art aus Kleinasien nebst einigen Bemerkungen über die Funktion der Kamme der Scorpione. *Zoologische Jahrbücher, Abtheilung für Systematik*, 44(6): 503–516. [issue 6 of vol. 44 was published February 2, 1922].
- VACHON, M. 1947a. Remarques préliminaires sur le faune des Scorpions de Turquie. *Bulletin du Muséum national d'Histoire naturelle*, Paris, 19(2): 161–164.
- VACHON, M. 1947b. Répartition et origine des scorpions de Turquie. *Comptes Rendus des Séances de Société de Biogéographie*, 206 (3): 26–29.
- VACHON, M. 1948. Scorpions récoltés dans l'île de Crète par Mr. le Docteur Otto von Wettstein. *Annalen des Naturhistorischen Museums in Wien*, 56: 60–69.
- VACHON, M. 1951. A propos de quelques scorpions de Turquie collectés par M. le Professeur Dr. Curt Kosswig. *Istanbul Üniversitesi Fen Fakültesi Mecmuası*, 16 (B): 341–344.
- VACHON, M. 1953. Sur la répartition du grand scorpion noir des îles de la mer Egée: *Jurus dufoureius* (Brullé). *Revue générale des Sciences pures et appliquées*, 60 (3/4): 96–100.
- VACHON, M. 1966a. À propos de la synonymie de deux genres de Scorpions: *Chaerilomma* Roewer, 1943 (Chactidae) et *Jurus* Thorell, 1877 (Vejovidae). *Senckenbergiana Biologica*, 47: 453–461.
- VACHON, M. 1966b. Liste des scorpions connus en Égypte, Arabie, Israël, Liban, Syrie, Jordanie, Turquie, Irak, Iran. *Toxicon*, 4: 209–218.
- VACHON, M. 1971. [Remarques sur le Scorpion caucasien *Calchas nordmanni* Birula (Scorpiones, Chactidae)]. *Entomologicheskoe Obozrenie (Revue d'Entomologie de l'URSS)*, 50(3): 712–718 (in Russian). English translation: *Entomological Review*, 1971, 50(3): 712–718.
- VACHON, M. 1974. Étude des caractères utilisés pour classer les familles et les genres de Scorpions (Arachnides). 1. La trichobothriotaxie en Arachnologie, Sigles trichobothriaux et types de trichobothriotaxie chez les Scorpions. *Bulletin du Muséum national d'histoire naturelle, Paris*, (3), 140 (Zool. 104), mai-juin 1973: 857–958.
- VACHON, M. & R. KINZELBACH. 1987. On the taxonomy and distribution of the scorpions of the Middle East. In F. Krupp, W. Schneider & R. Kinzelbach (eds.), *Proceedings of the Symposium on the Fauna and Zoogeography of the Middle East, Mainz, 1985. Beihefte zum Tübinger Atlas des Vorderen Orients, Reihe A (Naturwissenschaften)*, 28: 91–103.
- WERNER, F. 1902. Die Skorpione, Pedipalpen und Solifugen in der zoologisch-vergleichend-anatomischen Sammlung der Universität Wien. *Verhandlungen der zoologisch-botanischen Gesellschaft in Wien*, 52: 595–608.
- WERNER, F. 1934a. Ergebnisse einer zoologischen Studien- und Sammelreise nach den Inseln des Ägäischen Meeres. V. Arthropoden. *Sitzungsberichte der Akademie der Wissenschaften, Wien*, Abt. I, 143: 159–168.
- WERNER, F. 1934b. Scorpiones, Pedipalpi. In: H. G. Bronns Klassen und Ordnungen des Tierreichs. Akademische Verlagsgesellschaft, Leipzig. 5(IV) 8 (Scorpiones, pp. 1–316): 1–490.
- WERNER, F. 1936a. Neu-Eingänge von Skorpionen im Zoologischen Museum in Hamburg. *Festschrift zum 60. Geburtstage von Professor Dr. Embrik Strand*, 2: 171–193.
- WERNER, F. 1936b. Ergebnisse einer zoologischen Forschungsreise nach dem Dodekanes unternommen von Kustos Dr. Otto Wettstein, II.

- Skorpione des Dodekanes. *Sitzungsberichte der Akademie der Wissenschaften in Wien*, Abt. I, 145(1–2): 16–17.
- WERNER, F. 1937. Beiträge zur Kenntnis der Tierwelt der Peloponnes, der Inseln Kythira und Euboea sowie der kleinen Inseln im Saronischen Golf. I. Reisebericht. IV. Skorpione. *Sitzungsberichte der Akademie der Wissenschaften in Wien. Mathematisch-naturwissenschaftliche Klasse. Abteilung I. Biologie, Mineralogie, Erdkunde*, 146: 135–143.
- WERNER, F. 1938. Ergebnisse der achten zoologischen Forschungsreise nach Griechenland (Euboea, Tinos, Skiathos usw). *Sitzungsberichte der Akademie der Wissenschaften in Wien. Mathematisch-naturwissenschaftliche Klasse. Abteilung I. Biologie, Mineralogie, Erdkunde*, 147 (5–10): 151–173.
- YAĞMUR, E. A., H. KOÇ & A. AKKAYA. 2009. New localities for *Iurus dufoureius asiaticus* Birula, 1903 (Scorpiones: Iuridae) in Turkey. *Turkish Journal of Arachnology*, 1(2), December 2008 (published February 2009): 154–159.

Appendix A

Detailed Locality Data for *Iurus*

The following table includes all data that could be obtained from literature (with references) as well as all known unpublished label data (with collection depository listed). Published locality information is augmented where possible by administrative division. Administrative division of Greece (Prefecture and District) and Turkey (Province and District) is given as currently accepted. Geographic coordinates are given in traditional (DMS) format and decimal format, the latter used for digital map construction. Coordinates, when not provided in original labels, were estimated to closest identifiable point via GoogleEarth™ and GoogleMaps™. Toponyms were located and verified using gazetteers at <http://www.fallingrain.com/world> and <http://www.gtp.gr>. Spelling (especially of Greek toponyms) varies in literature.

No.	Species and Locality	Reference	Traditional (DMS) (lat., long.)	Decimal (lat., long.)	Coordinates
	<i>Iurus dufouriensis</i> (Brullé, 1832): Greece: Peloponnese, Crete, Kythira, Gavdos.				
1	Peloponnese, Achaea Prefecture, Kalavryta District, Kato Zachlorou, Vouraikos River gorge, 700 m asl	Facheris, 2007a, 2007b	38°05'27"N, 22°09'1"E	38.0908, 22.1531	
2	Peloponnese, Arcadia Prefecture, Gortyna District, Kakoureika (the northernmost locality of <i>I. dufouriensis</i>)	Facheris, 2007a, 2007b	37°34'46"N, 21°55'14"E	37.5794, 21.9206	
3	Peloponnese, Arcadia Prefecture, Gortyna District, Karitaina, Kalamiou Monastery	Facheris, 2007a, 2007b	37°28'52"N, 22°02'25"E	37.4811, 22.0403	
4	Peloponnese, Arcadia Prefecture Gortyna District, Karitaina, Alfios River	Crucitti, 1998	37°29'N, 22°02'E	37.4833, 22.0333	
5	Peloponnese, Arcadia Prefecture, Megalopolis District, Likosoura, Kastriti	Crucitti, 1998; Soleglad et al., 2009	34°42'N, 22°01'E	37.4, 22.0167	
6	Peloponnese, Arcadia Prefecture, Megalopolis District, Ano Karyes	Crucitti, 1998 ("Ano Karies")	37°26'17"N, 22°00'11"E	37.4381, 22.0031	
7	Peloponnese, Ilia Prefecture, Minthi Oros Mts., Zacharo District, Kalidona, Kurtaina, 35 km SE of Pyrgos	Crucitti, 1995, 1998; Soleglad et al., 2009	37°28'05"N, 21°42'17.27"E (for Kalidona)	37.4681, 21.7047	
8	Peloponnese, Ilia Prefecture, Minthi Oros Mts., Zacharo District, Kalidona, Ambula	Crucitti, 1998	37°28'05"N, 21°42'17.27"E (for Kalidona)	37.4681, 21.7047	
9	Peloponnese: Laconia Prefecture, Mani Peninsula	Parmakelis et al., 2006	36°45'40"N, 22°28'10"E	36.761, 22.469	
10	Peloponnese, Laconia Prefecture, Mani Peninsula, Parnon Mtns.	MESC	37°06'21.6"N, 22°43'48"E	37.106, 22.73	

11	Peloponnese, Laconia Prefecture, Mani Peninsula, Oitylo District, Areopolis	Soleglad et al., 2009 (as “Merropolis”, in error);	36°40'N, 22°23'	36.6667, 22.3833
12	Peloponnese, Laconia Prefecture, Mani Peninsula, Oitylo District, Oitylo (Itylo)	Soleglad et al., 2009; B. Ganzenbein, pers. comm., 2002	36°42'24"N, 22°23'18"E	36.7067, 22.3883
13	Peloponnese, Laconia Prefecture, Mani Peninsula, Oitylo District, Stavri	G. Bergthalter, pers. comm., 2003	36°31'17"N, 22°22'22"E	36.5214, 22.3728
14	Peloponnese, Laconia Prefecture, Gythio District, Selinitsa, 20 m asl	Crucitti, 1995, 1998; Soleglad et al., 2009	36°49'N, 22°17'E	36.8167, 22.2833
15	Peloponnese, Laconia Prefecture, Gythio District, Krimi, 160 m asl	Crucitti, 1995, 1998; Soleglad et al., 2009	36°47'56.98"N, 22°28'10.42"E	36.799, 22.4695
16	Peloponnese, Laconia Prefecture, Gythio District, Tripi (Tripis), Magoulitsa River, 410 m asl	Crucitti, 1995, 1998	37°05'N, 22°21'E	37.083, 22.35
17	Peloponnese: Laconia Prefecture, Gythio District, Passavas	Kinzelbach, 1975, 1982	36°45'22"N, 22°32'15"E	36.7561, 22.5375
18	Peloponnese: Laconia Prefecture, East Mani District, Sangias Ms., Mina	Kritscher, 1993	36°33'N, 22°25'01"E	36.55, 22.4167
19	Peloponnese: Laconia Prefecture, Mystras District, Mystras	Kinzelbach, 1982; Kovarik, 1992; Fet, 2000; Soleglad et al., 2009	37°04'N, 22°23"E	37.0667, 22.3833
20	Peloponnese: Laconia Prefecture, Mystras District, Anavyrti, 743 m asl	Werner, 1902; Crucitti, 1998; Soleglad et al., 2009	37°02'N, 22°22"E	37.0333, 22.3667
21	Peloponnese, Laconia Prefecture, Mystras District, Kalivia Sohas	Crucitti, 1998; Soleglad et al., 2009	37°01'N, 22°25"E	37.0167, 22.4167
22	Peloponnese, Laconia Prefecture, Mystras District, Ladha	Werner, 1902	37°05'N, 22°13"E	37.0833, 22.2167
23	Peloponnese, Laconia Prefecture, Mystras District, Patori (Parorion), 264 m asl	Kučera, 1992	37°04'N, 22°23"E	37.0667, 22.3833
24	Peloponnese, Laconia Prefecture, Mystras District, Parori, Sátiras	Crucitti, 1998	37°04'N, 22°23"E	37.0667, 22.3833
25	Peloponnese, Laconia Prefecture, Mystras District, Nea Mystras	Kinzelbach, 1975, 1982	37°04'N, 22°22'32"E	37.0667, 22.3756
26	Peloponnese: Laconia Prefecture, Sparti District, Kastorio	Crucitti, 1998	37°10'12.62"N, 22°8'24.76"E	37.1703, 22.3069
27	Peloponnese: Laconia Prefecture, Sparti District, Kastrí	Crucitti, 1998	37°10'N, 22°19"E	37.1667, 22.3167
28	Peloponnese, Laconia Prefecture, Sparti District, Taygetos Mts, 12 km W of Sparti	Kinzelbach, 1975	37°05'N, 22°16"E	37.0833, 22.2667
29	Peloponnese, Messinia Prefecture, Messini District, Messini (=Messene) (type locality of <i>Iurus dufouriensis</i>)	Brullé, 1832	37°03'04"N, 22°00'29"E	37.051, 22.008
30	Peloponnese, Messinia Prefecture, Andania District, Diavolitsi, Ano Psari	Crucitti, 1998	37°17'N, 21°58"E	37.2833, 21.9667

31	Peloponnese, Messinia Prefecture, Artemisia District, ca. 7 km on the road to Kalamata	Kritscher, 1993; Facheris, 2007a, 2007b	37°03'N, 22°08'E	37.05, 22.1333
32	Peloponnese, Messinia Prefecture, Artemisia District, Nedontas River, between Artemisia and Kalamata, 13 km from Kalamata, 310 m asl. (neotype locality)	Crucitti, 1995, 1998; Soleglad et al., 2009	37°05'N, 22°09'E	37.0833, 22.15
33	Peloponnese, Messinia Prefecture, Avia District, Vorio, W slope of Taygetos Mts, 600 m asl	Facheris, 2007a, 2007b	36°57'30"N, 22°14'19"E	36.9583, 22.2386
34	Peloponnese, Messinia Prefecture, Lefktro District, Kalyves Pefko	Peslier, 2005; pers. comm., 2009	36°54'12.72"N, 22°14'44.57"E	36.9035, 22.2457
35	Peloponnese, Messinia Prefecture, Oichalia District, Katsaros, Crete, Iraklio (formerly Kandia)	Crucitti, 1998	37°12'23.55"N, 22°04'50.28"E	37.2067, 22.0806
36	Crete, Katharo Plateau	Lucas, 1853; Birula, 1903	35°20'N, 25°08'E	35.333, 25.133
37	Crete, Kournas Lake	Stathī & Mylonas, 2001	35°08'47.88"N, 25°33'50.36"E	35.1467, 25.5639
38	Crete, Kritsa	Stathī & Mylonas, 2001	35°19'34.94"N, 24°16'40.61"E	35.3264, 24.2781
39	Crete, Mariou	I. Stathī, pers. comm., 2001	35°09'26.79"N, 25°38'36.50"E	35.1575, 25.6436
40	Crete, Mt Lefka Ori, south slope, 1200 m asl	Stathī & Mylonas, 2001	35°12'N, 24°25"E	35.20, 24.4167
41	Crete, Megalokastron	Raulin, 1869	35°15'01.78"N, 24°06'42.51"E	35.2506, 24.1119
42	Crete, Melisoudaki	Parmakelis et al., 2006	35°19'30"N, 25°07'50"E	35.325, 25.1306
43	Crete, Neapolis	Penther, 1906	35°15'14"N, 25°36'35"E	35.2539, 25.6097
44	Crete, Messara Valley (south of the island)	Lucas, 1853; Birula, 1903	35°04'N, 24°48"E	35.0667, 24.8
45	Crete, Sfakia	Vaction, 1948	35°12'39"N, 26°06'27"E	35.2108, 26.1075
46	Crete: Vianos (formerly Viano)	Soleglad et al., 2009	35°02'52.46"N, 25°24'08.96"E	35.0478, 25.4025
47	Crete, Lasithi	Kinzelbach, 1975	35°04'N, 25°42"E	35.0667, 25.7
48	Crete, Potami (Potamia, unclear locality)	Kinzelbach, 1975		
49	Gavdos Island	Facheris, 2007a, 2007b	34°50'N, 24°04"E	34.8333, 24.083
50	Kythira Island	Werner, 1937, 1938; Vachon, 1953; Kinzelbach, 1975 (unconfirmed); Parmakelis et	36°10'N, 23°00"E	36.1667, 23.00

		al., 2006 (Agia Sofia cave)	
	<i>Inurus sp. (status undetermined): Greece (eastern Aegean islands: Fourni, Karpathos, Kasos, ?Kos, ?Leros, Samos, Saria, Rhodes)</i>		
1	Fourni Island, Votsos Panagias pothole	Stathī & Mylonas, 2001 Werner, 1936b, 1938; Menozzi, 1941; Vachon, 1953; Kinzelbach, 1966, 1975, 1982; Kritscher, 1993; Stathī & Mylonas, 2001; Parmakelis et al., 2006; Kaltas et al., 2008. MESC	37°35'0.19"N, 26°29'07.42"E see detailed localities
2	Karpathos Island, Apella Beach, 2 km from Myrtonas	Kinzelbach, 1982 Werner, 1936b; Kritscher, 1993	35°36'12"N, 27°09'34"E 35°30'N, 27°14"E
3	Karpathos Island, Avlona, 401 m asl	Kinzelbach, 1975, 1982; Kritscher, 1993	35°46'N, 27°12"E 35.5, 27.2333
4	Karpathos Island, Karpathos town (=Pigadia)	Kinzelbach, 1975, 1982	35°34'N, 27°08"E
5	Karpathos Island, Kiriaki Peninsula, SE of Pigadia	Kinzelbach, 1975, 1982 Kritscher, 1993	35°29'38"N, 27°13'33"E 35.4939, 27.2258
6	Karpathos Island, western Lastos Mts.	Kinzelbach, 1975, 1982	35.5667, 27.1333
7	Karpathos Island, Menetes, Profitis Ilias	Kritscher, 1993	35°29'28.29"N, 27°10'02.88"E
8	Karpathos Island, Mesochori to Piles	Stathī & Mylonas, 2001; Parmakelis et al., 2006	35°32'38.42"N, 27°07'43"E
9	Karpathos Island, Myrtonas (Mertonas)	Kinzelbach, 1975, 1982	35°34'49"N, 27°10'14"E
10	Karpathos Island, between Myrtonas and Spoa	Kinzelbach, 1982	35°38'N, 27°09"E
11	Karpathos Island, Olympbos (Olympos)	Menozzi, 1941	35°44'22.73"N, 27°02'25.27"E
12	Karpathos Island, Othos, 700 m	Kritscher, 1993	35°32'30.98"N, 27°09'10.9"E
13	Karpathos Island, Volada	Menozzi, 1941; Kinzelbach, 1975, 1982	35°33'40.32"N, 27°09'17.32"E
14	Saria Island (Karpathos Archipelago)	Kinzelbach, 1982	35°52'N, 27°13"E
15	Kasos Island, Stylokamara Cave	Fet, 2000	35°24'N, 26°55'01"E 35.40, 26.917

	Rhodes Island	Borelli, 1913; Caporiacco, 1928; Werner, 1936b, 1938; Menozzi, 1941; Vachon, 1953; Kinzelbach, 1975, 1982; Krihscher, 1993; Fet, 2000; Kovářík & Whitman, 2005; Parmakelis et al., 2006	see detailed localities
16	Rhodes Island, Agios Isidoros, 678 m asl	Borelli, 1913	36°10'N, 27°51'E
17	Rhodes Island, Archangelos	Fet, 2000	36°11'N, 28°07'E
18	Rhodes Island, Mt. Ataviros (Attairo)	Menozzi, 1941	36°12'N, 27°52'E
19	Rhodes Island, Mt. Filerimos (Fileremo, Eremofilo)	Caporiacco, 1928; Kovářík & Whitman, 2005	36°24'N, 28°08'E
20	Rhodes Island, Kritinia (formerly Kastelos)	Soleglad et al., 2009 ("Kastelo")	36°14'55.4"N, 27°49'51.42"E
21	Rhodes Island, Lindos (Lindosa), 400 m asl	Kinzelbach, 1982; Stathi & Mylonas, 2001	36°05'57.20"N, 28°04'43.86"E
22	Rhodes Island, Masari	Parmakelis et al., 2006	35°30'55"N, 27°08'50"E
23	Rhodes Island, Mt. Profitis Ilias	Werner, 1936b; Menozzi, 1941; Stathi & Mylonas, 2001	36°16'34.44"N, 27°56'30.88"E
24	Rhodes Island, Rhodes town	Kinzelbach, 1982; Kritscher, 1993 (Rhodes town; Rodini Park)	36°26'27"N, 28°13'21"E
	Samos Island	Werner, 1934, 1938; Vachon, 1953; Kinzelbach, 1975; Krihscher, 1993; Parmakelis et al., 2006; Francke & Prendini, 2008	see detailed localities
25	Samos Island, Agios Nikolaos, 3 km W of Karlovasi	Francke & Prendini, 2008; Soleglad et al., 2009	37°47'25"N, 26°42'16"E
26	Samos Island, Manolates, 649 m asl	Krihscher, 1993	37°47'04"N, 26°49'43"E
27	Samos Island, Marathokampos	Werner, 1934a	37°43'35"N, 26°41'24"E
	? Kos Island, Asfendioú	Kinzelbach, 1975 (unconfirmed); dubious record (Stathi & Mylonas, 2001)	36°51'03"N, 27°12'32"E
	? Leros Island	Kinzelbach, 1975	37°09'N, 26°51"E
			37.15, 26.85

		(unconfirmed); dubious record (Stathi & Mylonas, 2001)	
<i>Iurus asiaticus</i> Birula, 1903: Turkey (southeast)			
1	Adana Province: Gülek Pass (Gülek Boğazı, Cilician Gates), Taurus Mts (type locality of <i>I. asiaticus</i>).	Birula, 1898, 1903	37°19'40"N, 34°47'40"E
2	Adana Province: Karaşalı District, Kızıldağ Plateau, 1600 m asl area, 450 m asl	Karataş, 2001	37°25'03"N, 35°02'25"E
3	Adana Province: Kozan District, Eski Mantaş Village, Beşiktaş area, 450 m asl	Yağmur et al., 2009	37°30'43"N, 35°52'31"E
4	Adana Province: Pozantı District, E of Pozantı	Yağmur et al., 2009	37°26'02"N, 34°53'57"E
5	Adana Province: Pozantı District, Belemedik	Kovařík, 2002 ("Belemedek Mara")	37°20'N, 34°54"E
6	Adiyaman Province: Tut District, Kaşlıca Village, S slopes of Akdağ Mts, 1183 m asl (the easternmost locality of <i>I. asiaticus</i> and genus <i>Iurus</i>)	Yağmur et al., 2009	37°48'34.6"N, 37°59'21.9"E
7	Kahramanmaraş Province: Central District, Süleymanlı Village (the northernmost locality of <i>I. asiaticus</i> and genus <i>Iurus</i>)	NHMW	37°52'35"N, 36°50'02"E
8	Kahramanmaraş Province: Central District, 2 km W of Yaylaüstü Village fork in the road to Andırın, 1237 m asl	Yağmur et al., 2009	37°34'33"N, 36°35'06"E
9	Kahramanmaraş Province: Göksun District, Gökşun, 1500 m asl	Lacroix, pers comm., 1992	38°01'N, 36°30"E
10	Mersin Province: Çamlıhayla District, Çamlıhayla (= Namrun) Soleglad et al., 2009	Franccke, 1981 ("Namrum"); Soleglad et al., 2009	37°10'35"N, 34°36'22"E
11	Mersin Province: Çamlıhayla District, Çamlıhayla Plateau, 425 m asl	Yağmur et al., 2009	37°08'19"N, 34°50'25"E
12	Mersin Province: Tarsus District, Tarsus, "Hacı Hamfai" (possibly Hacı Hamzalı)	Vachon, 1966, 1971	37°04' N, 34°50'E
13	Mersin Province: Tarsus District, Taşobası Village, 256 m asl	Karataş, 2001	37°05'27"N, 34°55'48"E
14	Mersin Province: Tarsus District, 1 km from Taşobası Village, 209 m asl	MTAS	37°05'55"N, 34°55'40"E
15	Niğde Province: Ulukışla District, Madenköy Village, 1710 m asl	NHMW	37°26'59"N, 34°37'32"E
<i>Iurus kraepelini</i> von Ubisch, 1922: Turkey (south); Greece (Megisti)			
1	Antalya Province: Akseli District, 12 km S of Akseli	Soleglad et al., 2009	37°03'07"N, 31°47'03"E
			37.0486, 31.79

2	Antalya Province: Akseli District, Bademli Village	Crucitti & Malori, 1998	37°38'22"N, 31°42'02"E	37.3092, 31.7367
3	Antalya Province: Akseli District, Güzelso Village	Crucitti & Malori, 1998	36°53'47"N, 31°51'20"E	36.896, 31.855
4	Antalya Province: Akseli District, Yapuz Village, 1800 m asl	MBCH	37°07'45"N, 31°51'27"E	37.129, 31.857
5	Antalya Province: between Akseli District and Gündoğmuş District, 26 km from Gündoğmuş (near Alacabel Pass)	Crucitti & Malori, 1998	36°58'44"N, 31°44'04"E	36.9789, 31.7344
6	Antalya Province: Alanya District, Alanya	Karatash, 2001; Soleglad et al., 2009	36°33'N, 31°59E	36.55, 31.9833
7	Antalya Province: Alanya District, Alanya Castle	MTAS	36°31'59.8"N, 31°59'28.8"E	36.5333, 31.9913
8	Antalya Province: Alanya District, Avsallar	Karatash, 2001	36°38'13"N, 31°45'04"E	36.6369, 31.7511
9	Antalya Province: Alanya District, 2 km from Alanya - Taşatan Plateau fork in the road, 1167 m asl	MTAS	36°38.498"N, 32°04.089E	36.6417, 32.0681
10	Antalya Province: Alanya District, Taşatan Plateau, 1208 m asl	MTAS	36°40.244"N, 32°10.210E	36.6706, 32.1767
11	Antalya Province: Alanya District, 38 km NE from Demirtaş	NHMW	36°33'N, 32°27"E	36.55, 32.45
12	Antalya Province: Alanya District, Uzunöz Village	Parmakelis et al., 2006; Francke & Prendini, 2008;	36°32'25"N, 32°12'19"E	36.5403, 32.2053
13	Antalya Province: Antalya	Kinzelbach, 1975; Soleglad et al., 2009	36°54'N, 30°41'E	36.913, 30.69
14	Antalya Province: Central District, Çakırlar Village, 17 km SE of Antalya	Kritscher, 1993	36°52'14"N, 30°33'43"E	36.8706, 30.5619
15	Antalya Province: Central District, Büyük Çaltıçak Village , 14 m asl	Yağmur et al., 2009	36°47'06"N, 30°34'09"E	36.785, 30.5722
16	Antalya Province: Central District, Küçük Çaltıçak Village, 2 m asl	Yağmur et al., 2009	36°46'26"N, 30°34'14"E	36.7739, 30.5706
17	Antalya Province: Demre District, 2 nd km of the road from Demre to Kaş	Yağmur et al., 2009	36°15'48.8"N, 29°56'37.7"E	36.2636, 29.9438
18	Antalya Province: Elmalı District, Çiglikara Nature Reserve, 1680 m asl	Kinzelbach, 1975; Kovařík, 2002 ("Giglicara")	36°37'34"N, 30°00'40"E	36.6261, 30.0111
19	Antalya Province: Elmalı District, near Elmalı	Yağmur et al., 2009	36°24'58"N, 29°40'18"E	36.4161, 29.6717
20	Antalya Province: Finike District, Finike ("Finika") (type locality of <i>I. kraepelini</i>).	von Ubisch, 1922	36°18N, 30°09E	36.295, 30.141
21	Antalya Province: Finike District, Arifköy Village, 30 km from Finike	MBCH	36°30'23"N, 30°03'35"E	36.5064, 30.0597

22	Antalya Province: Finike District, Avlanbeli Geçidi (Pass), ca. 25 km N of Finike, 1200 m asl	Soleglad et al., 2009	36°32'15"N, 29°59'49"E	36.5375, 29.9969
23	Antalya Province: Gazipaşa District, Gazipaşa	Karataş, 2001	36°16'N, 32°19"E	36.2667, 32.3167
24	Antalya Province: Gündoğmuş District, Gündoğmuş	Crucitti, 1999	36°48'39"N, 32°00'11"E	36.8108, 32.0031
25	Antalya Province: Kale District, Gölbaşı ("Gölbaktiche", "Gjolbaschi") (ancient Trysa, near Davazlar Village)	Soleglad et al., 2009	36°16'18"N, 29°52'20"E	36.2717, 29.8722
26	Antalya Province: Kale District, 2 nd km on the road from Demre to Kas, 476 m asl	MTAS	36°15'48.8"N, 29°56'37.7"E	36.2636, 29.9438
27	Antalya Province: Kale District, Tersane Island, 113 m asl	Yağmur et al., 2009	36°38'10"N, 29°05'19"E	36.6361, 29.0886
28	Antalya Province: Kaş District, Çamlık, near Kemerkoy Village	Crucitti & Malori 1998	36°29'35"N, 29°42'09"E	36.4931, 29.7025
29	Antalya Province: Kaş District, S of Gömüci Village, 986 m asl	MTAS	36°24'01"N, 29°41'56"E	36.4003, 29.6989
30	Antalya Province: Kaş District, 2 nd km of the road from Kalkan to Patara, 242 m asl	Yağmur et al., 2009	36°17'1"N, 29°24'26"E	36.2836, 29.4072
31	Antalya Province: Kaş District, Kmkk (ancient Xanthos)	Soleglad et al., 2009	36°21'19"N, 29°19'05"E	36.3553, 29.3181
32	Antalya Province: Korkuteli District, Güllük Mts. ("Güllük-Dagh") (ancient Termessos on Mt. Solymos)	Soleglad et al., 2009	36°58'57"N, 30°27'53"E	36.9825, 30.4647
33	Antalya Province: Manavgat District, Oymapınar Village, 65 m asl	Yağmur et al., 2009	36°53'52"N, 31°31'53"E	36.8978, 31.5314
34	Antalya Province: Manavgat District, İrmasan Geçidi (Pass), 1300 m asl	Soleglad et al., 2009	37°01'46"N, 31°14'43"E	37.0297, 31.2456
35	Antalya Province: Serik District, Çatallar	Soleglad et al., 2009	36°29'23"N, 30°04'14"E	37.135, 30.879
36	Antalya Province: Serik District, Aspendos (Belkis) Ruins, 4 km N of Serik	Kinzelbach, 1975; Soleglad et al., 2009	36°56'28"N, 31°10'17"E	36.9411, 31.1714
37	Isparta Province: Eğirdir District, Pazarköy Village, SE of Eğirdir (now Eğirdir), 1200 m asl	Kinzelbach, 1975; Kovářík, 2002	37°46'35"N, 31°02'35"E	37.7764, 31.0431
38	Isparta Province: Sütcüler District, Sütcüler ("Sütgüler")	Francke & Prendini, 2008	37°29'19"N, 30°59'37"E	37.4886, 30.9936
39	Karaman Province: Emenek District, Adiller Village	Crucitti & Malori, 1998	36°40'40"N, 32°37'33"E	36.6778, 32.6258
40	Konya Province: Beyşehir District, Bademli Village	Soleglad et al., 2009	37°17'18"N, 32°0'050"E	37.2883, 32.1805
41	Konya Province: Beyşehir District, Sıvalılin Cave, Yeşildağ, 1147 m asl	Karataş, 2001	37°32'40"N, 31°28'28"E	37.5444, 31.4744
42	Mersin Province: Anamur District, Abanoz Plateau, ca. 45 km N of Anamur	Crucitti & Malori, 1998	36°17'53"N, 32°54'51"E	36.2981, 32.9142
43	Mersin Province: Anamur District, Anemurium ("Anemouryon")	Francke & Prendini, 2008	36°01'27"N, 32°48'09"E	36.078, 32.834

	ruins, 2 km SW of Anamur			
44	Mersin Province: Aydıncık District, Aydıncık	Soleglad et al., 2009	36°10'N, 33°21"E	36.167, 33.35
45	Mersin Province: Erdemli District, Doğu Village, 161 m asl (the easternmost locality of <i>I. kraepelini</i>).	MTAS	36°44'58.9"N, 34°25'27.5"E	36.7497, 34.4243
46	Mersin Province: Gülnar District, Akkuyu road	KaratAŞ, 2001	36°20'N, 33°24"E	36.3333, 33.4
47	Mersin Province: Gülnar District, Gülnar	Soleglad et al., 2009	36°20'18"N, 33°24'28"E	36.3383, 33.4078
48	Mersin Province: Gülnar District, Manavgat Mts	Crucitti & Malori 1998	36°30'1"N, 33°15'7"E	36.5003, 33.2519
49	Mersin Province: Mersin [locality unclear]	Kinzelbach, 1975		
50	Mersin Province: Mut District, Alahan Village	Crucitti & Malori 1998	36°47'4"N, 33°20'47"E	36.7844, 33.3464
51	Mersin Province: Silifke District, Cennet Cave (Korikos or Corycos Cave), near Silifke	Vachon, 1951; Kinzelbach, 1975; Kovarık, 2002; Francke & Prendini, 2008; Soleglad et al., 2009	36°27'08.2"N, 34°06'22.3"E	36.378, 33.934
52	Mersin Province: Silifke District, Değirmendere Village, 425 m asl	Yağmur et al., 2009	36°25'53"N, 33°45'21"E	36.4314, 33.7558
53	Mersin Province: Silifke District, Göksu Delta Valley), 10 km S of Silifke	Vachon, 1951; Kinzelbach, 1975; Soleglad et al., 2009	36°16'21"N, 33°57'44"E	36.2725, 33.9622
54	Mersin Province: Silifke District, 5 km NW of Silifke	NHMW	36°25'34"N, 33°54'09"E	36.4261, 33.9025
55	Mersin Province: Silifke District, near Silifke, 425 m asl	Yağmur et al., 2009	36°23'03"N, 33°54'21"E	36.3842, 33.9058
56	Mersin Province: Silifke District, Silifke Castle, 159 m asl	KaratAŞ, 2001	36°22'36"N, 33°54'55"E	36.3767, 33.9153
57	Mersin Province: Silifke District, Taşucu Village	Yağmur et al., 2009	36°18'43"N, 33°51'41"E	36.3119, 33.8614
58	Mersin Province: Silifke District, Uzuncaburç Village (ancient Diocesarea-Olba)	Soleglad et al., 2009	36°35'2"N, 33°55'35"E	36.5839, 33.9263
59	Mersin Province: Silifke District, Liman Kalesi, Ağalar Limanı, 8 km SW of Taşucu	MBCH	36°16'40"N, 33°50'10"E	36.2778, 33.8361
60	Muğla Province: Bodrum District, Bodrum (ancient Halicarnassus)	Kinzelbach, 1975	37°02'N, 27°26"E	37.033, 27.433
61	Muğla Province: Bodrum District, Sariot Island (across Turgutreis) (the westernmost locality of <i>I. kraepelini</i>)	MTAS	36°59'29"N, 27°13'26"E	36.9914, 27.2239
62	Muğla Province: Dalaman District, Tersane Island, 178 m	MTAS	36°40'04"N, 28°55'05"E	36.6678, 28.9118
63	Muğla Province: Dalaman District, 7 km E of Dalaman	Kinzelbach, 1982	36°49'07"N, 28°55'50"E	36.8186, 28.9306
64	Muğla Province: Dalyan District	Yağmur et al., 2009	36°51'14"N, 28°37'25"E	36.8539, 28.6236

65	Muğla Province: Dalyan District, Dalyan, 28 m asl	Soleglad et al., 2009	36°50'03"N, 28°38'33"E	36.834, 28.6425
66	Muğla Province: Dalyan District, Kaşlak Village	MTAS	36°50'N, 28°37"E	36.8333, 28.6167
67	Muğla Province: Fethiye District	MTAS	36°37N, 29°07E	36.6167, 28.1167
68	Muğla Province: Fethiye	Francke & Prendini, 2008; Soleglad et al., 2009	36°39'05"N, 29°07'23"E	36.651, 29.123
69	Muğla Province: Fethiye District, 5 km S of Fethiye, Babadağ Mts, 499 m asl	Yağmur et al., 2009	36°33'39"N, 29° 09'12"E	36.5608, 29.1533
70	Muğla Province: Fethiye District, Akdağ Mts, Eren Hill,	Yağmur et al., 2009	36°43'51"N, 29°38'24"E	36.7308, 29.64
71	Muğla Province: Fethiye District, 10 km S of Arpacık Village, 70 m asl	Yağmur et al., 2009	36°43'08"N, 29° 01'48"E	36.7189, 29.03
72	Muğla Province: Fethiye District, Dodurga ("Dorduga")	Kinzelbach, 1975	36°23'54"N, 29°12'19"E	36.3983, 29.2053
73	Muğla Province: Fethiye District, Domuz Island, 8 m asl	Yağmur et al., 2009	36°39'41"N, 28°53'59"E	36.6614, 28.8997
74	Muğla Province: Fethiye District, Gemiler Island, 40 m asl	MTAS	36°33'11"N, 29°04'10"E	36.553, 29.0694
75	Muğla Province: Fethiye District, Göcek, 38 m asl	MTAS	36°45'25"N, 28°56'40"E	36.7569, 28.9444
76	Muğla Province: Fethiye District, Göcek Island, opposite to Göcek	MTAS	36°43'35"N, 28°56'22"E	36.7264, 28.9394
77	Muğla Province: Fethiye District, Gökbelen Village	MTAS	36°53'37"N, 28°15'22"E	36.8936, 28.2561
78	Muğla Province: Fethiye District, Kıdırak Village, near Ölüdeniz, S of Fethiye	Soleglad et al., 2009	36°31'52"N, 29°07'41"E	36.5311, 29.128
79	Muğla Province: Fethiye District, Kelebekler Valley (Butterflies Valley)	MTAS	36°29'48"N, 29°07'44"E	36.4967, 29.1289
80	Muğla Province: Fethiye District, Ovacık Village, 6 km S of Fethiye (=Mekri)	Werner, 1936a; Kovářík, 2002; Francke & Prendini, 2008	36°34'49"N, 29°08'1"E	36.5803, 29.1336
81	Muğla Province: Fethiye District, Yeşilzümlü Village, 990 m asl	Yağmur et al., 2009	36°48'03"N, 29°11'10"E	36.8008, 29.1861
82	Muğla Province: Fethiye District, Zeytin Island, opposite to Göcek, 38 m asl	MTAS	36°41'53"N, 28°55'36"E	36.6981, 28.9267
83	Muğla Province: Köyceğiz District	MTAS	36°56N, 28°44'E	36.9333, 28.7333
84	Muğla Province: Köyceğiz District, Ekinçik Village, 52 m asl	MTAS	36°50'39"N, 28°33'10"E	36.8442, 28.5528
85	Muğla Province: Köyceğiz District, near Karagöl Lake	Yağmur et al., 2009	37°04'06"N, 28°48'50"E	37.0683, 28.8139
86	Muğla Province: Köyceğiz District, Kaunos Ruins	MTAS	36°49'34"N, 28°37'21"E	36.8261, 28.6225
87	Muğla Province: Köyceğiz District, Sultanije Spring	Soleglad et al., 2009	36°53'25"N, 28°35'12"E	36.8903, 28.5867

88	Muğla Province: Marmaris District, 25 km N of Marmaris	MTAS	37°13'N, 28°14'E	37.2167, 28.9181
89	Muğla Province: Marmaris District, Nimara Island, 327 m asl	MTAS	36°48'15"N, 28°17'15"E	36.8042, 28.2875
90	Muğla Province: Ortaca District, Gökkbel Village, 145 m asl	Yağmur et al., 2009	36°47'4"N, 28°40'39"E	36.7844, 28.6775
91	Muğla Province: Seki District, Çiçekbaba Mts, 911 m asl	Yağmur et al., 2009	37°01'88"N, 28°45'73"E	37.0333, 28.7663
92	Muğla Province: Seki District, Çiçekbaba Mts, near Kartal Lake, 1763 m asl	Yağmur et al., 2009	37°03'66"N, 28°48'50"E	37.0664, 28.8139
93	Muğla Province: Seki District, Çiçekbaba Mts, near Kartal Lake, 1763 m asl	Yağmur et al., 2009	37°02'54"N, 28°46'37"E	37.0483, 28.7769
94	Muğla Province: Seki District, Göögübelen Pass, 1830 m asl	Yağmur et al., 2009	36°50'44"N, 29°44'76"E	36.8456, 29.7497
95	Muğla Province: Seki District, near Göögübelen Pass, 1794 m asl	Yağmur et al., 2009	36°50'54"N, 29°44'40"E	36.8483, 29.7444
96	Muğla Province: Seki District, near Göögübelen Pass, 1807 m asl	Yağmur et al., 2009	36°50'32"N, 29°45'16"E	36.8422, 29.7544
97	Muğla Province: Yatağan District, Bencik Mts, near fire watchtower, 1395 m asl	Yağmur et al., 2009	37°14'68"N, 28°01'29"E	37.2497, 28.0247
98	Muğla Province: Yatağan District, Bencik Mts, near fire watchtower, 1395 m asl	Yağmur et al., 2009	37°14'14"N, 28°03'28"E	37.2372, 28.0578
99	Greece: Megisti (Kastelorizo) Island: Palaiokastro	Fet & Braunwalder, 2000; Stathi & Mylonas, 2001; Parnakelis et al., 2006.	36°08'20"N, 29°34'50"E	36.1389, 29.5806
	<i>I. kalleci</i> sp. nov.: Turkey (south: Antalya Province)			
1	Antalya Province: Akseli District, 12 km S of Akseki (type locality of <i>I. kalleci</i>).	Soleglad et al., 2009 (as <i>I. dufourieius asiaticus</i>) MTAS	37°03'07"N, 31°24'03"E	37.0486, 31.79
2	Antalya Province: Alanya District, Dim Cave, 11 km E of Alanya, at 25 m depth, cave entrance 221 m asl		36°32'21"N, 32°06'33"E	36.5392, 32.1092
3	Mersin Province: Gülnar District, Gülnar	FKCP	36°20'N, 33°24'E	36.3333, 33.4
	<i>I. kinzelbachi</i> sp. nov.: Turkey (west: İzmir and Aydın Provinces)			
1	İzmir Province: Bornova District, Naldöken, formerly Narlıköy ("Narlı Kioi", "Marli Kioi"), population now extinct	Kinzelbach, 1975; Soleglad et al., 2009 (as <i>I. dufourieius asiaticus</i>)	38°27'31"N, 27°16'30"E	38.4586, 27.275
2	Aydın Province: Söke District, Dilek Peninsula National Park, Canyon (type locality of <i>I. kinzelbachi</i>).	Koç & Yağmur, 2007; Yağmur et al., 2009 (as <i>I. dufourieius asiaticus</i>)	37°41'37"N, 27°09'37"E	37.6936, 27.1603

3	Aydin Province: Söke District, Davutlar, 800 m asl	Francke & Prendini, 2008 (as <i>I. difforensis asiaticus</i>)	37°43'33"N, 27°18'15"E	37.7258, 27.3014
<i>Unclear or Erroneous Localities:</i>				
	Turkey: Gazane (BMNH)	Kinzelbach, 1975		
	Turkey: Gökcce-Kisik (=“Göktzsche-Kissik”, =“Koktsche-Kissik”) [SW of Eskisehir], Eskisehir Province, possibly mislabeled or introduction; specimen not found	Werner, 1902; Birula, 1903		
	Turkey: “Antakya, Adana, south Mersin” (FKCP, not a single locality)	Soleglad et al., 2009		
	Turkey: Antakya [in error, refers to Antalya]	Soleglad et al., 2009		
	Turkey: Şile (near Istanbul): possibly mislabeled or introduction	Kinzelbach, 1975		
	Lebanon: Beirut: possibly mislabeled or introduction	Kinzelbach, 1975		
	Egypt: possibly mislabeled or introduction	Thorell, 1877; Kraepelin, 1894, 1899		
	Cyprus (a large series in ZMHB; possibly mislabeled, most likely Crete)	Kamenz & Prendini, 2008		

Table A1: Locality data for *Iurus*.

Appendix B

Neobothriotaxy in *Iurus*

Neobothriotaxy in *Iurus* was reported for the first time by Soleglad, Kovařík & Fet (2009). In their study, 77 occurrences of neobothriotaxy were reported, segregated into nine separate “types”, spanning 101 specimens, and thoroughly described. Since Soleglad, Kovařík & Fet’s (2009) study, 341 specimens of *Iurus* have been examined for our current study, and additional cases of neobothriotaxy and new “types” were discovered.

Neobothriotoxic Types

Since Soleglad, Kovařík & Fet’s (2009) study, four new neobothriotoxic types were detected in our current analysis. Figure B1 illustrates all 13 types, occurring on the chela and the patella.

In three types (types 1–3), accessory trichobothria occur on the *internal* surface of the chelal palm, all in the vicinity of trichobothrium *ib*. Two of these accessory trichobothria are petite in size. One type (type 4) is found on the *ventral* surface of the chelal palm. This accessory trichobothrium is petite in size. Five types of neobothriotaxy (types 5–9) have been identified on the *external* surface of the chelal palm, three of which (types 6, 7, 9) are new. Except for type 5, all neobothriotaxy types found on the external surface are comprised of a solitary petite accessory trichobothrium. Type 5, in almost all cases, has full size accessory trichobothria, numbering from one to two.

The external surface of the patella exhibits four types of neobothriotaxy (types 10–13), one of which (type 10) is new. Types 10 and 11 are found in the *et* series, both represented by a single, petite trichobothrium. Type 12 is comprised of full size trichobothria, numbering from one to two, occurring close to the *em* series. Type 13 is represented by a single, petite trichobothrium, occurring in the *esb* series.

Number of Neobothriotoxic Instances

Table B1 presents detailed statistics of all neobothriotoxic occurrences in *Iurus*, grouped by the species in which they occur, and the general geographic distribution of these species.

247 occurrences of neobothriotaxy have been detected in *Iurus*. Generally, these occurrences involved a solitary accessory trichobothrium, though in some cases two accessory trichobothria are included within a

type. Statistically, accessory trichobothria are somewhat rare on the patella, with only 19 occurrences, accounting for 7.7 %. Of these accessory trichobothria, type 12 is found in more than half of all cases (10 occurrences). The chela accounts for a large majority of neobothriotoxic occurrences, 92.3 %. Of these, three types are most common: type 5, 100 occurrences (40.5 %), type 1, 78 occurrences (31.6 %), and type 8, 24 occurrences (9.7 %).

Distribution of Neobothriotaxy within *Iurus*

Figure B2 shows the geographical distribution of the 13 neobothriotoxic types in *Iurus*, involving the Greek Peloponnese and six provinces in Turkey.

Neobothriotaxy is quite rare in Greece, only three instances were detected in the 34 specimens of *I. dufouri* examined, representing three exclusive types (2, 6, 13), one specimen per each type, and only one chela, clearly minimal representation. The remaining ten types were detected in specimens from Turkey. Of particular interest are four types found exclusively in species *I. kinzelbachi* (types 8–11), which are considered diagnostic for this species. These types are distributed in extreme western Anatolia in İzmir and Aydın Provinces, isolated from the other types (Fig. B2). The Anatolian species *I. kraepelini*, which occupies the largest geographic range, has six neobothriotoxic types: 1, 3–5, 7, and 12. These types are found across the entire species’ range, in Muğla, Antalya, Konya, and Mersin Provinces; Antalya has all six types. In the third Anatolian species, *I. asiaticus*, neobothriotaxy (type 7) was detected only in a single specimen, (one chela), in extreme eastern Mersin, the most western edge of its distribution. Neothriotaxy was not found in *I. kадлеки*, where only five specimens are known.

It is worth mentioning that type 7, found in one specimen of *I. asiaticus*, was also found in *I. kraepelini* across most of its range. This is the only known case when two *Iurus* species share a certain type of neobothriotaxy.

The most common neobothriotoxic type in *I. kraepelini*, is type 5, occurring in all four provinces. This type also occurs in the “Taurus” population (actual locality unknown). This is an interesting type, accessory trichobothria are in general full size, and in many cases can occur in pairs. The second most prevalent type, type 1, is clustered in north-central Antalya and adjacent

	Turkey							Greece (34)
	İzmir (7)	Aydın (23)	Muğla (44)	Antalya (88)	Konya (4)	"Taurus" (8)	Mersin (15)	
Type 1: Chela Internal, ia Total = 78 (31.6 %)			8 (9 %)	55 (33 %)	8 (100 %)	7 (62.5 %)		
Type 2: Chela Internal, ia Total = 1 (0.04 %)				1 (4.5 %)				
Type 3: Chela Internal, ia Total = 1 (0.04 %)								1 (2.9 %)
Type 4: Chela Ventral, va Total = 1 (0.04 %)				1 (4.5 %)				
Type 5: Chela External, Et Total = 100 (40.5 %)			8 (9 %)	73 (42 %)	8 (100 %)	11 (75 %)		
Type 6: Chela External, Et Total = 1 (0.04 %)								1 (2.9 %)
Type 7: Chela External, Est Total = 7 (2.8 %)			2 (4.5 %)	4 (2.3 %)			1 (6.7 %)	
Type 8: Chela External, Est Total = 24 (9.7 %)	14 (100%)	10 (35 %)						
Type 9: Chela External, Eb Total = 15 (6.1 %)	3 (43 %)	12 (48 %)						
Type 10: Patella External, et Total = 2 (0.8 %)		2 (9 %)						
Type 11: Patella External, et Total = 6 (2.4 %)	4 (57 %)	2 (9 %)						
Type 12: Patella External, em Total = 10 (4.0 %)			2 (4.5 %)	7 (4.5 %)			1 (6.7 %)	
Type 13: Patella External, esb Total = 1 (0.04 %)								1 (2.9 %)
TOTAL = 247	21	26	20	141	16	18	2	3

Table B1: Neobothriotaxic occurrences in genus *Iurus* based on the examination of 343 specimens. Distribution in Turkey is broken down into provinces and in Greece all occurrences are found in the Peloponnese. For eight specimens, localities were simply stated as "Taurus" (GREY). We suspect this probably refers to Antalya or Konya Provinces, which also exhibit these two types of neobothriotaxy. 247 occurrences of neobothriotaxy have been detected (an occurrence represents a single pedipalp). Types 8–11 (BLUE) are found exclusively in *I. kinzelbachi*. Only three occurrences of neobothriotaxy were detected in *I. dufourei* (RED). The large majority of neobothriotaxic occurrences was found in *I. kraepelini* (GREEN). Only one occurrence was detected in *I. asiaticus* (WHITE) in Mersin Province. Percentages accompanying type totals are percentages of occurrences. Percentages accompanying occurrences counts are percentages of specimens exhibiting this type. Numbers accompanying province names are number of specimens examined in that province. See Fig. B1 for illustrations of these 13 types of neobothriotaxy and the map in Fig. B2 for their distribution.

Konya, sometimes found along with type 5 in the same population. Based on this distribution, type 1 could be possibly diagnostic for a local clade within *I. kraepelini*.

However, further investigation of additional material and the identification of new characters will be necessary before this can be determined.

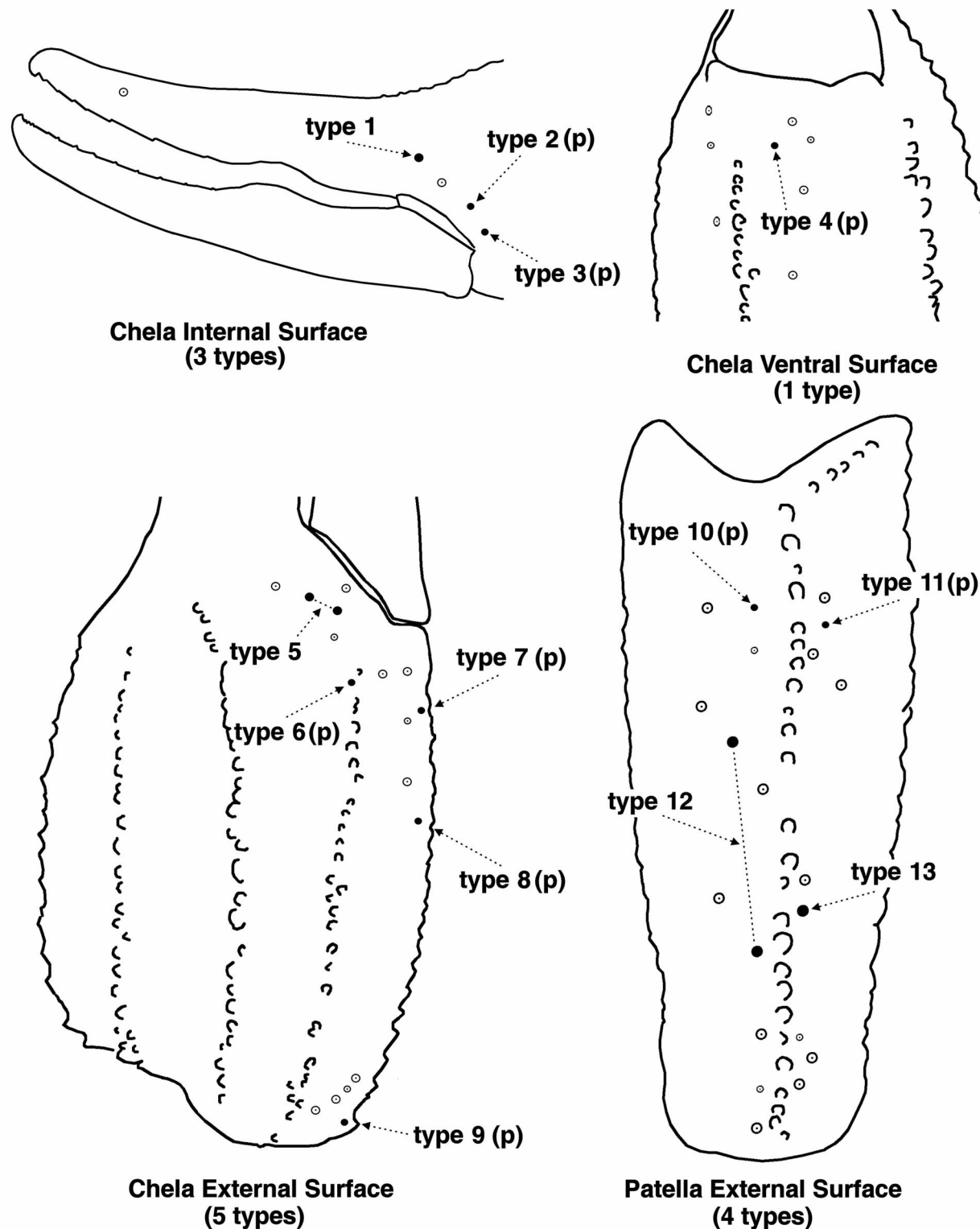


Figure B1: Diagrammatic trichobothria pattern (partial) of *Iurus* showing 13 types of neobothriotaxy. Also see map in Figure B2 that plots locations of specimens examined that exhibit these 13 accessory trichobothria types. Accessory trichobothria indicated by closed circles. (p) = petite.

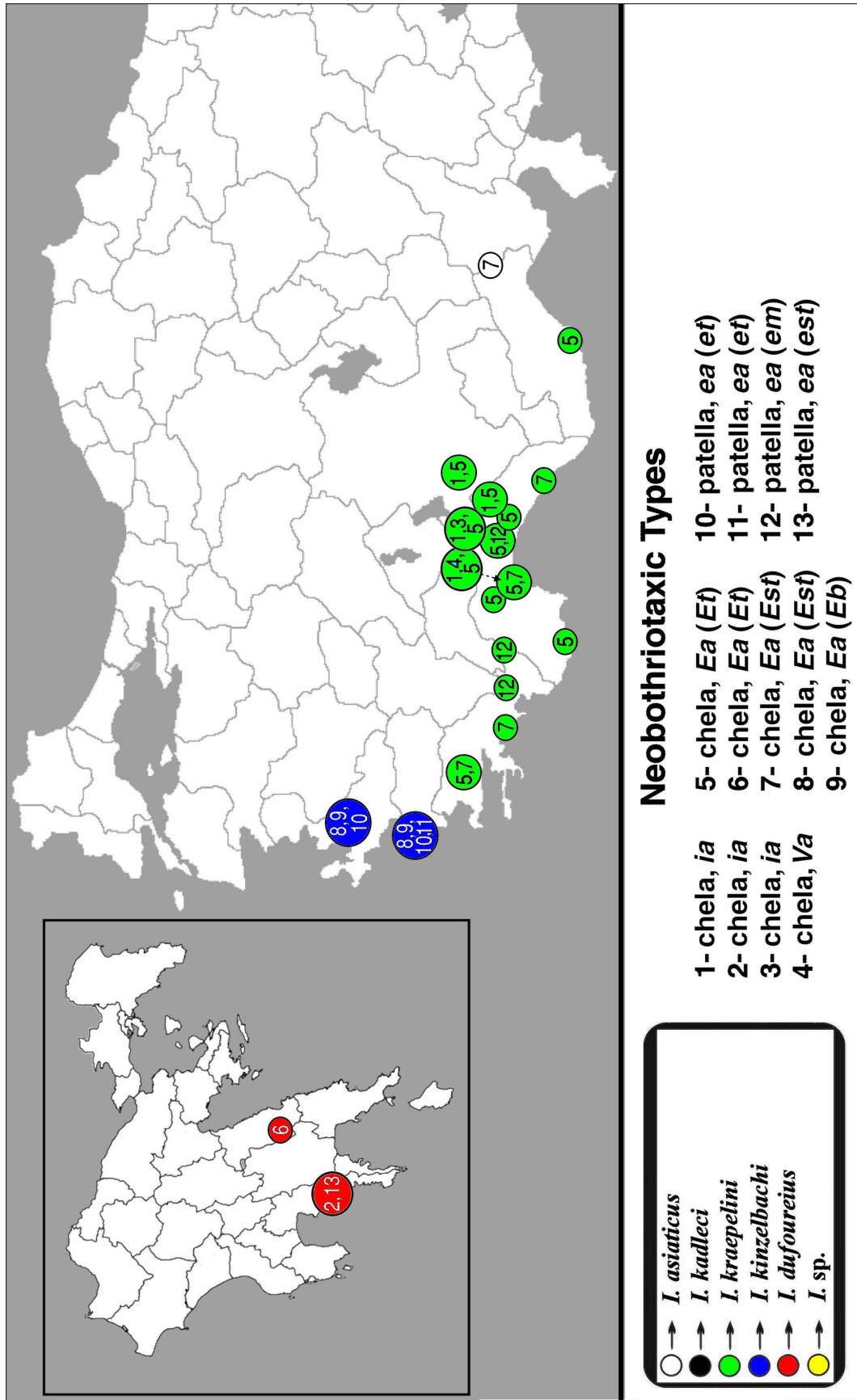


Figure B2: Map showing instances of neobothriotaxy in genus *Iurus*. Thirteen types of neobothriotaxy are identified (see Fig. B1 for illustrations of these types). Neobothriotaxy is found in four of the five *Iurus* species currently recognized in this paper (i.e., except for *I. kadleci* (BLACK)).

Appendix C

Morphometric Tendencies in *Iurus*

Based on 31 sets of measurements taken from the five species of *Iurus*, we conducted an extensive morphometric ratio analysis to determine tendencies in the relative segment proportions of these species. This involved a total of 762 measurements. We digitized 26 specific measurements (out of a total 33) of each specimen and computed all possible combinations of morphometric ratios, a total of 325 for each paired comparison (i.e., each species and each gender, a total of 20 comparison sets). Based on this analysis, we established a large subset (19 measurements) of the original measurement set, which included potentially diagnostic characters for one or more species. Full measurement sets of each species are presented in the body of this paper in Tables 4–7 and 10. The map (Figure C1) shows the distribution of *Iurus* species involved in this analysis. In all cases, with the exception of the subadult *I. kadlecii* female from the Dim Cave (Antalya, Turkey), all specimens used in this analysis were adult.

Each of the 19 measurements (listed in Tables C1, C2) were evaluated as to their dominance in a ratio comparison (i.e., a ratio involves two morphometrics). This evaluation was conducted for each species pair, male and female. Tables C1 and C2 present the results of this evaluation. The individual values depicted for each species for a specific morphometric states the number of ratio comparisons that the morphometric dominated in a species-by-species comparison, thus four sets of numbers. For example (Tab. C1), in *I. kraepelini* male the chelal depth dominated in *all* ratio comparisons. This means that no matter which other morphometric the chelal depth was combined with to form a ratio, its resulting ratio value was always the largest if the chelal depth was the numerator or the smallest if it was the denominator of the ratio. This implies unequivocally that the chelal depth in this species is significantly greater than in the other four species. We will discuss this further in the species discussions below. As a side note it must be stated that if a morphometric dominance value is small it implies that the measurement affected the ratio value in an opposite fashion, implying that the measurement is relatively small. This is equally important when considering potential diagnostic characters (see Fet & Soleglad (2002: 4–5) for further information on this technique).

In Tables C1 and C2, morphometrics that are considered useful diagnostically are shaded grey if they show high dominance values and yellow if they reflect low dominance values. Only the particular morphometrics (19 in all) used in the histograms in Figs. C2–C7 are shaded; therefore, not all high or low dominant

morphometrics are considered in this analysis. Each species will now be discussed as follows: first, we will provide an overview of the data in Tables C1 and C2 highlighting morphometric trends seen in the species as to its chela, metasoma, and telson. Second, specific ratios using high and low dominant measurement pairs will be discussed, as presented in Figs. C2–C7, illustrating their value as diagnostic characters. In some cases the ratio will separate the species from all other *Iurus* species, in other cases, it will contrast it with only one or two species. It is important to stress here, however, in general the 19 morphometrics presented in Tables C1 and C2 reflect the same dominance values in both genders across the five species, therefore providing excellence diagnostic potential. In the end, we present a key using only these ratios to separate the five species of *Iurus* based on adult material, male and female.

I. dufoureius. For the chela, the dominance values were somewhat low in *I. dufoureius*, only the chelal width, a value of 11.5, was above ten. This result can be seen also in the histogram in Fig. C2 where the chelal width is compared to the chelal length, exhibiting the second highest ratio value (though considerably less than *I. kraepelini*). The metasoma is quite interesting in *I. dufoureius*. Both its length and width exhibit somewhat high dominance values. Of course, this does not predict much about the stoutness or slenderness of the metasoma since both metrics dominated. The same is reflected in Figs. C4–C5 where the metasoma of *I. dufoureius* essentially clustered with three other species, all noticeably disjoint from the relatively slender *I. kadlecii*. *I. dufoureius* does, however, have the stoutest telson of the five species. This is reflected in Fig. C6 where the telson width and depth is compared to the telson length. Data in Tables C1 and C2 also indicate this result, the telson length with low to medium values and the telson width and depth with high values. As seen in the histogram in Fig. C6, *I. dufoureius*, though the species with the lowest ratio value, does cluster somewhat with *I. kraepelini* and *I. asiaticus*, species *I. kinzelbachi* and *I. kadlecii* showing considerable separation. From a diagnostic perspective, we would only use these two telson ratios to separate *I. dufoureius* from the latter two species.

I. kraepelini. The chelal width and depth provide outstanding diagnostic characters for this species, especially the latter. As discussed in detail elsewhere, the adult male in this species exhibits a highly vaulted chelal palm further exaggerating its overall depth. In Tables C1 and C2 ratio values for the depth and width

Male	<i>I. dufourii</i>	<i>I. kraepelini</i>	<i>I. kinzelbachi</i>	<i>I. kladeci</i>	<i>I. asiaticus</i>
CheIa_W	• 1 12 23 10 [11.5]	24 • 24 24 24 [24.0]	13 1 • 23 16 [13.25]	2 1 2 • 2 [1.75]	15 1 9 23 • [12.0]
CheIa_D	• 0 6 22 6 [8.5]	25 • 25 25 25 [25.0]	19 0 • 25 17 [15.25]	3 0 0 • 0 [0.75]	19 0 8 25 • [13.0]
CheIa_L	• 10 3 10 3 [6.5]	15 • 2 10 1 [7.0]	21 23 • 15 7 [16.5]	15 15 9 • 7 [11.5]	22 24 18 18 • [20.5]
Palm_L	• 3 2 16 2 [5.75]	22 • 6 23 5 [14.0]	23 19 • 24 12 [19.50]	9 2 1 • 1 [3.25]	23 20 13 24 • [20.0]
MF_L	• 2 0 6 5 [3.25]	23 • 9 15 17 [16.0]	25 16 • 20 23 [21.0]	19 10 4 • 15 [12.0]	20 7 2 10 • [9.75]
FF_L	• 8 1 4 9 [5.5]	16 • 0 8 8 [8.0]	24 25 • 14 25 [22.00]	21 17 10 • 17 [16.25]	16 17 0 8 • [10.25]
MS_I_L	• 20 15 2 11 [12.0]	5 • 7 0 4 [4.0]	10 18 • 1 4 [8.25]	23 25 24 • 22 [23.5]	14 21 21 3 • [14.75]
MS_II_L	• 24 22 8 21 [18.75]	1 • 11 2 7 [5.25]	3 14 • 2 14 [8.25]	16 23 23 • 20 [20.5]	4 18 11 5 • [9.5]
MS_III_L	• 23 16 3 23 [16.25]	2 • 1 1 10 [3.5]	9 24 • 3 21 [14.25]	22 24 22 • 24 [23.0]	2 15 4 1 • [5.5]
MS_IV_L	• 25 19 12 24 [20.0]	0 • 5 3 9 [4.25]	6 20 • 4 20 [12.50]	13 22 21 • 20 [19.0]	1 16 5 5 • [6.75]
MS_V_L	• 14 11 8 18 [12.75]	11 • 12 7 21 [12.75]	14 13 • 7 24 [14.5]	17 18 18 • 18 [17.75]	7 4 1 7 • [4.75]
MS_I_W	• 18 14 24 17 [18.25]	7 • 13 21 16 [14.25]	11 12 • 22 18 [15.75]	1 4 3 • 7 [3.75]	8 9 7 18 • [10.5]
MS_II_W	• 19 20 20 14 [18.25]	6 • 16 17 11 [12.5]	5 9 • 18 10 [10.5]	5 8 7 • 8 [7.0]	9 14 15 17 • [13.75]
MS_III_W	• 17 17 18 13 [16.25]	8 • 17 13 14 [13.0]	8 8 • 10 12 [9.5]	7 12 15 • 13 [11.75]	9 10 13 12 • [11.0]
MS_IV_W	• 16 23 21 19 [19.75]	7 • 19 18 17 [15.25]	2 6 • 14 6 [7.0]	4 7 10 • 10 [7.75]	6 7 19 15 • [11.75]
MS_V_W	• 22 25 25 25 [24.25]	3 • 18 22 13 [14.0]	0 7 • 20 2 [7.25]	0 3 5 • 4 [3.0]	0 11 23 21 • [13.75]
Tel_L	• 11 9 1 13 [11.0]	14 • 15 5 21 [13.75]	16 10 • 5 22 [13.25]	24 20 20 • 23 [21.75]	12 4 3 2 • [5.25]
Tel_W	• 13 24 19 22 [19.5]	12 • 23 20 23 [19.5]	1 2 • 10 10 [5.75]	6 5 14 • 13 [9.5]	3 2 15 12 • [8.0]
Tel_D	• 15 21 17 14 [16.75]	10 • 22 14 19 [16.25]	4 3 • 8 8 [5.75]	8 11 16 • 16 [12.75]	9 6 17 9 • [10.25]

Table C1: Summary of major measurements of males that show dominance in morphometric ratios across the five species of *Iurus* where all possible ratios are calculated. Each species is compared to the other four species, thus four sets of data per species. Each value states the number of ratios the measurement dominated for that species when compared to the other species. Highlighted entries indicate morphometrics used in constructing ratios, grey for high dominant and yellow for low dominant values.

Female	<i>I. dufouriius</i>	<i>I. kraepelini</i>	<i>I. kinzelbachi</i>	<i>I. kadleci</i>	<i>I. asiaticus</i>
Chela_W	• 2 15 20 9 [11.5]	23 • 21 23 17 [21.0]	9 4 • 22 5 [10.0]	5 2 3 • 2 [3.0]	16 8 19 23 • [16.5]
Chela_D	• 1 7 16 5 [7.25]	24 • 25 23 24.25]	18 0 • 21 7 [11.5]	9 0 4 • 3 [4.0]	20 2 17 22 • [15.25]
Chela_L	• 17 5 12 6 [10.0]	8 • 4 12 4 [7.0]	20 21 • 14 16 [17.75]	13 18 10 • 13 [13.5]	19 21 9 12 • [15.25]
Palm_L	• 9 2 18 0 [7.25]	16 • 3 17 0 [9.0]	23 22 • 25 5 [18.75]	6 8 0 • 0 [3.5]	25 25 19 25 • [23.5]
MF_L	• 11 3 10 6 [7.5]	14 • 3 10 7 [8.5]	22 22 • 15 21 [20.0]	15 14 10 • 16 [13.75]	19 18 7 9 • [13.25]
FF_L	• 19 0 8 10 [9.25]	6 • 0 5 5 [4.0]	25 25 • 18 25 [23.25]	17 20 7 • 17 [15.25]	15 20 0 8 • [10.75]
MS_I_L	• 21 18 1 14 [13.5]	4 • 11 0 6 [5.25]	7 14 • 0 4 [6.25]	24 25 21 • 23 [23.25]	10 19 21 2 • [13.0]
MS_H_L	• 23 20 3 24 [17.5]	2 • 9 1 11 [5.75]	4 15 • 1 18 [9.5]	22 24 24 • 25 [23.75]	1 14 7 0 • [5.5]
MS_III_L	• 25 20 4 21 [17.5]	0 • 6 2 8 [4.0]	4 19 • 2 14 [9.75]	21 23 23 • 24 [22.75]	3 17 11 1 • [8.0]
MS_IV_L	• 24 19 7 23 [18.25]	1 • 7 3 10 [5.25]	6 18 • 4 19 [11.75]	18 21 21 • 20 [20.0]	2 15 6 5 • [7.0]
MS_V_L	• 10 9 6 20 [11.25]	15 • 9 7 23 [13.5]	16 15 • 7 24 [15.5]	19 18 18 • 19 [18.5]	5 2 1 6 • [3.5]
MS_I_W	• 5 11 21 14 [12.75]	20 • 18 22 20 [20.0]	14 7 • 23 15 [14.75]	3 3 2 • 4 [3.0]	10 5 8 21 • [11.0]
MS_H_W	• 7 11 24 11 [13.25]	18 • 16 24 15 [18.25]	13 9 • 24 13 [14.75]	1 1 1 • 1 1 [1.0]	14 10 12 24 • [15.0]
MS_III_W	• 8 15 18 13 [13.5]	15 • 18 18 16 [16.75]	9 7 • 19 10 [11.25]	6 7 6 • 7 [6.5]	12 9 15 18 • [13.5]
MS_IV_W	• 3 17 17 12 [12.25]	22 • 22 19 19 [20.5]	8 3 • 15 6 [8.0]	8 6 10 • 8 [8.0]	13 6 18 17 • [13.5]
MS_V_W	• 12 24 23 18 [19.25]	13 • 23 20 18 [18.5]	1 2 • 11 1 [3.75]	2 5 13 • 6 [6.5]	7 7 24 19 • [14.25]
Tel_L	• 4 8 2 16 [7.5]	21 • 15 6 22 [16.0]	17 10 • 4 21 [10.5]	23 19 21 • 20 [20.75]	12 3 4 4 • [5.75]
Tel_W	• 18 25 25 25 [23.25]	7 • 24 21 25 [19.25]	0 1 • 18 10 [4.75]	0 4 6 • 9 [4.75]	0 0 15 15 • [7.5]
Tel_D	• 22 23 21 21 [21.75]	3 • 16 15 13 [11.75]	2 9 • 10 9 [7.5]	3 10 15 • 11 [9.75]	4 12 16 14 • [11.5]

Table C2: Summary of major measurements of females that show dominance in morphometric ratios across the five species of *Iurus* where all possible ratios are calculated. Each species is compared to the other four species, thus four sets of data per species. Each value states the number of ratios the measurement dominated for that species when compared to the other species. Highlighted entries indicate morphometrics used in constructing ratios, grey for high dominant and yellow for low dominant values.

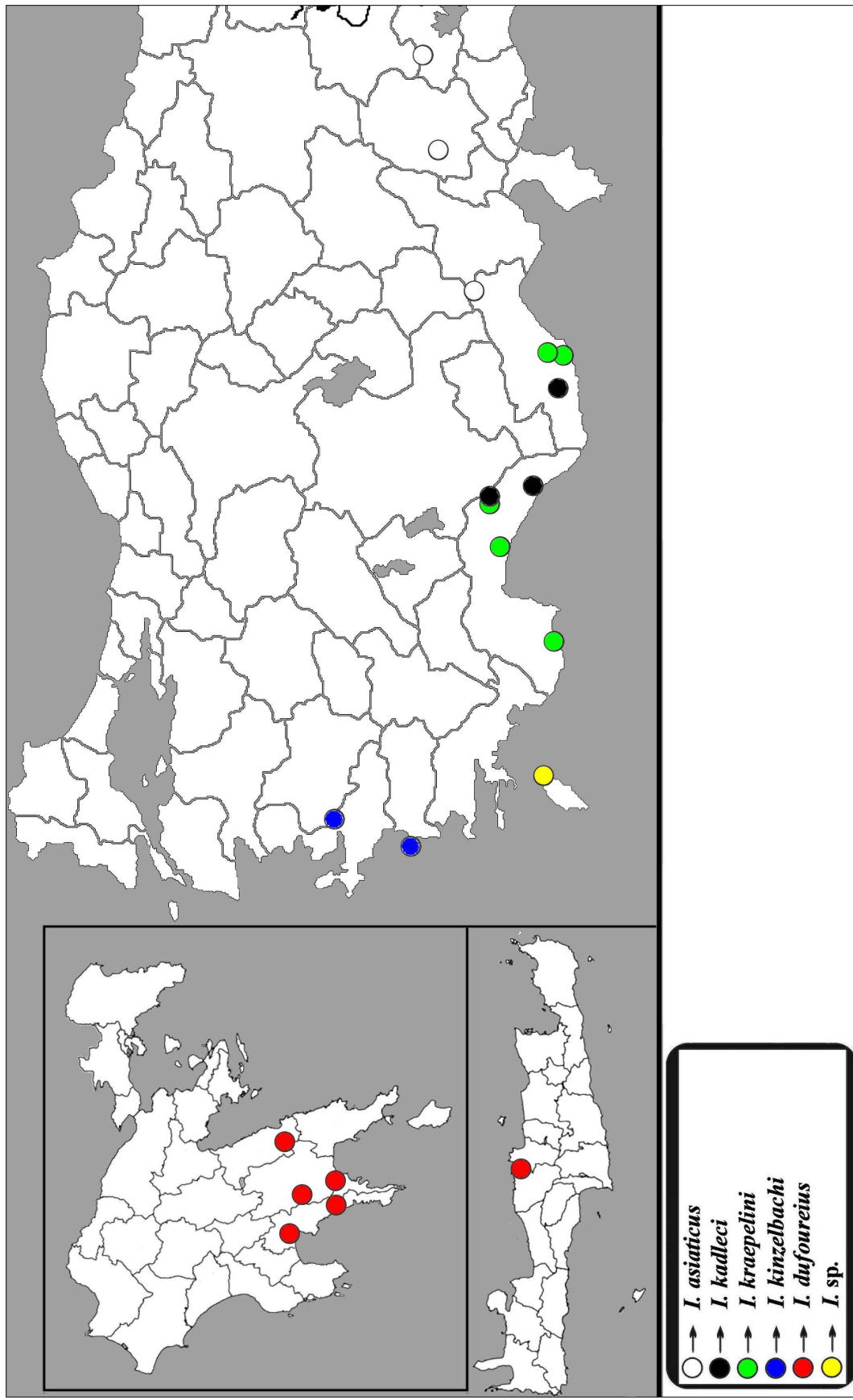


Figure C1: Localities of *Iurus* specimens measured.

are quite high, 21 or higher. These high values are accompanied by the somewhat low chelal length reflected both in the male and female. These three morphometrics form two ratios as shown in Fig. C2, chelal width and chelal depth compared to the chelal length. As seen from these histograms, *I. kraepelini* shows significant separation from the other four species with respect to the chelal depth. The metasoma of *I. kraepelini* is the stockiest in the genus, especially for segments I–IV. This is predictable by analyzing the data in Tables C1 and C2. The individual metasomal segment lengths show low dominant values whereas the segment widths all exceed 12.5. Figures C3–C4 also indicate the stocky metasoma in *I. kraepelini* for segments I–IV. The telson in *I. kraepelini* is somewhat stocky but less than that in *I. dufoureius*. Its vesicle width and depth ratios values approach that of *I. dufoureius*, but the telson is relatively longer thus decreasing its stockiness.

***I. kinzelbachi*.** The chela in *I. kinzelbachi* is somewhat elongated, especially the fingers. We purposefully constructed two ratios based on the elongated chelal fingers with a morphometric with a low dominance value, the telson width which exhibited values under 6. Fig. C illustrates the success of these two morphometric ratios, *I. kinzelbachi* showing considerable separation from all other species except *I. kadleci*. The two species closest geographically to *I. kinzelbachi*, *I. dufoureius* and *I. kraepelini*, show the most separation in these ratios. The low ratio values in these two species is caused by the relatively wide telson vesicle discussed elsewhere. *I. kadleci*, whose telson is somewhat narrow, also has the second longest chelal fingers, thus causing its clustering with *I. kinzelbachi*. The metasoma in *I. kinzelbachi* is somewhat slender on the terminal segments, especially IV–V. Interestingly, in Tables C1 and C2 we see the reason for this is the somewhat low values for these segment widths, all 8 or less. In *I. kinzelbachi*, telson is the second most slender in *Iurus*; only *I. kadleci* has a more elongated telson. This is apparent in the histograms presented in Fig. C6 where the telson width and depth are compared to its length.

***I. kadleci*.** *I. kadleci* has the thinnest chela in *Iurus*. Although its fingers are somewhat elongate, as discussed above, the overall thinness of the chela is due to its narrow width and depth. Tables C1 and C2 certainly support this observation where the dominance values are extremely low, all 4 or less, representing some of the lowest values in all. In Fig. C2 are two ratios based on the chelal width and depth as compared to its length. *I. kadleci* has the lowest ratio values in all four histograms, showing standard error separation from three of the four other species. Accompanying the thin chela in *I. kadleci* is the thinnest metasoma found in *Iurus*. This is predictable by inspecting Tables C1 and C2 where we

see not only large values for individual segment lengths, but low values for corresponding segment widths, both contributing to a thin ratio. Figs. C4–C5 also show the thin metasoma, with significant standard error separation for all five metasoma segments, for both male and female. Consistent with the thin chela and metasoma, *I. kadleci* also has the thinnest telson in *Iurus*. All data in Tables C1 and C2 point to this result as well as the histograms in Fig. C6. The ratio dominance values are high for the telson length and somewhat small for the vesicle width and depth. It is important to note here that these three ratios sets all confirm that *I. kadleci* is indeed a much more slender species than all other species in the genus.

***I. asiaticus*.** The chela of *I. asiaticus*, when compared to *I. kraepelini*, appears to be somewhat more elongated. This is due, in part, to the wider and much deeper chelal palm in *I. kraepelini*. However, in *I. asiaticus* the palm is somewhat elongated, contributing to the overall chelal length. The largest values for this morphometric in Tables C1 and C2 are for *I. asiaticus*. We purposefully combined this measurement with another that exhibited low values, the telson length. The telson length values for *I. asiaticus* are the lowest of all *Iurus* species. Fig. C7 shows the result of comparing the chelal palm length to the telson length. *I. asiaticus* shows decent separation from the other species, exhibiting the largest ratio values. The metasoma in *I. asiaticus* is somewhat stocky, typically showing lower ratio values in most segments in Figs. C4–C5, only exceeded by *I. kraepelini*. There is no particular tendency in telson of *I. asiaticus*, it is relatively short, as discussed above, but the vesicle width and depth also have somewhat low values, so the histograms in Fig. C6 place this species clustered with the others, only *I. kadleci* showing separation.

Key to *Iurus* species using morphometrics (male and female adults)

- 1 - Long fingered, narrow telson: Chelal fixed finger_length / Telson_width = 3.36–3.46 (3.412) male, 3.40–3.63 (3.532) female 2
- - Medium fingered, wide telson: Chelal fixed finger_length / Telson_width = 2.61–3.14 (2.837) male, 2.60–3.23 (2.883) female 3
- 2 - Thin metasoma: Metasomal segments I–III length / width = 1.09–1.25 (1.193), 1.36–1.45 (1.400), 1.63–1.68 (1.663) male, 1.11–1.12 (1.113), 1.39–1.53 (1.458), 1.58–1.68 (1.630) female; elongated telson: Telson_L / Telson_W = 4.34–4.34 (4.343) male, 4.04–4.29 (4.162) female *I. kadleci* sp. nov.
- - Medium metasoma: Metasomal segments I–III length / width = 0.82–0.86 (0.840), 1.13–1.17 (1.149),

1.34–1.49 (1.411) male, 0.76–0.80 (0.783), 1.03–1.10 (1.059), 1.26–1.34 (1.293) female; medium telson: Telson_L / Telson_W = 3.54–3.76 (3.674) male, 3.52–3.72 (3.637) female *I. kinzelbachi* sp. nov.

3 - Medium depth chelal palm; Chela_depth/ Chela_length = 0.32–0.36 (0.340) male, 0.31–0.34 (0.326) female **4**

■ - Deep chelal palm; Chela_depth /Chela_length = 0.40–0.45 (0.434) male, 0.37–0.38 (0.377) female
..... *I. kraepelini* von Ubisch, 1922

4 - Medium lengthed finger, narrow vesicle: Movable finger_length / Telson_width = 3.77–4.02 (3.897) male, 3.99–4.08 (4.033) female; elongated chelal palm, short telson: Palm_length / Telson_length = 0.85–0.92 (0.894) male, 0.90–0.95 (0.929) female
..... *I. asiaticus* Birula, 1903

■ - Short lengthed finger, wide vesicle: Movable finger_length / Telson_width = 3.19–3.38 (3.302) male, 3.37–3.70 (3.495) female; short chelal palm, medium telson: Palm_length / Telson_length = 0.73–0.77 (0.755) male, 0.73–0.85 (0.796) female
..... *I. dufoureius* (Brullé, 1832)

The statistics in the above key exhibit *absolute range separation* in all cases. The MVDs for the sixteen ratios (eight per male and female) ranged 18.0–42.0 (23.025) % for the male, and 14.4–42.1 (23.813) % for the female. In the primary key provided in the body of this paper, several of these morphometrics are used, supporting major morphology differences in the pedipalp chela and hemispermatophore.

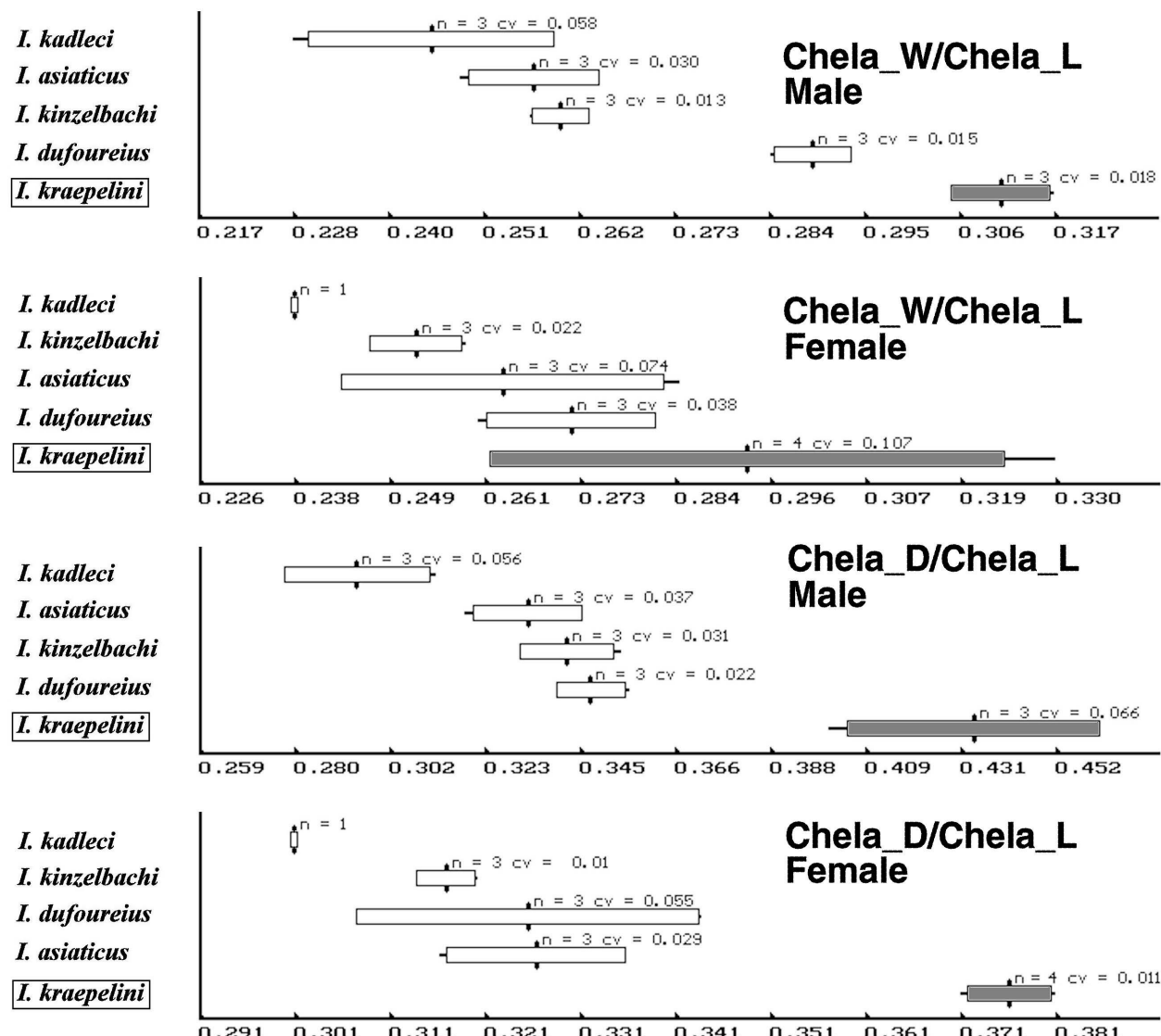


Figure C2: Morphometric ratio contrasting chelal width with chelal length (**top**) and chelal depth with chelal length (**bottom**). This histogram demonstrates two significant trends: the wide and deep chelal palm exhibited in *I. kraepelini* and, in contrast, the slender chelal palm, both in width and depth, in *I. kadleci*, sp. nov.

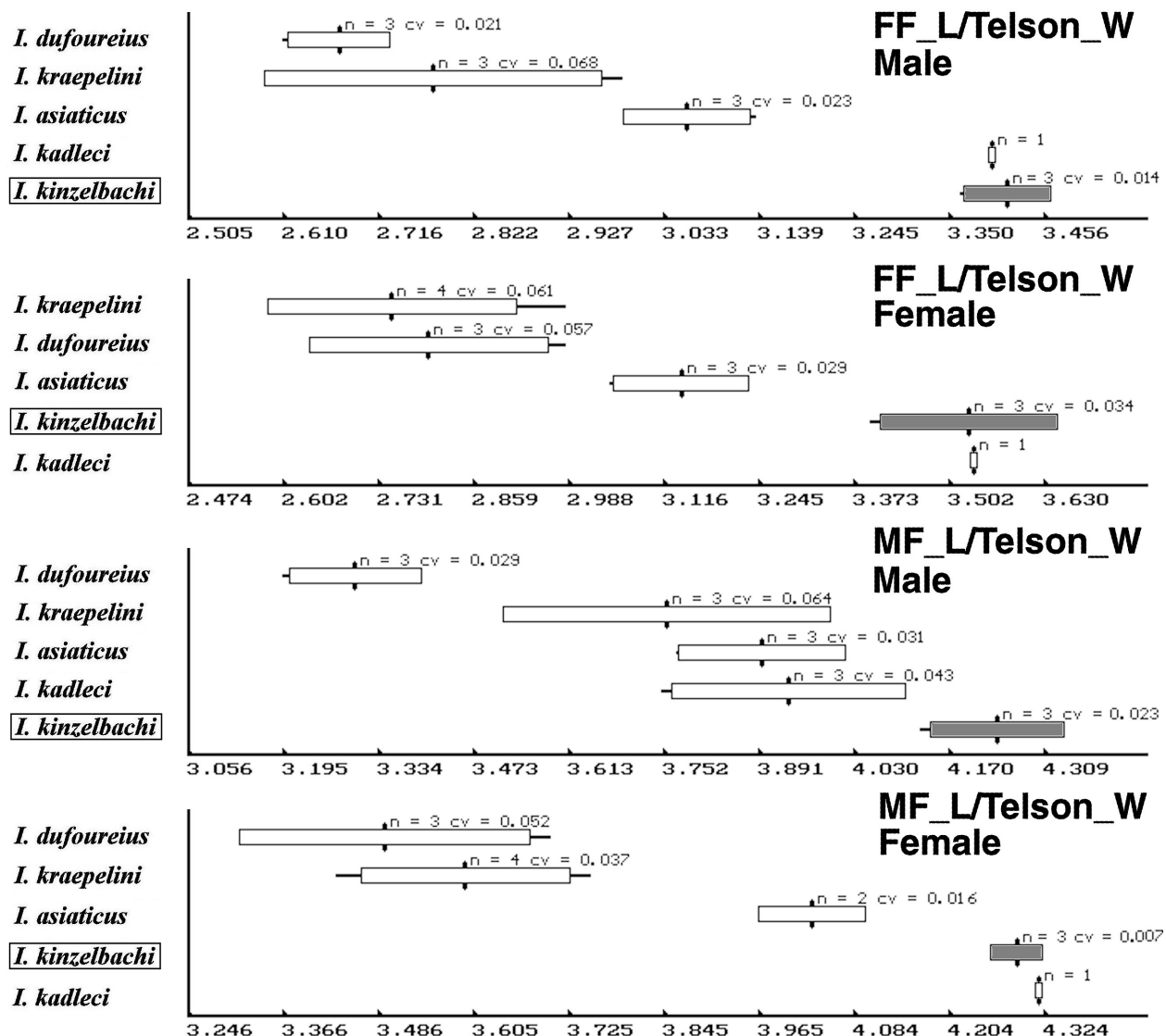


Figure C3: Morphometric ratio contrasting chelal fixed finger length with telson width (**top**) and chelal movable finger length with telson width (**bottom**). This histogram demonstrates the elongated chelal fingers exhibited in *I. kinzelbachi*, sp. nov. as compared to its somewhat narrow telson. In contrast, the relatively shorter fingers seen in *I. dufoureius* and *I. kraepelini* who also have a heavier telson, cluster the farthest from *I. kinzelbachi*. *I. kadleci*, sp. nov., whose fingers are somewhat elongate and telson narrow, clusters with *I. kinzelbachi*.

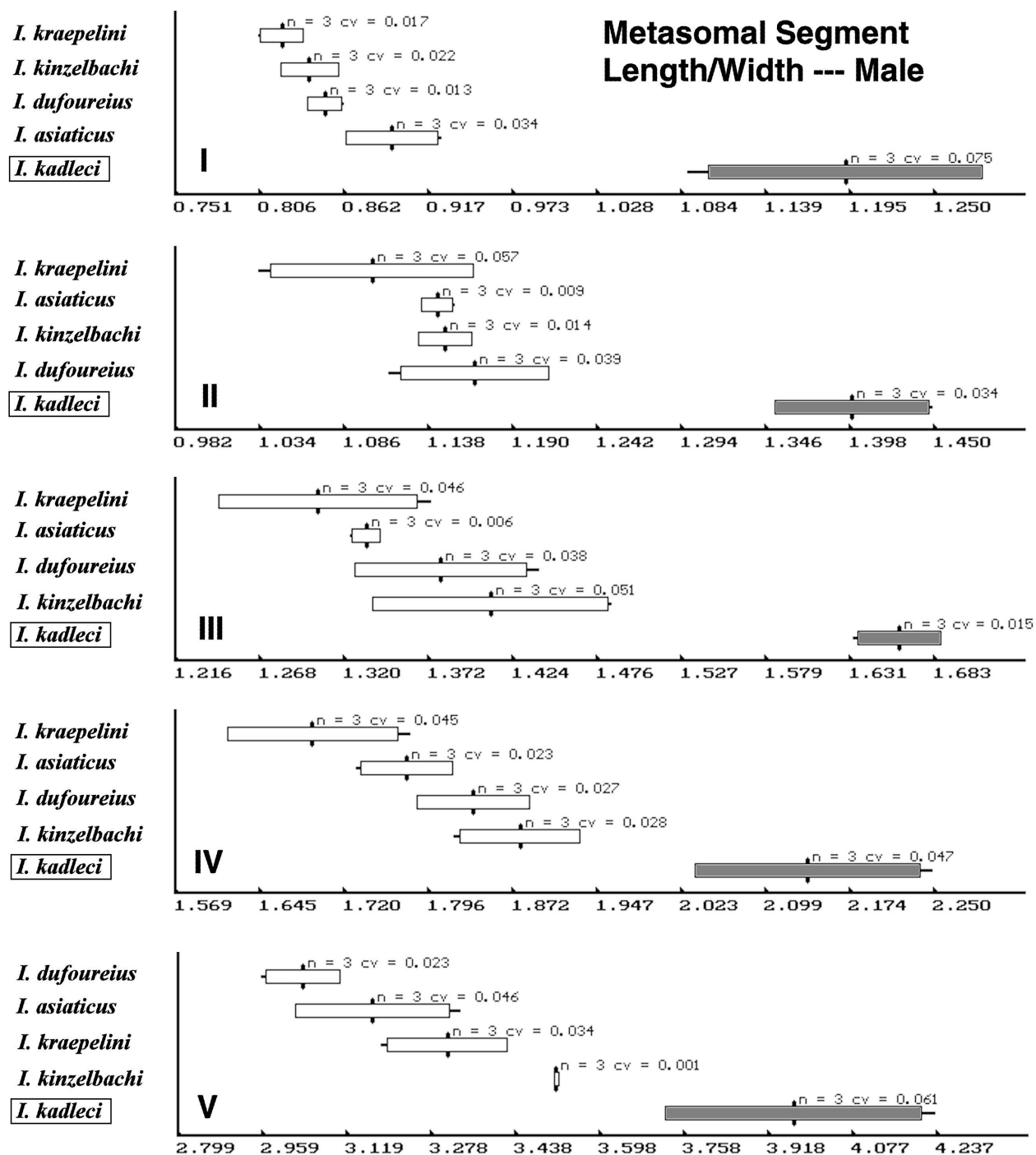


Figure C4: Morphometric ratio contrasting metasomal segments (length/width) for the **male**. This histogram demonstrates the elongated metasomal segments exhibited in *I. kadleci*, sp. nov. in contrast to the relatively stouter metasoma of *I. kraepelini*.

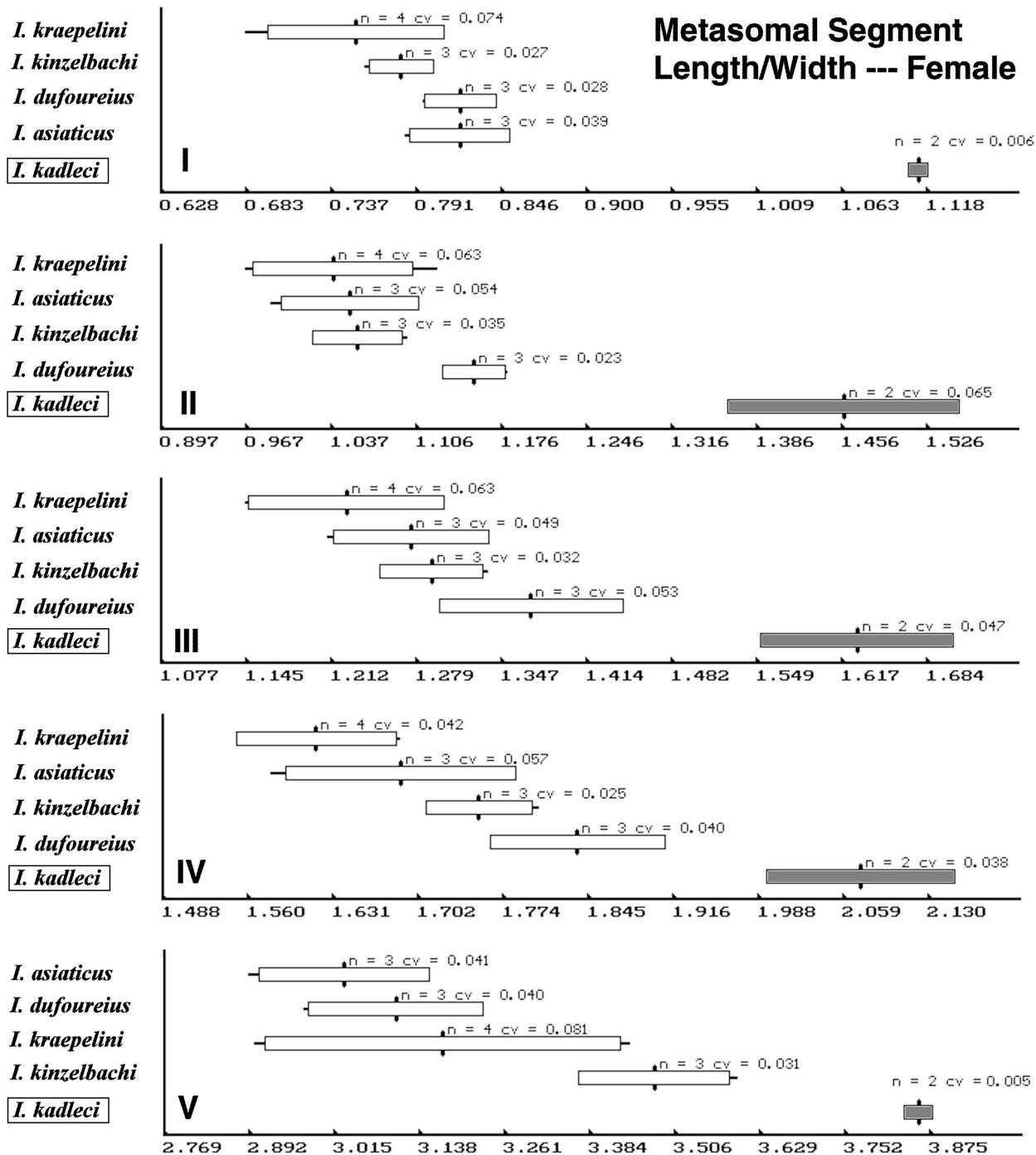


Figure C5: Morphometric ratio contrasting metasomal segments (length/width) for the female. This histogram demonstrates the elongated metasomal segments exhibited in *I. kadleci*, sp. nov. in contrast to the relatively stouter metasoma of *I. kraepelini*.

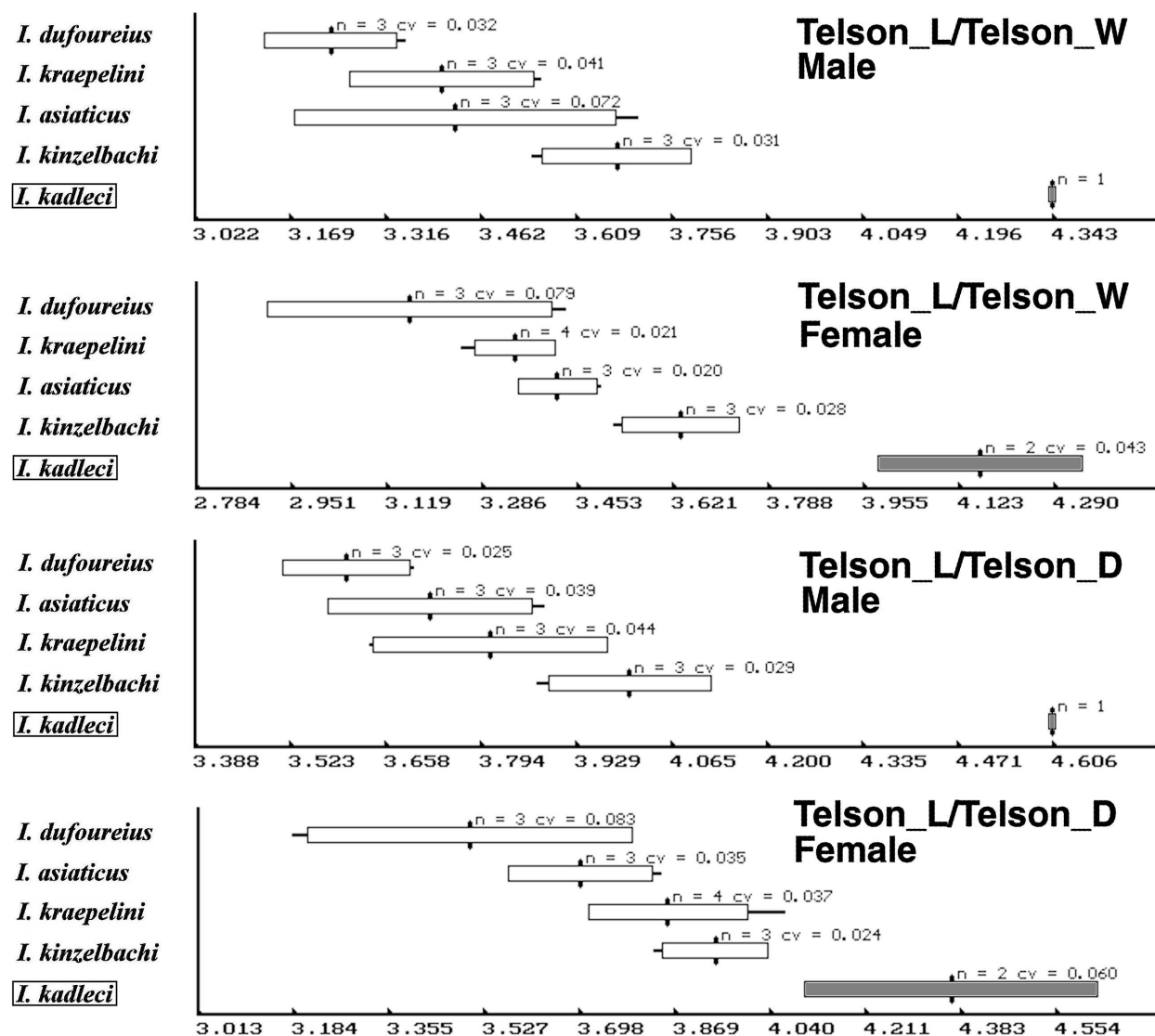


Figure C6: Morphometric ratio contrasting telson length with telson width (**top**) and telson length with telson depth (**bottom**). This histogram demonstrates the elongated, thin telson of *I. kadleci*, sp. nov. in contrast to the relatively stouter telson of *I. dufoureius*.

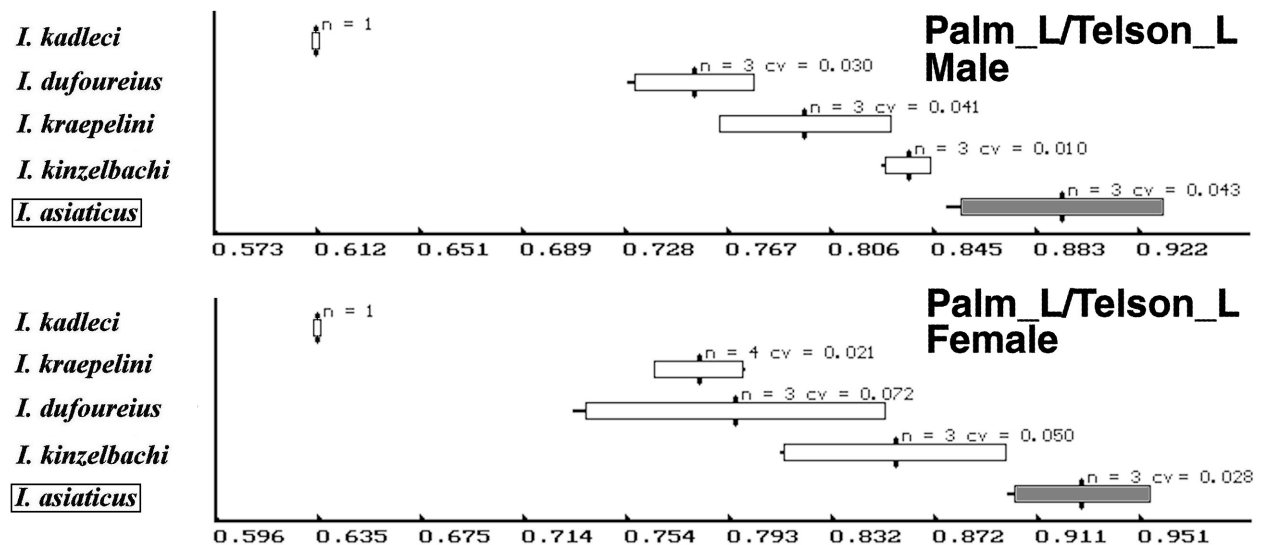


Figure C7: Morphometric ratio contrasting the chelal palm length to the telson length. This histogram demonstrates the relatively elongated chelal palm and short telson exhibited in *I. asiaticus* in contrast to the relatively shorter palm and elongated telson of *I. kadleci*, sp. nov.